



HAL
open science

Compressible turbulence in space and astrophysical plasmas : Analytical approach and in-situ data analysis for the solar wind

Supratik Banerjee

► **To cite this version:**

Supratik Banerjee. Compressible turbulence in space and astrophysical plasmas : Analytical approach and in-situ data analysis for the solar wind. Solar and Stellar Astrophysics [astro-ph.SR]. Université Paris Sud - Paris XI, 2014. English. NNT : 2014PA112206 . tel-01087024

HAL Id: tel-01087024

<https://theses.hal.science/tel-01087024>

Submitted on 25 Nov 2014

HAL is a multi-disciplinary open access archive for the deposit and dissemination of scientific research documents, whether they are published or not. The documents may come from teaching and research institutions in France or abroad, or from public or private research centers.

L'archive ouverte pluridisciplinaire **HAL**, est destinée au dépôt et à la diffusion de documents scientifiques de niveau recherche, publiés ou non, émanant des établissements d'enseignement et de recherche français ou étrangers, des laboratoires publics ou privés.

UNIVERSITÉ PARIS-SUD

ÉCOLE DOCTORALE ONDES ET MATIÈRE

Laboratoire: **Laboratoire de Physique des Plasmas**
Discipline: **PHYSIQUE**

THÈSE DE DOCTORAT

Soutenue le **25 septembre, 2014** par

Supratik BANERJEE

Compressible turbulence in space and astrophysical plasmas

Analytical approach and in-situ data analysis for the
solar wind

Directeur de thèse : **Prof. Sébastien GALTIER** (UPS, Orsay)

Composition du jury :

Président du jury :	M. T. PASSOT	-	Directeur de recherches (Obs. de Nice)
Rapporteurs :	M. S. NAZARENKO	-	Professor (Univ. of Warwick)
	M. W. SCHMIDT	-	Res. Asso. (Univ. of Göttingen)
Directeur de thèse :	M. S. GALTIER	-	Professeur (Univ. Paris-Sud, Orsay)
	M. F. SAHRAOUI	-	Chargé de recherches (LPP)
	M. L. SORRISO-VALVO	-	Chargé de recherches (Univ. della Calabria)
Membres invités:	M. J. SAUR	-	Professor (Univ. zu Koln)

Acknowledgments

At first I would like to convey my sincere gratitude to my thesis supervisor Prof. Sébastien Galtier, my co-supervisor Dr. Fouad Sahraoui and the other honourable members of the jury for making my thesis possible and successful. I acknowledge my laboratories Institut d'Astrophysique Spatiale (IAS), Orsay and Laboratoire de Physique des Plasmas (LPP), Palaiseau for their kind co-operation.

A special thanks to Dr. Thierry Passot, Dr. Alexei Kritsuk, Dr. Christoph Federrath, Dr. Olivier Le contel and Dr. Lucas Sorrison-Valvo for their valuable scientific advice and encouragement. I am also grateful to the team of Prof. Vincenzo Carbone (specially Dr. Fabio Lepreti) for introducing basic methods of data analysis to me.

I am indebted to AMDA database which allowed me to use THEMIS data at free of cost and also NASA copyrighted images which were important in explaining certain aspects of my thesis.

In my thesis, I used a number of images from different sources which included journals and books subject to copyright. In this context, I would like to formally acknowledge

- American Physical Society (APS)¹,
- Cambridge University Press,
- Institute of Physics (IOP publishing),
- Astronomy and Astrophysics,
- Dr. Alexei Kritsuk, Dr. Thierry Passot, Dr. Annick Pouquet, Dr. Bogdan Hnat, Dr. Chadi Salem and Dr. Lucas Sorrison-Valvo

for kindly allowing me to re-use those copyrighted images. For the other copyrighted images, the permissions are taken directly by *Rightslink*.

I would like to thank cordially to my friend Dr. Subimal Majee and all other friends who constantly supported me during last 3 years. A big thanks to all the members of Sammilani which is a bengali association in paris for making me happy always. I am thankful to all my friends, philosophers and guides. Finally I would like to thank all my teachers and my parents Mr. Ajit

¹"Readers may view, browse, and/or download material for temporary copying purposes only, provided these uses are for noncommercial personal purposes. Except as provided by law, this material may not be further reproduced, distributed, transmitted, modified, adapted, performed, displayed, published, or sold in whole or part, without prior written permission from the American Physical Society."

Kumar Banerjee and Mrs. Pratima Banerjee for all their contributions and sacrifices since my childhood.

I would like to acknowledge indian classical music and my guru (music teacher) Pandit Paritosh Pohankar for inspiring me at every moment.

And last but not the least ! A big thanks to my sister Indrani Banerjee and my grand mother Indira Mukherjee who always pray to god for me.

Contents

1	Introduction	1
1.1	General interest	1
1.2	Turbulence in space and astrophysical plasmas	2
1.3	An outline of my thesis	4
2	Compressibility in fluids	7
2.1	What is compressibility ?	7
2.2	Measure of compressibility for a fluid in motion	9
2.3	Closure for compressible fluids	11
2.4	Invariants in compressible barotropic fluid	12
2.4.1	Total energy	12
2.4.2	Kinetic helicity	14
2.4.3	Mass and linear momentum	14
2.5	Potential flow	15
2.6	Two dimensional compressible flow	16
2.7	One dimensional model for discontinuous compressible flow: Burgers' equation	16
2.8	Compressibility ratio for a polytropic gas across a normal shock	18
2.9	Baroclinic vector	20
3	Plasma physics and magnetohydrodynamics	21
3.1	What is a plasma ?	21
3.2	Two approaches to plasma	23
3.2.1	Kinetic approach	23
3.2.2	Fluid approach	25
3.3	Magnetohydrodynamics (MHD)	26
3.3.1	Mono-fluid model: Basic equations of MHD	27
3.3.2	Ideal MHD approximation from generalized Ohm's law	29
3.3.3	Linear waves in ideal MHD	31
3.3.4	Invariants of ideal MHD	33
3.3.5	Elsässer variables in magnetohydrodynamics	38
4	Turbulent flow : important notions	43
4.1	Turbulence - A phenomenon or a theory ?	44
4.2	Turbulent regime from Navier-Stokes : Reynolds number	45
4.3	Chaos and/or turbulence ?	48
4.4	Basic assumptions	50

4.4.1	Statistical homogeneity	50
4.4.2	Statistical isotropy	50
4.4.3	Stationary state	50
4.5	Two approaches to turbulence	51
4.5.1	Statistical approach	51
4.5.2	Spectral approach	54
4.6	Phenomenology	59
4.6.1	K41 phenomenology	60
4.6.2	IK phenomenology	63
4.6.3	Utilities of phenomenology	66
4.7	Dynamics and energetics of turbulence	70
4.7.1	Turbulent forcing	70
4.7.2	Turbulent cascade	71
4.7.3	Turbulent dissipation	73
4.8	Intermittency	74
4.8.1	β fractal model	77
4.8.2	Refined similarity hypothesis : Log-Normal model	78
4.8.3	Log-Poisson model	79
4.8.4	Extended self-similarity	80
5	Turbulence in compressible fluids	83
5.1	Why is it important ?	83
5.2	Primitive theoretical approaches	86
5.3	Numerical approaches using one dimensional model	88
5.4	Numerical Simulations in higher dimensions	90
5.4.1	Numerical methods for compressible turbulence	90
5.4.2	Piecewise Parabolic Method (PPM):	90
5.4.3	Compressible intermittency	97
5.4.4	Compressible and solenoidal forcing	99
5.4.5	Choice of inertial zone and sonic scale	101
5.4.6	Two-point closure in EDQNM model for compressible turbulence	102
5.5	Observational studies	102
6	Exact relations in turbulence	109
6.1	Exact relations in incompressible turbulence	109
6.1.1	Incompressible hydrodynamic turbulence	111
6.1.2	Incompressible MHD turbulence	113
6.2	Previous attempts for exact relations in compressible turbulence	116
6.2.1	Heuristic approach by Carbone et al. (2009)	116
6.2.2	FFO approach for a generalized exact equation	117

6.3	New exact relations and phenomenologies in compressible turbulence : My research work	120
6.3.1	Isothermal hydrodynamic turbulence	121
6.3.2	A new phenomenology for compressible turbulence	128
6.3.3	Isothermal MHD turbulence	130
6.3.4	Polytropic hydrodynamic turbulence	137
7	Solar wind data analysis	147
7.1	Introduction	147
7.2	The solar wind	148
7.2.1	The heliosphere	148
7.2.2	Prediction for the solar wind	149
7.2.3	The fast and the slow solar wind	149
7.2.4	Exploration of the solar wind	151
7.2.5	MHD fluctuations in the solar wind	152
7.2.6	Nature of the solar wind turbulence	152
7.3	Data source	154
7.3.1	The THEMIS mission	154
7.3.2	A brief description of instruments	154
7.4	Judicial selection of data	157
7.4.1	Selection of intervals	157
7.4.2	Relevant spatial and temporal scales	162
7.5	Analysis of the selected data	164
8	Resuming and looking ahead...	175
8.1	Answered and unanswered issues of compressible turbulence	175
8.2	Some future projects	177
	References	179

List of Figures

1.1	Turbulence in the mixing of milk in coffee, Credit: Daniel G. Walczyk.	2
1.2	Supercomputing simulation showing the formation of interstellar gas filaments in turbulent interstellar cloud; The highest density (red) fragments represent molecular self-gravitating cores leading to the star formation; Performed by researchers of University of California-Berkeley using the Pleiades supercomputer at the NASA Advanced Supercomputing facility, Credit: NASA.	3
2.1	Highly compressible dilute diffuse gas in the interstellar space; Credit: University of Leeds.	8
2.2	Evolution of a Burgers' shock in course of time (t); Credit: Ludovic Maas.	18
3.1	Different types of plasmas: argon glow discharge (left above), fusion plasma (right above), uv image of solar corona (left below) and highly dense Lagoon nebula (right below).	22
3.2	Experimental verification of Alfvén waves in a hydrogen filled tube of 34 inches and of diameter $5^{3/4}$ inches; The solid line corresponds to the theoretical estimation and the circles correspond to the experimental values which justifies the proportionality of Alfvén speed to the magnetic field in an incompressible or weakly compressible fluid; The discrepancy between the experimental and the theoretical values are due to instrumental reasons; <i>Reprinted with permission from (Allen et al., 1959); © (1959) American Physical Society. DOI: 10.1103/PhysRevLett.2.383</i>	34
3.3	Numerical simulation of twisted and knotted magnetic field lines for a system with non-zero magnetic helicity; Source: Oral presentation of Simon Candelaresi.	38
3.4	Order of magnitude of various plasma parameters for different types of plasmas.	42
4.1	Transition from laminar flow to turbulent flow as a function of increasing Reynolds number; Courtesy: Sébastien Galtier.	46
4.2	Behaviour of a second order auto-correlation function in space; Courtesy: Sébastien Galtier.	53

4.3	Schematic view of Richardson's energy cascade in turbulence by eddy fragmentation.	60
4.4	Normalized velocity power spectra from different experiments show universal $k^{-5/3}$ behaviour; <i>Reprinted with permission from Gibson & Schwarz (1963)</i> ; © (1963) Cambridge university press.	62
4.5	Sporadic interactions of Elsasser fields in IK phenomenology.	64
4.6	Clear deviation of the moments of velocity and magnetic fluctuations from the self-similar scaling laws of K41 and IK phenomenology in the solar wind; <i>Reprinted with author's permission from Salem et al. (2009)</i> ; © (2009) AAS. DOI: 10.1088/0004-637X/702/1/537	75
4.7	Scaling of second order longitudinal velocity structure functions (in logarithmic plot) in time domain using data obtained from S1 wind channel of ONERA; <i>Reprinted with permission from Frisch (1995)</i> ; © (1995) Cambridge university press.	77
4.8	Two dimensional representation of fractal cascade for $\beta = \frac{1}{2}$; Courtesy: Sébastien Galtier.	78
4.9	Comparison of different models of intermittency: plot of nth order moment for velocity structure function as a function of n, the discrete points with different colors and shapes (black and white triangles, white square, black circle and crosses) correspond to data obtained from different experiments, the straight chain line, dashed line, dotted line and the solid line correspond respectively the theoretical predictions of K41, beta-fractal with $D = 2.8$, log-Poisson and log-normal models; <i>Reprinted with permission from Frisch (1995)</i> ; © (1995) Cambridge university press.	81
5.1	WIND spacecraft data of velocity, density and radial magnetic field fluctuations (Days in 1995); <i>Reprinted with permission from Meyer-Vernet (2007)</i> ; © (2007) Cambridge university press.	84
5.2	Total mechanical energy spectra (left); step discontinuities for turbulent density and triangular discontinuities for turbulent velocity field (right); Source: Tokunaga (1976).	89
5.3	PDF of $s = \ln \rho$ for (i) isothermal case (left), (ii) $\gamma < 1$ (right-upper) and (iii) $\gamma > 1$ (right-lower) for one dimensional gas turbulence; <i>Reprinted with permission from Passot & Vazquez-Semadini (1998)</i> ; © (1998) American physical society. DOI: 10.1103/PhysRevE.58.4501	91

-
- 5.4 Vortex structures in numerical simulation (using PPM) of two dimensional compressible turbulence with 512^2 resolution (left) and power density spectra (right) for (i) solenoidal kinetic energy (E^S) (solid line), (ii) compressible kinetic energy (E^C) (dashed line) and (iii) total kinetic energy (E^v) (dotted line); *Reprinted with permission from Passot et al. (1988)*; © (1988) ESO. 92
- 5.5 Power density spectra for (in logarithmic graph) (i) solenoidal kinetic energy (E^S), (ii) compressible kinetic energy (E^C) and (iii) total kinetic energy (E^v) in three dimensional compressible turbulence PPM simulation with 256^3 resolution; the solenoidal and the total kinetic energy spectra follow a $k^{-0.95}$ law whereas the compressible kinetic energy spectrum follows a steeper $k^{-1.8}$ law; *Reprinted with permission from Porter et al. (1992)*; © (1992) American Physical Society. DOI: 10.1103/Phys-RevLett.68.3156 93
- 5.6 Power density spectra for (i) solenoidal kinetic energy (E^S) (left above), (ii) compressible kinetic energy (E^C) (left below) using 64^3 (Q40), 128^3 (Q41), 256^3 (Q42) and 512^3 (Q43) grid points and (iii) vortex tube structures in 512^3 numerical box of supersonic turbulence (right); *Reprinted with permission from Porter et al. (1994)*; © (1994) AIP publishing LLC. 94
- 5.7 Projected gas density of Mach 6 turbulence PPM simulation with 2048^3 resolution. White, blue and yellow colors represent respectively low, intermediate and high projected density values; *Reprinted with author's permission from Kritsuk et al. (2009)*. 95
- 5.8 Power density spectra corresponding to (a) total velocity (v), (b) solenoidal velocity (v_s), (c) compressional velocity (v_c), (d) $\rho^{1/2}v$ and $\rho^{1/2}v_s$, (e) $w \equiv \rho^{1/3}v$ and (f) ρ ; *Reprinted with permission from Kritsuk et al. (2007a)*; © (2007) AAS. DOI: 10.1086/519443 96
- 5.9 Scaling of third order structure functions of $w \equiv \rho^{1/3}v$ using data of three dimensional supersonic turbulence (r.m.s. Mach ~ 6) with 1024^3 resolution; *Reprinted with author's permission from Kritsuk et al. (2007b)*. 98
- 5.10 Compensated power density spectrum of $w \equiv \rho^{1/3}v$ using data of three dimensional supersonic turbulence (r.m.s. Mach ~ 6) with 2048^3 resolution; *Reprinted with author's permission from Kritsuk et al. (2009)*. 98

5.11	Compensated power spectra corresponding to different variables using solenoidal and compressible forcing; <i>Reprinted with permission from Federrath et al. (2010)</i> ; © (2010) ESO. . . .	100
5.12	Modified interpretation of power spectra with the newly defined sonic scale; <i>Reprinted with permission from Federrath et al. (2010)</i> ; © (2010) ESO.	101
5.13	Solenoidal and dilatational velocity power spectra for different turbulent Mach numbers at large times (left) and Pressure spectra at different time instants (right) obtained using EDQNM model for weakly compressible turbulence; <i>Reprinted with permission from Bertoglio et al. (2001)</i> ; © (2001) AIP publishing LLC.	103
5.14	Moments of proton density fluctuations and magnetic field magnitude fluctuations as a function of the order of moments in slow (left) and fast (right) solar wind; <i>Reprinted with permission from Hnat et al. (2005)</i> ; © (2005) American Physical Society. DOI: 10.1103/PhysRevLett.94.204502	105
5.15	Compressible and incompressible scaling (in log-log graph) in time domain of the fast solar wind data obtained from Ulysses spacecraft, Y^\pm W^\pm represent respectively the incompressible and compressible third order moments; <i>Reprinted with permission from Carbone et al. (2009)</i> ; © (2009) American Physical Society. DOI: 10.1103/PhysRevLett.103.061102	106
5.16	Heating energy supply by compressible pseudo-energy ε_I^\pm dissipation (Red and Blue squares) and incompressible pseudo-energy ε_I^\pm dissipation (Green and Violet circles) in comparison with two theoretical estimations of the radial temperature profile for fast solar wind; <i>Reprinted with permission from Carbone et al. (2009)</i> ; © (2009) American Physical Society. DOI: 10.1103/PhysRevLett.103.061102	107
6.1	Dilatation (left) and compression (right) phases in space correlation for isotropic turbulence. In a direct cascade scenario the flux vectors (blue arrows) are oriented towards the center of the sphere. Dilatation and compression (red arrows) are additional effects which act respectively in the opposite or in the same direction as the flux vectors.	125
6.2	Numerical verification of scaling (logarithmic plot) of the flux (F) and the source terms (Q) of equation (6.55) in supersonic turbulence using 1024^3 resolution; <i>Reprinted with permission from Kritsuk et al. (2013)</i> ; © (2013) Cambridge university press.	127

6.3	Phenomenological view of compressible MHD turbulence in the presence of a strong directive magnetic field; An axisymmetric total energy cascade is predicted in the perpendicular direction of the strong directive magnetic field following the same phenomenology of the hydrodynamic case; Source: Banerjee & Galtier (2013)	137
7.1	A schematic figure of the heliosphere; Credit: NASA.	149
7.2	Solar wind speed and the magnetic field polarity observations from the Ulysses spacecraft covering almost all the latitudes from the equatorial to the polar region; <i>Reprinted with permission from Biskamp (2008)</i> ; © (2003) Cambridge university press.	150
7.3	An artist view of the five spacecraft of the THEMIS mission; Credit: NASA.	153
7.4	Working principle of the fluxgate magnetometer (FGM).	155
7.5	A schematic view of ESA; Credit: Barkeley.	157
7.6	THEMIS spacecraft with its onboard instruments; Credit: NASA and oral presentation of Le Contel et al.	158
7.7	THEMIS spacecraft orbits during different periods; the red trajectory corresponds to THEMIS B and the grey region represents the solar wind; Credit : http://themis.ssl.berkeley.edu/	159
7.8	Spacecraft trajectories (red line) obtained by SSC Orbit Viewer along with the positions of the magnetopause (off-white net like region) and bow-shock (green net like region). D_{1x} , D_{2x} , D_{3x} represent respectively the distance of the spacecraft from the Earth, the magnetopause and the bow-shock along the x-direction.	160
7.9	Examination of the ionic fluid temperature for a 24-hour interval on 14/07/2008-15/07/2008.	161
7.10	Selection of Fast solar wind data for the periods of 15/06/2008 - 10/10/2008 and 15/06/2009 - 10/10/2009, the three components of velocity (in km/s) are given in three different colors (as explained in the image).	161

7.11	The fluctuation data scheme of 8h-11h of 11/08/2008 obtained from AMDA - the ion velocity components, ion density and magnetic field components are given in the respective three panels (top figure); calculated density fluctuations (in green) about the mean value (in violet) (middle panel) and the scaling of incompressible (in red) and partial compressible flux (in blue) as a function of time lag τ (bottom panel).	165
7.12	(a) Interval with negative incompressible and compressible flux, (b) Interval with positive incompressible and compressible flux.	167
7.13	(c) Interval with positive incompressible flux and negative compressible flux, (d) Interval with negative incompressible flux and positive compressible flux.	168
7.14	The effect of compressibility on the discrepancy between the incompressible and compressible flux.	169
7.15	Almost constant plasma beta parameter of order unity during a 10 hour interval of 10/08/2008 -11/10/2008 (second panel) .	170
7.16	Comparison of incompressible (in black), heuristic compressible (in green) and analytical compressible (in red) scalings in a 6-hour interval of 2008	172
7.17	Comparison of incompressible (in black), heuristic compressible (in green) and analytical compressible (in red) scalings in a 6-hour interval of 2009	172

List of Tables

4.1	Self-similarity with K41 phenomenology.	76
4.2	Self-similarity with IK phenomenology.	76
5.1	Different power spectra in supersonic turbulence (<i>Kritsuk et al., 2007a</i>).	95
7.1	Selected intervals of the fast solar wind with continuous data set	162
7.2	Average values of the flux terms (for 3 s. lag) for a number of three-hour intervals	171

Introduction

Contents

1.1	General interest	1
1.2	Turbulence in space and astrophysical plasmas	2
1.3	An outline of my thesis	4

1.1 General interest

TURBULENCE is said to be one of the last unsolved problems of classical physics. In a simplistic manner, one can describe turbulence as a very complicated non-linear fluid flow principally associated with vortices. It is easier to describe turbulence than to analyze it. Till date, no satisfactory analytical theory has been established to understand turbulence. It is even obscure to determine the suitable approach for understanding turbulence. Despite this enormous complexity, the most intriguing feature of turbulence is its ubiquity in nature. Starting from the everyday fluids like tap water or milk in a cup of hot coffee (see fig. 1.1), prominent signatures of turbulence are observed in the tropospheric air, the space plasmas (the solar wind, magnetospheric plasmas) and even in the interstellar clouds which give birth to the stars. Other than the usual hydrodynamical fluids and plasmas, turbulence is believed to describe various phenomena in non-linear optics (Garnier *et al.*, 2012), small scale biological fluids like microbial suspensions (Wensink *et al.*, 2012). Turbulence is also observed in quantum mechanics (Proment *et al.*, 2009). Most interestingly, turbulent behaviour is significantly perceived even in the field of finance and economics. This fact can be justified by a famous remark of Benoit Mandelbrot, who said

" The techniques I developed for turbulence, like weather, also apply to the stock market."

The formal study of turbulence is evoked from some practical interests. One of them is its efficiency in **mixing**. A spoon of milk gets uniformly mixed in coffee within some seconds only if we stir it to create turbulence.

Without turbulence the mixing would take place by pure molecular diffusion and would take several months to be completed. In case of weather forecasting,



Figure 1.1: Turbulence in the mixing of milk in coffee, Credit: Daniel G. Walczyk.

an understanding of turbulence is a must. The first theories of turbulence were indeed born out of that very interest (Richardson, 1922). Moreover, a thorough investigation of atmospheric turbulence or more precisely clear air turbulence (CAT) could be useful for reducing hazards to aircraft passengers across the zones of rough air and also to design more efficient aircrafts.

1.2 Turbulence in space and astrophysical plasmas

Clear signature of turbulence has been observed (Armstrong *et al.*, 1995; Bruno & Carbone, 2005) also in the space plasmas like solar wind, magnetospheric plasmas etc. and in the astrophysical plasmas. In several studies it is observed that the fluctuations in the aforesaid plasmas usually associate large number of spatial and temporal scales and the power spectrum of energy follows almost an identical power law (with index $-5/3$) to the one predicted by Kolmogorov for incompressible hydrodynamic turbulence (discussed in details in chapter 4). However, the plasma turbulence is not exactly identical to ordinary fluid turbulence due to the presence of electromagnetic fields.

Moreover, the space plasmas are usually non-collisional and hence a viscous dissipation mechanism cannot be associated. One has thus to consider the plausibility of kinetic turbulence in such plasmas (Belmont *et al.*, 2014). In case of the solar wind, low frequency fluctuations are modelled by ordinary MHD turbulence whereas more sophisticated models like Hall MHD, electron MHD or purely kinetic approaches are needed to explain high frequency fluctuations (Meyrand & Galtier, 2010; Salem *et al.*, 2012). An understanding of solar wind turbulence is necessary in order to understand the acceleration and the anomalous heating of solar wind (Tu & Marsch, 1997). In course of this thesis, analytical studies along with some spacecraft data analysis have been performed in order to address these issues. On the other hand, turbulence in the cold molecular highly compressible interstellar clouds is believed to bring about the formation of a star by preventing the collapse of a self-gravitating cloud. The scientists of University of California-Berkeley have recently performed large scale supercomputing simulations (see figure 1.2) for understanding the underlying mechanisms.

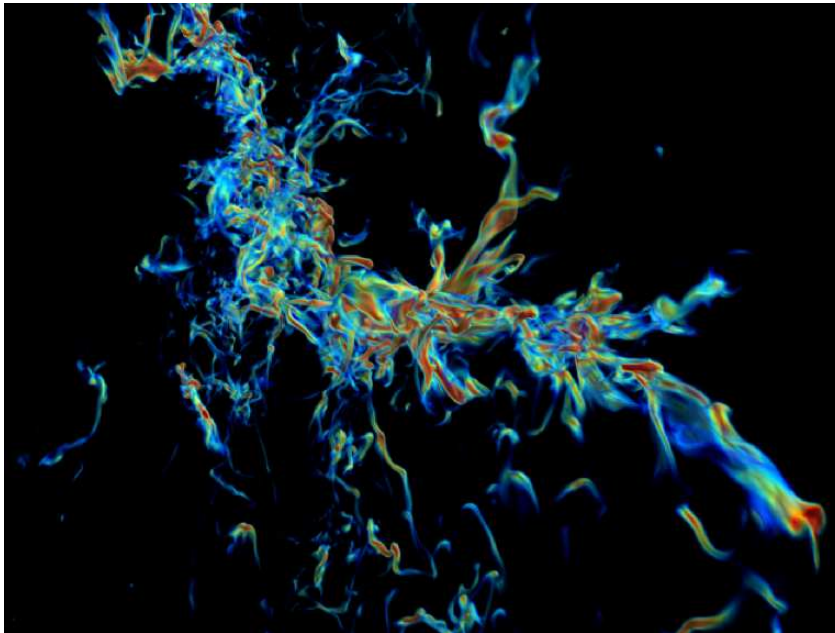


Figure 1.2: Supercomputing simulation showing the formation of interstellar gas filaments in turbulent interstellar cloud; The highest density (red) fragments represent molecular self-gravitating cores leading to the star formation; Performed by researchers of University of California-Berkeley using the Pleiades supercomputer at the NASA Advanced Supercomputing facility, Credit: NASA.

1.3 An outline of my thesis

Compressibility in fluids is a non trivial issue which becomes more complicated when discussed in the framework of turbulence¹. The principal work of my thesis consists of deriving analytical statistical constraints or so-called exact relations for compressible turbulence. A clear theoretical background is thus necessary to be developed before presenting my work. Besides, the subject of my thesis largely covers fluid mechanics, plasma physics and also space physics. The composition of this thesis is accomplished from a pedagogical point of view so as to render it accessible to all the persons having knowledge of at least one of the three domains. Besides, discussing the main problematic of the thesis, parallel attempts are also taken to address some misconceptions or unanswered issues in a more general context. Including this introduction, this thesis consists of eight chapters.

In the second chapter of this thesis, different concepts and measures of compressibility have been introduced in a general context for a neutral fluid. Some simple thermodynamic closures (polytropic, barotropic etc.) have been discussed along with the associated inviscid invariants (mass, linear momentum, total energy and kinetic helicity). Very familiar one dimensional model of [Burgers \(1948\)](#) is also discussed including some properties of shock waves in a compressible flow.

The third chapter presents a brief overview of plasma physics. The reductions of kinetic Boltzmann equations² into fluid equations and finally into monofluid Magnetohydrodynamic (MHD) equation have been worked out in a detailed manner. The approximation of ideal MHD, the corresponding linear wave modes (Alfvén and magnetosonic modes) and integral invariants (mass, total energy, cross-helicity, magnetic helicity etc.) are discussed in a schematic way. The notions of Elsässer variables and pseudo-energies both in incompressible ([Elsässer, 1950](#)) and compressible MHD ([Marsch & Mangeney, 1987](#)) have been introduced at the end of the chapter.

The fourth chapter is dedicated to introduce turbulence or rather incompressible turbulence both in neutral and MHD fluids. The chapter begins with some interesting debatable issues like the proper definition of turbulence or the distinction between chaos and turbulence. This part is followed by a schematic discussion of different statistical symmetry considerations in the study of turbulence. The notions of correlation functions, structure functions

¹The construction of the sentence was done deliberately in order to present an alternative point of view than the usual one where we say that turbulence in fluids is complicated and becomes more complicated in compressible fluids.

²In usual books, the fluid equations are derived from collisionless Vlasov's equation which is physically not correct.

and energy power spectra have been elucidated always in incompressible turbulence. With all these elements two different phenomenological views K41 and IK are described respectively for hydrodynamical and magnetohydrodynamic turbulence along with the corresponding power laws which predict respectively a $-5/3$ and a $-3/2$ power law index for the energy power spectra. The dynamics and the physics of energy cascade in turbulence are explained using those phenomenological views. Finally, the aspect of self-similarity or the scale invariance in turbulence is investigated using different models of intermittency and also a slightly different notion of extended self similarity (ESS). This chapter practically sets up the theoretical background for presenting my thesis work thereby rendering the later more accessible to someone who is not very familiar to the fundamentals of turbulence.

The fifth chapter contains a very brief review of different types of research works which have been accomplished in exploring the fundamental properties of compressible turbulence upto the beginning of my thesis and have played some role in conglomerating my ideas over compressible turbulence and possible scopes in that said field. Some initial theoretical approaches are discussed along with their predictions in a separate section. This part is followed by another discussion of some important numerical approaches in compressible turbulence and their different predictions in physical space and Fourier space scaling. High resolution numerical simulations (Kritsuk *et al.*, 2007*a,b*; Kritsuk *et al.*, 2010; Federrath *et al.*, 2010) employing piecewise parabolic method (PPM) for supersonic turbulence are discussed in an elaborate way. Unlike incompressible turbulence, no $-5/3$ power law is found for the fluid velocity power spectrum for compressible fluids. However, the Kolmogorov type $-5/3$ spectrum is found to be recovered even in compressible turbulence if one considers the power spectra for cube-root density weighted velocity instead of normal fluid velocity. For the MHD turbulence simulations, an identical situation is noticed for the Elsässer variables. A theoretical rather analytical explanation for this behaviour is tried to investigate in scope of my thesis. The chapter ends with some significant research works on the compressible turbulence in astrophysical plasmas and space plasmas. Specially the work of Carbone *et al.* (2009) using Ulysses spacecraft data revealed significant improvement in fast solar wind turbulence scaling laws when density fluctuations are taken into account and also hints at the importance of a cube-root density weighted velocity variable in compressible turbulence.

The sixth chapter comprises of my research works on compressible turbulence. It begins with the derivations of some exact relations in incompressible hydrodynamic and MHD turbulence. After describing some shortcomings of previous theoretical approaches in compressible case, we have derived our exact relations for (a) isothermal neutral fluid (Galtier & Banerjee, 2011), (b)

isothermal MHD fluid and (Banerjee & Galtier, 2013) (c) polytropic neutral fluid (Banerjee & Galtier, 2014). With each derivation, we have tried to understand the corresponding phenomenology and thereby predicting some spectral indices. Interestingly, the justification behind the scaling of density weighted velocity becomes clearer owing to these relations. Although the aspect of anisotropy is beyond the scope of my thesis, a simple anisotropic phenomenology is proposed in compressible MHD turbulence in the presence of a very strong mean or external magnetic field. In case of polytropic turbulence, fluctuations of local sound speed and the algebraic value of polytropic index are predicted to play an important role.

In the chapter 7, a brief but formal introduction of the solar wind is given. The applicability of MHD in case of the large scale fluctuations are also discussed. The following part is dedicated to test our exact relation for compressible MHD turbulence using the THEMIS spacecraft data. After giving a very brief introduction of the THEMIS mission and some of its instruments, a step-by-step description of the data selection process is provided. In case of fast solar wind, incompressible scaling is compared with the compressible scaling whence an attempt to quantify the compressibility in the fast solar wind turbulence is taken. All these studies in case of slow solar wind are kept as future projects in order to compare the role of compressibility between these two types of winds.

Finally, in the chapter 8, the significance of my work is resumed briefly along with some unanswered issues. The chapter ends with a list of propositions of future works both in theory of compressible turbulence and in spacecraft data analysis of the space plasmas.

Compressibility in fluids

Contents

2.1	What is compressibility ?	7
2.2	Measure of compressibility for a fluid in motion . . .	9
2.3	Closure for compressible fluids	11
2.4	Invariants in compressible barotropic fluid	12
	2.4.1 Total energy	12
	2.4.2 Kinetic helicity	14
	2.4.3 Mass and linear momentum	14
2.5	Potential flow	15
2.6	Two dimensional compressible flow	16
2.7	One dimensional model for discontinuous compressible flow: Burgers' equation	16
2.8	Compressibility ratio for a polytropic gas across a normal shock	18
2.9	Baroclinic vector	20

2.1 What is compressibility ?

COMPRESSIBILITY of a matter (solid, liquid or gas) can be described as a measure of **ease** with which its density can be altered either locally or globally. So, in a sense compressibility is inverse to the elasticity of a material. An increase in density (for a given mass) with respect to an initial density corresponds to lower volume with respect to the initial volume and is called *compression* whereas a decrease in density and hence a rise in volume is known as *rarefaction* or *dilatation*.

The solids are highly elastic and very hard to deform. Their compressibility is very low. The liquids are a bit less elastic but the compressibility is very low too. Compressible fluid family is primarily represented by gases. They

are usually very easy to be compressed or rarefied i.e. for a given pressure change a gas will respond the best in comparison with solids and liquids (which are almost indifferent to it). Formally **compressibility** (β) is defined as the **inverse of bulk modulus** i.e. the fractional change in volume for unit change in pressure (for a given temperature T) and is written as

$$\beta = \frac{1}{V} \left(\frac{\partial V}{\partial P} \right)_T. \quad (2.1)$$

It is important to note that the compressibility of a material is a function of instantaneous temperature and pressure (Fine & Millero, 1973). Typically, at 273 K, the compressibility of water is $5.1 \times 10^{-10} \text{ Pa}^{-1}$ in the neighbourhood of zero pressure. Under the same condition, the compressibility of air is about 10^{-5} Pa^{-1} which shows that air is much more compressible than water. The

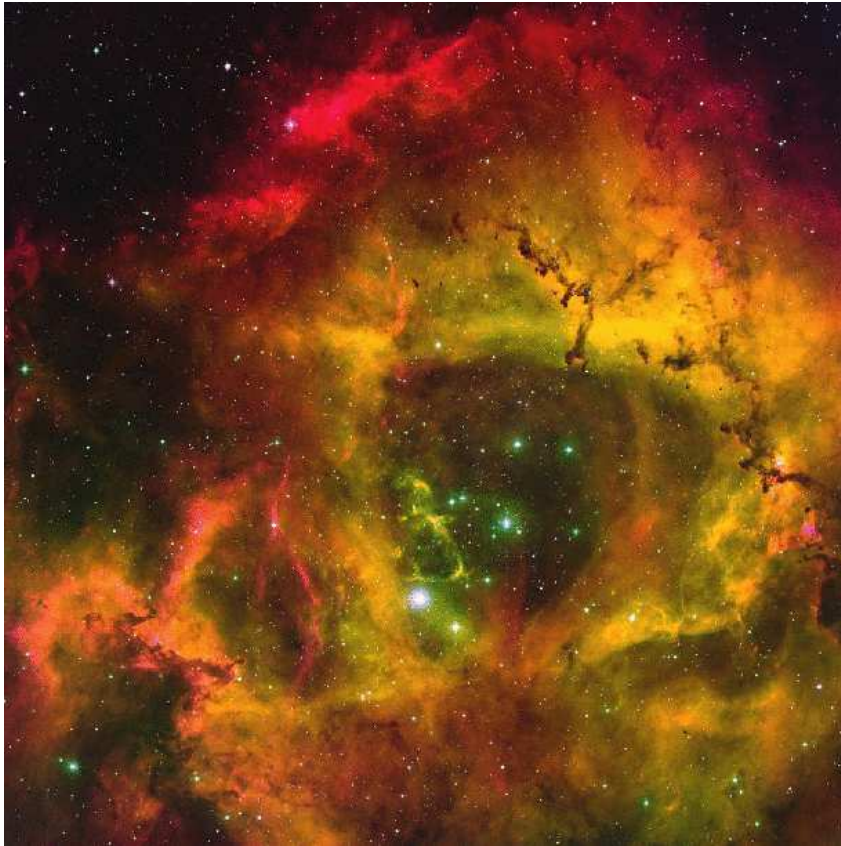


Figure 2.1: Highly compressible dilute diffuse gas in the interstellar space; Credit: University of Leeds.

above discussion, however, is appropriate for a solid or liquid or gas in static condition. If we study a fluid in motion, then we have two points of view for

studying the fluid. The first one is Lagrangian view which consists of studying the flow by following a fluid blob (of given mass) and recording the changes of different dynamical variables in course of time. Compressibility of the fluid here is presented by the variation of density of the given blob with time. In order to use the other one which is Eulerian point of view, a fixed geometric volume in space is considered and the dynamical variables at each space and time point in that volume are studied. In this context compressibility is said to exist if the density functions ($\rho(\mathbf{x}, t)$) have a non-zero temporal or spatial derivative almost everywhere.

2.2 Measure of compressibility for a fluid in motion

Unlike the static case, it is difficult to give a consistent measure of compressibility for a fluid in flow. It is because in the second case the compressibility is no more a pure material property but gets influenced by the corresponding flow dynamics. We thus talk of **compressible flow**. The basic dynamical equations for a neutral (without charge) fluid is given by

$$\frac{\partial \rho}{\partial t} + \nabla \cdot (\rho \mathbf{v}) = 0, \quad (2.2)$$

$$\frac{\partial \mathbf{v}}{\partial t} + (\mathbf{v} \cdot \nabla) \mathbf{v} = -\frac{\nabla P}{\rho} + \mathbf{f} + \nu \Delta \mathbf{v} + \frac{\nu}{3} \nabla (\nabla \cdot \mathbf{v}), \quad (2.3)$$

where $\mathbf{v}(\mathbf{x}, t)$ is the Eulerian fluid velocity, $P(\mathbf{x}, t)$ is the fluid pressure, \mathbf{f} is the body force per unit mass and ν is the kinematic viscosity (which is the ratio of dynamic viscosity to the fluid density). For an incompressible flow, at each point (\mathbf{x}, t) of the flow field, density is constant and the above two equations get reduced to

$$\nabla \cdot \mathbf{v} = 0, \quad (2.4)$$

$$\frac{\partial \mathbf{v}}{\partial t} + (\mathbf{v} \cdot \nabla) \mathbf{v} = -\nabla P + \mathbf{f} + \nu \Delta \mathbf{v}. \quad (2.5)$$

It is however noteworthy that in Eulerian case, the condition (2.4) is an outcome of incompressibility and not necessarily imply incompressibility (one can check immediately) whereas it corresponds directly to Lagrangian incompressibility. Throughout our discussion, we shall consider the **Eulerian point of view**.

Despite its difficulty, it is important to have a measuring parameter to compare the degree of compressibility of different fluid flows so that the effect of

compressibility on different phenomena can be analyzed easily. In the following we try to construct a quantity which can be a consistent measure of compressibility. We assume an ideal (no viscosity) fluid which was initially at rest with uniform initial density ρ_0 and not necessarily uniform initial pressure P_0 . The initial pressure gradient is equal to the body force (which is independent of the flow) thereby producing zero acceleration. Now we assume very small perturbation in density $\rho_1 (\ll \rho_0)$ which causes small perturbations in velocity (which was initially zero) and pressure and are respectively given by \mathbf{v} and P_1 . The non-linearity, consisting of terms which are negligible with one order higher, does not contribute to the modified dynamics and so we are left with

$$\rho_0 \frac{\partial \mathbf{v}}{\partial t} + \nabla P_1 = 0, \quad (2.6)$$

$$\frac{\partial \rho_1}{\partial t} + \rho_0 \nabla \cdot \mathbf{v} = 0. \quad (2.7)$$

Assuming plane wave solution for the perturbations, we obtain simply

$$\omega_f^2 = \left(\frac{P_1}{\rho_1} \right) k^2 = C_S^2 k^2, \quad (2.8)$$

where ω_f and k denote respectively the angular frequency and the wavenumber of the linear mode(s). The above equation shows that one mode is possible and that can easily be identified to acoustic mode (or sound wave) with phase velocity (and group velocity) equal to $C_S = \sqrt{P_1/\rho_1}$. Hence we can conclude that any small perturbation in a compressible ideal fluid can propagate with sound speed. Alternatively speaking, any information of small density fluctuation can be propagated between two points with mutual separation l in a characteristic **compressible time** $\tau_C = l/C_S$. For an incompressible fluid, C_S is infinity and so $\tau_C = 0$. We can hence argue that higher the τ_C , higher is the compressibility of the fluid. Following the same reasoning, we can say that for a given flow with velocity $\mathbf{v}(\mathbf{x}, t)$, a reliable measure of its compressibility can be given by the dimensionless ratio $|\mathbf{v}|/C_S$ which is known as the local Mach number of the flow and is denoted by $\mathcal{M}(\mathbf{x}, t)$. So for small density perturbation, the supersonic flow is more compressible than a subsonic flow and the compressibility is linear with the Mach number according to our present method. This formalism is done for ideal fluid. The insertion of viscosity cannot, however, alter the propagation speed but attenuates the amplitude of the wave.

Another approach for measuring the compressibility is by the method of **Helmholtz decomposition** (Helmholtz, 1867). We learnt previously that incompressible fluid velocity is solenoidal or divergenceless (2.4). Helmholtz

decomposition expresses the fluid velocity vector, in general case, as a vector sum of two components - i) Solenoidal part (\mathbf{v}_S) and ii) Compressible part (\mathbf{v}_C) where by definition, $\nabla \cdot \mathbf{v}_S = 0$ and $\nabla \times \mathbf{v}_C = \mathbf{0}$. A possible measure for compressibility can be given simply by the ratio $|\mathbf{v}_C|/|\mathbf{v}_S|$. By construction, these two components are mutually orthogonal in Fourier space as

$$\mathbf{k} \cdot \hat{\mathbf{v}}_S = 0 ; \quad \mathbf{k} \times \hat{\mathbf{v}}_C = \mathbf{0}. \quad (2.9)$$

This fact enables us to decompose the velocity in longitudinal (parallel to \mathbf{k}) and transverse components ($\hat{\mathbf{v}}_S$ and $\hat{\mathbf{v}}_C$ respectively) in Fourier space.

In the community of turbulence, however, some different quantities are used to quantify the influence of compressibility in a turbulent fluid. The simplest one can just be given as $|\nabla \cdot \mathbf{v}|/|\nabla \times \mathbf{v}|$ which is approximately analogous to the last definition using Helmholtz decomposition. Another measure is obtained from the so-called **small scale compressive ratio** (r_{CS}) (Kida & Orszag, 1990, 1992; Kritsuk *et al.*, 2007a) which is given by

$$r_{CS} = \frac{\langle |\nabla \cdot \mathbf{v}|^2 \rangle}{\langle |\nabla \cdot \mathbf{v}|^2 \rangle + \langle |\nabla \times \mathbf{v}|^2 \rangle}, \quad (2.10)$$

and is believed to reflect the compressible effects in length scales near the viscous length scale in a turbulent fluid. In their paper, Federrath *et al.* (2010) used another slightly different version. In order to quantify the relative importance of compressive motion over rotational motion, they used the ratio $E_C(k)/E_{tot}(k)$ where the numerator and the denominator are defined as

$$\begin{aligned} \int_0^\infty E_C(k) dk &= \frac{1}{2} \int_0^\infty \hat{\mathbf{v}}_C \cdot \hat{\mathbf{v}}_C^* 4\pi k^2 dk, \\ \int_0^\infty E_{tot}(k) dk &= \frac{1}{2} \int_0^\infty \hat{\mathbf{v}} \cdot \hat{\mathbf{v}}^* 4\pi k^2 dk. \end{aligned}$$

A simple measure of compressibility can also be obtained by the quantity $\rho_1/(\rho_0 P_1)$ which reflects the static case but this measure does not take into account the flow velocity and hence does not consider the correlation between the compressibility and the kinetics.

2.3 Closure for compressible fluids

As shown in the previous section, the basic equations for a hydrodynamic fluid consist of the mass continuity equation and the momentum conservation equation which get a simpler form (2.4 and 2.5) for an incompressible fluid.

These two equations (in fact four equations, the second being a vector equation) form a closed system¹. Precisely speaking, we have one vector variable \mathbf{v} and one scalar variable P (of course it is a simplification for an isotropic fluid otherwise P would be a tensor of rank two) - and we have one vector equation and a scalar one. For compressible fluids, density appears to be an additional scalar variable. So we need another scalar type relation in order to close the system. A usual practice is to express the fluid pressure as a function of fluid density. The corresponding fluid or flow-field is known as **barotropic fluid**. A more simplified closure is obtained if we express the fluid pressure proportional to an arbitrary power law of the density i.e.

$$P = K\rho^\gamma.$$

This type of closure is called **polytropic closure**. Depending on the values of γ , we have the following cases. The case $\gamma = 1$ corresponds to **isothermal** case where the proportionality constant K comes to be the square of sound speed of the flow field. $\gamma = c_p/c_v$ is the **adiabatic** closure, where c_p and c_v denote respectively the specific heat of a fluid at constant pressure and in constant volume. For $\gamma = 0$ we get an **isobaric** fluid where the fluid pressure is constant throughout. Incompressible limit can be derived from this polytropic closure if $\gamma \rightarrow \infty$ and can be shown as follows:

$$\partial_t(P\rho^{-\gamma}) = 0 \Rightarrow \partial_t P + \mathbf{v} \cdot \nabla P + \gamma P(\nabla \cdot \mathbf{v}) = 0. \quad (2.11)$$

The limit $\gamma \rightarrow \infty$ leads to the condition $\nabla \cdot \mathbf{v} = 0$ which represents an incompressible flow.

Another possible closure may be the irrotationality of the flow which means $\nabla \times \mathbf{v} = \mathbf{0}$, although this is a vector closure and cannot readily be applied to serve our purpose.

For the flow field where energy transport is important, we have to go further and write the evolution equation for temperature too. Then for closing the system, we have to use some closure relating heat flux, pressure, density etc.

2.4 Invariants in compressible barotropic fluid

2.4.1 Total energy

In general for three dimensional compressible flows whose dynamics is governed by the Navier-Stokes equations, the total energy is a conserved quantity

¹In the present context, the concept of closure is used in a view to having a closed system of algebraic equations obtained after having linearized the fluid equations which themselves cannot be closed so easily due to the non-linearity in the Navier-Stokes equations.

if the viscosity of the fluid is neglected (inviscid case). This fact is an immediate consequence of translational symmetry in time of inviscid Navier-Stokes equations. If the system of equation is closed with a barotropic closure i.e. $P = P(\rho)$ we can show that the total energy density is given as

$$\mathcal{E} = \rho \left[\frac{v^2}{2} - \int Pd \left(\frac{1}{\rho} \right) \right] = \rho \left[\frac{v^2}{2} + \int P \frac{d\rho}{\rho^2} \right].$$

One can easily identify that the above expression consists of two terms - kinetic energy and compressive internal energy. The internal energy per unit mass is formally defined as $e = - \int Pd(1/\rho)$. The total energy conservation is shown below. First we have :

$$\frac{\partial \int \mathcal{E} d\tau}{\partial t} = \int \frac{\partial \mathcal{E}}{\partial t} d\tau = \int \frac{\partial}{\partial t} \left[\rho \frac{v^2}{2} - \rho \int Pd \left(\frac{1}{\rho} \right) \right] d\tau. \quad (2.12)$$

Now we show that (using elementary vector calculus identities)

$$\frac{\partial}{\partial t} \left(\rho \frac{v^2}{2} \right) = \left(\frac{v^2}{2} \frac{\partial \rho}{\partial t} + \rho \mathbf{v} \cdot \frac{\partial \mathbf{v}}{\partial t} \right) = -\nabla \cdot \left(\rho \frac{v^2}{2} \mathbf{v} \right) - \mathbf{v} \cdot \nabla P \quad (2.13)$$

and

$$\begin{aligned} -\frac{\partial}{\partial t} \left(\rho \int Pd \left(\frac{1}{\rho} \right) \right) &= -e \nabla \cdot (\rho \mathbf{v}) + \frac{1}{\rho} \frac{\partial \rho}{\partial t} \frac{\partial}{\partial \left(\frac{1}{\rho} \right)} \left[\int Pd \left(\frac{1}{\rho} \right) \right] \\ &= -e \nabla \cdot (\rho \mathbf{v}) - \frac{P}{\rho} \nabla \cdot (\rho \mathbf{v}) = -e \nabla \cdot (\rho \mathbf{v}) - P (\nabla \cdot \mathbf{v}) - \frac{P}{\rho} \mathbf{v} \cdot \nabla \rho. \end{aligned} \quad (2.14)$$

We note further that

$$\rho \mathbf{v} \cdot \nabla e = -\rho \mathbf{v} \cdot \nabla \left[\int Pd \left(\frac{1}{\rho} \right) \right] = -\rho \mathbf{v} \cdot P \nabla \left(\frac{1}{\rho} \right) = \frac{P}{\rho} \mathbf{v} \cdot \nabla \rho. \quad (2.15)$$

Using (2.13), (2.14) and (2.15), we obtain

$$\frac{\partial \mathcal{E}}{\partial t} = -\nabla \cdot \left(\rho \frac{v^2}{2} \mathbf{v} + \rho e \mathbf{v} + P \mathbf{v} \right) = -\nabla \cdot \mathcal{F}. \quad (2.16)$$

The above equation has the conservative form. The rate of change of total energy density equals to the divergence of flux \mathcal{F} . Using Gauss' divergence theorem and assuming that the normal component of the flux vanishes at the boundary surface of our chosen volume, we can show that the total energy ($\int \mathcal{E} d\tau$) is an inviscid invariant in three dimensional compressible flow.

2.4.2 Kinetic helicity

Kinetic helicity is a pseudo scalar and is defined as $\int H_\omega d\tau$ where $H_\omega = \mathbf{v} \cdot \boldsymbol{\omega}$ and $\boldsymbol{\omega} = \nabla \times \mathbf{v}$ is the vorticity vector. The introduction of kinetic helicity was also thanks to Helmholtz decomposition (Wu *et al.*, 2007) discussed above. The velocity vector as well as the vorticity vector can be decomposed in lateral and transverse components with respect to one another and can be written as

$$v^2 \boldsymbol{\omega} = H_\omega \mathbf{v} + \mathbf{v} \times \boldsymbol{\Lambda}, \quad (2.17)$$

$$\omega^2 \mathbf{v} = H_\omega \boldsymbol{\omega} - \boldsymbol{\omega} \times \boldsymbol{\Lambda}, \quad (2.18)$$

where the longitudinal and transverse components of velocity and vorticity are respectively proportional to the kinetic helicity density H_ω and the vector $\boldsymbol{\Lambda}$ called the Lamb vector. In case of an inviscid barotropic fluid (under possible conservative body force) total kinetic helicity is a conserved quantity thereby describing the frozen vortex lines in the flow and hence a conservation of the number of linkage or knottedness of those lines within them (Thomson, 1869). Here, in the following, we examine the conservation of kinetic helicity of an inviscid barotropic fluid :

$$\frac{\partial H_\omega}{\partial t} = \frac{\partial \mathbf{v}}{\partial t} \cdot \boldsymbol{\omega} + \frac{\partial \boldsymbol{\omega}}{\partial t} \cdot \mathbf{v} \quad (2.19)$$

$$= \left[-(\mathbf{v} \cdot \nabla) \mathbf{v} - \frac{\nabla P(\rho)}{\rho} \right] \cdot \boldsymbol{\omega} + [\nabla \times (\mathbf{v} \times \boldsymbol{\omega})] \cdot \mathbf{v} \quad (2.20)$$

$$= -\nabla \cdot \left(\frac{v^2}{2} \boldsymbol{\omega} \right) - \frac{\nabla P(\rho)}{\rho} \cdot \boldsymbol{\omega} + \nabla \cdot [\mathbf{v} \times (\mathbf{v} \times \boldsymbol{\omega})]. \quad (2.21)$$

In the step (2.20), we have used the fact that for a barotropic fluid, the baroclinic vector ($\nabla P \times \nabla \rho$) is always zero. The expression (2.21) however does not guarantee the conservation of kinetic helicity. Under the condition where the $\nabla P/\rho$ can be written as a pure gradient, (2.21) is reduced to a pure divergence form thereby guaranteeing the conservation of total kinetic helicity under the assumption that either the corresponding flux vector disappears at every point on the flow-field boundary surface or at the boundary surface it is purely tangential to the surface. Fortunately, the usual closures of type polytropic (non-isothermal) ($P = K\rho^\gamma$) or isothermal ($P = C_s^2 \rho$) satisfies the necessary condition for kinetic helicity conservation in a compressible flow.

2.4.3 Mass and linear momentum

The above two conservations are non-trivial and they are not in general available (as they are derived here) in the text-books. For the total mass ($\int \rho d\tau$)

and the total linear momentum ($\int \rho \mathbf{v} d\tau$) conservation, the demonstration is more or less trivial and can immediately be obtained respectively from equations (2.2) and (2.3). Is it noteworthy that these two quantities are conserved even in the presence of finite fluid viscosity. The conservation of linear momentum (as one can expect) is a direct consequence of the absence of any net external force on the system whereas the mass conservation shows that the fluid flows in a closed system which prohibits any mass exchange with the exterior.

2.5 Potential flow

In the above section we have presented the irrotationality ($\nabla \times \mathbf{v} = \mathbf{0}$) as a closure. But the significance of irrotationality is deeper than that and represents a specific class of flow which is known as *potential flow*. The basic reason behind the name resides in the fact that for an irrotational fluid, the flow velocity vector can be expressed as a gradient of a scalar potential ϕ i.e. $\mathbf{v} = -\nabla\phi$ (Zakharov & Sagdeev, 1970). If the fluid is additionally incompressible then the potential satisfies Laplace's equation i.e. $\Delta\phi = 0$. The flow can be determined just by its kinetics (no information on the dynamics i.e. the applied force is required to determine the local velocity field). An important field of application for the potential flow is compressible flows. Remembering the Helmholtz's equation, we can understand that the flow velocity has only its compressible part which means $\mathbf{v} \equiv \mathbf{v}_C$ and $\mathbf{v}_S = \mathbf{0}$ and thus such a fluid is infinitely compressible according to our measure of compressibility using Helmholtz decomposition.

For this type of flow, the kinetic helicity is trivially conserved as it is identically zero ($\boldsymbol{\omega} = \mathbf{0}$) in this case. Interestingly for an irrotational inviscid fluid the baroclinic vector is also identically zero. The fact can easily be verified by taking the curl of (2.3) omitting the viscous and the forcing term. It is thus concluded that a barotropic fluid need not be, in general, irrotational but an irrotational fluid necessarily implies barotropicity when the viscosity is neglected. The total energy is thus always conserved by the virtue of 2.4.1. In the following, we shall search for the conservation of the total fluid dilatation i.e. $\int (\nabla \cdot \mathbf{v}) d\tau$.

Throughout our study, we have searched for flow invariants in the inviscid limit in the absence of any net external forcing. This very procedure, although not general, is appropriate in the framework of our study of completely developed turbulence in the **inertial zone** - a zone which is supposed to be independent of the external forcing and the small scale viscous effects. A detailed discussion on this point will be done later while introducing the fluid

turbulence and its different aspects.

2.6 Two dimensional compressible flow

Discussion over two dimensional flows builds an essential part of fluid dynamics owing to its numerous practical applications. It is however a bit tricky to talk about the two dimensional flows. The number of available spatial coordinates are three but the fluid velocity vector is spanned in two dimensions and any variation in the third dimension is neglected. This type of flow field are thus sometimes called 2.5 dimensional. The velocity field is assumed to be in x-y plane (by choice) and is defined as

$$\mathbf{v} = v_x(x, y)e_x + v_y(x, y)e_y, \quad (2.22)$$

and the gradient operator is defined as

$$\nabla \equiv \frac{\partial}{\partial x}e_x + \frac{\partial}{\partial y}e_y. \quad (2.23)$$

The corresponding vorticity vector (pseudo-vector to be precise) is then defined as

$$\boldsymbol{\omega} = \nabla \times \mathbf{v} = \left(\frac{\partial v_y}{\partial x} - \frac{\partial v_x}{\partial y} \right) e_z = \omega e_z. \quad (2.24)$$

This above construction makes the kinetic helicity density ($\mathbf{v} \cdot \boldsymbol{\omega}$) identically zero ($\mathbf{v} \perp \boldsymbol{\omega}$) everywhere in the flow field. The total kinetic helicity is thus trivially conserved irrespective of the closure of the fluid. An interesting family of invariants has been obtained for two dimensional flow of a barotropic, inviscid fluid by Pedlosky (1987). These invariants are function of a newly defined quantity called **potential vorticity** ($\boldsymbol{\omega}_\rho = \boldsymbol{\omega}/\rho$). Using eqn. (2.2) and taking the curl of the eqn (2.3), we can show that in the inviscid limit, for a three dimensional flow we have

$$\frac{\partial \boldsymbol{\omega}_\rho}{\partial t} + (\mathbf{v} \cdot \nabla) \boldsymbol{\omega}_\rho = (\boldsymbol{\omega}_\rho \cdot \nabla) \mathbf{v}. \quad (2.25)$$

By the above construction, we obtain additionally for a two dimensional flow $(\boldsymbol{\omega}_\rho \cdot \nabla) = 0$, which renders $\boldsymbol{\omega}_\rho$ to be a Lagrangian invariant or material invariant of the flow.

2.7 One dimensional model for discontinuous compressible flow: Burgers' equation

From the above discussion, we can understand that for compressible fluids we cannot derive any separate evolution equation for the velocity field right

2.7. One dimensional model for discontinuous compressible flow: Burgers' equation 17

from the Navier-Stokes equations. However, if we consider a compressible flow in one dimension, there exists a simplistic yet very useful scalar evolution equation for the fluid velocity field - this equation is called **Burgers' equation** after J. M. Burgers who played an essential role in popularizing this equation in the framework of compressible turbulence (Burgers, 1948). The equation is written as

$$\frac{\partial v}{\partial t} + v \frac{\partial v}{\partial x} = \nu \frac{\partial^2 v}{\partial x^2}. \quad (2.26)$$

This equation was known to the mathematicians and physicists well before Burgers. Burgers' equation was implemented, possibly for the first time, to the problem of discontinuities in the viscous fluid flows in the seminal paper by Bateman (1915). The above equation was proposed in a view to obtaining discontinuous solution for the fluid motion in the limit of very weak kinematic viscosity (approaching zero). Unlike Navier-Stokes, this equation neglects the effect of fluid pressure gradient with respect to the advection term. Here we search for a **travelling wave** type solution of the equation (2.26) where the solution can be expressed as

$$v(x, t) = F(x + Vt) = F(X),$$

where $X = x + Vt$ (with V constant). Under this assumption, the equation (2.26) reduces to

$$V \frac{dF}{dX} + F \frac{dF}{dX} = \nu \frac{d^2 F}{dX^2}, \quad (2.27)$$

whence we can derive

$$2\nu \frac{dF}{dX} = (F + V)^2 \pm a^2, \quad (2.28)$$

where a is an arbitrary constant of integration. The final solution can be obtained by integrating (2.28) once more and is given by (taking the +ve sign in equation (2.28))

$$v = a \tan \left[\frac{a}{2\nu} (x + Vt - C) \right] - V, \quad (2.29)$$

with C being the constant of integration or (taking the -ve sign in equation (2.28))

$$\left| \frac{v + V - a}{v + V + a} \right| = e^{\frac{a}{\nu}(x+Vt-C)}. \quad (2.30)$$

For the first type of solution, we do not have any definite value for v when $\nu \rightarrow 0$ whereas in the second case (which can be re-written in using tanh function) we get $v = -(V + a)$ or $v = (V - a)$ according as $a(x + Vt - c) > 0$

or < 0 whence comes the discontinuity in the solution and the notion of one-dimensional Burgers' shock. The shock is developed essentially due to the non-linearity whereas it dissipates in course of time under the influence of fluid viscosity (see figure 2.2).

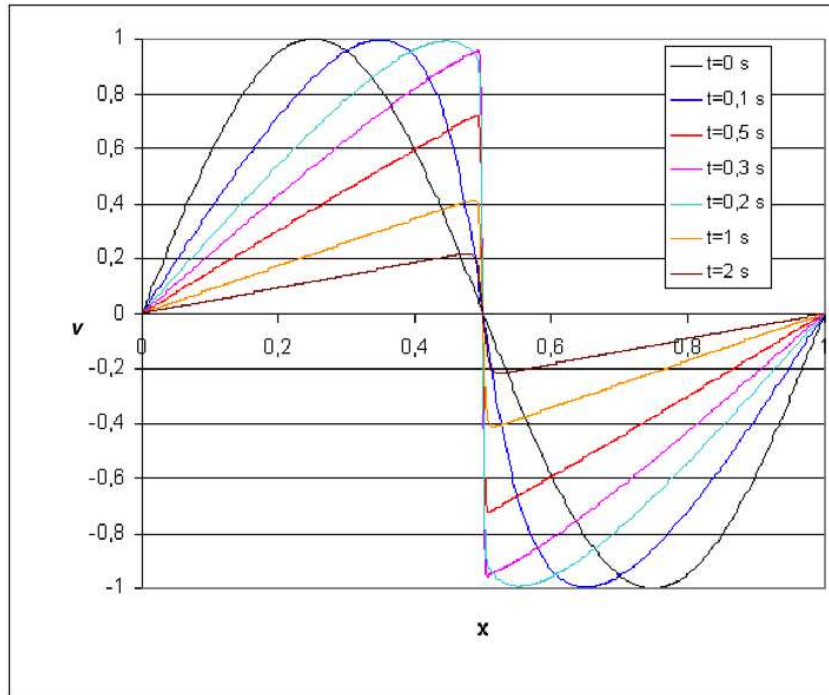


Figure 2.2: Evolution of a Burgers' shock in course of time (t); Credit: Ludovic Maas.

2.8 Compressibility ratio for a polytropic gas across a normal shock

If a normal shock² develops in a compressible polytropic fluid ($P = K\rho^\gamma$), we can derive (Vázquez-Semadeni *et al.*, 1996) an equation across the interface of the shock for the compressibility ratio (the ratio of the densities of the forth and the back of the shock). This study is useful as it describes (as we will see) the role of Mach number and the polytropic index on the compressibility ratio. If the two sections of fluid across the shock are characterized respectively by (ρ_1, v_1, P_1) and (ρ_2, v_2, P_2) , then by the continuity equation and the energy

²A shock wave which is developed in the perpendicular direction to the flow of shock creating fluid medium.

2.8. Compressibility ratio for a polytropic gas across a normal shock

19

conservation equation (Bernoulli principle), we can have

$$\rho_1 v_1 = \rho_2 v_2, \quad (2.31)$$

$$\rho_1 v_1^2 + P_1 = \rho_2 v_2^2 + P_2, \quad (2.32)$$

where v_1 and v_2 are respectively the normal components of fluid velocity across the shock interface. Eliminating v_2 in (2.31) and (2.32), we obtain

$$v_1^2 + K \rho_1^{\gamma-1} = \frac{\rho_1}{\rho_2} v_1^2 + K \left(\frac{\rho_2}{\rho_1} \right) \rho_2^{\gamma-1} \quad (2.33)$$

$$\Rightarrow v_1^2 \left(1 - \frac{\rho_1}{\rho_2} \right) = K \rho_1^{\gamma-1} \left[\left(\frac{\rho_2}{\rho_1} \right)^\gamma - 1 \right], \quad (2.34)$$

denoting the compressibility ratio as $\chi (\equiv \rho_2/\rho_1)$ and using the fact that the sound speed is given by $C_S^2 = \gamma K \rho_1^{\gamma-1}$, we can show that χ satisfies the following equation

$$\chi^{\gamma+1} - (1 + \gamma M_1^2) \chi + \gamma M_1^2 = 0, \quad (2.35)$$

where $M_1 = v_1^2/C_S^2$ is defined as the **upstream Mach number**. From the above equation, it is easy to verify that when $\gamma \rightarrow 1$, $\chi \rightarrow M_1^2$. So for a nearly isothermal fluid, the compressibility ratio across a normal shock can be estimated by the square of its upstream Mach number. When $\gamma \ll 1$ but $\gamma \neq 0$, then according to *Vázquez-Semadeni et al. (1996)*, $\chi \sim e^{M^2}$. Unfortunately this limit is not evident to verify and it is thought that their conclusion is suffering from calculation problem. One can simply understand this problem just by taking different very small values of γ and by checking whether χ is of the order of e^{M^2} . In fact, a very small value of γ corresponds to a near isobaric case which in turn would weaken any discontinuity of pressure and thus density in the fluid i.e. across a shock (even if it develops) the compressibility ratio comes to be nearly unity (being independent of upstream Mach number) and this fact is immediate to verify from (2.35). One can do a similar elimination of v_1 in the conditions of continuity and is left with

$$\gamma M_2^2 \chi^{\gamma+1} - (1 + \gamma M_2^2) \chi^\gamma + 1 = 0, \quad (2.36)$$

where M_2 is the downstream Mach number. In the isothermal limit, we obtain that $\chi \rightarrow 1/M_2^2$. So the compressibility ratio becomes inversely proportional to the square of downstream Mach number which is not difficult to imagine. The compressibility ratio, here also, tends to unity for very small value of polytropic index.

2.9 Baroclinic vector

In course of our investigation for different properties and invariants of compressible flow, several times we came across the **baroclinic vector** (a pseudo-vector in fact) which is defined as $\mathcal{B} = (\nabla P \times \nabla \rho) / \rho^2$. For barotropic flow this vector is zero. It is however interesting to discuss the role of this vector. Without considering barotropy, we can show that

$$\frac{\partial \boldsymbol{\omega}}{\partial t} = \frac{\nabla P \times \nabla \rho}{\rho^2} + \nabla \times (\mathbf{v} \times \boldsymbol{\omega}). \quad (2.37)$$

This equation reveals that the baroclinic term can act as a vorticity generator. This term was believed to be active behind curved shocks or at their collisions after (Passot & Pouquet, 1987; Fleck, 1991; Klein & McKee, 1994). Vázquez-Semadeni *et al.* (1996) numerically tested the effect of this term and concluded that actually the baroclinic term is dominated by the stretching term (the curl) in the above equation and thus affects the vortex generation rate very slightly. However, baroclinic vector can be important if there is a thermal heating in the flow field.

Plasma physics and magnetohydrodynamics

Contents

3.1	What is a plasma ?	21
3.2	Two approaches to plasma	23
3.2.1	Kinetic approach	23
3.2.2	Fluid approach	25
3.3	Magnetohydrodynamics (MHD)	26
3.3.1	Mono-fluid model: Basic equations of MHD	27
3.3.2	Ideal MHD approximation from generalized Ohm's law	29
3.3.3	Linear waves in ideal MHD	31
3.3.4	Invariants of ideal MHD	33
3.3.5	Elsässer variables in magnetohydrodynamics	38

3.1 What is a plasma ?

PLASMA is popularly known to be the fourth fundamental state of ordinary matter. It is the only ionized state of matter whereas the other three states i.e. the solid, liquid and gas correspond to neutral state. Interestingly this 4th state constitutes 99.9% of the visible (or ordinary) matter of our universe. Starting from the laboratory low pressure discharges, plasmas can be seen in fusion reactors, atmospherical fluids, stellar cores, stellar winds and even in the cold interstellar clouds (see figure 3.1). Although the word plasma is loosely used to indicate any ionized gas or suspension in common parlance, in physics we define a plasma in a more systematic way. Formally speaking a plasma is an ionized continuous medium which contains charged (positive ions, negative ions, electrons) and neutral (atoms) species, and is macroscopically quasi-neutral i.e. beyond a specified spatial and temporal

scale, a plasma is almost chargeless. The corresponding spatial scale is known as Debye scale (λ_D) within which charge neutrality is not required and the corresponding time scale is defined by $\tau_P = 2\pi/\omega_P$ where ω_P is known as the plasma frequency. τ_P can more clearly be defined as the time required for a

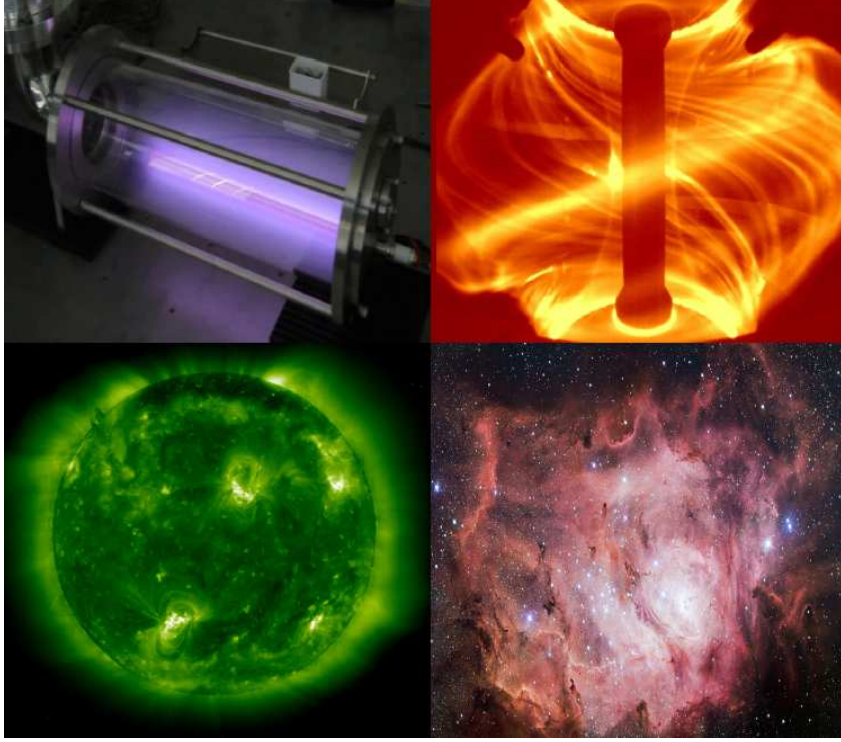


Figure 3.1: Different types of plasmas: argon glow discharge (left above), fusion plasma (right above), uv image of solar corona (left below) and highly dense Lagoon nebula (right below).

plasma to re-establish its original state if one of its dynamical variables (density, fluid velocity, pressure etc.) undergoes a small (first-order) perturbation. (λ_D) and ω_P are fundamental parameters of each type of charged species in a plasma. For clarity, we indicate the ionic Debye length and the corresponding plasma frequency as λ_{Di} and ω_{Pi} respectively. For the electrons, the respective parameters are λ_{De} and ω_{Pe} . In terms of the known quantities they are expressed as

Parameter	λ_{Di}	λ_{De}	ω_{Pi}	ω_{Pe}
Expression	$\sqrt{\frac{\epsilon_0 k_B T_i}{n_i Z^2 e^2}}$	$\sqrt{\frac{\epsilon_0 k_B T_e}{n_e e^2}}$	$\sqrt{\frac{n_i Z^2 e^2}{m_i \epsilon_0}}$	$\sqrt{\frac{n_e e^2}{m_e \epsilon_0}}$

where n_i and n_e denote respectively ionic and electronic number density, e is the electronic charge, Z is the ionic valency, T_i and T_e are respectively

the ionic and electronic temperatures, m_i and m_e being respectively the ionic and electronic masses and finally ε_0 is the free space permittivity. From these aforesaid definitions one can easily realize that (considering $Z = 1$) for a plasma

$$\frac{\lambda_{Di}}{\lambda_{De}} \approx \sqrt{\frac{T_i}{T_e}}, \quad \frac{\omega_{Pi}}{\omega_{Pe}} \approx \sqrt{\frac{m_e}{m_i}}, \quad (3.1)$$

where quasi-neutrality is assumed. In laboratory plasmas, electrons are in general more energetic than the ions and so usually $T_e > T_i$ which implies $\lambda_{Di} < \lambda_{De}$. On the other hand for fusion plasmas or space plasmas, these two temperatures are nearly equal thereby giving the same Debye length both for the ions and electrons. On the other hand, since $m_e \ll m_i$, we find $\omega_{Pe} > \omega_{Pi}$ for any kind of plasma.

3.2 Two approaches to plasma

A plasma can be treated microscopically or macroscopically according to the interest. The microscopical approach is known as the kinetic approach whereas the macroscopic treatment is called the fluid approach.

3.2.1 Kinetic approach

A plasma is a system of mutually interacting charged particles (ions, electrons) which sometimes can contain considerable number of neutral atoms too. A kinetic theory for plasma consists in analyzing different properties of the plasma by the help of the individual probability distribution functions (PDF) of each particle species in phase space. This approach takes into account the collective behaviour of the particles as well as their individual behaviour. We thus need to know the nature of the microscopic interaction forces along with external macroscopic forces in order to construct a kinetic description of a plasma phenomenon. In the current context, a brief and schematic presentation of kinetic approach to plasma will be presented without entering into formal and detailed derivations.

Basic equations

If the distribution function of i^{th} species of a plasma at a given point $\mathbf{X} \equiv (\mathbf{x}, \mathbf{V}, t)$ is given by $f_i(\mathbf{x}, \mathbf{V}, t)$, then for a collisional plasma, the governing kinetic equation for the corresponding species is given by Boltzmann equation (Rax, 2005):

$$\frac{\partial f_i}{\partial t} + \mathbf{V} \cdot \nabla f_i + \mathbf{a} \cdot \nabla_{\mathbf{V}} f_i = \left(\frac{\delta f_i}{\delta t} \right)_{collision}, \quad (3.2)$$

where \mathbf{a} denotes the acceleration and the right hand side term represents the change in $f_i(\mathbf{x}, \mathbf{V}, t)$ with respect to time due to collisional forces i.e. short range interaction terms. Of course we do not exactly know the nature of the collision term which is, in turn, approximated either by simplistic relaxation model or by more rigorous Boltzmann collision integral and Fokker-Planck collision term (Bittencourt, 2003).

In case where we neglect intra-particle short range collisional effects but we wish to take the long range interactions (Coulomb or electro-magnetic interaction for example) between the charged particles into account, the right-hand term vanishes and the acceleration is expressed as

$$m_i \mathbf{a} = \mathbf{F}_{ext} + q_i (\mathbf{E}_{int} + \mathbf{V} \times \mathbf{b}_{int}), \quad (3.3)$$

where F_{ext} includes all types of external force including Lorentz force associated to some external electric and magnetic field. \mathbf{E}_{int} and \mathbf{b}_{int} , on the other hand, present respectively resultant electric and magnetic field due to all the moving charges inside the plasma. Under that condition, the plasma dynamics can be described by

$$\boxed{\frac{\partial f_i}{\partial t} + \mathbf{V} \cdot \nabla f_i + \frac{1}{m_i} [\mathbf{F}_{ext} + q_i (\mathbf{E}_{int} + \mathbf{V} \times \mathbf{b}_{int})] \cdot \nabla_{\mathbf{V}} f_i = 0,} \quad (3.4)$$

which is popularly known as collisionless Boltzmann equation or Vlasov equation.

Macroscopic quantities

Macroscopic variables corresponding to each species i can be derived as the moments of different kinetic variables under their PDF f_i according to the following definitions:

$$density \equiv n_i(\mathbf{x}, t) = \int_{\mathbf{V}} f_i(\mathbf{x}, \mathbf{V}, t) d\mathbf{V}, \quad (3.5)$$

$$velocity \equiv \mathbf{v}_i(\mathbf{x}, t) = \frac{1}{n_i} \int_{\mathbf{V}} \mathbf{V} f_i(\mathbf{x}, \mathbf{V}, t) d\mathbf{V}, \quad (3.6)$$

$$pressure \equiv \mathcal{P}_i(\mathbf{x}, t) = m_i \int_{\mathbf{V}} (\mathbf{v}_i - \mathbf{V}) \otimes (\mathbf{v}_i - \mathbf{V}) f_i(\mathbf{x}, \mathbf{V}, t) d\mathbf{V}. \quad (3.7)$$

It is noteworthy that the internal fields of Vlasov equation i.e. \mathbf{E}_{int} and \mathbf{b}_{int} must be self-consistent i.e. they should satisfy Maxwell equations where the charge density ρ_c and the current density \mathbf{J} should be deducible from the sum of the moments of the PDFs of individual species according to the following

definitions:

$$\rho_c = \sum_i q_i \int_{\mathbf{V}} f_i(\mathbf{x}, \mathbf{V}, t) d\mathbf{V}, \quad (3.8)$$

$$\mathbf{J} = \sum_i q_i \int_{\mathbf{V}} \mathbf{V} f_i(\mathbf{x}, \mathbf{V}, t) d\mathbf{V}, \quad (3.9)$$

where q_i is the particular charge of i^{th} species in plasma.

3.2.2 Fluid approach

In this approach, the plasma dynamics is described only in terms of the macroscopic variables (which themselves are derived from the kinetic approach) and not by the microscopic details. The fluid description of a plasma is not always suitable for explaining a plasma phenomenon. It can only be relevant if a perfect or a near thermodynamic equilibrium can be ascertained for the individual population of each species. The fluid equations can be derived as different moments of Boltzmann's equations in the velocity space. The zeroth order moment (corresponding to i^{th} species) is given by

$$\int_{\mathbf{V}} \left(\frac{\partial f_i}{\partial t} + \mathbf{V} \cdot \nabla f_i + \frac{1}{m_i} [q_i (\mathbf{E} + \mathbf{V} \times \mathbf{b})] \cdot \nabla_{\mathbf{V}} f_i \right) d\mathbf{V} = \int \left(\frac{\delta f_i}{\delta t} \right)_c d\mathbf{V}, \quad (3.10)$$

where \mathbf{E} and \mathbf{b} correspond to the total electric and magnetic fields. Noting that \mathbf{x} , \mathbf{V} , t are mutually independent variables, we can show by definition (3.6)

$$\int \mathbf{V} \cdot \nabla f_i d\mathbf{V} = \nabla \cdot (n_i \mathbf{V}_i) \quad \text{and} \quad (3.11)$$

$$\int (\mathbf{E} + \mathbf{V} \times \mathbf{b}) \cdot \nabla_{\mathbf{V}} f_i d\mathbf{V} = \int \nabla_{\mathbf{V}} \cdot [(\mathbf{E} + \mathbf{V} \times \mathbf{b}) f_i] d\mathbf{V} = \mathbf{0}. \quad (3.12)$$

In deriving the second expression, we use the fact that \mathbf{E} and \mathbf{b} do not have any explicit \mathbf{V} dependence and also we use Gauss-Ostrogradsky theorem assuming the distribution function will vanish at infinity. Using the above two expressions and multiplying both sides of (3.10) by m_i (mass of i^{th} species), we get

$$\boxed{\frac{\partial \rho_i}{\partial t} + \nabla \cdot (\rho_i \mathbf{v}_i) = S_i}, \quad (3.13)$$

which gives us a continuity equation for the i^{th} species, $S_i = \int m_i \left(\frac{\delta f_i}{\delta t} \right)_c d\mathbf{V} = \delta \rho_i / \delta t$ being the source term for the respective species due to collisions. In

the same manner, integrating the first order moment of Boltzmann's equation in velocity space i.e.

$$\int_{\mathbf{V}} \mathbf{V} \left(\frac{\partial f_i}{\partial t} + \mathbf{V} \cdot \nabla f_i + \frac{1}{m_i} [q_i (\mathbf{E} + \mathbf{V} \times \mathbf{b})] \cdot \nabla_{\mathbf{V}} f_i \right) d\mathbf{V} = \int_{\mathbf{V}} \mathbf{V} \left(\frac{\delta f_i}{\delta t} \right) d\mathbf{V}, \quad (3.14)$$

and following some straightforward algebra (see [Bittencourt \(2003\)](#) book page 200), we finally obtain (again by multiplying both sides by m_i)

$$\rho_i \left[\frac{\partial \mathbf{v}_i}{\partial t} + (\mathbf{v}_i \cdot \nabla) \mathbf{v}_i \right] = -\nabla \cdot \mathcal{P}_i + \rho_i \mathbf{f}_i + \mathbf{A}_i - \mathbf{v}_i S_i, \quad (3.15)$$

where \mathbf{f} denotes the external force term, \mathbf{A}_α accounts for the momentum transport due to collision and \mathcal{P} represents the pressure tensor.

As one can remark that the evolution equation for the zeroth order moment ρ is coupled with the first order moment \mathbf{v} and that of the first order moment is coupled with the second order moment \mathcal{P} . This is also true (one can verify) for higher order moments. It is thus necessary to close the system by some additional closure information. For simplicity, where we can assume an almost thermodynamic equilibrium, the required closure may be obtained just by assuming an algebraic relation between the density and the scalar fluid pressure P . Further simplification is achieved by using an isothermal closure i.e. $P = C_s^2 \rho$, C_s being the constant sound speed where a very quick heat transfer is assumed. A more general polytropic closure i.e. $P = K \rho^\gamma$, K being a constant, is however used very often for astrophysical plasma. In case of important convection, we cannot, however, restrict ourselves to the evolution equation of the first order moment and then we have to solve the evolution equation for P which associates the heat flux tensor which is the third order moment.

3.3 Magnetohydrodynamics (MHD)

As discussed above, the fluid approach gives a much simpler method for describing a plasma compared with rigorous kinetic approach. Multi-fluid models are appropriate where (i) the departure from thermodynamic equilibrium is very weak but, (ii) the departure from quasi-neutrality is not necessarily weak (in case of sheath for example). In case of a bi-species plasma (ions and electrons) where the quasi-neutrality is perturbed very weakly, the ionic and the electronic fluids are strongly coupled by the ambipolar electric field and the electronic charge density evolves according to the ionic charge density. The plasma dynamics can, in that case, be described by a single fluid whose inertia is governed by the massive ions and mobility by the lighter electrons.

This fluid, being quasi-neutral, is almost free of any net electrostatic force and is therefore called a hydromagnetic (old nomenclature) or a magnetohydrodynamic (MHD) fluid.

3.3.1 Mono-fluid model: Basic equations of MHD

Here we shall carry out a general derivation of mono-fluid equations by summing the equations of a multi-fluid plasma over all the species of the plasma (denoted by index α). For that we have to define some new quantities. The mass density of the resulting single fluid is given by

$$\rho = \sum_{\alpha} n_{\alpha} m_{\alpha}, \quad (3.16)$$

and the respective charge density is defined as

$$\rho_c = \sum_{\alpha} n_{\alpha} q_{\alpha}, \quad (3.17)$$

Again, the mean fluid velocity is defined as the density weighted average of the fluid velocities of each species and is expressed as

$$\mathbf{v} = \frac{\sum_{\alpha} n_{\alpha} m_{\alpha} \mathbf{v}_{\alpha}}{\sum_{\alpha} n_{\alpha} m_{\alpha}}, \quad (3.18)$$

The relative velocity of each species-fluid with respect to the resultant fluid is called the diffusion velocity of the corresponding species and is given by

$$\mathbf{w}_{\alpha} = \mathbf{v}_{\alpha} - \mathbf{v}, \quad (3.19)$$

The resultant current density for the single fluid will be expressed as

$$\mathbf{J} = \sum_{\alpha} n_{\alpha} q_{\alpha} \mathbf{v}_{\alpha}. \quad (3.20)$$

For individual fluids corresponding to each species α , the continuity equation and the momentum evolution equation are respectively written as

$$\frac{\partial \rho_{\alpha}}{\partial t} + \nabla \cdot (\rho_{\alpha} \mathbf{v}_{\alpha}) = S_{\alpha}, \quad (3.21)$$

$$\rho_{\alpha} \left[\frac{\partial \mathbf{v}_{\alpha}}{\partial t} + (\mathbf{v}_{\alpha} \cdot \nabla) \mathbf{v}_{\alpha} \right] = \rho_{\alpha} (\mathbf{E} + \mathbf{v}_{\alpha} \times \mathbf{b}) + \rho_{\alpha} \mathbf{f} - \nabla \cdot \mathcal{P}_{\alpha} + \mathbf{A}_{\alpha} - \mathbf{v}_{\alpha} S_{\alpha}. \quad (3.22)$$

The continuity equation for the mono-fluid is then given by

$$\sum_{\alpha} \frac{\partial \rho_{\alpha}}{\partial t} + \sum_{\alpha} \nabla \cdot (\rho_{\alpha} \mathbf{v}_{\alpha}) = \sum_{\alpha} S_{\alpha}, \quad (3.23)$$

$$\frac{\partial \sum_{\alpha} \rho_{\alpha}}{\partial t} + \nabla \cdot \left(\sum_{\alpha} \rho_{\alpha} \mathbf{v}_{\alpha} \right) = \sum_{\alpha} S_{\alpha}. \quad (3.24)$$

Using the definitions of the single fluid variables given above, we obtain

$$\boxed{\frac{\partial \rho}{\partial t} + \nabla \cdot (\rho \mathbf{v}) = 0}, \quad (3.25)$$

where the total source term contribution is made to be zero as we consider a closed system whose total mass is conserved.

In order to obtain the equation of motion for the resultant fluid, we add up also the individual equation of motions and we are left with

$$\begin{aligned} \sum_{\alpha} \rho_{\alpha} \left[\frac{\partial \mathbf{v}_{\alpha}}{\partial t} + (\mathbf{v}_{\alpha} \cdot \nabla) \mathbf{v}_{\alpha} \right] &= \sum_{\alpha} \rho_{c\alpha} (\mathbf{E} + \mathbf{v}_{\alpha} \times \mathbf{b}) + \\ &\sum_{\alpha} \rho_{\alpha} \mathbf{f} - \sum_{\alpha} \nabla \cdot \mathcal{P}_{\alpha} + \sum_{\alpha} \mathbf{A}_{\alpha} - \sum_{\alpha} \mathbf{v}_{\alpha} S_{\alpha}. \end{aligned} \quad (3.26)$$

Now the collision term $\sum_{\alpha} \mathbf{A}_{\alpha}$ should vanish as it gives the total internal force which is zero under mutual action-reactions. Using the single fluid variables, the above equation can be expressed as

$$\begin{aligned} \sum_{\alpha} \rho_{\alpha} \left[\frac{\partial \mathbf{v}_{\alpha}}{\partial t} + (\mathbf{v}_{\alpha} \cdot \nabla) \mathbf{v}_{\alpha} \right] &= \rho_c (\mathbf{E} + \mathbf{J} \times \mathbf{b}) + \\ \rho \mathbf{g} - \nabla \cdot \mathcal{P} + \sum_{\alpha} \nabla \cdot (\rho_{\alpha} \mathbf{w}_{\alpha} \otimes \mathbf{w}_{\alpha}) &- \sum_{\alpha} \mathbf{v}_{\alpha} S_{\alpha}. \end{aligned} \quad (3.27)$$

As we know by the equation of continuity,

$$\sum_{\alpha} \mathbf{v}_{\alpha} S_{\alpha} = \sum_{\alpha} \mathbf{v}_{\alpha} \left[\frac{\partial \rho_{\alpha}}{\partial t} + \nabla \cdot (\rho_{\alpha} \mathbf{v}_{\alpha}) \right], \quad (3.28)$$

we can show that

$$\sum_{\alpha} \rho_{\alpha} \left[\frac{\partial \mathbf{v}_{\alpha}}{\partial t} + (\mathbf{v}_{\alpha} \cdot \nabla) \mathbf{v}_{\alpha} \right] + \sum_{\alpha} \mathbf{v}_{\alpha} S_{\alpha} = \sum_{\alpha} \left[\frac{\partial \rho_{\alpha} \mathbf{v}_{\alpha}}{\partial t} + \nabla \cdot (\rho_{\alpha} \mathbf{v}_{\alpha} \otimes \mathbf{v}_{\alpha}) \right]. \quad (3.29)$$

Again we note $\sum_{\alpha} \rho_{\alpha} \mathbf{w}_{\alpha} = \mathbf{0}$ by definition. Using this and replacing \mathbf{v}_{α} by $\mathbf{v} + \mathbf{w}_{\alpha}$ in the right hand side expression of equation (3.29), we obtain

$$\begin{aligned} & \sum_{\alpha} \left[\frac{\partial \rho_{\alpha} \mathbf{v}_{\alpha}}{\partial t} + \nabla \cdot (\rho_{\alpha} \mathbf{v}_{\alpha} \otimes \mathbf{v}_{\alpha}) \right] \\ &= \frac{\partial \rho \mathbf{v}}{\partial t} + \nabla \cdot (\rho \mathbf{v} \otimes \mathbf{v}) + \sum_{\alpha} \nabla \cdot (\rho_{\alpha} \mathbf{w}_{\alpha} \otimes \mathbf{w}_{\alpha}) \\ &= \rho \left[\frac{\partial \mathbf{v}}{\partial t} + (\mathbf{v} \cdot \nabla) \mathbf{v} \right] + \sum_{\alpha} \nabla \cdot (\rho_{\alpha} \mathbf{w}_{\alpha} \otimes \mathbf{w}_{\alpha}), \end{aligned} \quad (3.30)$$

where we use eqn. (3.25) in deriving the final step. Using the above derived relation in (3.27), finally we are left with

$$\rho \left[\frac{\partial \mathbf{v}}{\partial t} + (\mathbf{v} \cdot \nabla) \mathbf{v} \right] = \rho_c \mathbf{E} + \mathbf{J} \times \mathbf{b} + \rho \mathbf{f} - \nabla \cdot \mathcal{P}. \quad (3.31)$$

In the framework of a plasma mono-fluid, the Coulomb force is negligible with respect to the magnetic Lorentz force due to quasi-neutrality. Under this approximation the above relation reduces for an MHD fluid to

$$\rho \left[\frac{\partial \mathbf{v}}{\partial t} + (\mathbf{v} \cdot \nabla) \mathbf{v} \right] = \mathbf{J} \times \mathbf{b} + \rho \mathbf{f} - \nabla \cdot \mathcal{P}. \quad (3.32)$$

Decomposing the kinetic pressure dyad tensor \mathcal{P} in its principal pressure part and deviatoric parts, we finally write

$$\boxed{\rho \left[\frac{\partial \mathbf{v}}{\partial t} + (\mathbf{v} \cdot \nabla) \mathbf{v} \right] = \mathbf{J} \times \mathbf{b} + \rho \mathbf{f} - \nabla P + \mu \Delta \mathbf{v} + \frac{\mu}{3} \nabla (\nabla \cdot \mathbf{v})}, \quad (3.33)$$

where μ is the dynamic viscosity. For the sake of simplicity, we assume the case of plasmas which are sufficiently collisional in order to close the system by a simple thermodynamic closure like a barotropic one [$P = P(\rho)$] or more specifically an isothermal or polytropic closure (simple barotropes). The equation for the evolution of magnetic field for the resultant fluid is given by Faraday's law:

$$\boxed{\frac{\partial \mathbf{b}}{\partial t} = -\nabla \times \mathbf{E}}. \quad (3.34)$$

3.3.2 Ideal MHD approximation from generalized Ohm's law

In order to close the system of MHD equations, we need to express the electric field in terms of the other fluid variables (\mathbf{v} , \mathbf{b} , P , ρ). It is the Ohm's law by

which we get the required information. The generalized form of Ohm's law can be derived following the same formalism as that we used in order to obtain the equivalent Navier-Stokes equation for the resultant mono-fluid in the previous section - the mass density being replaced by the charge density (for detailed derivation, see [Bittencourt \(2003\)](#)). Depending on the form of Ohm's law used, several types of MHD models can be obtained. The generalized form of non-relativistic Ohm's law is written as ([Boyd & Sanderson, 2003](#))

$$\mathbf{E} + \mathbf{v} \times \mathbf{b} - \frac{\mathbf{j}}{\sigma} - \frac{1}{\sigma\nu_C} \frac{\partial \mathbf{j}}{\partial t} = \frac{m_i}{Ze\rho} (\mathbf{j} \times \mathbf{b} - \nabla P_e), \quad (3.35)$$

where σ denotes the coefficient of conductivity, ν_C is the electron collision frequency, m_i and Ze are respectively the ionic mass and charge. \mathbf{j} represents the current density and ∇P_e denotes the electronic pressure gradient.

In the MHD approximation, \mathbf{j} is supposed to vary on hydrodynamic time scale τ_H . By virtue of Bogoliubov hierarchy we can say $\tau_H\nu_C \gg 1$. Hence we have

$$\left| \frac{\mathbf{j}}{\sigma} \right| \left| \frac{1}{\sigma\nu_C} \frac{\partial \mathbf{j}}{\partial t} \right| \gg 1. \quad (3.36)$$

Again the term $m_i\nabla P_e/Ze\rho$ can be neglected with respect to the term $(\mathbf{v} \times \mathbf{b})$ considering the ionic Larmor radius to be very small in comparison with the characteristic fluctuation length scale (for detailed justification see [Boyd & Sanderson \(2003\)](#)). The generalized Ohm's law then gets reduced to

$$\mathbf{E} + \mathbf{v} \times \mathbf{b} - \frac{\mathbf{j}}{\sigma} = \frac{m_i}{Ze\rho} (\mathbf{j} \times \mathbf{b}). \quad (3.37)$$

The right hand side term is the Hall term and the corresponding MHD is called Hall MHD. Now comparing the Lorenz force term to the Hall term, we get

$$\left| \frac{m_i}{Ze\rho} (\mathbf{j} \times \mathbf{b}) \right| \left| (\mathbf{v} \times \mathbf{b}) \right| \sim \frac{bm_i}{\mu_0 e \rho l v} \sim \frac{d_i v_A}{lv}, \quad (3.38)$$

where d_i is the ion inertial length and is defined as

$$d_i \equiv \frac{c}{\omega_{Pi}},$$

where c is the speed of light in vacuum. The above estimate shows that the Hall term becomes relevant if the ratio $d_i v_A/lv$ is at least of the order of unity. In case where $v \sim v_A$ (case of solar wind), Hall effect is perceived if the characteristic length scale l is at least of the order of d_i ([Galtier \(2013\)](#), page 39). In case of solar wind, $d_i \sim 10^2 km$ and thus the Hall effect cannot be effective for the length scales comparable to astronomical unit (1 A.U. = 1.5×10^8 km).

Without the Hall term, Ohm's law takes the following form

$$\mathbf{E} + \mathbf{v} \times \mathbf{b} = \frac{\mathbf{j}}{\sigma}, \quad (3.39)$$

and corresponds to resistive MHD. In the limit where we neglect the resistivity of an MHD fluid, we have $\sigma \rightarrow \infty$ and we are thus left with

$$\mathbf{E} + \mathbf{v} \times \mathbf{b} = \mathbf{0}. \quad (3.40)$$

This equation is called idealized Ohm's law. Substituting the above expression in the equation (3.34), finally we get

$$\boxed{\frac{\partial \mathbf{b}}{\partial t} = \nabla \times (\mathbf{v} \times \mathbf{b})}. \quad (3.41)$$

Equations (3.25), (3.33) and (3.41) constitute the complete set of **ideal MHD equations**.

3.3.3 Linear waves in ideal MHD

It is crucial to examine the existence of waves in an ideal MHD fluid for understanding the corresponding dynamics and the nature of response created by the fluid to any external attempt of perturbation with respect to a steady state flow. Of the waves, the linear modes are the simplest to obtain. These are the eigen modes corresponding to a very small or first order perturbation in an ideal MHD fluid. In order to obtain the linear waves, we have to linearize the ideal MHD equations. Under the assumption of a polytropic closure and zero steady state velocity (which can be obtained without losing generality just by a suitable Galilean transformation), these equations are written as (following the same formalism as that of 2.2):

$$\omega P_1 = \rho_0 C_s^2 \mathbf{k} \cdot \mathbf{v}_1, \quad (3.42)$$

$$\omega \mathbf{v}_1 = \mathbf{k} \left(\frac{P_1}{\rho_0} + \frac{\mathbf{b}_0 \cdot \mathbf{b}_1}{\mu_0 \rho_0} \right) - \frac{b_0}{\mu_0 \rho_0} k_{\parallel} \mathbf{b}_1, \quad (3.43)$$

$$\omega \mathbf{b}_1 = -b_0 k_{\parallel} \mathbf{v}_1 + \mathbf{b}_0 (\mathbf{k} \cdot \mathbf{v}_1), \quad (3.44)$$

where the terms with subscript 0 denotes the equilibrium quantities and those with subscript 1 correspond to the linear perturbations. $C_s = \sqrt{\gamma P_0 / \rho_0}$ represents the equilibrium sound speed and k_{\parallel} and k_{\perp} denote respectively the parallel and the perpendicular components of the wave propagation vector along and perpendicular to the equilibrium field b_0 . Combining the above

three algebraic relations, we obtain finally the following relation (for simplicity, we assume $\mu_0 = \rho_0 = 1$)

$$\left[\omega^2 - (\mathbf{k} \cdot \mathbf{b}_0)^2\right] \mathbf{v}_1 = [(C_s^2 + b_0^2)(\mathbf{k} \cdot \mathbf{v}_1) - (\mathbf{k} \cdot \mathbf{b}_0)(\mathbf{v}_1 \cdot \mathbf{b}_0)] \mathbf{k} - (\mathbf{k} \cdot \mathbf{b}_0)(\mathbf{k} \cdot \mathbf{v}_1) \mathbf{b}_0. \quad (3.45)$$

Without losing generality, now if we choose $\mathbf{k} = k_\perp \mathbf{e}_y + k_\parallel \mathbf{e}_z$, the above relation can be written in the following matrix form (Galtier Book):

$$\begin{pmatrix} \omega^2 - k_\parallel^2 b_0^2 & 0 & 0 \\ 0 & \omega^2 - k_\perp^2 C_s^2 - k^2 b_0^2 & -k_\perp k_\parallel C_s^2 \\ 0 & -k_\perp k_\parallel C_s^2 & \omega^2 - k_\parallel^2 C_s^2 \end{pmatrix} \begin{pmatrix} v_{1x} \\ v_{1y} \\ v_{1z} \end{pmatrix} = \begin{pmatrix} 0 \\ 0 \\ 0 \end{pmatrix}$$

In order that the equations have non-trivial solution, the determinant of the coefficient matrix should vanish. We therefore obtain the following dispersion relation:

$$(\omega^2 - k_\parallel^2 b_0^2) [\omega^4 - (C_s^2 + b_0^2) k^2 \omega^2 + k^2 C_s^2 k_\parallel^2 b_0^2] = 0. \quad (3.46)$$

The solutions of the above equation are given as:

$$\omega_A = \pm k_\parallel b_0, \quad (3.47)$$

$$\omega_F = \pm \sqrt{\frac{k^2}{2} \left[(C_s^2 + b_0^2) + \sqrt{(C_s^2 + b_0^2)^2 - 4C_s^2 b_0^2 \frac{k_\parallel^2}{k^2}} \right]}, \quad (3.48)$$

$$\omega_S = \pm \sqrt{\frac{k^2}{2} \left[(C_s^2 + b_0^2) - \sqrt{(C_s^2 + b_0^2)^2 - 4C_s^2 b_0^2 \frac{k_\parallel^2}{k^2}} \right]}, \quad (3.49)$$

where ω_A corresponds to the **Alfvén mode** (after the discoverer Hannes Alfvén) and ω_F and ω_S are respectively the fast and the slow magnetosonic modes. Alfvén mode is a purely incompressible and transverse mode (in incompressible hydrodynamics we do not have any linear mode) whereas the last two waves are compressional modes and cannot get excited in incompressible case. The group velocity of the Alfvén mode is called **Alfvén velocity** and is expressed as (re-putting μ_0 and ρ_0)

$$\mathbf{V}_A = \frac{\mathbf{b}_0}{\sqrt{\mu_0 \rho_0}} \quad (3.50)$$

and the corresponding phase speed is given by $(V_A k_\parallel)/k$. Alfvén waves were theoretically predicted by Alfvén (1942) and was verified, for the first time, in ionized hydrogen tube experiment (see figure 3.2) 17 years later (Allen *et al.*,

1959). The phenomenology of incompressible MHD turbulence in presence of a directional field b_0 is explained by the interaction of fluctuating Alfvén waves (IK phenomenology) and will be discussed in details in the chapter 4. Whether the phenomenology of compressible MHD turbulence can be modeled by a combined effect of Alfvén, fast and slow compressional modes, is yet to be understood.

It is noteworthy that turbulence which is a complete non-linear phenomenon, can sometimes be described by the linear modes. For collisionless plasmas, it is also very interesting to note that even for a compressible fluid, the compressional modes damp rapidly and finally the dynamics is governed by the only incompressible mode which is Alfvén mode.

3.3.4 Invariants of ideal MHD

In this section, we shall examine the invariance of some dynamical variables in an ideal MHD flow. As mentioned earlier, the main objective of finding inviscid invariants lies on the fact that the knowledge of these invariants will help us determine the possibility of cascades (explained in the next chapter) in the inertial zone (defined in the previous chapter) which is supposed to be free from any large scale forcing effect and small scale viscous effect. For simplicity, here we derive those conservation principles right from the inviscid ideal MHD equations ($\nu = 0, \eta = 0$). The generalized expressions with the viscous terms can be found in standard text books (Galtier, 2013).

The choice of boundary conditions plays a key role in obtaining the invariants. In the following demonstrations, we use the most common and realistic boundary conditions i.e. at the surface of the chosen Eulerian volume (in which the flow is confined), the velocity and the magnetic fields are purely tangential i.e. $\mathbf{v} \cdot \mathbf{n} = 0$ and $\mathbf{b} \cdot \mathbf{n} = 0$ at each point of the boundary surface, \mathbf{n} being the unit normal vector at an arbitrary point of the surface. We shall also see that some quantities, which are not invariant under the said boundary condition, can be invariant if we assume $\mathbf{v} = \mathbf{b} = \mathbf{0}$ at every point of the boundary surface.

Mass and linear momentum

As in the hydrodynamic case, conservation of total mass ($\int \rho d\tau$) can immediately be seen from the continuity equation which itself is in conservative form. For the linear momentum, we can show that for ideal MHD,

$$\frac{\partial \rho \mathbf{v}}{\partial t} = -\nabla \cdot (\rho \mathbf{v} \otimes \mathbf{v}) - \nabla \left(P + \frac{b^2}{2\mu_0} \right) + \frac{1}{\mu_0} (\mathbf{b} \cdot \nabla) \mathbf{b}. \quad (3.51)$$

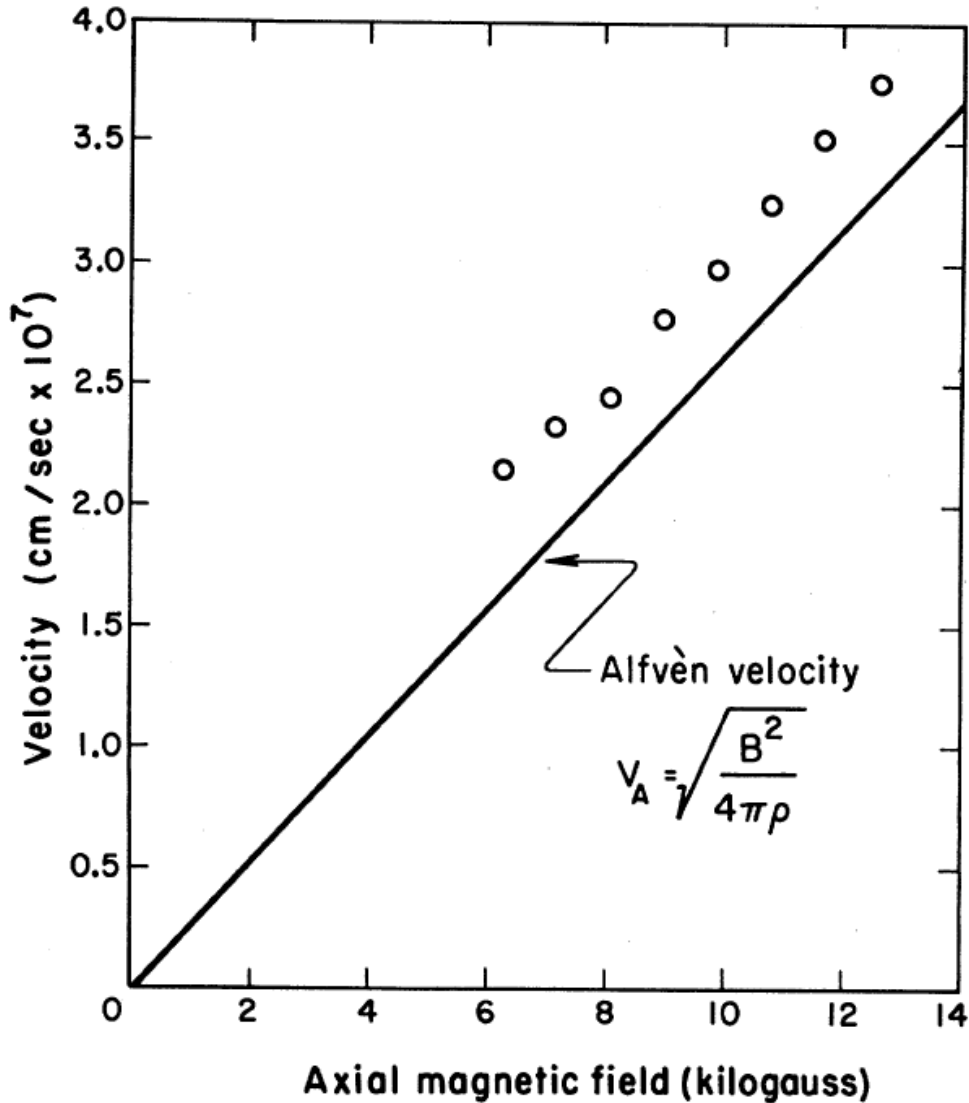


Figure 3.2: Experimental verification of Alfvén waves in a hydrogen filled tube of 34 inches and of diameter $5^{3/4}$ inches; The solid line corresponds to the theoretical estimation and the circles correspond to the experimental values which justifies the proportionality of Alfvén speed to the magnetic field in an incompressible or weakly compressible fluid; The discrepancy between the experimental and the theoretical values are due to instrumental reasons; Reprinted with permission from (Allen *et al.*, 1959); © (1959) American Physical Society. DOI: 10.1103/PhysRevLett.2.383

There is a priori no reason for the tensors consisting \mathbf{b} vanish at the boundary surface. As a result, linear momentum is not an invariant under our boundary conditions. If we relax the boundary conditions by making both the velocity and magnetic field vanish at surface, then too we cannot show the conservation. The physical reason for this is simply the fact that linear momentum is transported by the magnetic field even at the surface.

Total energy

The total energy of a compressible MHD fluid is composed of three parts - kinetic, magnetic and compressional. As earlier, we consider a barotropic MHD fluid for which the total energy density is:

$$\mathcal{E} = \rho \left[\frac{v^2}{2} + \frac{b^2}{2\mu_0\rho} - \int Pd \left(\frac{1}{\rho} \right) \right] = \rho \left[\frac{v^2}{2} + \frac{b^2}{2\mu_0\rho} + \int P \frac{d\rho}{\rho^2} \right].$$

Now from the ideal MHD equations, we can obtain (using vector calculus identities) at first:

$$\frac{\partial}{\partial t} \left(\rho \frac{v^2}{2} \right) = -\nabla \cdot \left(\rho \frac{v^2}{2} \mathbf{v} \right) - \mathbf{v} \cdot \nabla P - \mathbf{j} \cdot (\mathbf{v} \times \mathbf{b}), \quad (3.52)$$

and then for the magnetic part of the energy, we obtain

$$\frac{1}{2\mu_0} \frac{\partial b^2}{\partial t} = \frac{1}{\mu_0} [\nabla \cdot (\mathbf{v} \times \mathbf{b}) \times \mathbf{b}] + \mathbf{j} \cdot (\mathbf{v} \times \mathbf{b}), \quad (3.53)$$

and finally for the compressive part we find finally,

$$\frac{\partial(\rho e)}{\partial t} = -\nabla \cdot (\rho e \mathbf{v}) - P (\nabla \cdot \mathbf{v}), \quad (3.54)$$

adding up the above three components, we get finally

$$\frac{\partial \mathcal{E}}{\partial t} = -\nabla \cdot \left(\rho \frac{v^2}{2} \mathbf{v} + \rho e \mathbf{v} + P \mathbf{v} + \left(\frac{\mathbf{b} \times (\mathbf{v} \times \mathbf{b})}{\mu_0} \right) \right) = -\nabla \cdot \mathcal{F}, \quad (3.55)$$

which is a conservative form with \mathcal{F} being the total energy flux density. The vector $(\mathbf{b} \times (\mathbf{v} \times \mathbf{b})) / \mu_0$ is called **Poynting vector** which measures the out-flux of electromagnetic energy. Following the same prescription given in the previous chapter, we can show that the total energy ($\int \mathcal{E} d\tau$) is conserved in ideal MHD under barotropic closure.

Cross helicity

Another crucial invariant of ideal MHD is the total cross helicity and was introduced by [Woltjer \(1958\)](#). The density of cross helicity is defined by $H_c = \mathbf{v} \cdot \mathbf{b}$. Being a scalar product of a polar vector (\mathbf{v}) and a pseudo-vector (\mathbf{b}), H_c is a pseudo-scalar i.e. it changes sign under parity. In an intuitive manner we can say that by virtue of cross helicity, kinetic energy and magnetic energy can be transferred to one another. In the following we shall initially investigate the conservation of total cross helicity (i.e. $\int H_c d\tau$), under barotropic closure. From the ideal MHD equations, we get

$$\begin{aligned} \frac{\partial H_c}{\partial t} &= \frac{\partial(\mathbf{v} \cdot \mathbf{b})}{\partial t} = \mathbf{v} \cdot \frac{\partial \mathbf{b}}{\partial t} + \mathbf{b} \cdot \frac{\partial \mathbf{v}}{\partial t} \\ &= \mathbf{v} \cdot [\nabla \times (\mathbf{v} \times \mathbf{b})] + \mathbf{b} \cdot \left[-\frac{\nabla P}{\rho} - (\mathbf{v} \nabla) \mathbf{v} - \frac{\mathbf{b} \times (\nabla \times \mathbf{b})}{\mu_0 \rho} \right] \\ &= -\nabla \cdot (\mathbf{v} \times (\mathbf{v} \times \mathbf{b})) + (\mathbf{v} \times \mathbf{b}) \cdot \omega - \mathbf{b} \cdot \left[\frac{\nabla P}{\rho} + (\mathbf{v} \cdot \nabla) \mathbf{v} \right], \end{aligned} \quad (3.56)$$

where the last term is vanished as two members (\mathbf{b}) of the scalar triple product are identical. We also show that

$$\mathbf{b} \cdot [(\mathbf{v} \cdot \nabla) \mathbf{v}] = \mathbf{b} \cdot \left[\nabla \left(\frac{v^2}{2} \right) - \mathbf{v} \times \omega \right] = \nabla \cdot \left(\frac{v^2}{2} \mathbf{b} \right) - \mathbf{b} \cdot (\mathbf{v} \times \omega). \quad (3.57)$$

Now the term with fluid pressure cannot immediately be expressed as a pure divergence under generalized barotropic closure. It is only a sub-class of barotropic closure for which $\nabla P/\rho = \nabla h$ (where h is a scalar function), we can write

$$\mathbf{b} \cdot \frac{\nabla P}{\rho} = \mathbf{b} \cdot \nabla h = \nabla \cdot (\mathbf{b}h). \quad (3.58)$$

Now using the expressions of (3.57) and (3.58) in (3.56), we get finally

$$\frac{\partial H_c}{\partial t} = \nabla \cdot \left[v^2 \mathbf{b} - (\mathbf{v} \cdot \mathbf{b}) \mathbf{v} - h \mathbf{b} - \frac{v^2}{2} \mathbf{b} \right], \quad (3.59)$$

which ensures the conservation of total cross helicity under the abovesaid boundary conditions using Gauss-Ostrogradsky theorem.

Polytropic closure ($P = k\rho^\gamma$) is such a type of barotropic closure which indeed permits $\nabla P/\rho = \nabla h$, where for a polytropic fluid (given that $\gamma \neq 0$ and 1),

$$h = \frac{\gamma P}{(\gamma - 1)\rho}. \quad (3.60)$$

The conservation of cross helicity is hence assured for a polytropic fluid. Now $\gamma = 0$ corresponds to an isobaric fluid and the term vanishes trivially. For an

isothermal fluid, $\gamma = 1$ and it is also possible to write $\frac{\nabla P}{\rho} = \nabla h$ where

$$h = C_s^2 \ln \frac{\rho}{\rho_0}, \quad (3.61)$$

C_s and ρ_0 being the constant sound speed and the equilibrium density of the fluid. Cross helicity is thus invariant even when $\gamma = 0$ or 1 . Topologically cross helicity measures the inter field line junctions between the magnetic and the velocity field lines. A global conservation of this quantity thus describes the frozen nature of one of them with respect to the other thereby keeping the number of inter field lines knots a constant.

It is crucial to note that even in compressible MHD, it is the incompressible cross helicity which is conserved. However, the compressible cross helicity with density $\rho \mathbf{v} \cdot \mathbf{v}_A$ (where $\mathbf{v}_A = \mathbf{b}/\sqrt{\mu_0 \rho}$) is not a conserved quantity in compressible MHD.

Magnetic helicity

Magnetic helicity is another type of helicity which is of purely magnetic origin. This variable is introduced by [Woltjer \(1958\)](#). The corresponding density is defined as $H_m = \mathbf{a} \cdot \mathbf{b}$ where \mathbf{a} is a vector potential of magnetic field \mathbf{b} . H_m is also a pseudo scalar as \mathbf{a} is a true vector. Due to the presence of vector potential \mathbf{a} , H_m is also expected to be dependent on the choice of gauge. The Faraday's equation in ideal MHD is written as

$$\frac{\partial \mathbf{b}}{\partial t} = \nabla \times (\mathbf{v} \times \mathbf{b}). \quad (3.62)$$

As we know $\mathbf{b} = \nabla \times \mathbf{a}$ by definition, we obtain

$$\frac{\partial \mathbf{a}}{\partial t} = (\mathbf{v} \times \mathbf{b}) + \nabla \Phi, \quad (3.63)$$

where Φ is an arbitrary scalar potential corresponding to the chosen gauge. Using the above two equations we get

$$\begin{aligned} \frac{\partial H_m}{\partial t} &= \frac{\partial (\mathbf{a} \cdot \mathbf{b})}{\partial t} = \mathbf{a} \cdot \frac{\partial \mathbf{b}}{\partial t} + \mathbf{b} \cdot \frac{\partial \mathbf{a}}{\partial t} \\ &= \mathbf{b} \cdot [(\mathbf{v} \times \mathbf{b}) + \nabla \Phi] + \mathbf{a} \cdot (\nabla \times (\mathbf{v} \times \mathbf{b})) \\ &= \nabla \cdot (\mathbf{b} \Phi) + \nabla \cdot ((\mathbf{v} \times \mathbf{b}) \times \mathbf{a}) + 2\mathbf{b} \cdot (\mathbf{v} \times \mathbf{b}) \\ &= \nabla \cdot (\mathbf{b} \Phi) + \nabla \cdot ((\mathbf{v} \times \mathbf{b}) \times \mathbf{a}) \quad [:\mathbf{b} \cdot (\mathbf{v} \times \mathbf{b}) = 0]. \end{aligned} \quad (3.64)$$

These two terms are vanished by Gauss-Ostrogradsky theorem under our boundary conditions. For the first term it is immediate whereas for the second term we have to use the identity $((\mathbf{v} \times \mathbf{b}) \times \mathbf{a}) = (\mathbf{v} \cdot \mathbf{a}) \mathbf{b} - (\mathbf{b} \cdot \mathbf{a}) \mathbf{v}$ to apply

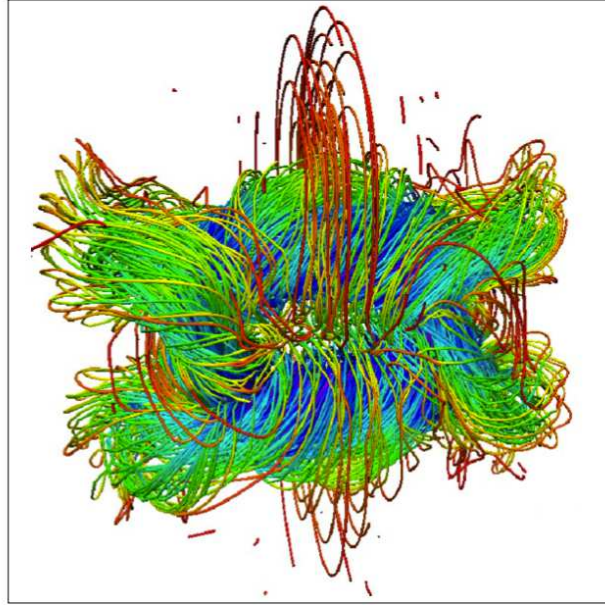


Figure 3.3: Numerical simulation of twisted and knotted magnetic field lines for a system with non-zero magnetic helicity; Source: Oral presentation of Simon Candelaresi.

our boundary conditions where both the velocity and magnetic field are purely tangential at the boundary surface of the Eulerian volume. Total magnetic helicity is thus proved to be an invariant of ideal MHD.

Magnetic helicity measures the degree of twists and knots (see figure 3.3) in the magnetic field lines in a plasma (Moffatt, 1969). Conservation of total magnetic helicity hence indicates that the magnetic field lines are frozen in the flow field and thus the total number of the intra-fieldline knots is conserved.

3.3.5 Elsässer variables in magnetohydrodynamics

For incompressible fluids, resistive MHD equations are written as

$$\frac{\partial \mathbf{v}}{\partial t} + (\mathbf{v} \cdot \nabla) \mathbf{v} = -\frac{\nabla P}{\rho} - \alpha \mathbf{b} \times (\nabla \times \mathbf{b}) + \nu \Delta \mathbf{v}, \quad (3.65)$$

$$\frac{\partial \mathbf{b}}{\partial t} = \nabla \times (\mathbf{v} \times \mathbf{b}) + \eta \Delta \mathbf{b}, \quad (3.66)$$

$$\nabla \cdot \mathbf{v} = 0, \quad (3.67)$$

$$\nabla \cdot \mathbf{b} = 0, \quad (3.68)$$

where $\alpha = 1/(\mu_0 \rho)$ is a constant for incompressible flow and η is the magnetic resistivity. These equations can be re-written in a more symmetric form if we

carry out a variable transformation (Elsässer, 1950) from (\mathbf{v}, \mathbf{b}) to $(\mathbf{z}^+, \mathbf{z}^-)$ where

$$\boxed{\mathbf{z}^\pm = \mathbf{v} \pm \alpha^{1/2} \mathbf{b}.} \quad (3.69)$$

These variables are called **Elsässer variables** after the name of the discoverer W.M. Elsässer. By virtue of this transformation, the above equations can be written as

$$\nabla \cdot \mathbf{z}^\pm = 0 \quad (3.70)$$

$$\frac{\partial \mathbf{z}^+}{\partial t} + (\mathbf{z}^- \cdot \nabla) \mathbf{z}^+ = -\nabla P_T + \Delta (\nu_+ \mathbf{z}^+ + \nu_- \mathbf{z}^-), \quad (3.71)$$

$$\frac{\partial \mathbf{z}^-}{\partial t} + (\mathbf{z}^+ \cdot \nabla) \mathbf{z}^- = -\nabla P_T + \Delta (\nu_+ \mathbf{z}^- + \nu_- \mathbf{z}^+), \quad (3.72)$$

where $P_T = P + b^2/2\mu_0$ is the total pressure and $\nu_\pm = (\nu \pm \eta/2)$. As mentioned by the author in his 1950 letter, this notable symmetrical form of these above equations along with their analogy to the Navier-Stokes equations led to an intuitive theoretical evidence for the possibility of turbulence in a 'hydromagnetic system' similar to ordinary hydrodynamic case. The existence of turbulent magnetic field, coupled with the mechanical fluid motion, can thus be theoretically understood. The fundamental importance of Elsässer variables will be explained precisely when we shall discuss the Iroshnikov-Kraichnan (IK) phenomenology in MHD turbulence in the next chapter.

Compressible Elsässer variables

Despite the success of Elsässer variables in incompressible MHD, Elsässer was sceptical about their utility in compressible MHD. He ended his 1950 letter by admitting the fact that "... we have thus been unable to ascertain whether similarly simple, symmetrized equations exist for the compressible case."

The generalization of these Elsässer variables to compressible MHD was finally done after 37 years by Marsch & Mangeney (1987). In the compressible case, no change in definition of the \mathbf{z}^\pm is needed. However, the density, being a variable in compressible fluids, cannot retain the Elsässer symmetry in compressible MHD equations. In order to construct the compressible Elsässer variables, we have to replace \mathbf{b} by $\mathbf{v}_A = \mathbf{b}/\sqrt{\mu_0\rho}$ where \mathbf{v}_A can be called

compressional Alfvén velocity. The ideal MHD equations are then written as:

$$\frac{\partial \ln \rho}{\partial t} + (\mathbf{v} \cdot \nabla) \ln \rho = -\nabla \cdot \mathbf{v}, \quad (3.73)$$

$$\frac{\partial \mathbf{v}}{\partial t} + (\mathbf{v} \cdot \nabla) \mathbf{v} - (\mathbf{v}_A \cdot \nabla) \mathbf{v}_A = -\frac{\nabla P_T}{\rho} - \mathbf{v}_A (\nabla \cdot \mathbf{v}_A), \quad (3.74)$$

$$\frac{\partial \mathbf{v}_A}{\partial t} + (\mathbf{v} \cdot \nabla) \mathbf{v}_A - (\mathbf{v}_A \cdot \nabla) \mathbf{v} = -\frac{1}{2} \mathbf{v}_A (\nabla \cdot \mathbf{v}), \quad (3.75)$$

$$\frac{\partial (P \rho^{-\gamma})}{\partial t} = 0, \quad (3.76)$$

$$(\mathbf{v}_A \cdot \nabla) \ln \rho = -2 (\nabla \cdot \mathbf{v}_A). \quad (3.77)$$

The first one is the continuity equation, the second and the third one correspond respectively to the force equation and Faraday's equation. The fourth and the fifth relations present respectively the polytropic closure and the solenoidal magnetic field. These equations prove to be very useful in deriving the exact relation of compressible MHD turbulence (Banerjee & Galtier, 2013) which is of central interest of my thesis. A few steps of simple and straightforward algebra finally gives us the following equations

$$\frac{D^\pm}{Dt} \ln \rho = -\frac{1}{2} \nabla \cdot (\mathbf{z}^\pm - \mathbf{z}^\mp), \quad (3.78)$$

$$\frac{D^\mp}{Dt} \mathbf{z}^\pm = \pm \frac{1}{4} (\mathbf{z}^+ - \mathbf{z}^-) \frac{D^\pm}{Dt} \ln \rho - \frac{1}{8} \nabla (\mathbf{z}^+ - \mathbf{z}^-)^2 - \left[C_s^2 + \frac{1}{8} (\mathbf{z}^+ - \mathbf{z}^-)^2 \right] \nabla \ln \rho, \quad (3.79)$$

where $C_s = \sqrt{\gamma P / \rho}$, gives the sound speed. These equations are important in understanding the possible phenomenology of compressible MHD turbulence and will be discussed later in the chapter on compressible turbulence.

Incompressible limit : From the above equations we can also verify the incompressible limit which is already known. This limit can easily be achieved by letting the fluid density constant. However, care should be taken for the term $C_s^2 \nabla (\ln \rho)$. In the incompressible limit, although $\nabla (\ln \rho) \rightarrow 0$, the sound velocity comes to be infinite due to the polytropic exponent which tends to infinity and thereby rendering the product $C_s^2 \nabla (\ln \rho)$ to be finite (Error in Marsch & Mangeney (1987)). In the incompressible limit, the above equations are hence written as

$$\nabla \cdot \mathbf{z}^\pm = 0, \quad (3.80)$$

$$\frac{D^\mp}{Dt} \mathbf{z}^\pm = -\frac{1}{8} \nabla (\mathbf{z}^+ - \mathbf{z}^-)^2 - \frac{\nabla P}{\rho}, \quad (3.81)$$

which are nothing but the equations (3.70), (3.71) and (3.72) in the inviscid limit.

Pseudo energies

By using the compressible Elsässer variables, one can re-write the densities of total energy and cross helicity respectively as

$$\mathcal{E} = \frac{1}{4}\rho (\mathbf{z}^+ \cdot \mathbf{z}^+ + \mathbf{z}^- \cdot \mathbf{z}^-) + \rho e, \quad (3.82)$$

$$\mathcal{H}_C = \frac{1}{4}\rho (\mathbf{z}^+ \cdot \mathbf{z}^+ - \mathbf{z}^- \cdot \mathbf{z}^-). \quad (3.83)$$

The quantities $\mathcal{E}^\pm = \frac{1}{2}\rho \mathbf{z}^\pm \cdot \mathbf{z}^\pm$ are called **pseudo-energies** corresponding to the two Elsässer variables. In compressible case, the total energy is an inviscid invariant of MHD whereas the total compressible cross helicity ($\int \mathcal{H}_C d\tau = \int \rho H_C d\tau$) is not a conserved quantity. In the incompressible case, both the total energy and the cross helicity are conserved and so are the incompressible pseudo-energies $\frac{1}{2}\mathbf{z}^\pm \cdot \mathbf{z}^\pm$. In case where $z^+ \gg z^-$ (or $z^- \gg z^+$), it is the pseudo energy density \mathcal{E}^+ (or \mathcal{E}^-) which approximates the total energy density and the cross helicity (for the cross helicity the sign changes according to the positive correlation or anti-correlation).

Different plasma sources	Ionic parameters				Electronic parameters				Magnetic field (T)
	n_i (m^{-3})	f_{pi} (Hz)	T_i (K)	λ_{Di} (m)	n_e (m^{-3})	f_{pe} (Hz)	T_e (K)	λ_{De} (m)	
Reactor plasma	10^{18}	10^8	10^2	10^{-6}	10^{18}	10^{10}	10^4	10^{-5}	10^{-2}
Cylindrical confinement	10^{22}	10^{10}	10^8	10^{-5}	10^{22}	10^{12}	10^8	10^{-5}	5
Tokamak	10^{20}	10^9	10^8	10^{-4}	10^{20}	10^{11}	10^8	10^{-4}	5
Terrestrial Ionosphere	$10^9 - 10^{12}$	$10^4 - 10^5$	$10^2 - 10^3$	10^{-4}	$10^9 - 10^{12}$	$10^6 - 10^7$	$10^2 - 10^3$	10^{-4}	10^{-5}
Terrestrial magnetosphere	10^7	10^3	10^5	10	10^7	$10^4 - 10^5$	$10^4 - 10^5$	10	10^{-8}
Solar wind (1 AU)	10^7	10^3	10^5	10	10^7	$10^4 - 10^5$	10^5	10	10^{-9}
Solar corona	10^{14}	10^6	10^6	10^{-2}	10^{14}	10^8	10^6	10^{-2}	10^{-4}
Solar photosphere	10^{23}	10^{11}	10^4	10^{-8}	10^{23}	10^{13}	10^4	10^{-8}	10^{-2}
Interstellar cloud	$10^8 - 10^9$	$10^3 - 10^4$	$10 - 10^2$	10^{-2}	$10^8 - 10^9$	$10^5 - 10^5$	$10 - 10^2$	10^{-2}	10^{-8}

Figure 3.4: Order of magnitude of various plasma parameters for different types of plasmas.

Turbulent flow : important notions

Contents

4.1	Turbulence - A phenomenon or a theory ?	44
4.2	Turbulent regime from Navier-Stokes : Reynolds number	45
4.3	Chaos and/or turbulence ?	48
4.4	Basic assumptions	50
4.4.1	Statistical homogeneity	50
4.4.2	Statistical isotropy	50
4.4.3	Stationary state	50
4.5	Two approaches to turbulence	51
4.5.1	Statistical approach	51
4.5.2	Spectral approach	54
4.6	Phenomenology	59
4.6.1	K41 phenomenology	60
4.6.2	IK phenomenology	63
4.6.3	Utilities of phenomenology	66
4.7	Dynamics and energetics of turbulence	70
4.7.1	Turbulent forcing	70
4.7.2	Turbulent cascade	71
4.7.3	Turbulent dissipation	73
4.8	Intermittency	74
4.8.1	β fractal model	77
4.8.2	Refined similarity hypothesis : Log-Normal model	78
4.8.3	Log-Poisson model	79
4.8.4	Extended self-similarity	80

4.1 Turbulence - A phenomenon or a theory ?

TURBULENCE is described by very complex dynamics of fluids necessarily associating non-linearity. Turbulence is ubiquitous and hence it is very easy to give a natural example of turbulent flow (the mixing of milk in a coffee cup, atmospheric turbulence in troposphere, solar wind, self-gravitating molecular clouds in astrophysics etc.) but it is extremely hard to set up a formal definition for this type of motion. In his 1954 lecture (Chandrasekhar, 1954), Chandrasekhar defined turbulence as **a phenomenon associated with the velocity state of a fluid medium**. This shows, in fact, the difficulty of setting up a concrete and quantitative definition of turbulence. In the different communities of turbulence, we have different definitions for turbulence depending on their specific approach to understand turbulence. Mathematically speaking, a turbulent flow can be defined to be a dynamical system having infinitely large number of degrees of freedom (DF). Later we shall give an estimation of the DF of a natural turbulent system. A chaotic motion differs from a turbulent motion due to the fact that the previous one is defined for particle dynamics (and not for a continuous medium) and possesses finite and low number of degrees of freedom. There is no strict definition of turbulence. **However, turbulence can formally be defined as a non-equilibrium statistical system whose state can be determined by the flux rate of the flow invariants rather than the thermodynamic variables**. Another popular definition is given using Lyapunov exponents. According to this definition, **a turbulent flow-field is associated with an exponential divergence between the dynamical variables of two neighbouring points in course of time**. In terms of a dynamical variable \mathbf{z} , this definition is mathematically written as

$$|\delta\mathbf{z}(t)| = |\mathbf{z}(\mathbf{x} + \mathbf{r}, t) - \mathbf{z}(\mathbf{x}, t)| = e^{\lambda t} |\delta\mathbf{z}(0)|,$$

where λ is called the Lyapunov exponent. Unlike the time-independent first definition, this definition describes the evolution of a turbulent system. For the astrophysicists neither of these two is very useful. Here the objective is to identify whether an astrophysical system is turbulent or not right from their fluctuation spectra. Another definition, which may be called an operational definition, is thus given in terms of the fluctuation power spectra. It defines turbulence to be a non-linear random motion of fluids or plasmas whose corresponding **fluctuation power spectra ($F(k)$) span a broad range of lengthscales and/or timescales with a power law ($F(k) \sim k^\alpha \Rightarrow \ln F(k) \sim \alpha \ln k$)**. A more detailed use and discussion on this definition will be done throughout.

Although a fluid need not be incompressible in order to produce a turbulent

flow, the systematic theoretical development for turbulence has primarily been done under the assumption of incompressibility. It is because *i*) mathematically incompressible turbulence is much more simple than the compressible one and *ii*) phenomenologically incompressible turbulence is easier to understand in terms of its structures which are the vortices. In this chapter, we shall introduce different assumptions, notions and approaches of fluid turbulence principally for incompressible flow. The existence and validity of these notions are not entirely obvious in case of compressible turbulence and will be discussed in the next chapter.

4.2 Turbulent regime from Navier-Stokes : Reynolds number

In three dimensions, Navier-Stokes equations are believed (to date) to describe satisfactorily a neutral fluid motion in the presence of viscosity. Considering compressibility, we can write the equation as

$$\frac{\partial \mathbf{v}}{\partial t} + (\mathbf{v} \cdot \nabla) \mathbf{v} = -\frac{\nabla P}{\rho} + \mathbf{f} + \nu \Delta \mathbf{v} + \frac{\nu}{3} \nabla (\nabla \cdot \mathbf{v}). \quad (4.1)$$

For an incompressible fluid ($\rho = \text{constant}$, $\nabla \cdot \mathbf{v} = 0$), the equations then get reduced to

$$\frac{\partial \mathbf{v}}{\partial t} + (\mathbf{v} \cdot \nabla) \mathbf{v} = -\nabla P + \mathbf{f} + \nu \Delta \mathbf{v}, \quad (4.2)$$

where $(\mathbf{v} \cdot \nabla) \mathbf{v}$ represents the non-linear term (non-linear in velocity) and $\nu \Delta \mathbf{v}$ corresponds to the viscous term which tries to retain the laminar flow. The ratio of these two terms gives us a dimensionless number which is obtained as

$$\mathfrak{R}_e \equiv \frac{|(\mathbf{v} \cdot \nabla) \mathbf{v}|}{\nu \Delta \mathbf{v}} \approx \frac{vl}{\nu} \approx \frac{\rho vl}{\mu}, \quad (4.3)$$

where the length scale is derived as $\nabla \equiv 1/l$ and $\mu = \rho\nu$ is the dynamic viscosity. This dimensionless quantity is called **Reynolds number**. A small value (< 1) of \mathfrak{R}_e corresponds to viscosity dominating laminar motion whereas a large value (> 100) leads to the case where non-linearity prevails the viscous effects and hence the regime of non-linear, chaotic motion of the fluid is attained. Typically for a value $\mathfrak{R}_e \sim 2000$, the flow field is characterised as a turbulent flow for which the afore-said definitions can be used with various perspectives. A completely developed turbulence is reached when $\mathfrak{R}_e \sim 10^4$. Theoretically speaking, with the rise in \mathfrak{R}_e , all the symmetries (Frisch, 1995) of Navier-Stokes equations are lost. **But at a very high \mathfrak{R}_e those symmetries are restored in a statistical sense (which will be discussed**

below) - this state is called the state of **completely developed turbulence** and therefore can be treated more easily in an analytical way than the states of transition. In the following figure various steps of the transition from a calm laminar flow to a chaotic complex motion is shown as a function of Reynolds number.

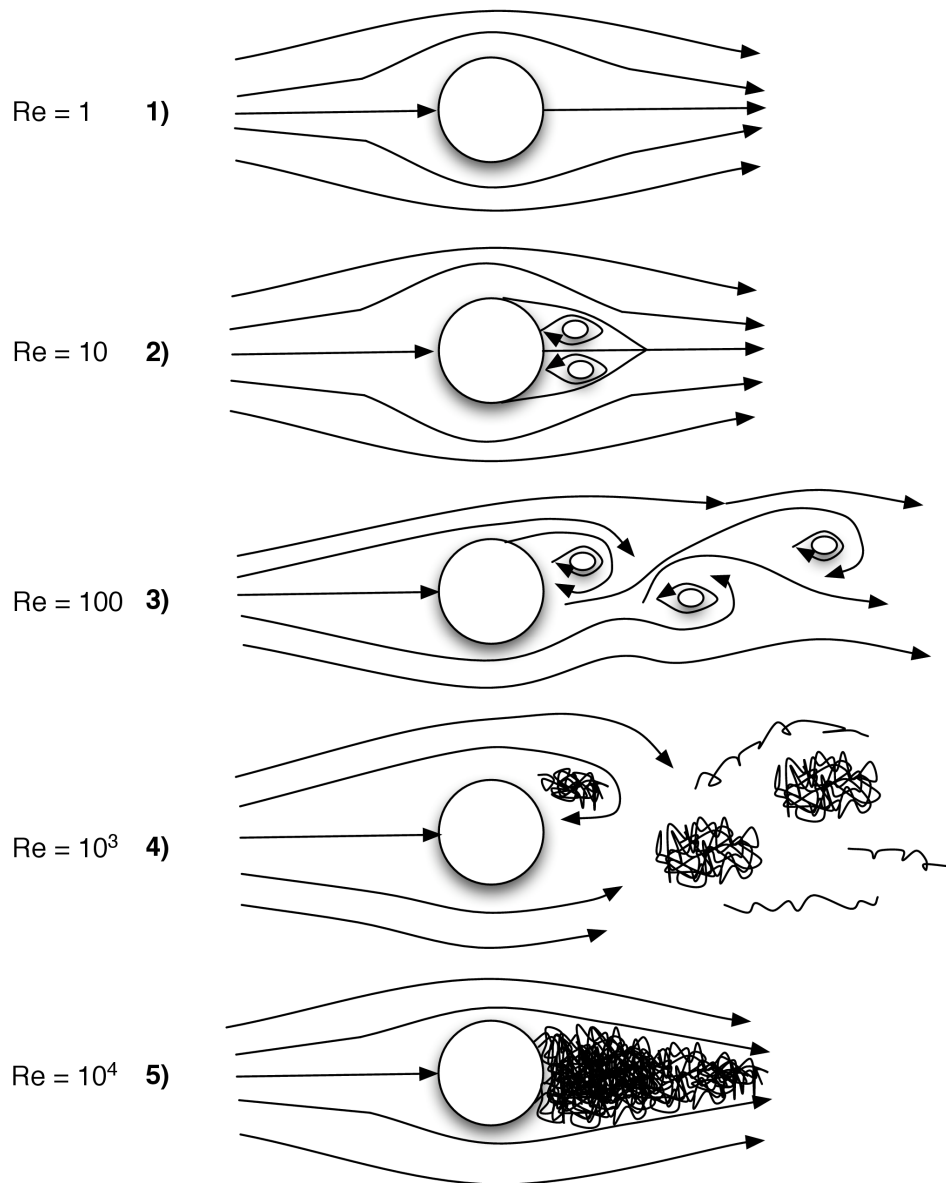


Figure 4.1: Transition from laminar flow to turbulent flow as a function of increasing Reynolds number; Courtesy: Sébastien Galtier.

The notion of Reynolds number can also be generalised in case of plasmas. For MHD fluids (as we have seen in the previous chapter) additionally we

need Faraday's equation from which another dimensionless quantity can be derived and can be written as

$$\mathfrak{R}_m \approx \frac{vl}{\eta}, \quad (4.4)$$

which is the ratio of the non-linear rotational term in Faraday's equation (after the substitution of resistive Ohm's law) to the magnetic-diffusion term. This quantity is known as Magnetic Reynolds Number. $\mathfrak{R}_m \ll 1$ indicates that the magnetic field will be diffused principally and hence the corresponding state is determined by the boundary conditions rather than the flow whereas $\mathfrak{R}_m \gg 1$ represents the predominance of the advection of the magnetic field lines along with the flow. Evidently, a total random, chaotic, turbulent type of motion therefore requires a very high value of both \mathfrak{R}_e and \mathfrak{R}_m .

In incompressible case, as the density is constant, dynamic viscosity (μ) and kinematic viscosity (ν) are equivalent. But in compressible flows, they are not the same. It is still a subject of debate which one of the two viscous coefficients is more fundamental and independent of the fluid density. One thus must use the general expression of Reynolds number including the density in defining a turbulent regime in compressible turbulence.

The notion of Reynolds number is not exclusive to the Navier-Stokes equations. As discussed in the chapter 2, a one dimensional compressible flow with discontinuities can be described by an ordinary differential equation called **Burger's equation**. It is trivial to verify that the corresponding turbulence regime, which is sometimes called **Burgulence** (Frisch & Bec, 2001), is simply characterised by \mathfrak{R}_e .

In an interesting note (page 998, A new kind of science) on Reynolds number, Wolfram (2002) mentioned that the turbulent regime is not always determined only by the Reynolds number. In fact modern-day experiments (ref needed) with dye water stream show a laminar-turbulence transition at a significantly lower \mathfrak{R}_e than that obtained by Osborne Reynolds in 1880s (Reynolds, 1883). The possible reason for this shift is suspected to be excessive external perturbations of the "modern mechanized world". Despite this, according to Wolfram, the randomness in a fully developed turbulence can still be attributed to the so called "intrinsic randomness" of the system and be expected to be unaffected by any external perturbation.

Historically it is interesting to note that the concept of Reynolds number was introduced by George Gabriel Stokes (Stokes, 1851). The number is later named after Osborne Reynolds who pioneered its implementation into the study of self-similar flows (Rott, 1990) in the year 1883. The term **Reynolds Number** was however introduced 25 years later by Sommerfeld (Sommerfeld, 1908).

Self-similar flow and Reynolds number

A fluid flow is said to be self-similar if it remains unchanged under certain rescaling of spatial and temporal scales. For such a flow, the governing equation for the corresponding dynamics should be scale-invariant with respect to such scaling transformation. Force-free Navier Stokes equation also possesses such scale-invariance. One can easily show that for incompressible Navier-Stokes equations with non-zero finite viscosity, the following transformation

$$\mathbf{x} \longrightarrow \lambda \mathbf{x}; \quad t \longrightarrow \lambda^{1-h} t; \quad \mathbf{v} \longrightarrow \lambda^h \mathbf{v} \quad (4.5)$$

keeps the equation globally unchanged when $h = -1$. With zero viscosity, the scale invariance is retained for any real value of h . Reynolds number, being dimensionless, remains also unaffected under a similarity transformation corresponding to finite viscosity¹ i.e. $h = -1$. A fixed finite value of Reynolds number thus characterizes self-similar flows. In incompressible flow, the scaling of pressure need not be considered separately because of the existence of a Poisson's equation between the pressure and the fluid velocity (Frisch, 1995). In compressible case, however the similarity transformation is a bit different and sensitive to the nature of closure used. One can easily verify that for isothermal closure ($P = C_S^2 \rho$), the required transformation is given by

$$\mathbf{x} \longrightarrow \lambda \mathbf{x}; \quad t \longrightarrow \lambda t; \quad \mathbf{v} \longrightarrow \mathbf{v}; \quad \rho \longrightarrow \lambda^{-1} \rho \quad (4.6)$$

and for a polytropic closure ($P = K \rho^\gamma$) the corresponding transformation is

$$\mathbf{x} \longrightarrow \lambda \mathbf{x}; \quad t \longrightarrow \lambda^{\frac{2\gamma}{1+\gamma}} t; \quad \mathbf{v} \longrightarrow \lambda^{\frac{1-\gamma}{1+\gamma}} \mathbf{v}; \quad \rho \longrightarrow \lambda^{-\frac{2}{1+\gamma}} \rho. \quad (4.7)$$

The isothermal and the incompressible cases can be recovered just by putting $\gamma = 1$ and $\gamma \longrightarrow \infty$ respectively. Without much surprise, one can show that here in compressible case, Reynolds number remains unchanged under similarity scale transformation if we consider the general expression of Reynolds number including density and the dynamic viscosity to be the intrinsic property of the fluid. The similarity transformations are not exactly the same in case of turbulence where statistical self-similarity is defined with respect to the structure functions. This aspect will be discussed later in this chapter in the section of intermittency.

4.3 Chaos and/or turbulence ?

This section is dedicated to a long-lasting debate and probably the most fundamental debate in turbulence physics - the relation between turbulence and

¹For inviscid case, Reynolds number is identically infinite.

deterministic chaos. Before coming to the actual controversy, it should be clear that *chaos* which is also known as *deterministic chaos* is a well-defined (mathematically) state of disordered motion of a many particle system whereas turbulence is not a theoretical concept but a real, natural phenomenon which describes highly non-linear, disordered, unpredictable and complex motion in a real fluid (e.g. poured milk in a coffee cup, the flow of tap water, the atmosphere, the solar flare, the interstellar clouds etc.) when the Reynolds number attains a very high value. Turbulence thus does not (as we saw above) have a universal and unique mathematical definition. So of course categorically they are different. Now the debate can be revitalised if we ask - Is turbulent disorder originated from chaos or due to some another 'unknown' fact ?

The correct answer being yet to be known, in the literature, we often see the clear existence of these two institutions. One can refer to "The lectures on geophysical fluid dynamics" by Salmon (1998) where turbulence is characterized in the following words :

"However, one further property of turbulence seems to be more fundamental than all of these because it largely explains why turbulence demands a statistical treatment. This property is variously called instability, unpredictability, or lack of bounded sensitivity. In more fashionable terms, turbulence is chaotic."

A diametrically opposite view can be found in Stephen Wolfram's book "A new kind of science" where the author claims (page 998):

"And as it turns out I suspect that despite subsequent developments the original ideas of Andrei Kolmogorov about complicated behaviour in ordinary differential equations were probably more in line with my notion of intrinsic randomness generation than with the chaos phenomenon".

The reason behind Wolfram's view is basically the presence of dissipation of a fluid in Navier-Stokes equations. Turbulent randomness, in order to be chaotic, should have been originated from the excessive sensitivity of the constituent particles to the initial conditions of their corresponding motions. But if the fluid dissipation is included, according to Wolfram, most details of the initial conditions would have been damped out intuitively at the large scale of the collective fluid behaviour and it is therefore very unlikely to trace chaotic unpredictability in the large scale randomness manifested in a turbulent system.

Another fact is that every chaotic motion associates moderately finite number of degrees of freedom whereas a turbulent system is believed to consist of infinitely large number of motion. An estimation of the number of degrees of freedom of a turbulent system is given later in this chapter by using Kolmogorov's phenomenology of incompressible turbulence.

4.4 Basic assumptions

4.4.1 Statistical homogeneity

The notion of statistical homogeneity is a crucial hypothesis for the study of turbulence. In usual terms, homogeneity describes the translational symmetry of a function in space (which is defined at every point of the concerning space) i.e. $f(\mathbf{x}) = f(\mathbf{x} + \mathbf{r})$. For statistical homogeneity it is sufficient to replace them by their corresponding statistical (or ensemble) average. For two-point study, homogeneity is said to exist if **the statistical averages of two-point correlators are only the function of the difference vector between the positions of the two points and not on their individual positions.** In mathematical expressions that can be written as

$$\langle f(\mathbf{x}) \cdot g(\mathbf{x} + \mathbf{r}) \rangle = \phi(\mathbf{r}), \quad (4.8)$$

where the $\langle \cdot \rangle$ denotes the statistical average. The above property reduces to the usual one point definition of statistical homogeneity for a function ψ if we just replace the function g by function f , set $\mathbf{r} = \mathbf{0}$ and define $\psi(\mathbf{0}) = f^2(\mathbf{x})$ in the above equation.

4.4.2 Statistical isotropy

The properties of an isotropic system are independent of the direction chosen. **In case of statistical isotropy, directional invariance holds good for the ensemble averages of the dynamic variables.** For two-point statistics, the corresponding correlators are functions of the magnitude of the mutual distance of those two points. Mathematically it can be written simply as

$$\langle f(\mathbf{x}) \cdot g(\mathbf{x} + \mathbf{r}) \rangle = \phi(r). \quad (4.9)$$

Statistical mirror symmetry is also an important notion in turbulence. It is a partial isotropy (in statistical sense) where we have

$$\langle f(\mathbf{x} + \mathbf{r}) \rangle = \langle f(\mathbf{x} - \mathbf{r}) \rangle. \quad (4.10)$$

4.4.3 Stationary state

A dynamical state is said to be statistically stationary **if the statistical averages of its dynamical variables or rather flow variables are independent of time.** So in a stationary state, for any variable Z we have

$$\frac{\partial \langle Z \rangle}{\partial t} = 0. \quad (4.11)$$

An essential element of Richardson's cascade is embedded in the consideration of a statistical stationary state. For such a state, the average energy injection rate is equal to the average energy dissipation rate. A simple demonstration using the incompressible Navier-Stokes equations (equation 4.2) can be given as the following:

$$\begin{aligned} \frac{\partial E}{\partial t} &= \frac{\partial}{\partial t} \int \frac{v^2}{2} d\tau = \int \frac{\partial}{\partial t} \left(\frac{v^2}{2} \right) d\tau \\ &= \int \left[-\nabla \cdot \left(\frac{v^2}{2} \mathbf{v} \right) - \nabla \cdot (P\mathbf{v}) + \nu \mathbf{v} \cdot \Delta \mathbf{v} + \mathbf{v} \cdot \mathbf{f} \right] d\tau. \end{aligned} \quad (4.12)$$

The divergence terms can be thrown away by using Gauss-Ostrogradsky divergence theorem assuming the surface of the closed volume containing the flow to be at infinity and also assuming that the velocity vector at the surface is purely tangential. Now for a steady state, the left hand term vanishes and we are led to the conclusion that

$$-\nu \mathbf{v} \cdot \Delta \mathbf{v} = \mathbf{v} \cdot \mathbf{f}. \quad (4.13)$$

For a turbulent flow which is statistically homogeneous (and therefore the statistical average and space average are equivalent), we can say that the rate of average energy injection is equal to the average energy dissipation and is formally written as

$$-\langle \nu \mathbf{v} \cdot \Delta \mathbf{v} \rangle = \langle \mathbf{v} \cdot \mathbf{f} \rangle = \varepsilon. \quad (4.14)$$

Note that the existence of this type of statistical steady state is not obvious. For compressible turbulence the existence of a stationary state and its consequences will be discussed later.

Interestingly from equation (4.13), we notice that the non-linear term or the inertial term does not finally contribute to the time rate of change of total energy (or even average energy). This fact leads to the important conclusion that in the inertial zone energy is neither gained nor lost on average but gets transferred from one scale to another thereby ensuring the possibility of an energy cascade within the said interval.

4.5 Two approaches to turbulence

4.5.1 Statistical approach

Application of statistical tools in the study of turbulence is justified by its random nature (whatever be the origin of this) and also by the fact that a completely developed turbulence, by definition, is expected to recover the

symmetries in Navier-Stokes equations in a statistical sense within the inertial zone (Frisch, 1995). In the study of turbulence fluctuations, two-point statistics seems to be more relevant than mere one point statistics. Two-point statistics consists of one-point statistical averaged quantities and two-point covariances which can also be (in a less rigorous way) considered as a measure of the correlation between any two points \mathbf{x} and $\mathbf{x} + \mathbf{r}$. In the following, $\langle \cdot \rangle$ will denote the statistical or ensemble average of a variable. Two-point correlator corresponding to the variables φ and ψ can be expressed in two ways i.e. $\langle \varphi(\mathbf{x} + \mathbf{r})\phi(\mathbf{x}) \rangle$ and $\langle \phi(\mathbf{x} + \mathbf{r})\varphi(\mathbf{x}) \rangle$. A priori they are different quantities and there is no reason for them to be equal even under the assumption of statistical homogeneity (as we see below).

Auto-correlation and spatio-temporal memory The correlation functions involving only one single variable is called the auto-correlation function. The simplest non-trivial auto-correlation functions are the second order functions. For an arbitrary flow variable ϕ , the second order space and time auto-correlators are respectively defined by $\langle \phi(\mathbf{x} + \mathbf{r}, t)\phi(\mathbf{x}, t) \rangle$ and $\langle \phi(\mathbf{x}, t + \tau)\phi(\mathbf{x}, t) \rangle$. The typical behaviour of a second order space auto-correlation function is shown in the figure (4.2). The correlation function remains considerable within a length scale r_C called the **correlation length** of the variable ϕ . Beyond that scale $\phi(\mathbf{x} + \mathbf{r}, t)$ comes to be almost independent of $\phi(\mathbf{x}, t)$. r_C can therefore be taken as a measure of spatial memory of ϕ . Identical treatment can be carried out for the temporal correlation functions in order to determine the correlation time corresponding to the concerned variable. In case of a statistically isotropic turbulence, a two-point longitudinal space correlator of velocity of order n (where n is a natural number) is defined as (Biskamp, 2008)

$$C_n(r) = \langle v_{\parallel}(\mathbf{x})^{n-1} v_{\parallel}(\mathbf{x} + \mathbf{r}) \rangle, \quad (4.15)$$

where v_{\parallel} denotes the component of velocity in the direction of \mathbf{r} . Similar definitions can be made for the temporal correlations too.

Structure functions In the context of incompressible turbulence, structure functions of a flow variable represent the statistical moments (of different orders) of the fluctuations of the corresponding quantity. The n -th order moment (where n is usually a natural number but can be positive fraction too) of a flow variable ψ gives the n -order structure function and is written as $S_n = \langle (\delta\psi)^n \rangle$. Initially Kolmogorov (1941a), Monin *et al.* (1975) defined structure functions for locally isotropic turbulence - following them, for two points \mathbf{x} and $\mathbf{x} + \mathbf{r}$, the longitudinal and transverse n -th order structure functions are

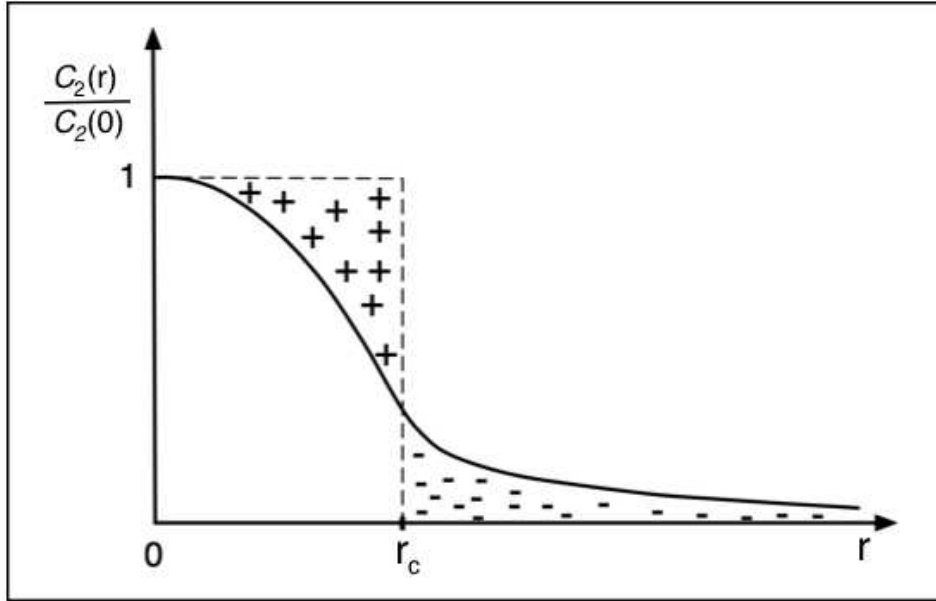


Figure 4.2: Behaviour of a second order auto-correlation function in space; Courtesy: Sébastien Galtier.

respectively defined by

$$S_n(r) = \langle [\delta v_{\parallel}(r)]^n \rangle, \quad T_n(r) = \langle [\delta v_{\perp}(r)]^n \rangle, \quad (4.16)$$

where δv_{\parallel} is the projection of δv in the direction of l and δv_{\perp} gives the two components which are perpendicular to \mathbf{r} . It is noteworthy that the local isotropy in statistical sense leads the moments or rather the components of the moments to be a function of the magnitude of \mathbf{r} vector instead of the vector itself. One should be careful that the isotropy does not necessarily make the parallel and perpendicular moments equal.

Following the above definition, we can have both positive and negative values of the structure functions depending on the values of n i.e. an even n always gives a positive value whereas an odd n may give a negative as well as a positive value. This definition is not however universal. In [Constantin & Fefferman \(1994\)](#), where several inequalities have been established relating the different order structure functions, the authors defined the structure functions as

$$S_n^a(r) = \langle |\delta v(r)|^n \rangle, \quad (4.17)$$

which always gives positive $S_n(l)$ irrespective of the values of n . In the following, we shall be more interested in longitudinal structure functions which is equivalent to the probability distribution function of the velocity increments

and their enhanced tails which correspond to the events of relatively large amplitude (Biskamp, 2008). The longitudinal structure functions are related to the longitudinal correlation functions by algebraic equations. One can easily prove that

$$S_2(r) = 2 [C_2(0) - C_2(r)], \quad S_3(r) = 3 [C_3(r) - C_3(-r)]. \quad (4.18)$$

Similar type (not exactly identical) of relations can be obtained in case of higher order moments and also for lateral structure functions (Monin *et al.*, 1975). In obtaining these relations, incompressibility condition i.e. $\nabla \cdot \mathbf{v} = 0$ is a must. For compressible turbulence, the possibility of these type of relation is therefore not guaranteed.

Structure functions are proved to be more fruitful than the correlators for high n . Unlike the higher order correlation functions which do not carry satisfactory information, the higher order longitudinal structure functions are found to obey a scaling law (Kolmogorov, 1941*b*) within inertial range and can be expressed as

$$S_n(r) = \alpha_n r^{\xi_n}, \quad (4.19)$$

where α_n is a proportionality constant but parametrized by the order of the structure function. The function $S_n(r)$ can be studied in two different ways for two interests. One is just by varying r and keeping n constant which helps us understand the extent (the range of length scale) to which a turbulent flow shows self-similarity with respect to the statistical moments of given order. Similarly varying n for a given length scale r is an appropriate tool for the study of intermittency which will be discussed below.

It is however important to note that the scaling relations of the structure functions remain the same if one uses the definition of equation (4.17) for the structure functions (Nie & Tanveer, 1999).

4.5.2 Spectral approach

Spectral approach to the study of turbulence consists of analytical study in Fourier space and plays a complementary role to the aforesaid statistical approach which is based on physical space. The basic reasons for the popularity of this approach can be understood by virtue of the following points (Galtier, 2013):

- a) The transfer of energy in turbulence from one length scale to another is believed to be an outcome of the interaction between different linear and non-linear wave modes in the turbulent media (Lesieur, 2008).
- b) Construction of closures in Fourier space is found to model turbulence more easily and reproduce theoretically the experimental energy spectrum law (see K41 phenomenology below) immediately with remarkable precision.

c) Spectral numerical codes are more precise than finite difference method. Moreover, they are easier to handle numerically in direct numerical simulations.

d) Spectral approach is indispensable in the analytical study of wave turbulence in weakly turbulent flows where the turbulent dynamics and the energy exchange from one scale to another is supposed to be caused by the interaction of three or more linear modes (Nazarenko, 2011).

In this approach, turbulent dynamics is studied in Fourier space and so we need the basic equation(s) of dynamics, here for example Navier-Stokes equations and the energy transport equation, to be expressed in Fourier space. Thus we have to construct the Fourier transform of each relevant dynamical variable which includes one point variables (velocity, pressure, energy etc.) as well as multi-point quantities like two-point or three-point energy correlation functions etc. Below we shall give some formal definitions and then construct some relevant quantities in Fourier space under the assumption of statistical homogeneity. Then we shall re-write incompressible Navier-Stokes equations in Fourier space which bears substantial importance in understanding the origin of inter-scale energy cascading in direct space which will be discussed in the following section.

4.5.2.1 Correlators in Fourier space and Energy spectra

The three dimensional Fourier transform (FT) of a one-point random stationary function $f(\mathbf{x})$ is defined as (in the sense of distribution)

$$\hat{f}(\mathbf{k}) \equiv \frac{1}{(2\pi)^3} \int_{\mathbf{R}^3} f(\mathbf{x}) e^{-i\mathbf{k}\cdot\mathbf{x}} d\mathbf{x}. \quad (4.20)$$

For homogeneous turbulence, the two-point correlators are defined as $\langle f(\mathbf{x})f(\mathbf{x}') \rangle = \langle f(\mathbf{x})f(\mathbf{x} + \mathbf{r}) \rangle = G(\mathbf{r})$ which let the Fourier transform of the direct space correlators be expressed as

$$M(\mathbf{k}) \equiv \frac{1}{(2\pi)^3} \int_{\mathbf{R}^3} G(\mathbf{r}) e^{-i\mathbf{k}\cdot\mathbf{r}} d\mathbf{r}. \quad (4.21)$$

Considering the case of second order velocity correlation tensors, we can define the corresponding FT as

$$\phi_{ij}(\mathbf{k}) \equiv \frac{1}{(2\pi)^3} \int_{\mathbf{R}^3} R_{ij}(\mathbf{r}) e^{-i\mathbf{k}\cdot\mathbf{r}} d\mathbf{r}, \quad (4.22)$$

where $R_{ij}(\mathbf{r}) \equiv \langle v_i(\mathbf{x})v_j(\mathbf{x} + \mathbf{r}) \rangle$ is two-point direct space velocity correlator. $\phi_{ij}(\mathbf{k})$ is called the spectrum of velocity field. For the quantity $\phi_{ij}(\mathbf{k})$ to be

defined mathematically, R_{ij} should be integrable which is physically possible because R_{ij} tends to zero for $|\mathbf{r}| \rightarrow \infty$. Furthermore, due to statistical homogeneity, one can easily verify that $R_{ij}(\mathbf{r}) = R_{ji}(-\mathbf{r})$ which, in turn, gives

$$\phi_{ji}(\mathbf{k}) = \phi_{ij}(-\mathbf{k}) = \phi_{ij}^*(\mathbf{k}). \quad (4.23)$$

We also suppose that the physical space correlation functions (here two-point correlators) can be expressed as inverse Fourier transform of ϕ_{ij} . Then we can write

$$R_{ij}(\mathbf{r}) = \int_{\mathbf{R}^3} \phi_{ij}(\mathbf{k}) e^{i\mathbf{k}\cdot\mathbf{r}} d\mathbf{k}. \quad (4.24)$$

The total average energy (in incompressible case which is equal to the kinetic energy) per unit mass at a point \mathbf{x} is then written as

$$E = \frac{1}{2} \langle u_i(\mathbf{x}) u_i(\mathbf{x}) \rangle = \frac{1}{2} R_{ii}(\mathbf{0}) = \frac{1}{2} \int_{\mathbf{R}^3} \phi_{ii}(\mathbf{k}) d\mathbf{k}, \quad (4.25)$$

whence we can finally obtain the general expression for the **energy spectrum** tensor in homogeneous turbulence and is given by

$$E(\mathbf{k}) \equiv \frac{1}{2} \phi_{ii}(\mathbf{k}). \quad (4.26)$$

For the special case of isotropic turbulence, the energy spectrum gets reduced to a scalar and is written as $\mathcal{E}(k)$ where

$$\mathcal{E}(k) \equiv \frac{dE}{dk} = \frac{1}{2} \frac{d \int \phi_{ii}(\mathbf{k}) d\mathbf{k}}{dk} = \frac{d \int 2\pi k^2 \phi_{ii}(k) dk}{dk} = 2\pi k^2 \phi_{ii}(k). \quad (4.27)$$

$\mathcal{E}(k)$ is called the **modal spectral density** of energy and is highly important and popular in the community of turbulence.

One can also verify that in homogeneous and isotropic incompressible turbulence, the general expression for the energy spectrum tensor is given by

$$\phi_{ij}(k) = \left(\delta_{ij} - \frac{k_i k_j}{k^2} \right) \frac{\mathcal{E}(k)}{4\pi k^2}. \quad (4.28)$$

4.5.2.2 Navier-Stokes equation and energy equation in Fourier space

Here we write incompressible Navier-Stokes equations in terms of the Fourier transform of the original dynamical variables and then we express the energy equation in Fourier space too. Rewriting the equation (4.2) omitting the force term, we get

$$\frac{\partial \mathbf{v}}{\partial t} + (\mathbf{v} \cdot \nabla) \mathbf{v} = -\nabla P + \nu \Delta \mathbf{v}. \quad (4.29)$$

Taking the FT on both sides, we obtain

$$\frac{\partial \widehat{\mathbf{v}}(\mathbf{k})}{\partial t} + (\widehat{\mathbf{v} \cdot \nabla}) \mathbf{v} = -i\mathbf{k}\widehat{P}(\mathbf{k}) - \nu|\mathbf{k}|^2 \widehat{\mathbf{v}}(\mathbf{k}), \quad (4.30)$$

where ' $\widehat{}$ ' denotes the corresponding Fourier transform. The next step is to eliminate the pressure term using incompressibility. Taking the divergence on both sides of equation (4.2) and using $\nabla \cdot \mathbf{v} = 0$ we get a Poisson's equation for pressure and is given by

$$\Delta P = -\nabla \cdot [(\mathbf{v} \cdot \nabla) \mathbf{v}]. \quad (4.31)$$

Taking FT on both sides of this equation, we get

$$k^2 \widehat{P}(\mathbf{k}) = ik_j [(\widehat{\mathbf{v} \cdot \nabla}) \mathbf{v}]_j \quad (4.32)$$

$$\Rightarrow \widehat{P}(\mathbf{k}) = i \frac{k_j}{k^2} [(\widehat{\mathbf{v} \cdot \nabla}) \mathbf{v}]_j, \quad (4.33)$$

using the definition of Kronecker delta, we can reduce the i^{th} component of the equation 4.30 to

$$\frac{\partial \widehat{v}_i(\mathbf{k})}{\partial t} + \nu k^2 \widehat{v}_i(\mathbf{k}) = - \left(\delta_{ij} - \frac{k_i k_j}{k^2} \right) [(\widehat{\mathbf{v} \cdot \nabla}) \mathbf{v}]_j, \quad (4.34)$$

here the repetition of the dummy index j indicates summation over j . The following step is to derive the FT of the non-linear term. We can write for the i^{th} component

$$\begin{aligned} [(\widehat{\mathbf{v} \cdot \nabla}) \mathbf{v}]_i &= \frac{1}{(2\pi)^3} \int (v_j(\mathbf{r}) \partial_j v_i(\mathbf{r})) e^{-i\mathbf{k} \cdot \mathbf{r}} d\mathbf{r} \\ &= \frac{1}{(2\pi)^3} \int \left(\int \widehat{v}_j(\mathbf{p}) e^{i\mathbf{p} \cdot \mathbf{r}} d\mathbf{p} \right) \left(i \int \widehat{v}_i(\mathbf{q}) q_j e^{i\mathbf{q} \cdot \mathbf{r}} d\mathbf{q} \right) e^{-i\mathbf{k} \cdot \mathbf{r}} d\mathbf{r} \\ &= i \int_{\mathbf{p}} \int_{\mathbf{q}} \widehat{v}_j(\mathbf{p}) q_j \widehat{v}_i(\mathbf{q}) \delta(\mathbf{k} - \mathbf{p} - \mathbf{q}) d\mathbf{p} d\mathbf{q}, \end{aligned} \quad (4.35)$$

where by definition, $(1/(2\pi)^3) \int e^{-i(\mathbf{k}-\mathbf{p}-\mathbf{q}) \cdot \mathbf{r}} d\mathbf{r} = \delta(\mathbf{k} - \mathbf{p} - \mathbf{q})$. The above expression, being inserted in (4.34), gives

$$\frac{\partial \widehat{v}_i(\mathbf{k})}{\partial t} + \nu k^2 \widehat{v}_i(\mathbf{k}) = -i \left(\delta_{ij} - \frac{k_i k_j}{k^2} \right) \sum_{\mathbf{k}=\mathbf{p}+\mathbf{q}} \widehat{v}_m(\mathbf{p}) q_m \widehat{v}_j(\mathbf{q}). \quad (4.36)$$

Now substituting q_m by $k_m - p_m$ and inserting the incompressibility condition i.e. $\widehat{v}_m(\mathbf{p}) p_m = 0$ in the above relation, we obtain the final form which is given by (Biskamp, 2008; Ditlevsen, 2010)

$$\boxed{\frac{\partial \widehat{v}_i(\mathbf{k})}{\partial t} + \nu k^2 \widehat{v}_i(\mathbf{k}) = -i \left(\delta_{ij} - \frac{k_i k_j}{k^2} \right) \sum_{\mathbf{k}=\mathbf{p}+\mathbf{q}} \widehat{v}_m(\mathbf{p}) k_m \widehat{v}_j(\mathbf{q}).} \quad (4.37)$$

The evolution equation for the energy spectral density is therefore obtained from the following expression

$$\frac{\partial E(\mathbf{k})}{\partial t} = \frac{\partial(\hat{v}_i \hat{v}_i^*)}{\partial t} = \frac{\partial \hat{v}_i}{\partial t} \hat{v}_i^* + \frac{\partial \hat{v}_i^*}{\partial t} \hat{v}_i. \quad (4.38)$$

Moreover using the fact that the velocity vector is real, we can show $\hat{v}_i^*(\mathbf{k}) = \hat{v}_i(-\mathbf{k})$. Using this relation in the equations (4.37) and (4.38) and finally using a few steps of algebrae, we obtain (Rose, H.A. & Sulem, P.L., 1978),

$$\frac{\partial E(\mathbf{k})}{\partial t} + 2\nu k^2 E(\mathbf{k}) = \int \int T(\mathbf{k} | \mathbf{p}, \mathbf{q}) \delta(\mathbf{k} + \mathbf{p} + \mathbf{q}) d\mathbf{p} d\mathbf{q}, \quad (4.39)$$

where

$$T(\mathbf{k} | \mathbf{p}, \mathbf{q}) = -Im [(\mathbf{k} \cdot \hat{\mathbf{v}}(\mathbf{q})) (\hat{\mathbf{v}}(\mathbf{p}) \cdot \hat{\mathbf{v}}(\mathbf{k})) + (\mathbf{k} \cdot \hat{\mathbf{v}}(\mathbf{p})) (\hat{\mathbf{v}}(\mathbf{q}) \cdot \hat{\mathbf{v}}(\mathbf{k}))] \quad (4.40)$$

is called the transfer function. For an inviscid fluid ($\nu = 0$), the total energy equation can be written as

$$\frac{\partial E}{\partial t} = \frac{\partial}{\partial t} \int E(\mathbf{k}) d\mathbf{k} = \int \int \int T(\mathbf{k} | \mathbf{p}, \mathbf{q}) \delta(\mathbf{k} + \mathbf{p} + \mathbf{q}) d\mathbf{k} d\mathbf{p} d\mathbf{q}. \quad (4.41)$$

By symmetry, one can write

$$\begin{aligned} \frac{\partial E}{\partial t} &= \frac{1}{3} \frac{\partial}{\partial t} \left[\int E(\mathbf{k}) d\mathbf{k} + \int E(\mathbf{p}) d\mathbf{p} + \int E(\mathbf{q}) d\mathbf{q} \right] \\ &= \frac{1}{3} \int_{\mathbf{k}, \mathbf{p}, \mathbf{q}} [T(\mathbf{k} | \mathbf{p}, \mathbf{q}) + T(\mathbf{p} | \mathbf{q}, \mathbf{k}) + T(\mathbf{q} | \mathbf{k}, \mathbf{p})] \delta(\mathbf{k} + \mathbf{p} + \mathbf{q}) d\mathbf{k} d\mathbf{p} d\mathbf{q}. \end{aligned} \quad (4.42)$$

$$(4.43)$$

Now by using the incompressibility, one can easily show that

$$[T(\mathbf{k} | \mathbf{p}, \mathbf{q}) + T(\mathbf{p} | \mathbf{q}, \mathbf{k}) + T(\mathbf{q} | \mathbf{k}, \mathbf{p})] = 0. \quad (4.44)$$

The above relation proves the total energy conservation and also energy conservation for each triad interaction. The above equation is crucial for understanding the localness of interactions in turbulence (discussed in the following section) in terms of the **triads** and can be considered to be the key equation for shell models in turbulence (Ditlevsen, 2010) which are beyond the scope of our current discussion. Kolmogorov's $-5/3$ law for isotropic turbulence can also be reproduced from the relation (4.41) by using Weiner-Khinchin formula (for detailed derivation see page 11 of Ditlevsen (2010)).

4.5.2.3 Triadic interaction and localness of interactions

It is clear from the equation (4.37) that the non-linear term, which efficiently transfers energy, essentially associates three modes \mathbf{k} , \mathbf{p} and \mathbf{q} in Fourier space. For an effective non-zero energy transfer, those three modes should obey the condition of resonance i.e. $\mathbf{k} + \mathbf{p} + \mathbf{q} = \mathbf{0}$. This introduces the notion of **triadic or three-wave interaction**. As the non-linear term is believed to bring about the energy cascade, the corresponding mechanism is thus believed to be driven by this type of triad interactions. Let the wave numbers be ordered by a sequence say k_n . As energy cascading should be a process of inter-scale step-by step energy transfer (can be shown theoretically for hydrodynamic turbulence), it is necessarily local in wave space which means then the efficient energy transferring interactions corresponding to scale k_n^{-1} will involve either k_n or $k_{n\pm 1}$. Now practically in order to implement the locality in the triadic interactions, all the triads for which the smallest wave number is less than the half of the largest one are eliminated selectively. So if we consider an interacting triad of wave vectors \mathbf{k}_n , \mathbf{p}_n and \mathbf{q}_n with an ordering (by choice) that $|\mathbf{k}_n| > |\mathbf{p}_n| > |\mathbf{q}_n|$, the selected triads will be those which would have $2|\mathbf{q}_n| \geq |\mathbf{k}_n|$. It is noteworthy that energy is conserved in each triad interaction. Interestingly, in three dimensions, triad interactions can be reduced to pair interactions (two-mode interaction) which is not feasible in two dimensional turbulence due to enstrophy which is also conserved in each triad in 2d turbulence (Kraichnan, 1967a). This result of triad-wise conservation is also valid for incompressible MHD turbulence (Biskamp, 2008). In MHD turbulence both the energy and cross-helicity can be shown to be conserved for each interacting triad thereby validating the localness of interactions in MHD case as well.

4.6 Phenomenology

As described earlier that a turbulent flow necessarily associates fluctuations of the flow variables over a broad range of spatial and temporal scales. Phenomenology in turbulence refers to a possible physical image by which these multiscale dynamics and energetics of a turbulent flow can be understood in a general way. So it is clear that phenomenology is neither an absolute reality nor a unique entity. Schematically, there are four episodes in a turbulence phenomenology : (i) Determination (by intuition or any other rigorous method) of one or more scale invariant quantity(s), (ii) Derivation of an approximate expression (by dimensional analysis) of that (or those) scale invariant quantity(s) as a function of other turbulence flow variables (length scale, corresponding velocity fluctuation, characteristic time, magnetic field

fluctuation, density fluctuation etc.), (iii) Determination of the characteristic time(s) governing any transfer (energy, helicity etc.) corresponding to the flow and finally (iv) Prediction of a power law of relevant spectral density(s) as a function of the wave numbers corresponding to different length scales and also derivation of other relevant characteristic scales as a function of different scale variables. In the following we shall give a brief description of two well-known phenomenologies namely (a) K41 (Kolmogorov's phenomenology) for 3D incompressible hydrodynamic isotropic turbulence and (b) IK (Iroshnikov-Kraichnan phenomenology) for 3D incompressible MHD turbulence in the presence of a strong external magnetic field.

4.6.1 K41 phenomenology

K41 phenomenology is a direct outcome of Kolmogorov's 1941 theories. It can be described by the image of Richardson's cascade (Richardson, 1922) i.e. self-similar energy cascading inside the inertial zone. In the absence of forcing or external energy injection and viscous dissipation, net energy flux rate (ε) is assumed to be the scale invariant quantity within inertial zone. Moreover, using the existence of a stationary state, ε can be thought to be

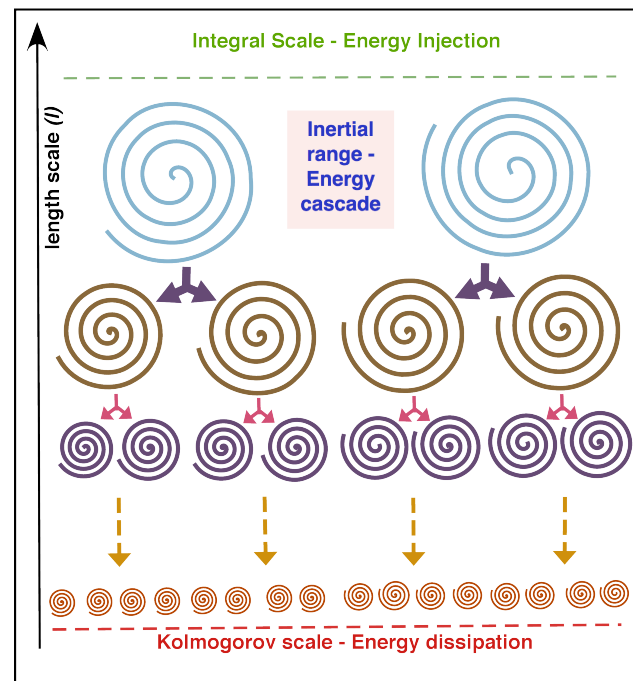


Figure 4.3: Schematic view of Richardson's energy cascade in turbulence by eddy fragmentation.

equal to the energy injection and dissipation rate respectively at the integral and Kolmogorov scale of the flow. By dimensional analysis, we can show that for an incompressible flow (density being normalised to unity), the inertial range energy flux rate is given by

$$\varepsilon \sim \frac{v_l^2}{\tau_l}. \quad (4.45)$$

Next step is to determine the characteristic time τ_l . According to Richardson's image, τ_l should be given by the time required for a complete distortion of a vortex of length scale l and is given by (as according to Kolmogorov, the distortion is caused by relative velocity and not the individual velocities at each point) so called **eddy turnover time** (ETT)

$$\tau_l \sim \frac{l}{v_l}, \quad (4.46)$$

where v_l is the velocity fluctuation corresponding to length scale l and physically it is nothing but the relative velocity (rather the magnitude of the relative velocity vector) between two points separated by a distance l . The use of ETT as the characteristic time expresses the scale invariant to be written as

$$\varepsilon \sim \frac{v_l^3}{l}. \quad (4.47)$$

Using the aforesaid definition of energy spectral density in homogeneous turbulence, we can write

$$E(k) \sim v_l^2 k^{-1} \sim (\varepsilon k^{-1})^{\frac{2}{3}} k^{-1} \sim \varepsilon^{\frac{2}{3}} k^{-\frac{5}{3}}.$$

This law is the most famous law in turbulence physics and is commonly known as **Kolmogorov's 5/3 law**. This approximate relation can be converted to an equation by introducing a dimensionless constant C called Kolmogorov's constant and the equation is written as

$$\boxed{E(k) = C \varepsilon^{\frac{2}{3}} k^{-\frac{5}{3}}}. \quad (4.48)$$

The value of C is determined experimentally and is about 1.4 – 1.6.

The equation (4.47) is also obtained from the exact relation (Antonia *et al.*, 1997) in a more direct way (without introducing the characteristic time) if we use the following definition

$$v_l \sim \sqrt{\langle (\delta \mathbf{v})^2 \rangle}. \quad (4.49)$$

The derivation of the final spectra is however not an immediate offspring of the exact relation which uses no a priori assumption on the scale invariance of ε .

★★ Another approach of obtaining the $k^{-5/3}$ spectrum (Nazarenko, 2011) consists in assuming that the energy spectral density i.e. $E(k)$ to depend only on ε and k then the only possibility is to obtain the above law given C is a dimensionless constant. This argument, however, is useful only if the energy spectral density depends on two variables in incompressible case (as only the length and the time are independent variables). In fact in MHD case (which we shall treat in the following subsection), the energy spectral density depends also on another variable called Alfvén speed and thus by using the previous method, one cannot obtain unique solution for the spectral law.

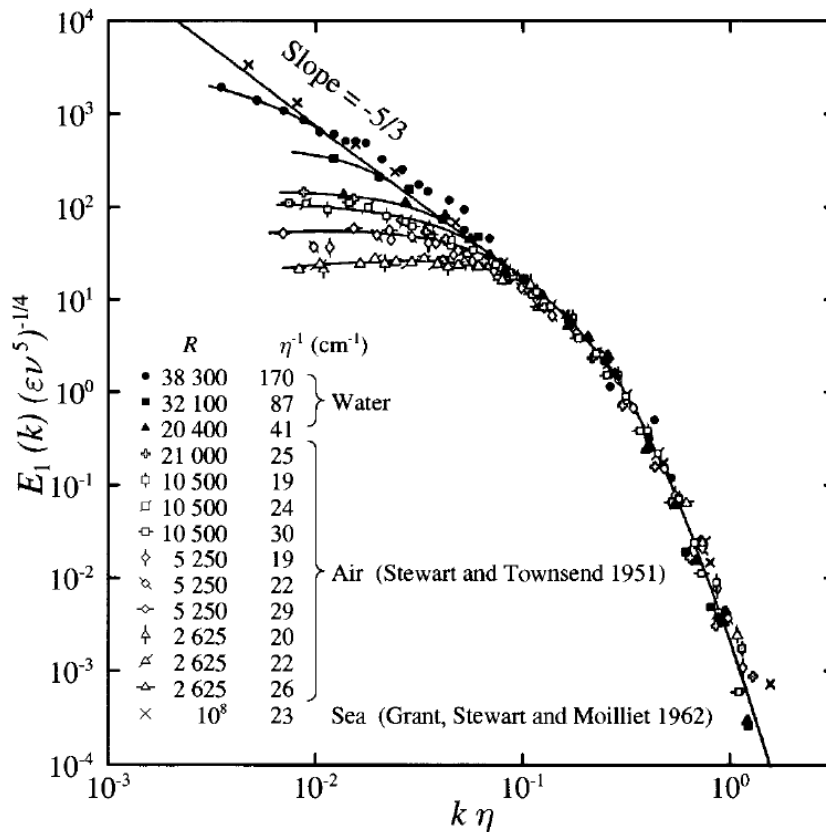


Figure 4.4: Normalized velocity power spectra from different experiments show universal $k^{-5/3}$ behaviour; Reprinted with permission from Gibson & Schwarz (1963) ; © (1963) Cambridge university press.

Universality in turbulence The most intriguing feature of turbulence is believed to be its universal properties despite the presence of enormous complex dynamics. That means, the regime of turbulence flow exhibits some common properties or features irrespective of the origin of the fluid (as far as the governing equations are the same) and the macroscopic conditions imposed on the flow regime. One of the formal ways to define this universality is in terms of the index of the power spectra. A considerable number of experiments have been carried out using different fluids in turbulence. Surprisingly, each of them has presented a zone with $-5/3$ power law (see figure 4.4). The interval for which we get the universal behaviour, is expected to represent the inertial zone (which will be discussed later) which is free from both the macroscopic and microscopic effects. However, the width of the zone with $-5/3$ is different from different experiments and can partly be attributed to difference in the initial Reynolds number of the corresponding flow. It is however important to note that, the parameter of universality (for example the index $-5/3$ of velocity power spectra in incompressible hydrodynamic turbulence) is not absolutely universal and can be different for different fluids (e.g. a plasma).

4.6.2 IK phenomenology

This phenomenology depends on the image of non-linear interaction of two oppositely propagating weakly fluctuating linear modes. According to this phenomenology energy is transferred from one length scale to another length scale by the deformation of one fluctuating linear wave by the other one. This phenomenology was independently proposed by [Iroshnikov \(1964\)](#) and [Kraichnan \(1965\)](#). They applied this concept in understanding the turbulence in a plasma fluid or more precisely in an MHD fluid. In incompressible MHD (as seen in the previous chapter), we have only one linear mode which is Alfvén mode. Now, in presence of a strong magnetic field (sometimes called the guiding magnetic field) \mathbf{B}_0 , which is supposed to be constant in space and time, the dynamical equation for the Elsässer variables ($\mathbf{z}^\pm = \mathbf{v} \pm \mathbf{b}$) is written as ([Elsässer, 1950](#))

$$\frac{\partial \mathbf{z}^\pm}{\partial t} \mp (\mathbf{V}_A \cdot \nabla) \mathbf{z}^\pm + (\mathbf{z}^\mp \cdot \nabla) \mathbf{z}^\pm = -\nabla \left(P + \frac{v_A^2}{2} \right) + \frac{1}{2} (\varpi^+ \Delta z^\pm + \varpi^- \Delta z^\mp), \quad (4.50)$$

where $\mathbf{V}_A = \frac{\mathbf{B}_0}{\sqrt{\mu_0 \rho}}$ and $\mathbf{v}_A = \frac{\mathbf{b}}{\sqrt{\mu_0 \rho}}$ represent respectively the true Alfvén speed and the normalized local magnetic field. The terms $\varpi^\pm = \left(\frac{\nu \pm \eta}{2} \right)$ correspond to the combination of kinematic viscosity and magnetic diffusivity. This equation indicates that in incompressible MHD turbulence, the non-linear interaction takes place between two oppositely propagating Elsässer fields where the fields

\mathbf{z}^+ and \mathbf{z}^- convect respectively with velocity $-\mathbf{V}_A$ and \mathbf{V}_A along the external magnetic field (see figure 4.5). This is called **Alfvén effect** which causes even the small scale fluctuations to be highly affected by the macroscopic magnetic field thereby modifying the inertial range spectra.

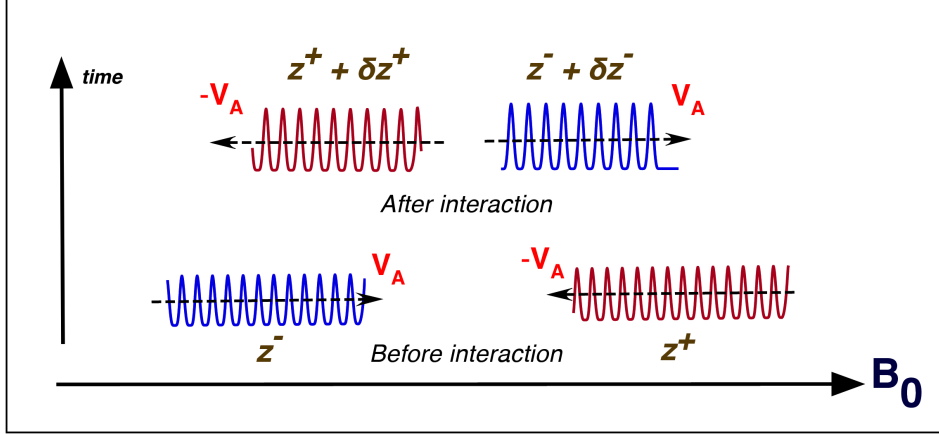


Figure 4.5: Sporadic interactions of Elsasser fields in IK phenomenology.

Unlike pure hydrodynamical case, here we can define two characteristic times (i) Alfvén time ($\tau_{Al} = l/V_A$) which corresponds to the time necessary for one single interaction between \mathbf{z}^+ and \mathbf{z}^+ and (ii) Non-linear time (τ_l) which measures the time required for a sufficient distortion of \mathbf{z}^+ or \mathbf{z}^- by one another and hence they are respectively given by

$$\tau_l^\pm = l/z_l^\mp. \quad (4.51)$$

Interestingly the transfer time (τ_{tr}) is not simply the non-linear time in general case and depends on the relative importance of the two dynamic time scales. Three cases are possible :

- (a) $\tau_{Al} \ll \tau_l$ - corresponds to weak turbulence regime,
- (b) $\tau_{Al} \sim \tau_l$ - corresponds to the critical balance regime in turbulence and
- (c) $\tau_{Al} \gg \tau_l$ which corresponds to K41 turbulence regime

IK phenomenology dwells on the first situation of the above three. $\tau_{Al} \ll \tau_l$ indicates that the deformation in one single interaction (δz_l^\pm) is too weak to transfer energy to the next length scale as

$$\frac{\delta z_l^\pm}{z_l^\pm} \approx \frac{\tau_{Al}}{\tau_l^\pm} \ll 1. \quad (4.52)$$

We need $N (\gg 1)$ number of interactions to have a sufficient deformation i.e. $\delta z_l^\pm \sim z_l^\pm$. Considering this interaction process to be completely random an

estimate for N can be obtained using the law of big numbers according to which

$$\frac{\delta z_l^\pm}{z_l^\pm} \sim \frac{1}{\sqrt{N}}. \quad (4.53)$$

The resulting transfer time is then given by

$$\tau_{tr_l}^\pm \sim N\tau_{Al} \sim \left(\frac{z_l^\pm}{\delta z_l^\pm}\right)^2 \tau_{Al} \sim \left(\frac{\tau_l^\pm}{\tau_{Al}}\right)^2 \tau_{Al} = \frac{\tau_l^{\pm 2}}{\tau_{Al}}. \quad (4.54)$$

The remaining part of the story is no doubt the determination of the scale invariants. Unlike the hydrodynamical case, here we have more than one scale invariant quantities. Alfvén speed, being a constant of the system, is invariant by scale by default. The total energy (sum of kinetic and magnetic energy) flux rate is considered to be scale invariant (but not necessarily a constant). The cross helicity (as we saw in the previous chapter) is also a conserved quantity and so its flux rate can also be assumed as a scale invariant quantity. This leads us to the fact that the pseudo-energies $\int (\mathbf{z}^\pm)^2 d^3x$ are conserved individually (shown in the previous chapter). So for them we have a couple of scale invariant flux rates which are given by ε^\pm . Their expressions can be written as

$$\varepsilon^\pm \sim \frac{(z_l^\pm)^2}{\tau_{tr_l}^\pm} \sim \frac{z_l^{+2} z_l^{-2} \tau_{Al}}{l^2}. \quad (4.55)$$

For the sake of simplicity we consider very weak velocity-magnetic field fluctuation correlation (for the general case, see [Grappin *et al.* \(1983\)](#) which leads to $z_l^+ \simeq z_l^-$. In that case $\tau_{tr_l}^+ \simeq \tau_{tr_l}^-$ and the dimensional relation (4.55) can be re-written as

$$\varepsilon \sim \frac{z_l^4 \tau_{Al}}{l^2}, \quad (4.56)$$

where ε may be regarded as (neglecting the constant factor 2) the total energy flux rate. Expressing $z_l^2 \sim E(k)k$, we get

$$\varepsilon \sim v_A^{-1}(E(k)k)^2 k \Rightarrow E(k) \sim (\varepsilon v_A)^{1/2} k^{-3/2}. \quad (4.57)$$

For inserting the equality, we introduce a dimensionless constant C_{IK} and we write

$$\boxed{E(k) = C_{IK}(\varepsilon v_A)^{1/2} k^{-3/2}}. \quad (4.58)$$

Although the mechanism of IK type transfer is different than that for K41 type transfer in inertial range cascade, the difference in spectral indices is practically very hard to realise (-1.5 and -1.67). It is the higher order moments who reflect the difference more prominently (ref. needed). One can easily understand that the transfer time in IK mechanism is larger than that of K41

as $\tau_l \gg \tau_{Al}$. This is because in Alfvénic turbulence, energy is transferred by the sporadic interactions of the oppositely propagating Elsasser fields and not by a continuous process of dissociation of the vortices.

Under the same assumption of isotropy, scale invariants and very weak velocity-magnetic field fluctuation correlation, if we consider the situation where $\tau_{Al} \lesssim \tau_l$, Alfvén effect can still be used where the number of interactions N necessary for a sufficient deformation of z_l is not estimated by the law of big numbers but can just be estimated as

$$N \sim \frac{\tau_l}{\tau_{Al}} \quad (4.59)$$

and so the resulting transfer time (τ_{tr_l}) is simply given as

$$\tau_{tr_l} \sim N\tau_{Al} \simeq \frac{\tau_l}{\tau_{Al}}\tau_{Al} = \tau_l, \quad (4.60)$$

which indicates the possibility of a $-5/3$ spectrum. For the case where $\tau_{Al} \gg \tau_l$, the effect of 'guiding' field is negligible and the flow basically behaves as a K41 flow with the velocity fields are replaced by the Elsasser fields.

★★ Very often for deriving the transfer time in critical balanced state, τ_{Al} is just replaced by τ_l in the expression of τ_{tr_l} obtained in (4.54). This is physically wrong (by construction) although it gives $\tau_{tr_l} \sim \tau_l$ too.

Here in defining the characteristic times, we assumed isotropy which was also a primary assumption of Kraichnan too. But physically it is somewhat inconsistent to maintain three dimensional isotropy in presence of a strong magnetic field. Without using any mean field, the idea of isotropy is theoretically saved by assuming the strong field \mathbf{B}_0 to be generated by the largest coherent structures of the system. But this explanation is not really consistent to its scale invariance which we used in the dimension analysis. Kraichnan's $-3/2$ spectrum is thus put into question in the framework of isotropic MHD turbulence (Biskamp, 2008). The phenomenology, on the other hand, is relevant if we consider an anisotropic or at least an axisymmetric (i.e. an isotropy in the plane perpendicular to that of the strong 'guiding' magnetic field) turbulent flow.

4.6.3 Utilities of phenomenology

The importance of phenomenology is not only limited in predicting different power spectra but also in understanding various aspects of turbulence:

(i) By phenomenological argument we can estimate the number of degrees of freedom (which is theoretically infinitely large) for a turbulent system.

(ii) We can also have an idea of the extent to which fluid equations can be valid for a turbulent system by comparing its macroscopic and microscopic length scales.

(iii) The law of energy decay in decaying turbulence can be obtained.

(iv) Probability distribution functions can also be approximated by phenomenological elements.

In the following four subsections, these points will be elaborated in a quantitative manner using dimensional analysis.

4.6.3.1 Degrees of freedom of a turbulent flow

A turbulent system is said to possess infinitely large number of degrees of freedom (references). Theoretically it can serve our purpose but in practical cases, for numerical simulations for example, we need to have an idea of that *infinitely large* value for a real system. More precisely, an estimation of the minimum number of grid points necessary to simulate a completely developed three dimensional turbulence is required. In the following we shall give an approximate order of that quantity using the above K41 phenomenology. From the expression of the mean energy injection rate (which is equal to the mean energy dissipation rate in a stationary state) the integral scale (l_0) can be written as

$$l_0 \sim \frac{v_0^3}{\varepsilon}, \quad (4.61)$$

and the dissipation scale or the Kolmogorov scale is expressed as

$$l_\eta \sim \sqrt{\nu \tau_l} \sim \sqrt{\nu l^{2/3} \varepsilon^{-1/3}} \Rightarrow l_\eta \sim \left(\frac{\nu^3}{\varepsilon} \right)^{1/4}. \quad (4.62)$$

The ratio of these two length scales can give an estimation of the spanning range for a "healthy inertial zone" which is

$$\frac{l_0}{l_\eta} \sim \left(\frac{\nu^3}{l_0^3 \varepsilon} \right)^{-1/4} \sim \mathfrak{Re}_e^{3/4}, \quad (4.63)$$

and for a simulation in three dimensions, the minimum number of grid points in a uniform grid is thus given by

$$\boxed{N \sim \mathfrak{Re}_e^{9/4}}, \quad (4.64)$$

Surprisingly this number is also controlled by the integral Reynolds number. For a completely developed turbulence, in general, we have $\mathfrak{R}_e \sim 10^4$ and so $N \sim 10^9$. As a completely developed turbulence is supposed to be spanned in all the available scales from the integral to the dissipative one, this above estimated N can be a reasonable measure of the number of degrees of freedom of a turbulent flow. This estimation works if we assume the inertial range motion is entirely disorganised. In reality, as the experiments show, the inertial range motion is often consisting of coherent structures like vortex filaments etc. This reduces significantly the number of degrees of freedom thereby paving the way for future simulation prospects (Frisch, 1995).

4.6.3.2 Applicability of fluid equations

The above estimation, by default, is adapted to incompressible turbulence. For compressible turbulence, the issue is more subtle and we have even to check the applicability of the hydrodynamic model by comparing the fluid dissipation scale and the kinetic mean free path of the molecules. Usually for the most of the fluids in our surroundings (water, air etc.) the speed of the sound is of the order of the thermal velocity (v_{th}) of the molecules. Additionally we suppose that the kinematic viscosity is written as the product of the molecular mean free path (λ) and the thermal speed (following usual formulation of transport co-efficients). Using these two facts, the ratio of the Kolmogorov scale and the molecular mean free path is given as (Corrsin, 1959; Frisch, 1995)

$$\Upsilon \equiv \frac{l_\eta}{\lambda} \sim \frac{\eta}{l_0} \frac{l_0 v_0}{\lambda v_{th}} \frac{v_{th}}{v_0} \sim M^{-1} \mathfrak{R}_e^{1/4}, \quad (4.65)$$

where M is the Mach number. Attention should be paid on the fact that the hydrodynamical model is applicable if $\Upsilon \gg 1$ i.e. $M \ll \mathfrak{R}_e^{1/4}$. For a typical system with $\mathfrak{R}_e \sim 10^4$, the condition reduces to $M \ll 10$. This, in turn, puts a question to the validity of hydrodynamical model for high Mach number ($M \sim 10$) compressible turbulence both from theoretical and numerical point of view. However, very high ($10^5 - 10^7$) Reynolds numbers are estimated both for cold interstellar molecular clouds (Elmegreen & Scalo, 2004) and the solar wind (Borovsky & Gary, 2008) which retains the validity of fluid approach in astrophysical or space plasma turbulence even for $M \simeq 10$.

4.6.3.3 Energy decay in non-forced turbulence

If a turbulent flow is not forced, it will dissipate energy in time due to viscous effects. An approximate law for this decay can be derived by two following assumptions:

(1) An "**infrared asymptotic self similarity**" (**IRSS**) for velocity with a negative² scaling exponent α which means for $l \rightarrow \infty$, $v_l \approx Cl^\alpha$, C being a constant.

(2) **Principle of permanence of large eddies** which asserts that if a freely decaying turbulent flow initially possesses IRSS, this symmetry will be preserved at later instants with same scaling exponent α and constant C .

Using the definition of IRSS and that of the spectral density of energy, we write for $l \rightarrow \infty$,

$$v_l^2 = C^2 l^{2\alpha} \Rightarrow E(k) = C^2 k^{-2\alpha-1}, \quad (4.66)$$

for $k \rightarrow 0$. As α is negative, the above law indicates a growing energy spectrum at small scales which is not physical. It is therefore necessary to have a lower cut-off scale l_0 below which the turbulence is of completely developed type and the scaling law $v_l \sim l^{\frac{1}{3}}$ is obeyed instead. This l_0 is called the integral scale which translates also with time. Corresponding v_0 scales as $v_0 \sim Cl_0^\alpha$. For integral scale Reynolds number $\mathcal{R}_0 \sim \frac{l_0 v_0}{\nu} \gg 1$, the mean energy dissipation rate can be estimated by

$$\frac{d}{dt} v_0^2 \sim -\varepsilon \sim -\frac{v_0^3}{l_0}. \quad (4.67)$$

Substituting the scaling law of v_l for large scales in the above equation, we get

$$\frac{d}{dt} (C^2 l_0^{2\alpha}) \sim -C^3 \frac{l_0^{3\alpha}}{l_0}, \quad (4.68)$$

Integrating the above equation, we get

$$l_0 \sim (t + t_0)^{\frac{1}{1-\alpha}}, \quad v_0 \sim (t + t_0)^{\frac{\alpha}{1-\alpha}}, \quad (4.69)$$

which further gives

$$E \sim (t + t_0)^{\frac{2\alpha}{1-\alpha}}, \quad \mathcal{R} \sim (t + t_0)^{\frac{1+\alpha}{1-\alpha}}, \quad (4.70)$$

where t_0 is a constant of integration. As α is negative, v_l and E always decrease with time whereas the integral scale increases with time. Reynolds number increases with time for $\alpha > -1$. On the other hand, for $\alpha < -1$, Reynolds number decreases and the above derivation fails once Reynolds number takes a value of the order of unity. This derivation is a general one. In his classic 1941b paper, Kolmogorov treated the three dimensional case $\alpha = -\frac{5}{2}$ and hence obtained $E \sim t^{-10/7}$ as the law of decay of energy. Interestingly, this particular choice of α was based on time independence of Loitsyansky's integral (1939) which was later invalidated by **Batchelor & Proudman (1956)**.

²Otherwise the velocity field is not homogeneous but only consists of homogeneous increments (**Frisch, 1995**).

4.6.3.4 PDF for velocity gradients

Using K41 phenomenology along with Landau argument, we can derive (following Frisch's book) probability distribution function (PDF) for velocity gradients given that the PDF for **velocity fluctuations at inertial scale** (v_0) is known. For that we assume the turbulence to be homogeneous and isotropic and $P_v(v_0)$ is known. The characteristic velocity fluctuation corresponding to Kolmogorov scale l_η is estimated by

$$(v_\eta) \sim v_0 \left(\frac{l_\eta}{l_0} \right)^{\frac{1}{3}}, l_\eta \sim \nu^{\frac{3}{4}} l_0^{\frac{1}{4}} v_0^{-\frac{3}{4}}. \quad (4.71)$$

The corresponding velocity gradient is then estimated by

$$s \sim \left(\frac{v_\eta}{l_\eta} \right) \sim v_0^{\frac{3}{2}} \nu^{-\frac{1}{2}} l_0^{-\frac{1}{2}}. \quad (4.72)$$

We know that if a random variable x follows a PDF $P_x(x)$, then a monotonic function of x denoted as $y = f(x)$ will follow a PDF which is given by

$$P_y(y) \sim \left| \frac{df^{-1}(y)}{dy} \right| P_x[f^{-1}(y)], \quad (4.73)$$

where f^{-1} is the inverse function of f .

In our case, identifying $s = f(v_0) = v_0^{\frac{3}{2}} \nu^{-\frac{1}{2}} l_0^{-\frac{1}{2}}$, we get

$$f^{-1}(s) = v_0 = s^{\frac{2}{3}} \nu^{\frac{1}{3}} l_0^{\frac{1}{3}}, \quad (4.74)$$

whence we get the resulting PDF for s which can be approximately written as

$$P_s(s) \sim \nu^{\frac{1}{3}} l_0^{\frac{1}{3}} s^{-\frac{1}{3}} P_v \left(s^{\frac{2}{3}} \nu^{\frac{1}{3}} l_0^{\frac{1}{3}} \right). \quad (4.75)$$

This relation is of dubious validity for the central part of the PDFs where the variables are comparable to their r.m.s values and can only be applied to the tail of the PDFs. Therefore low order moments of the velocity derivatives such as skewness, flatness etc. cannot be predicted by the above relation. According to Landau argument, PDFs of velocity fluctuations are believed to be non-universal due to its dependence of the detailed mechanism of the turbulence production. Non universality of velocity PDF propagates to the dissipative scale velocity gradient PDF by virtue of the above relation.

4.7 Dynamics and energetics of turbulence

4.7.1 Turbulent forcing

A flow field whose dynamics is governed by Navier-Stokes equations, dissipates energy by virtue of its viscosity. For such a system the turbulent regime decays

with time and we cannot get a stationary state. An external source of energy is therefore needed to sustain the turbulent regime and obtain a stationary state. This source is called a forcing term and the corresponding flow is said to be forced. In a stationary state, the injected energy rate equals to the dissipated energy rate (shown earlier). To obtain a considerable inertial zone, the forcing should act only at the largest scales i.e. at the smallest wave numbers ($\sim k_0$) of the system. In general the introduction of the forcing term in the Navier-Stokes equations may break its invariance under Galilean transformation. However the invariance is retained if the forcing term is delta-correlated in time (Frisch, 1995). In case of numerical simulations, the usual functional forms of forcing is chosen to follow

$$\mathbf{f}(k, t) \sim \mathcal{F}(k) e^{-\lambda(k-k_0)} \delta(t - t_0), \quad (4.76)$$

where λ is positive. Forcing means, in general sense, injection of a quantity into the system from exterior. In hydrodynamic turbulence, the only possibility of forcing is in the velocity field through Navier-Stokes equations. In MHD turbulence, forcing can be done through NS and Faraday equation by respective excitation of velocity field and magnetic field. Forcing the magnetic field is, however, not compulsory and is often avoided for the sake of simplicity both in theoretical and numerical works. One should understand that an exclusive forcing on velocity field can equally nourish the magnetic field and the corresponding energy through cross-helicity i.e. the coupling between turbulent velocity and magnetic field.

In order to avoid any adulteration of compressibility by the forcing, the forcing itself should be solenoidal (divergenceless) i.e. $\nabla \cdot \mathbf{f} = 0$ in the simulation of incompressible turbulence. For compressible turbulence, the determination of forcing scheme is a bit complicated story and the nature of forcing, in fact, affects the nature of turbulence i.e. the corresponding scaling and spectra (Mac Low *et al.*, 1998; Kritsuk *et al.*, 2007a; Federrath *et al.*, 2010).

4.7.2 Turbulent cascade

The concept of cascade is of key importance in the study of turbulence. By definition, turbulence associates a sequence of length and time scales. For incompressible turbulence, Richardson (1922) proposed an image where the vortices, which are considered to be the coherent structures of an ideal incompressible flow, get fragmented into smaller vortices and so on. In an interval of length scales which are sufficiently larger than the viscous or the dissipation length scale (l_η), the energy (in incompressible case it just means the kinetic energy in the absence of any body force field), which is a conserved quantity, therefore seems to be spent by the larger vortices in order to feed

the smaller vortices. If we associate a wave number k which is roughly equal to the inverse of the length parameter (for circular vortices, the diameter, for example) of the vortices, within the said interval, the energy is said to **flow** step by step (can be shown theoretically in hydrodynamic turbulence) from the lower wave number to higher wave number whence the notion of cascade takes birth. The energy must be cascaded through because for the aforesaid length scale interval, no mechanism is present to dissipate the energy from the system. This interval, where the inertial terms dominate over the viscous terms, is called the **inertial zone**. Without any difficulty we can understand that the energy cascade takes place within that inertial zone. The idea of turbulent cascade is extended for other conserved quantities too (like the kinetic helicity in 3D hydrodynamic turbulence, enstrophy in 2D hydrodynamic turbulence, magnetic helicity in 3D MHD turbulence etc.). One should not forget that Richardson image is a *possible image* and not *the only image* for explaining the energy cascade.

The concept of cascade is more adapted in terms of the energy spectra and triad interactions. One can show that both in incompressible hydrodynamic and MHD turbulence, spectral energy is conserved for individual triads (Biskamp, 2008). More generally speaking, the spectra of ideal invariants are conserved in non-linear interactions. If such a quantity is added or injected externally to the system (by forcing for example) at an inertial range wave number k_{in} , it gets scattered into other regions of k -space by triad interactions. For local interactions, this scattering should be in small steps thereby setting up a cascade of that invariant. Note that, there is no restriction which says that the cascade should be unidirectional. It is however observed that the net transfer always takes place in a direction either from larger scale to smaller scale or the contrary. Depending on the direction of the transfer of a quantity, we have two types of cascades. The quantities which cascade from larger scale to smaller scale (i.e. from lower k to higher k) are said to undergo a **direct cascade** (energy in 3D HD and MHD turbulence, enstrophy in 2D HD turbulence etc.). For the opposite case, where the net transfer is from lower length scale to higher length scale, an **inverse cascade** (energy in 2D HD turbulence, magnetic helicity in 3D MHD turbulence etc.) is said to take place. Theoretically it is not very evident to determine the cascade direction. However there exist some theoretical attempts which can be useful, under certain circumstances, to determine the cascade direction. Kolmogorov never insisted on the theoretical determination of the cascade direction. Historically for the first time interesting rigorous methods of understanding the cascade direction for both evolving and stationary turbulence were proposed by Fjortoft (1953). These methods were simple but indirect (Nazarenko, 2011). In addition they were structured to treat hydrodynamic

turbulence. The approach conceived by Kraichnan (1967a) was the same as that of Fjortoft. In addition, he used the locality assumptions to predict the direct and inverse cascade spectra in 2D hydrodynamic turbulence. But it is lengthy and does not seem to be adapted readily for MHD turbulence. Some years later Kraichnan & Montgomery (1980) proposed another method of determining cascade direction using Gibbs functional under the assumption of **absolute equilibrium**. This method can successfully be applied to 2D and 3D turbulence for both hydrodynamic and MHD turbulence. However, in this method one needs to know the exhaustive set of invariants for a given dynamical system and thus cannot be readily applied for a complex system³. All the above discussions was for incompressible turbulence. For compressible turbulence a priori we do not have the Richardson's view of cascade as the velocity fields are no more divergence-less and even if we create some initial vortices, sequential fragmentation of those structures will not be guaranteed due to the fluid compressibility (figure 7.1 Frisch (1995)). A phenomenological view equivalent to the Richardson cascade is thus required to understand the transfer of the conserved quantities in the inertial zone which itself is of questionable existence in case of compressible turbulence. A discussion will be done later while discussing different aspects and studies of compressible turbulence.

4.7.3 Turbulent dissipation

In his 1954 lecture series, Chandrasekhar specified **dissipation** to be one of the two most fundamental aspects (the second being interscale energy transfer) of turbulence. In his words, "[Viscous dissipation is the only mechanism available to a fluid medium to dissipate the energy input and thus maintain an energy balance. Because of this, and because it is physically clear that turbulence cannot exist in an inviscid medium, viscosity and viscous dissipation are necessary aspects of the turbulence phenomenon.](#)" According to the above idea of cascading, energy is getting transferred in a stepwise manner from the integral scale to smaller scale and so on by the consecutive fragmentation of vortices. Dissipation occurs at very small length scales where the corresponding vortex size scale is such that the $\nu\Delta\mathbf{v}$ dominates over the inertial terms. It is simply because of the Laplacian in the viscous term which makes the term inversely proportional to the square of the length scale. Energy is then dissipated from the system as a consequence of the intermolecular collisions. The length scale l_η which initiates the dissipation is known as Kolmogorov scale. For hydrodynamic turbulence an estimation of Kolmogorov scale can

³In weak turbulence (beyond the scope of my thesis) regime, we can however prove rigorously the sense of the cascade (Nazarenko, 2011).

be obtained by using the K41 phenomenology and is given as (see equation 4.62)

$$l_\eta \sim \left(\frac{\nu^3}{\varepsilon} \right)^{1/4}. \quad (4.77)$$

In reality, however, it is usually found that dissipation becomes important at scales $\sim 30l_\eta$. This fact can trivially be attributed to the neglect of the dimensionless constant in the dimension analysis. A possibility of weaker non-linear interactions than those predicted by the phenomenology can nevertheless be thought to be a relevant reason for this discrepancy.

For MHD turbulence, similarly, the application of IK phenomenology, estimates the corresponding dissipation scale (l_D) to be

$$l_D \sim \left(\frac{\nu^2 V_A}{\varepsilon} \right)^{1/3}, \quad (4.78)$$

where the kinematic viscosity and magnetic resistivity are assumed to be of the same order and so is for the kinetic energy and magnetic energy flux rate. Considering ε and V_A to be of the order unity (which is realistic), the dissipation scale in MHD turbulence can be shown to be larger than that for ordinary turbulence (for real instances where $\nu \ll 1$). This represents earlier dissipation and therefore weaker cascading in MHD turbulence (in comparison with hydrodynamic turbulence) which is caused by the sporadic nature of non-linear interaction between Alfvén waves. It is noteworthy that the existence of turbulence in an inviscid fluid is not impossible physically. Nevertheless, for theoretical consideration, a finite non-zero dissipation is essential for the fluid in order to guarantee the convergence of various global variables like total energy, total helicity etc.

4.8 Intermittency

Intermittency is basically a concept of chaos dynamics revealing the irregular variation of the phases of a dynamics which is apparently periodic and chaotic. In the framework of turbulence (incompressible turbulence is concerned here), intermittent behavior is perceived in various situations such as dissipation of kinetic energy in fully turbulent flows, transition between turbulent and non-turbulent regime in turbulent jets, scaling of structure functions even in the inertial zone of a completely developed turbulence.

Intermittency in the dissipation range of turbulence is very often seen in experimental and observational data (see figure 4.6). But it is not in contradiction with traditional image of self-similar K41 phenomenology which is valid within inertial range. Dissipation range intermittency was discovered

by (Batchelor & Townsend, 1949) and was, for the first time, explained by Kraichnan (1967b) using arguments a la Landau by claiming that very minute fluctuations in the energy dissipation rate get enormously amplified in the far dissipation zone when the energy spectrum is assumed to fall off faster than an algebraic fall. For an intermittent flow, the fluctuations of a quantity are not uniformly distributed statistically but become increasingly sparse as the spatial or temporal resolution increases. A quantitative measurement of intermittency can statistically be carried out by the quantity **flatness** or kurtosis of the fluctuations and is defined as

$$F = \frac{S_4(l)}{(S_2(l))^2} \quad (4.79)$$

and intermittency is said to exist if flatness is independent of the scale chosen. In the K41 phenomenology (discussed earlier), one of the fundamental

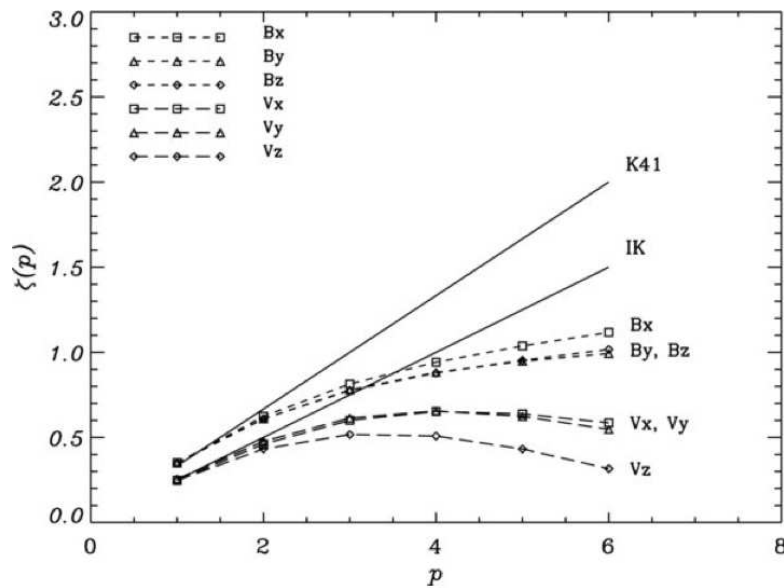


Figure 4.6: Clear deviation of the moments of velocity and magnetic fluctuations from the self-similar scaling laws of K41 and IK phenomenology in the solar wind; *Reprinted with author's permission from Salem et al. (2009);* © (2009) AAS. DOI: 10.1088/0004-637X/702/1/537

assumptions was the **spatial self-similarity** of the random velocity fields in the inertial zone. That means within inertial zone, the spatial distribution of the coherent structures (eddies in case ordinary turbulence) is identical at any length scale chosen. Mathematically self-similarity requires the mean turbulent state corresponding to a length scale to be mapped to that at another

length scale by a simple scale factor which, in turn, requires the scaling exponent ξ_n to be proportional to n . In terms of the structure functions this can be written as (for isotropic turbulence)

$$S_n(l) = \alpha_n l^{pn} \quad (4.80)$$

where p is a constant with respect to n but changes with different choice of phenomenology. For K41 phenomenology, we get $p = \frac{1}{3}$ and so we should obtain table 4.1

n	1	2	3	4	5
ξ_n	1/3	2/3	1	4/3	5/3

Table 4.1: Self-similarity with K41 phenomenology.

This value of p can also be justified by the Kolmogorov's exact relation in turbulence which predicts a linear scaling between the longitudinal third order velocity structure functions and the fluctuating length scale. Moreover, in the experiment performed in S1 wind tunnel of ONERA the second order longitudinal structure function is found to scale as $l^{2/3}$ for a substantial large range (see figure 4.7).

On the other hand, for IK phenomenology, we have $p = \frac{1}{4}$ and so the table becomes 4.2

n	1	2	3	4	5
ξ_n	1/4	1/2	3/4	1	5/4

Table 4.2: Self-similarity with IK phenomenology.

In the current context, any deviation from self-similar values i.e. the tabular values of ξ_n represents intermittency in the inertial zone. Even if $\xi_n = pn + q$ with q a non-zero constant, the flow is no more self-similar and becomes intermittent. Experiments and observational data show clear deviation for the moments higher than 3. Unlike dissipation range intermittency, inertial range intermittency contradicts K41 phenomenology and the reason for this type of intermittency is not very easy to explain. As inertial zone intermittency is prominent for higher order moments, an intuitive explanation may be attributed to the tail of the velocity PDFs of the corresponding flow. Various attempts have been taken to model the behavior of the higher order moments. These models are explained in a brief and qualitative manner in the following as a function of their increasing complexity.

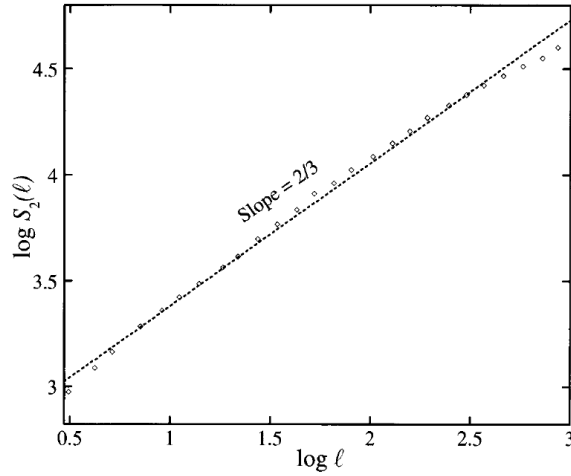


Figure 4.7: Scaling of second order longitudinal velocity structure functions (in logarithmic plot) in time domain using data obtained from S1 wind channel of ONERA; *Reprinted with permission from Frisch (1995)*; © (1995) Cambridge university press.

4.8.1 β fractal model

The simplest of all the models for inertial range intermittency is the β - fractal model which was proposed by Frisch *et al.* (1978). This model uses the concept of fractal which is also self-similar by construction. Intermittency in this model is introduced due to the fact that the coherent structures of a length scale occupy an effective volume which is a fraction of the effective volume occupied by its immediate predecessor structures. The ratio of the current and the previous volume is given by a constant factor β where $0 < \beta < 1$. A phenomenological view of this model is given in the figure 4.8. For three dimensional turbulence, the corresponding scaling exponent (following K41 phenomenology) is given by

$$\xi_n = \frac{n}{3} + (3 - D)\left(1 - \frac{n}{3}\right), \quad (4.81)$$

where D is the fractal dimension i.e. the effective spatial dimension covered by the coherent structures of a turbulent flow. D is formally written as $D = d + (\ln\beta/\ln B)$ where B is the ratio of consecutive smaller to the larger length scale (in general we assume $B = \frac{1}{2}$). If $D = 3$ i.e. the smaller eddies are supposed to occupy the same volume as that occupied by their parent eddies, the intermittent correction is zero. On the other hand, even if $D \neq 3$, intermittency is not perceived for the 3rd order moments. This latter fact is visibly linked with the value of n and thus the chosen phenomenology. For

higher order ($n \geq 4$) moments, if $D < 3$, the correction part is negative and ξ_n versus n graph shows a good agreement with the experimental or measured values upto 8th order moments. A ξ_n vs. n graph for the specific choice of $D = 2.8$ is shown in figure (4.9) along with the measured values. This

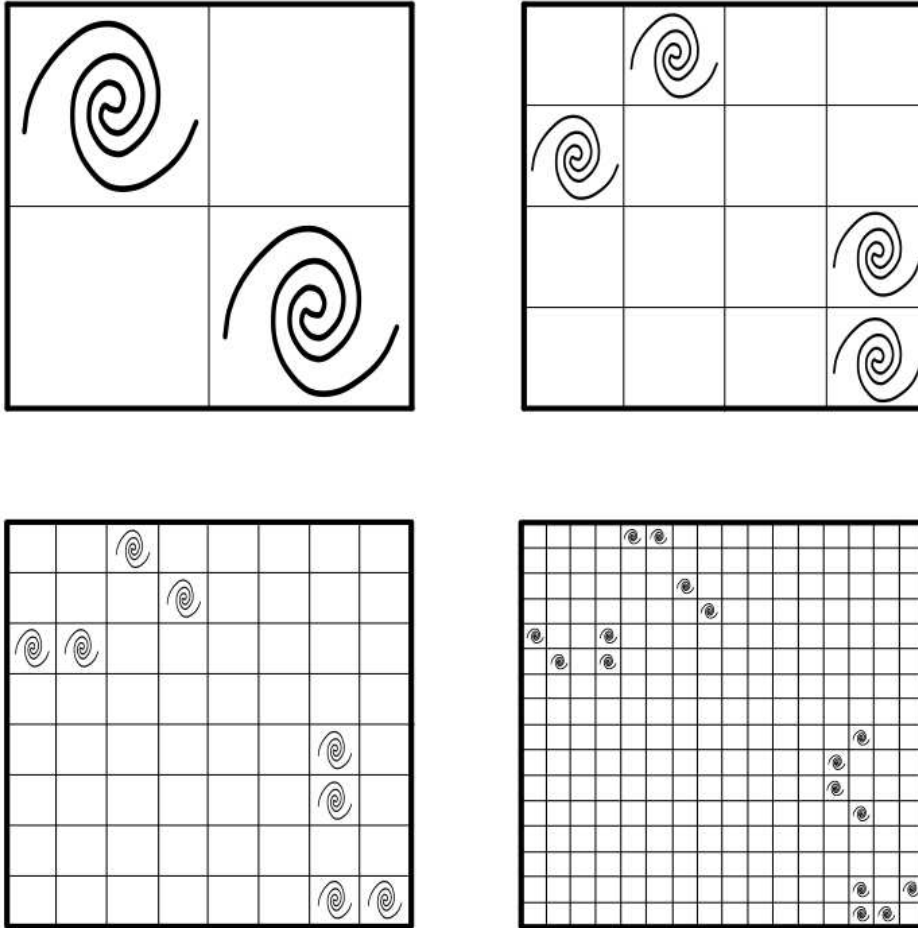


Figure 4.8: Two dimensional representation of fractal cascade for $\beta = \frac{1}{2}$; Courtesy: Sébastien Galtier.

model is later generalized using bi-fractal and multi-fractal model for a better agreement with the experimental values or the values measured from observed data. Bi-fractal model, at its trivial version, corresponds to the Kolmogorov law for $n \leq 3$ and to the β fractal model for $n > 3$.

4.8.2 Refined similarity hypothesis : Log-Normal model

Landau objected (Frisch, 1995) to K41 phenomenology where the local velocity fluctuations (δv_l) corresponding to a single length scale l are linked to

a scale averaged net energy flux rate of dissipation ($\langle\langle\varepsilon\rangle\rangle$). In order to solve this inconsistency, Oboukhov (1962) replaced the scale averaged quantity by $\langle\varepsilon_l\rangle$, a mean energy flux rate averaged on a sphere of length scale l . Finally in order to quantitatively apply the idea of Oboukhov in turbulence scaling, Kolmogorov (1962) proposed **refined similarity hypothesis** which can be expressed mathematically as

$$S_n(l) = C \langle\varepsilon_l^{n/3}\rangle l^{n/3}. \quad (4.82)$$

This hypothesis is adapted to inertial zone as well as the dissipative zone in an equal footing thereby leading to a realistic model of dissipative zone intermittency. Historically this model precedes β fractal model and is the first ever model of intermittency in turbulence. The model is called log-normal as the PDF of the fluctuations of flux rate of energy corresponding to length scale l i.e. ε_l is supposed to follow a **log-normal law**. As a consequence, this model expresses ξ_n as a non-linear function of n unlike the fractal model. Indeed one finally obtain (assuming K41 phenomenology)

$$\xi_n = \frac{n}{3} - \frac{\mu}{18}n(n-3), \quad (4.83)$$

where μ is a parameter to be adjusted according to the measured data set. This model holds satisfactory agreement with the measured values for $n < 10$ for $\mu \simeq 0.2$. Recent experiments however show a net divergence for moments $n > 10$ which cannot be predicted by this model and thus requires a more sophisticated model (see figure 4.9).

4.8.3 Log-Poisson model

This model was proposed by She & Leveque (1994) and is considered to date to be the most successful model in hydrodynamic turbulence. The model fits well with the experimental and numerical results upto $n = 16$. In this model, the PDF of ε_l is supposed to obey a log-Poisson law. The scaling exponent, hence obtained, is given by

$$\xi_n = \frac{n}{3} + \frac{2}{3} \left(\frac{1 - \lambda^{n/3}}{1 - \lambda} - \frac{n}{3} \right), \quad (4.84)$$

where λ represents the degree of intermittency and decreases with increasing intermittency. This is also a parameter and can be adjusted externally in order to have the best fit with the experimental and numerical measures. For hydrodynamic turbulence $\lambda = \frac{2}{3}$ shows considerable agreement with measured values for $n = 16$ whereas for MHD turbulence, a choice of $\lambda = \frac{1}{3}$ gives a good agreement for $n \leq 8$ (the best fit obtained to date by this model) with

the velocity fields being replaced by Elsasser variables. The reason of this difference in values of 'best' λ is not clear. It is however thought that the best beta should approximately be the ratio of the effective dimension available for the dissipative structures to the total accessible dimension for the flow. For 3D hydrodynamic turbulence, the dissipative structures are one dimensional vortex filaments (so the effective available dimension is $3 - 1 = 2$) whereas for 3D MHD case we find two dimensional current sheets (the effective available dimension is $3 - 2 = 1$) to be the corresponding dissipative structures. It is important to note that this model is readily applicable to study the exact scaling relation of MHD turbulence (for 3rd order moments) only if the velocity and the magnetic field fluctuations are very weakly correlated.

In case of compressible turbulence, the notion of intermittency is not very clearly established. No satisfactory model is made to date for the corresponding intermittency principally because of our ignorance of the phenomenology of the compressible turbulence. A brief discussion on the modeling of intermittency in compressible turbulence is given in the chapter 5.

4.8.4 Extended self-similarity

All of the above discussion of intermittency was based on the deviation from the scaling relation of type equation (4.19). Both from the numerical and observational studies, it is seen that the scaling relation associates minimum error at $n = 3$. Moreover, the exact relations in turbulence theoretically prove (discussed in chapter 6) the linear scaling between S_3 and the fluctuation length scale. Using this fact, a modified scaling relation can be proposed in the following form

$$S_n(l) = \alpha'_n S_3^{\xi_n}, \quad (4.85)$$

which indeed gives a substantially larger "inertial range of scaling" (Benzi *et al.*, 1993) along with a remarkable precision in the determination of the scaling exponents. This formulation is called **extended self-similarity** (ESS) or extended scaling relation (Biskamp, 2008). In addition, the scaling exponents determined from ESS do not depend on the Reynolds number and hence completely developed turbulent scaling can be achieved even at considerably lower Reynolds number just owing to this relation. However, ESS scaling is found to degrade (Biskamp, 2008) with increasing value of n and hence only a limited number of scaling indices can be determined with high precision.

Besides velocity structure function scaling, ESS also assures a broader inertial range and a better precision in case of passive scalar⁴ scaling. For a

⁴A scalar which flows with the fluid without affecting the flow field by its own evolution. e.g. fluid temperature.

passive scalar θ , the ordinary scaling relation can be written as (Monin *et al.*, 1975)

$$\langle [(\delta\theta)^2 \delta v]^{n/3} \rangle = \alpha_n'' I^{\xi_n}, \quad (4.86)$$

whereas using ESS, the modified relation becomes

$$\langle [(\delta\theta)^2 \delta v]^{n/3} \rangle = \alpha_n'' \langle (\delta\theta)^2 \delta v \rangle^{\xi_n}. \quad (4.87)$$

However, ESS cannot produce better results for scaling of pure moments of passive scalars like $(\delta\theta)^n$ which do not associate any exact relation unlike $(\delta\theta^2 \delta v)$.

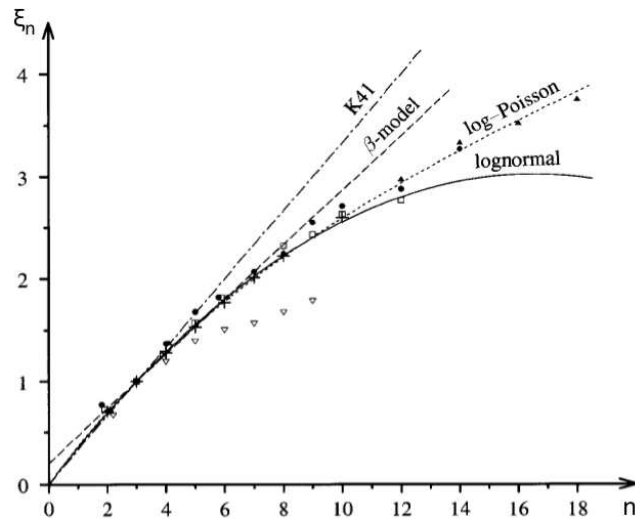


Figure 4.9: Comparison of different models of intermittency: plot of n th order moment for velocity structure function as a function of n , the discrete points with different colors and shapes (black and white triangles, white square, black circle and crosses) correspond to data obtained from different experiments, the straight chain line, dashed line, dotted line and the solid line correspond respectively the theoretical predictions of K41, beta-fractal with $D = 2.8$, log-Poisson and log-normal models; *Reprinted with permission from Frisch (1995)*; © (1995) Cambridge university press.

Turbulence in compressible fluids

Contents

5.1	Why is it important ?	83
5.2	Primitive theoretical approaches	86
5.3	Numerical approaches using one dimensional model .	88
5.4	Numerical Simulations in higher dimensions	90
5.4.1	Numerical methods for compressible turbulence	90
5.4.2	Piecewise Parabolic Method (PPM):	90
5.4.3	Compressible intermittency	97
5.4.4	Compressible and solenoidal forcing	99
5.4.5	Choice of inertial zone and sonic scale	101
5.4.6	Two-point closure in EDQNM model for compressible turbulence	102
5.5	Observational studies	102

5.1 Why is it important ?

DIFFERENT notions, characteristics and exact relations which we have discussed till now are all based on incompressible turbulence. Historically, incompressible turbulence was approached first because of two basic reasons: (i) the laboratory experimental results (Frisch, 1995), to which any newly established theory could be matched, were all liquids which are fairly incompressible fluids and atmospheric turbulence which was of central interest for the aerodynamic engineers was associated with atmosphere which is weakly compressible as the velocity fluctuations are considerably inferior to the sound speed and (ii) incompressible turbulence dynamics is much easier to handle mathematically than the compressible one. In some communities it was (rather is still) however believed that turbulence in highly compressible fluids is not physical. In his 1954 lectures (Chandrasekhar, 1954), S. Chandrasekhar clearly mentioned, "It exists in incompressible fluids or with small

(with respect to the velocity of sound) velocities in a compressible fluid, so that to sufficient accuracy, the problems of turbulence may be discussed in terms of incompressible fluids." Interestingly in the year 1948, J.M. Burgers proposed (Burgers, 1948) a simplified form of Navier-Stokes equations in a view to describing a one-dimensional highly compressible flow with shock discontinuities. He also predicted the law of energy spectra $E(k) \sim k^{-2}$ for the corresponding turbulence in such a fluid using a new phenomenology of his own.

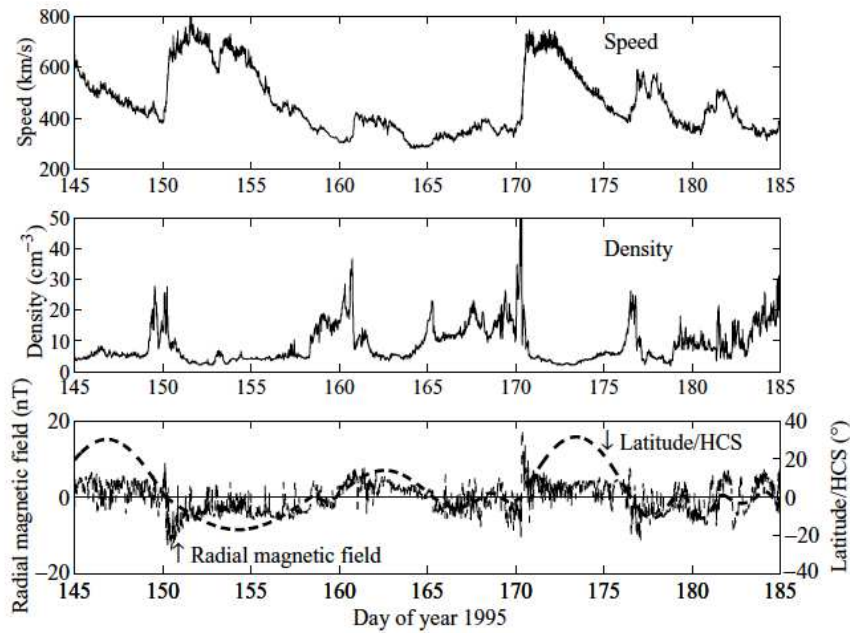


Figure 5.1: WIND spacecraft data of velocity, density and radial magnetic field fluctuations (Days in 1995); *Reprinted with permission from Meyer-Vernet (2007)* ; © (2007) Cambridge university press.

Interest for compressible turbulence increased with the gradual developments in (i) aeronautics, (ii) space-physics and (iii) astrophysics. The modern flights are made high speed including the supersonic ones which are used for military purpose. These necessarily bring about the formation of shock waves thereby bringing forth compressible turbulence .

Starting from 1960s, several missions like Mariner 2, Helios 1 and 2, Wind, ACE, Ulysses etc. are employed to study the space plasma properties in the solar wind and planetary magnetospheres using in-situ measurements. Density fluctuations of the solar wind plasma always drew attention due to their non-trivial correlation with the velocity and magnetic field fluctuation data.

In the figure 5.1, we can clearly visualize the density fluctuation peaks are associated with the abrupt changes of radial velocity fluctuation and also with the change of sign of the radial magnetic field. These data are obtained by the WIND spacecraft from the ecliptic solar wind in the year 1995. This indicates that the density fluctuates considerably in solar wind turbulence which, in turn, justifies the compressible character of the corresponding turbulence. The degree of fluctuation is found to be more profound in slow wind than in fast wind. Furthermore compressibility in solar wind turbulence is believed to play a key role in the heating of the fast solar wind (Carbone *et al.*, 2009). A study of compressible turbulence is thus essential for understanding the physics of the solar wind.

Cold interstellar molecular clouds which collapse under their self-gravitational force are also found to be turbulent associating non-negligible density fluctuations. The competition between gravitational collapse and the convective turbulence in such a cloud is indeed considered to be responsible in star formation mechanism (Vázquez-Semadeni *et al.*, 1996). Moreover, power laws corresponding to turbulent Mach number and density fluctuations are predicted from the astrophysical and space plasma data analysis.

Several numerical works on compressible turbulence have been carried out (Passot *et al.*, 1988; Vázquez-Semadeni *et al.*, 1996; Hennebelle & Audit, 2007; Kritsuk *et al.*, 2007a,b; Schmidt *et al.*, 2009; Schmidt, 2009; Federrath *et al.*, 2010) in order to verify the above space physical or astrophysical predictions and also to understand the basic physics and phenomenology in compressible turbulence – specially the distinction between sub-sonic and supersonic turbulence.

From a theoretician’s point of view, compressible turbulence is also interesting as well as challenging. The variation of density destroys the quadratic nature of the total energy density which is no longer $v^2/2$ (in hydrodynamic case) or $(v^2 + v_A^2)/2$ (in MHD case) and also includes an internal energy term which can be calculated from the corresponding thermodynamic closure and has, in general a non-trivial form (as described in the chapter 2). The role of density fluctuations in scaling, spectral laws and phenomenology is an important matter to investigate analytically. In case of compressible plasmas, the coupling between the density fluctuations and the magnetic field fluctuations is also of key importance and thus should be understood theoretically.

In this chapter we shall try to give a structured review on some theoretical, observational and numerical works in the framework of compressible turbulence which had been performed until the debut of my thesis and played significant role in the motivation and progress of my thesis work. Different sections will correspond to different problematics and interests in compressible turbulence. Within a section, significant and relevant works on that theme

will be discussed in a chronological order. No pretension is made to cover ¹ all the important works in compressible turbulence. An important skip relevant to my thesis interest is however regretted in advance. This review part will be followed by a schematic discussion on how different notions and features of incompressible turbulence are modified in case of compressible turbulence. In the next chapter, we shall discuss exact relations in incompressible and compressible turbulence which will further clarify the intrinsic difference between these two turbulences by the help of analytical approaches.

5.2 Primitive theoretical approaches

This section will basically consist of some initial but significant theoretical approaches to compressible turbulence. These works were done from a pure theoretical interest and without any significant experimental or numerical background (which was difficult to achieve at that period).

Despite his scepticism for turbulence in highly compressible fluid medium, S. Chandrasekhar was the first to publish an analytical paper in compressible isotropic turbulence (Chandrasekhar, 1951). In this paper he showed analytically that for an isotropic turbulence the correlation (R) between the density fluctuations (about their statistical mean value) of two arbitrary points associates a constant of motion which is given by $I = \int_0^\infty r^2 R dr$. Using this he predicted a k^2 spectrum for the power spectral density (PSD) of R for the largest scales of the system. This spectral behaviour indicates that the largest eddies of density fluctuations are determined by the initial conditions of the flow and thus reflect permanent features of the system. In the same paper he also deduced an evolution equation of R which couples the velocity fluctuations and density fluctuations in a compressible fluid with an adiabatic closure. However he solved that equation in the very restricted case of subsonic turbulence for which he obtained spherical wave solutions for R with phase speed $\sqrt{2}C_S$ where C_S is the sound speed in the flow medium. Unfortunately, at that time we had neither satisfactory observational data nor numerical data to test his predictions.

Another important theoretical approach was made in the year 1970 by V.E. Zakharov and R.Z. Sagdeev (Zakharov & Sagdeev, 1970). Their work was based on "acoustic turbulence" which concerns an irrotational potential flow. In their approach, they investigated the development of a turbulent flow in the wave space under very weak density perturbations (of first order) and derived

¹In this review, we will mainly discuss the works related to the fundamental characteristics of compressible turbulence; important engineering and aeronautical works are unfortunately beyond the scope of this review.

a continuity equation in Fourier space of the form

$$\frac{\partial \mathcal{E}}{\partial t} + \frac{\partial P_k}{\partial k} = 0, \quad (5.1)$$

where \mathcal{E} and P_k represent respectively the kinetic energy power spectrum and the corresponding flux. Both by analytical method and dimensional arguments, they obtained a $k^{-3/2}$ spectrum for the energy spectrum which was similar to the energy spectrum obtained by Zakharov for weak turbulence regime in a previous work (Zakharov, 1965). In the year 1973, Kadomtsev & Petviashvili published (Kadomtsev & Petviashvili, 1973) an alternative theory based on the dominance of shocks in turbulent scaling. They introduced a delta correlated random, potential force which they concluded to be indispensable in maintaining a stationary acoustic turbulence regime. Without that forcing, the sawteeth of acoustic modes (which they obtained as the solution) are dissipated in time. They also realized that the consideration of "relay energy transfer" from one scale to another cannot be valid in acoustic turbulence because the harmonics of a sawtooth are phase correlated and hence get damped together due to energy absorption behind the shock front. However, energy transfer along the spectrum becomes possible if the phase correlations are neglected. But in that situation absorption of individual harmonics should be taken into account which finally lead to the phenomenological equation

$$\frac{\partial v_k^2}{\partial t} + \frac{\partial \Gamma_k}{\partial k} = -\alpha \frac{\Gamma_k}{k}, \quad (5.2)$$

where v_k is the Fourier transform of velocity and $\Gamma_k = Av_k^2 k^3 / C_S$, A and C_S being respectively a constant and the isothermal constant sound speed. α denotes another constant. The novelty in their equation with respect to that of Zakharov & Sagdeev resides at the right hand term which reflects the absorption term of a given harmonic in the shocks. In order to evaluate α , they considered a steady state for which they obtained $\Gamma_k \sim k^{-\alpha}$. Finally assuming $v_k^2 \sim k^{-2}$ in presence of shock wave (as obtained from Burgers' equation), they found $\alpha = 1$ which renders the final form as

$$\boxed{\frac{\partial v_k^2}{\partial t} + \frac{\partial \Gamma_k}{\partial k} = -\frac{\Gamma_k}{k}}. \quad (5.3)$$

Using Hopf characteristic functionals (Hopf, 1952) to "liquid particles" in sub-sonic turbulence, Moiseev *et al.* (1981) predicted self-similar spectrum for the compressible vortices² in an adiabatic fluid and is written as

$$E_k = K \rho_0 C_{S0}^{\frac{2}{1-3\gamma}} \bar{\varepsilon}^{\frac{2\gamma}{3\gamma-1}} k^{-\frac{5\gamma-1}{3\gamma-1}}, \quad (5.4)$$

²In sub-sonic turbulence, they assumed a weak compressible effect which does not modify the vortex structures but just add compressible perturbations on them.

where $E_k \equiv v_k^2 K$ is a constant of proportionality, ρ_0 and C_{S0} are respectively the equilibrium density and sound speed, $\bar{\varepsilon}$ denotes the dissipation rate of kinetic energy (the compressible energy was not taken into account) and γ is the adiabatic index. In addition, for a very small turbulent Mach number ($M \ll 1$), they predicted

$$\boxed{\frac{v_c}{v_s} \sim M^2}, \quad (5.5)$$

where v_c and v_s are respectively the compressible and the solenoidal components of the average velocity fluctuations (see Helmholtz decomposition, Chapter 2).

Finally for $M \leq 1$, they derived another power law for kinetic energy spectrum from equation (5.3) and is written as

$$E_k = K \rho_0 \bar{\varepsilon}^{\frac{2}{3}} L^{\frac{5}{3}} (kL)^{-\frac{5-M^2}{3-M^2}}, \quad (5.6)$$

where L is the forcing scale of the system and the other symbols carry their usual meaning. The above equation is not self-similar due to the presence of Mach number. The equation (5.6) is shown to reduce to the self-similar equation (5.4) when M^2 is assumed to be independent of L .

5.3 Numerical approaches using one dimensional model

In this section we shall try to discuss very briefly some important theoretical works on one dimensional compressible turbulence which are accompanied by numerical verifications.

A statistical plus numerical study of one dimensional polytropic fluid with finite viscosity was accomplished by Tokunaga (1976). The numerical study was performed by Lax-Wendroff discretization method. In their numerical study, they obtained step shocks for the density and triangular shocks for the velocity field (figure 5.2). Total mechanical energy (kinetic and compressive energy) was numerically found to decay as $t^{-0.9}$ which was close enough to their heuristic prediction with t^{-1} . They also reported an equipartition of average kinetic and compressible energy. Finally they calculated the velocity power spectrum numerically which gave a k^{-2} trend at low k and an exponential fall at higher wave numbers (see figure 5.2).

Density structures in highly compressible turbulence are believed to play a key role in astrophysics. This aspect was investigated theoretically and numerically for one dimensional polytropic gas turbulence (Passot & Vazquez-Semadini, 1998) where the polytropic index is very close to unity. Using a

simple one-dimensional model, it was found that density PDF follows a log-normal distribution in isothermal turbulence (for which the polytropic index $\gamma = 1$) whereas for $\gamma \neq 1$ we have power-law distribution. For $\gamma < 1$ an asymptotic power-law regime is obtained at high density limit and for $\gamma > 1$ we have an asymptotic power law behaviour in the low density regime (figure (5.3)). The isothermal log-normal distribution was symmetric with respect to its centre whereas the power laws were not. Interestingly they noticed that moreover the power laws for $\gamma > 1$ and $\gamma < 1$ are almost mirror images of one another. This comparative study is important in order to understand the basic difference between isothermal and polytropic turbulence which indeed inspired me in deriving an exact relation for polytropic turbulence (which is done for an arbitrary value of γ but $\neq 0$ and 1) which will be discussed in the chapter 6.

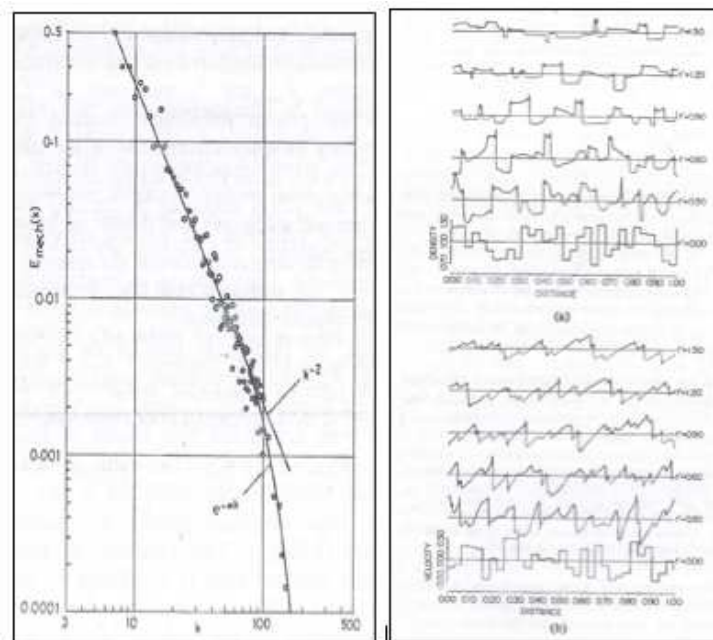


Figure 5.2: Total mechanical energy spectra (left); step discontinuities for turbulent density and triangular discontinuities for turbulent velocity field (right); Source: Tokunaga (1976).

5.4 Numerical Simulations in higher dimensions

5.4.1 Numerical methods for compressible turbulence

Unlike incompressible turbulence, spectral and pseudo-spectral methods are not suitable for tackling turbulence both in compressible hydrodynamics and magnetohydrodynamics. Quasi-discontinuous shock waves are difficult to handle in a finite Fourier representation due to the Gibbs phenomenon. However, a number of numerical studies for compressible MHD turbulence have been accomplished using spectral and pseudo-spectral methods (Passot & Pouquet, 1987; Dahlburg & Picone, 1989; Kida & Orszag, 1992).

The recent development of the numerical methods in compressible turbulence is deeply indebted to the astrophysical fluid dynamics and more precisely to the vast amount of research works in astrophysical plasma turbulence (for a review see Schmidt (2013)). Typically, there are two different approaches for simulating astrophysical plasma turbulence. The first one consists of applying traditional time advancement schemes like Lax-Wendroff or Runge-Kutta. These methods are of high accuracy but lacking in stability. To get rid of unwelcome oscillations at the steep gradients, numerical viscosity is introduced in order to broaden the thickness of the shock fronts without affecting the high accuracy. The best known code of this type is ZEUS code (Stone & Norman, 1992a,b; Stone *et al.*, 1992) which is vastly used in astrophysical MHD flows with radiation transport (Biskamp, 2008). The same basic algorithm has been used in developing MOCCT method (Hawley & Stone, 1995). Another similar type code was developed by Nordlund & Brandenburg (1992) for studying solar convection.

The second approach is based on Godunov's method (Richtmyer & Morton, 1967) essentially implementing Lagrangian tracking and is appropriate for dealing with the flow discontinuities. This method is of first order and hence the drawback of this method is poor accuracy. However, several approaches have been taken in order to improve the accuracy by using sophisticated interpolation schemes. Among these, piecewise parabolic method (PPM), which is a higher order extension of Godunov's method, has become very popular and is specifically useful for simulating both two and three dimensional turbulence. In the following we shall discuss some important numerical works which have been performed using PPM.

5.4.2 Piecewise Parabolic Method (PPM):

The advent of modern computational fluid dynamics (CFD) was accompanied by the development of Piecewise Parabolic Method (PPM) which employed

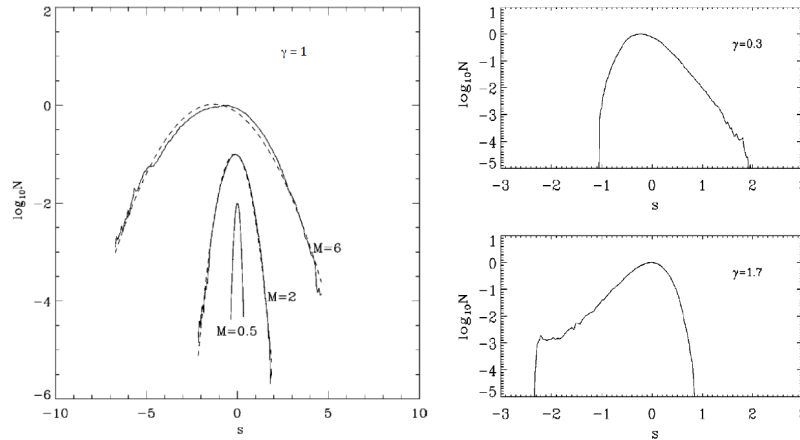


Figure 5.3: PDF of $s = \ln \rho$ for (i) isothermal case (left), (ii) $\gamma < 1$ (right-upper) and (iii) $\gamma > 1$ (right-lower) for one dimensional gas turbulence; *Reprinted with permission from Passot & Vazquez-Semadini (1998)*; © (1998) American physical society. DOI: [10.1103/PhysRevE.58.4501](https://doi.org/10.1103/PhysRevE.58.4501)

higher-order interpolation in constructing relevant flow variables everywhere in the flow field. This method was developed (Colella & Woodward, 1984) in order to simulate unsteady flows associated with strong shocks and discontinuities in astrophysical contexts (e.g. supernova explosions, supersonic jets etc.). Moreover, PPM changes its ordinary smooth flow algorithm in the vicinity of a discontinuity in order to capture the corresponding structure and also detects shock regions in order to adjust the amount of local numerical dissipation. Another practical advance of this method lies on the fact that it uses directional splitting algorithm (Strang, 1968) which applies alternating one-dimensional schemes for a multidimensional flow thereby adding a high accuracy and better performance to the simulation. Several frameworks in order to improve the accuracy and resolution have been proposed in later years (Harten *et al.*, 1987; Liu *et al.*, 1994). Although originated as a pure hydrodynamic code, PPM got its MHD version (in two dimensions) thanks to Dai & Woodward (1994).

A significant numerical study was accomplished for two dimensional compressible polytropic turbulence by Passot *et al.* (1988) using PPM on a 512^2 grid using periodic boundary conditions. They performed two runs with respective Mach numbers 1 and 4. In order to understand the effect of vortices and the shocks in turbulence they studied spectra corresponding to compressible and solenoidal velocity components separately (figure 5.4). They observed a slightly steeper slope than k^{-2} for the compressible part which they explained

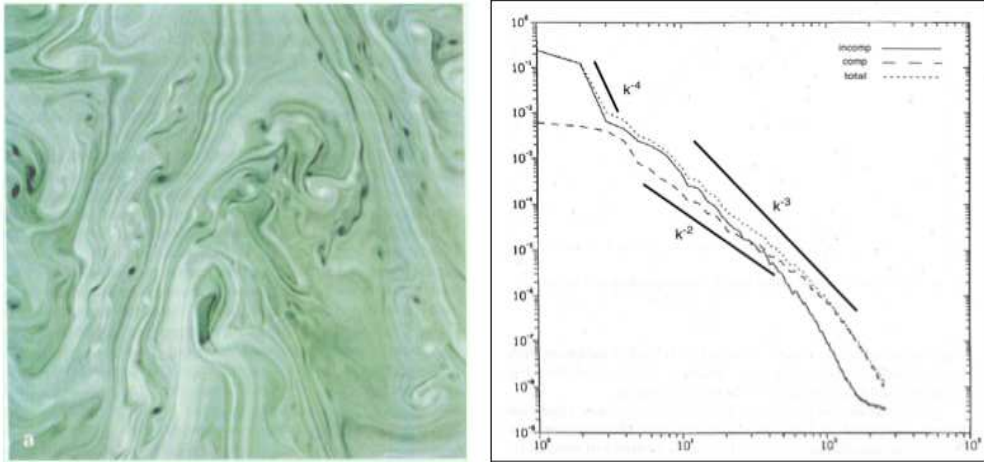


Figure 5.4: Vortex structures in numerical simulation (using PPM) of two dimensional compressible turbulence with 512^2 resolution (left) and power density spectra (right) for (i) solenoidal kinetic energy (E^S) (solid line), (ii) compressible kinetic energy (E^C) (dashed line) and (iii) total kinetic energy (E^v) (dotted line); Reprinted with permission from [Passot *et al.* \(1988\)](#); © (1988) ESO.

in the light of "dimension independent" shock analysis. The solenoidal part represented an initial k^{-4} slope followed by a less steeper k^{-3} slope which was explained by the piling up of vorticity sheets ([Brachet *et al.*, 1986](#)). The numerically obtained solenoidal slope was also in agreement with their theoretical prediction of Kolmogorov-type self similar spectrum which they established by following [Moiseev *et al.* \(1981\)](#) in case of two dimensional turbulence. In their study, they noticed a lack of equipartition between the vortices and the shocks which violated the statistical prediction of [Kraichnan \(1953\)](#). This discrepancy was more pronounced in some previous DNSs of polytropic turbulence using pseudo-spectral methods ([Léorat & Pouquet, 1986](#); [Passot & Pouquet, 1987](#)) of Navier-Stokes equations and seemed to get reduced in PPM where the true turbulence regime is believed to be attained owing to a very large Reynolds number. They also found spectral indices for three dimensional compressible turbulence which associates respectively $k^{-5/3}$, k^{-2} and k^{-2} spectra from the solenoidal, compressible and total velocity power spectrum. In order to understand the coherent structures, energy cascading and the distinction between subsonic and supersonic phases, direct numerical simulations (DNS) of the Euler equations are one of the best possible numerical approaches. Thanks to PPM, high resolution simulation of three dimensional supersonic turbulence became feasible (at least to my knowledge). The initial attempts consisted

of notable works of Porter *et al.* (1992); Porter *et al.* (1994) on decaying turbulence (without forcing) using ideal (without viscosity) compressible fluids with polytropic closure. They performed simulations using upto 256^3 (1992) and 512^3 (1994) uniform grid points and keeping their initial rms Mach number unity. In order to categorize the incompressible and compressible effects at the onset and during the development of turbulence, they used Helmholtz decomposition of the fluid velocity. In both cases, two temporal phases i.e. a quasi-supersonic and a post-supersonic phase are reported. In the first phase,

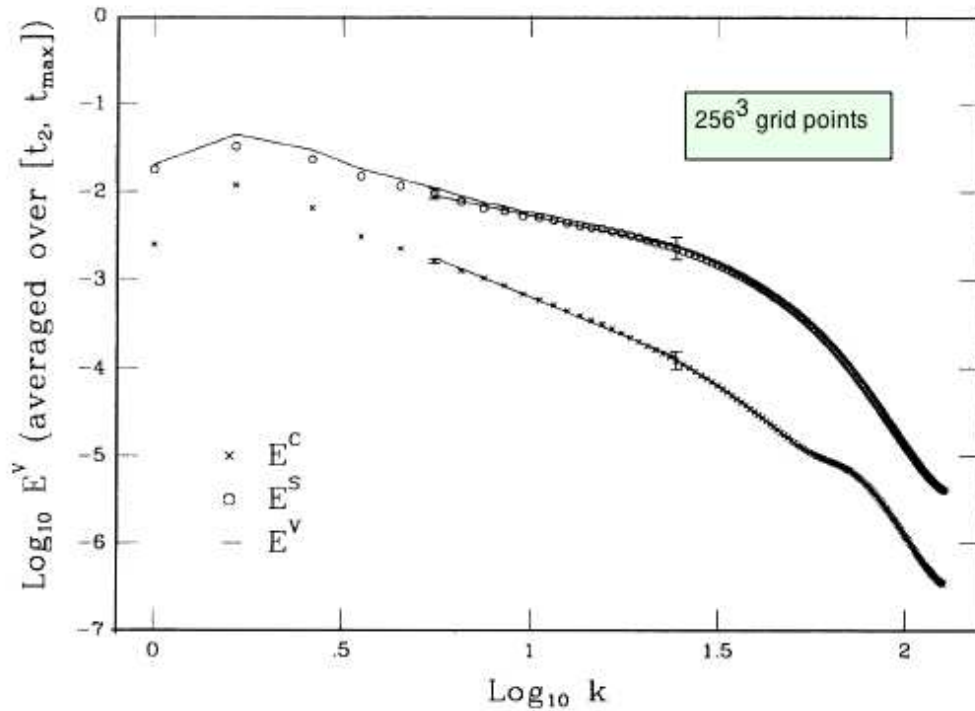


Figure 5.5: Power density spectra for (in logarithmic graph) (i) solenoidal kinetic energy (E^S), (ii) compressible kinetic energy (E^C) and (iii) total kinetic energy (E^V) in three dimensional compressible turbulence PPM simulation with 256^3 resolution; the solenoidal and the total kinetic energy spectra follow a $k^{-0.95}$ law whereas the compressible kinetic energy spectrum follows a steeper $k^{-1.8}$ law; Reprinted with permission from Porter *et al.* (1992); © (1992) American Physical Society. DOI: 10.1103/PhysRevLett.68.3156

vortices are formed due to strong interaction between the shocks whereas in the second phase the kinetic energy spectrum decays in a self-similar way. In their PRL 1992 (with max resolution of 256^3 points), they found that the spectrum of decaying compressional kinetic energy followed a $k^{-1.8}$ behaviour

whereas the solenoidal kinetic energy as well as the total kinetic energy spectra were found to produce a shallower curve with $k^{-0.95}$ (see figure 5.5). No Kolmogorov like regime with $k^{-5/3}$ was detected. A Kolmogorov spectrum was however reported for both the solenoidal and compressional part in their 1994 article with higher resolution (see figure 5.6). Another interesting finding was

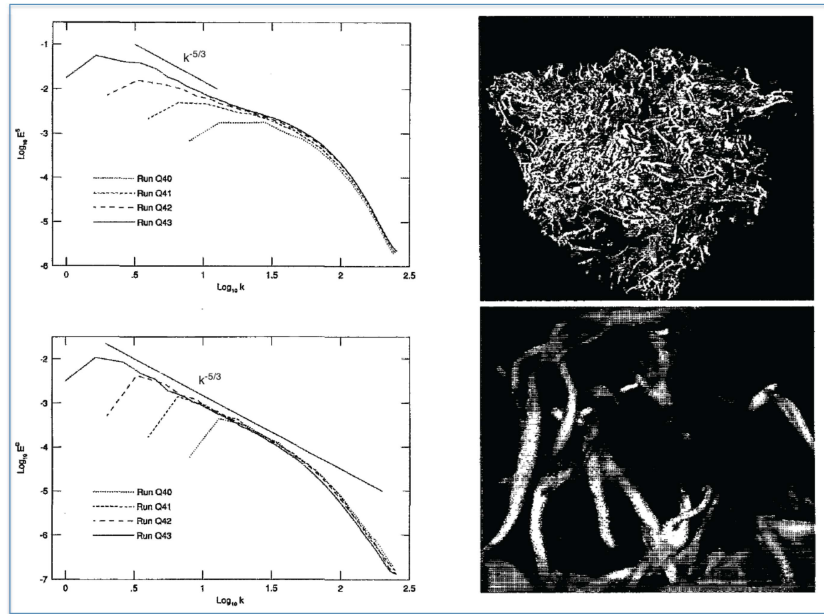


Figure 5.6: Power density spectra for (i) solenoidal kinetic energy (E^S) (left above), (ii) compressible kinetic energy (E^C) (left below) using 64^3 (Q40), 128^3 (Q41), 256^3 (Q42) and 512^3 (Q43) grid points and (iii) vortex tube structures in 512^3 numerical box of supersonic turbulence (right); *Reprinted with permission from Porter et al. (1994); © (1994) AIP publishing LLC.*

vortex tubes almost covering the available space which could indicate some conclusive phenomenology in compressible turbulence (see figure 5.6). It is in recent years that high resolution ($\geq 1024^3$) DNS employing PPM have been performed by Kritsuk et al. (2007a) (hereafter referred as K07) for simulating supersonic turbulence. The rms Mach number is maintained at 6. Like the previous attempts described above, they studied supersonic turbulence in an ideal fluid but added a forcing term in order to obtain a stationary turbulence regime and hence stationary spectra. In this paper, for the first time, the power spectra of density weighted velocities ($\rho^{1/2}v$, $\rho^{1/3}v$) are studied along with the fluid velocity, its solenoidal and compressional components. In 1024^3 simulation, the spectra (see figure 5.8) along with their indices are given in

the following table 5.1.

Interestingly neither the fluid velocity v nor $\rho^{1/2}v$ follows a Kolmogorov $-5/3$ spectrum whereas $w \equiv \rho^{1/3}v$ does (see figure 5.8). This can be seen as a direct consequence of the constancy of compressible kinetic energy transfer rate (Lighthill, 1955) from one scale to another. Besides they obtained a k^{-1} law for the power spectrum of fluid density. In order to provide with a theoretical explanation for Kolmogorov scaling of this new density weighted velocity w , they used a simple hierarchical model relating density and length scales. No rigorous analytical explanation was however furnished. In course of my master internship and thesis, by virtue of the newly derived exact relations (discussed in next chapter), this issue is addressed principally over a rigorous analytical basement.

Variable	v	v_S	v_c	$\rho^{1/2}v$	$\rho^{1/2}v$	ρ
Power spectral index	-1.95	-1.92	-2.02	-1.58	-1.69	-1.07

Table 5.1: Different power spectra in supersonic turbulence (Kritsuk *et al.*, 2007a).

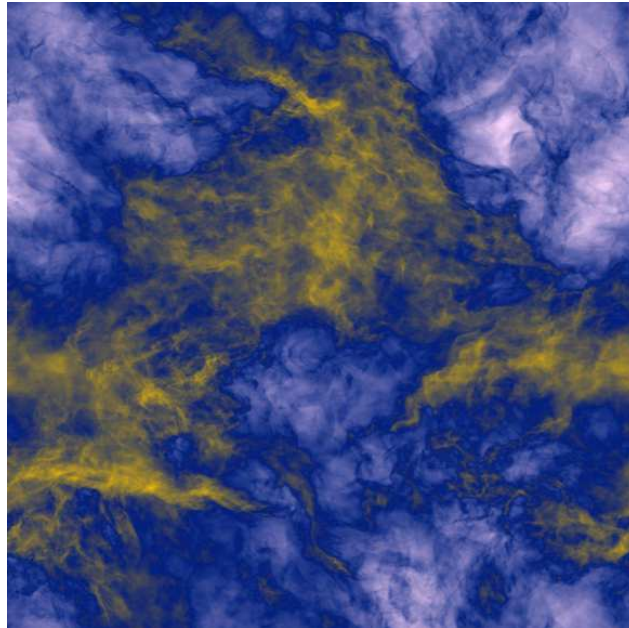


Figure 5.7: Projected gas density of Mach 6 turbulence PPM simulation with 2048^3 resolution. White, blue and yellow colors represent respectively low, intermediate and high projected density values; *Reprinted with author's permission from Kritsuk et al. (2009).*

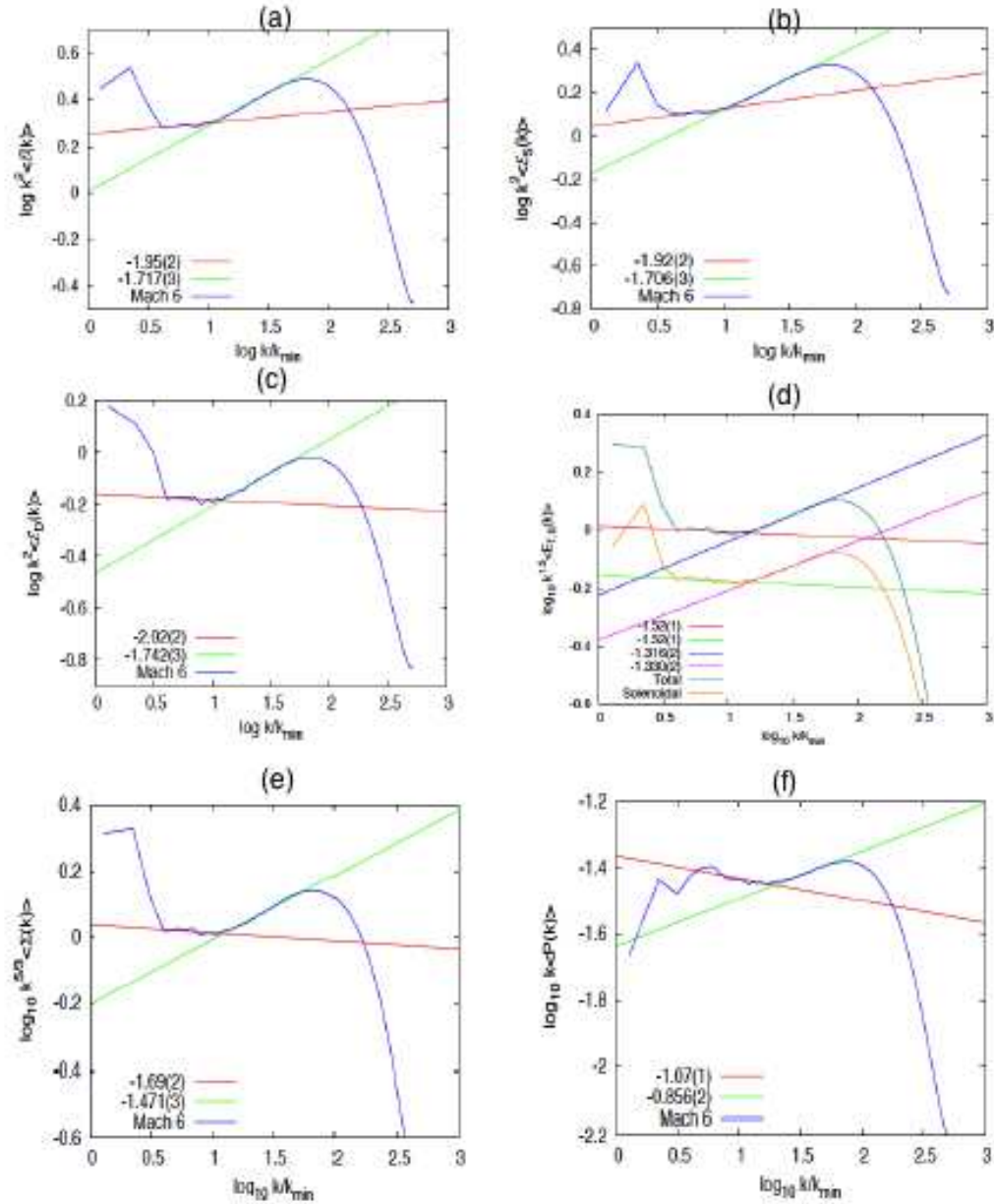


Figure 5.8: Power density spectra corresponding to (a) total velocity (v), (b) solenoidal velocity (v_s), (c) compressional velocity (v_c), (d) $\rho^{1/2}v$ and $\rho^{1/2}v_s$, (e) $w \equiv \rho^{1/3}v$ and (f) ρ ; Reprinted with permission from Kritsuk *et al.* (2007a); © (2007) AAS. DOI: 10.1086/519443

In their 2007 article, Kritsuk et al. did not publish any direct space scaling of the structure functions corresponding to the variable $\rho^{1/3}v$. This study was performed in (Kritsuk *et al.*, 2007b) (figure 5.9). Furthermore, their inertial range is usually³ spanned within $\sqrt{10}k_{min} < k < 10k_{min}$ which is considerably narrow and the spectra suffered from bottleneck effect in the high wave number range. These points were improved in a following article using 2048^3 grid points where they obtained a wider inertial range for hydrodynamic turbulence (figure 5.10) with $\sqrt{10}k_{min} < k < 10^{1.5}k_{min}$ along with a less pronounced bottleneck.

In the same paper they discussed their MHD simulation results using 512^3 resolution and using three plasma betas namely 20, 2 and 0.2. For $\beta = 20$ they again obtained a $-5/3$ scaling for the variable w whereas they did not precise any spectral index for magnetic energy. In addition, they obtained (in all three cases) a satisfactory linear scaling for the third order structure function corresponding to density weighted Elsässer fields $W^\pm \equiv \rho^{1/3}z^\pm$ which supports their empirical 1/3 rule even in scaling in compressible MHD turbulence. A considerable part of my thesis is devoted to address this point from an analytic point of view and will be discussed in details in the next chapter.

5.4.3 Compressible intermittency

Intermittency in compressible turbulence is another important issue to be clearly understood. Although this aspect of intermittency is not directly addressed in course of my thesis, some important works on compressible turbulence provided me with indirect motivation for bulding up my research work and interest. Performing a 256^3 compressible MHD turbulence simulation, Padoan *et al.* (2004) proposed a unified approach for modelling the self-similarity in compressible, super Alfvénic (Alfvénic mach number > 1) turbulence. Their generalized model was described in terms of usual She-Lévêque formalism (She & Leveque, 1994) where the Hausdorff dimension of the most intense dissipative structures was made to be a function of sonic Mach number. This work prescribes a general method for studying the intermittency of interstellar media once the corresponding sonic Mach numbers are known from the observational data.

A model of extended self-similarity in compressible turbulence was suggested by Schmidt *et al.* (2008) depending on the numerical data of compressible turbulence of an isothermal fluid (Kritsuk *et al.*, 2007a). They inferred that refined self-similarity can be achieved in compressible turbulence, if we

³Except the case of the density spectrum where the inertial range is found to get shifted towards higher wave numbers.

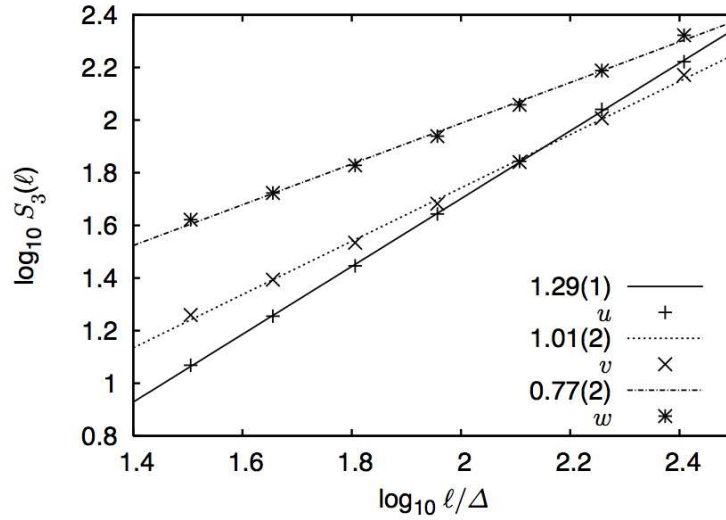


Figure 5.9: Scaling of third order structure functions of $w \equiv \rho^{1/3}v$ using data of three dimensional supersonic turbulence (r.m.s. Mach ~ 6) with 1024^3 resolution; *Reprinted with author's permission from Kritsuk et al. (2007b)*.

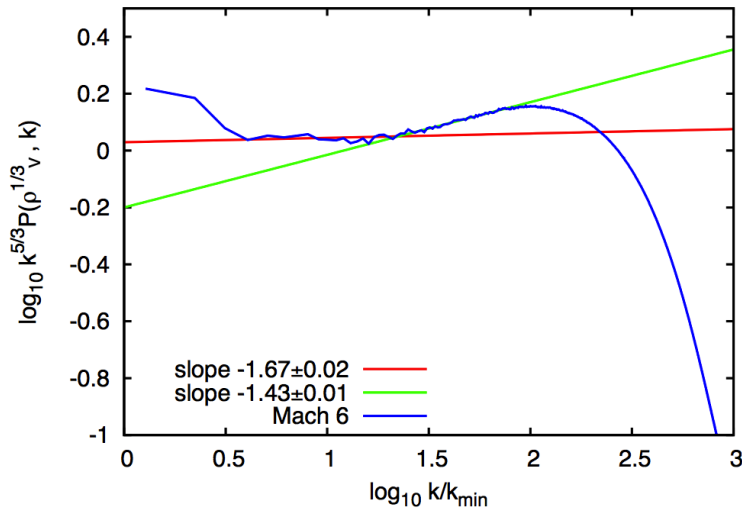


Figure 5.10: Compensated power density spectrum of $w \equiv \rho^{1/3}v$ using data of three dimensional supersonic turbulence (r.m.s. Mach ~ 6) with 2048^3 resolution; *Reprinted with author's permission from Kritsuk et al. (2009)*.

use density-weighted velocity ($\rho^{1/3}\mathbf{v}$) in place of fluid velocity. This conclusion, in turn, justifies again the density weighted velocity to be the appropriate variable for compressible turbulence. The scaling exponents are proved to obey log-Poisson model even in compressible turbulence thereby ascertaining the Burgers shocks to be the dissipative structures for intermittence.

5.4.4 Compressible and solenoidal forcing

The role of forcing is also non-trivial in compressible turbulence. In incompressible turbulence, we are bounded to apply a solenoidal forcing whereas for compressible case, we have an option to choose. For a solenoidal force, the compressibility of turbulence is governed by the intrinsic fluid compressibility whereas for a compressible force, the regulation of compressibility in turbulence is partially executed externally thereby reducing the universality of such a flow and a judicious choice of forcing scheme is needed. On the other hand, for a pure solenoidal forcing, the compressible effect would decay in time and could not be reflected properly in the stationary regime of turbulence. A mixture of solenoidal and compressible forcing can also be a choice. A mixture with compressible to solenoidal forcing ratio ≈ 0.7 was employed by K07 for hydrodynamic simulations ⁴.

The aspect of forcing is significantly studied by Federrath *et al.* (2008, 2010); Schmidt *et al.* (2008); Schmidt *et al.* (2009) in the framework of their DNS and also by Schmidt (2009) in his large eddy simulations. Unlike previous numerical works, Federrath *et al.* obtained a non-lognormal density PDF for isothermal turbulence while using compressible driving. In K07, interestingly for high turbulent Mach number, the compressible power spectra (P_c) locks at half of the value of solenoidal power spectra (P_s) (Kritsuk *et al.*, 2010). This locking was justified by some geometrical reasoning in a previous paper (Nordlund & Padoan, 2003). In case of Federrath *et al.* (2010), for hydrodynamic isothermal simulations using 1024^3 points, the compressible to solenoidal power spectra ratio comes to 1.2 for a pure compressible driving whereas for a solenoidal one the natural 0.5 ratio is obtained in the inertial zone. Most interestingly, Federrath *et al.* observed an important discrepancy between the turbulence scaling and spectral properties of isothermal turbulence in function of pure solenoidal and pure compressive forcing (figure 5.11). Using solenoidal scheme they obtained $k^{-1.85}$ and $k^{-1.45}$ spectra respectively for v , $\rho^{1/2}v$ whereas they obtained an approximate Kolmogorov scaling $k^{-1.64}$ for the variable $\rho^{1/3}v$. However, no Kolmogorov scaling is found for these three variables under compressible driving (figure 5.11).

⁴Whereas pure solenoidal scheme was adapted to drive their MHD simulations in 2007.

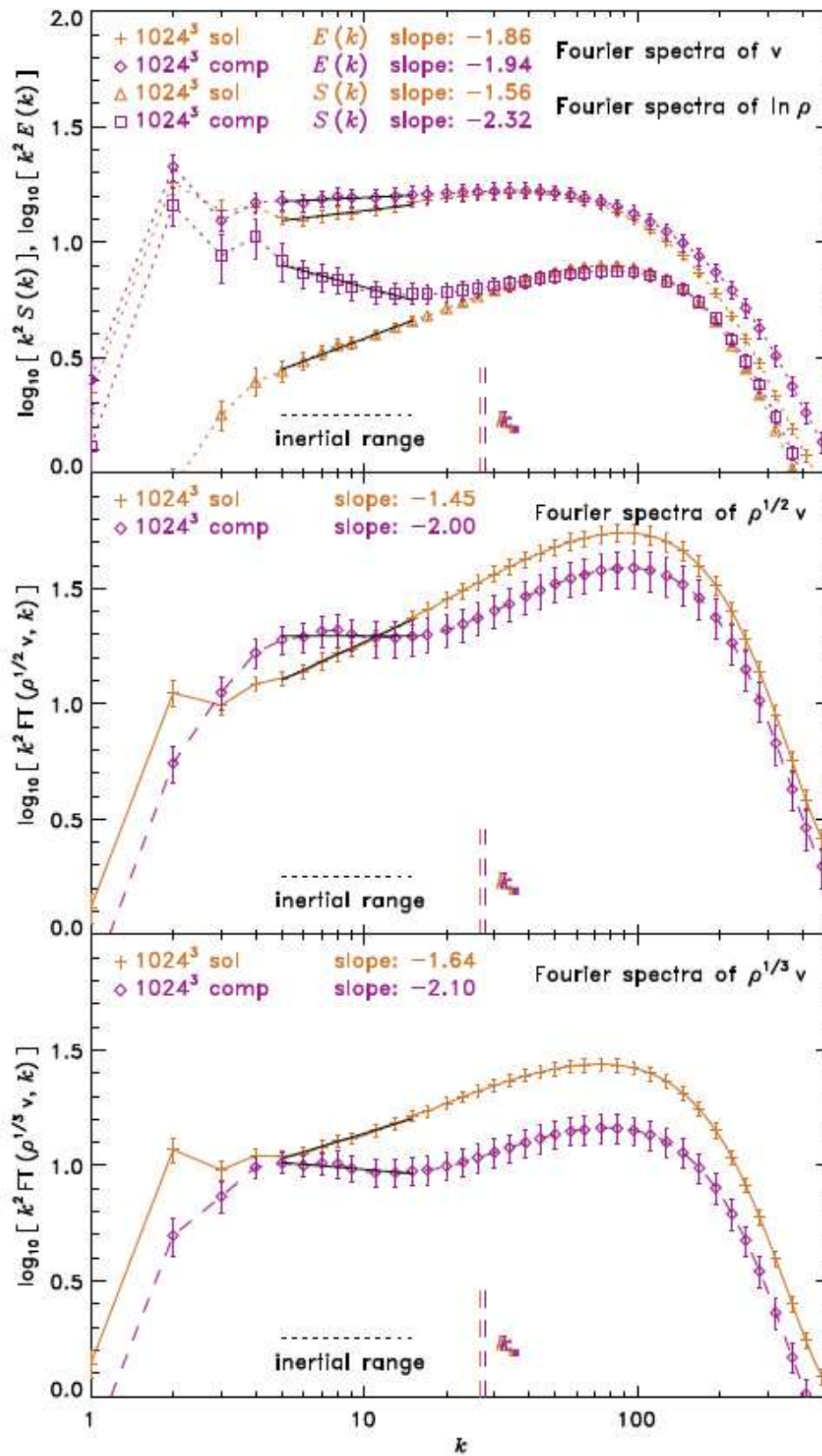


Figure 5.11: Compensated power spectra corresponding to different variables using solenoidal and compressible forcing; Reprinted with permission from Federrath *et al.* (2010); © (2010) ESO.

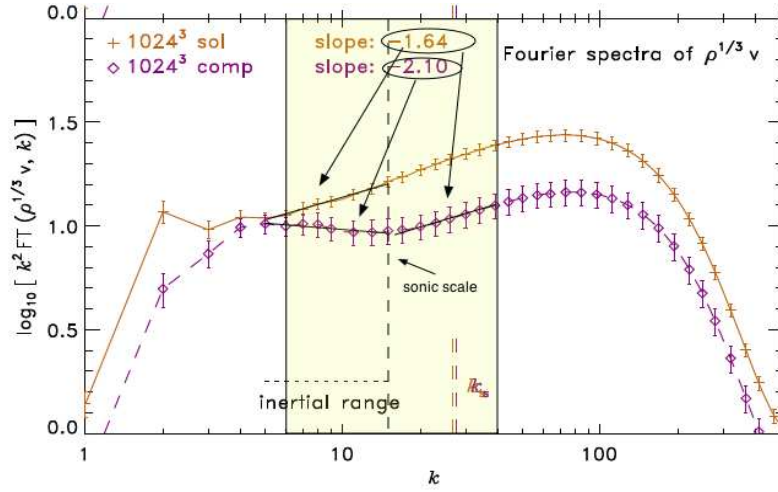


Figure 5.12: Modified interpretation of power spectra with the newly defined sonic scale; *Reprinted with permission from Federrath et al. (2010)*; © (2010) ESO.

5.4.5 Choice of inertial zone and sonic scale

In order to distinguish the subsonic and supersonic regime, they provided with an estimate for the sonic scale ($1/k_s$) which can be obtained by solving the equation

$$\int_{k_s}^{k_d} E^v(k) dk \simeq \frac{1}{2} C_S^2, \quad (5.7)$$

where k_d is the dissipation wave vector, C_S is the isothermal sound speed and the other symbols have their usual meaning. After their estimate of sonic scale they have defined their inertial range inside the super-sonic regime ($k < k_s$) and more precisely within the range $5 \leq k \leq 15$ whereas they admit the fact that bottleneck should not affect the turbulence statistics for $k < 40$. The spectra obtained in K07 are also suspected to suffer from the same problem. In fact, I think that their results are satisfactory but lack suitable complete interpretation. For clarifying the point I take their power spectra corresponding to $\rho^{1/3}v$ and try to indicate the maximum possible inertial zone i.e. $5 \lesssim k \lesssim 40$ (see figure 5.12). Within the newly defined inertial zone, we obtain one single spectral index -1.64 if we use solenoidal forcing whereas we get two spectral indices, a -2.1 law for the low wavevector regime and a Kolmogorov type -1.64 law in the sub-sonic regime if we use pure compressible forcing. The existence of the double slope can be attributed to the sub-sonic and supersonic regime (Passot et al., 1988) of compressible turbulence and therefore the modified estimate for the sonic scale can be given

by the break point of the two slopes (as drawn by the dotted line in the figure 5.12). A plausible explanation for these slopes is given in the next chapter by the help of compressible exact relations.

5.4.6 Two-point closure in EDQNM model for compressible turbulence

EDQNM or Eddy Damped Quasi-Normal Markovian is a useful model of turbulence in which the dynamical equations of statistical moments of fluid velocity components are closed in wave space assuming a linear "eddy damping" effect by the fourth or higher order moments thereby preventing the strong development of third order moments and the corresponding non-linear energy transfer (Lindborg *et al.*, 1993). This model is developed and adapted principally for incompressible turbulence. An extension of this model in case of very weakly compressible turbulence is worked out by Bertoglio *et al.* (2001). In their model they considered linear terms with density variation but neglected all the non-linear terms comprising density fluctuations. At very low turbulent Mach number (0.01 or 0.1), the dilatational velocity power spectrum starts at giving $k^{-5/3}$ and evolves towards $k^{-11/3}$ at large time. For the pressure spectra, we get $k^{-7/3}$ in the beginning which is followed by a $k^{-5/3}$ and a $k^{-11/3}$ at later instants (figure 5.13). At large times, at a given time instant, the solenoidal component seems to follow -5/3 law whereas the dilatational component follows a -5/3 at turbulent Mach near unity but conceives a -11/3 slope for smaller turbulent Mach Numbers (figure 5.13). These results are in agreement with their theoretical predictions based on a simple model of weakly compressible turbulence discussed in the same paper. Furthermore, for very low turbulent Mach number ($M_t \ll 1$), the dilatational velocity component seems to vary as M_t^2 which does not hold any longer for $M_t \sim 1$. A detailed discussion of EDQNM is however beyond the scope of this review and can be found in text books on turbulence (Biskamp, 2008) or in research papers (Orszag, 1970; Lindborg *et al.*, 1993).

5.5 Observational studies

Compressible turbulence in interstellar clouds Interstellar clouds are proved to be turbulent due to having fluctuations spanning over a large range of length scales. Moreover considerable density fluctuations certainly justifies the compressible character of interstellar turbulence. In fact it is believed that the convective turbulence in cold interstellar dense clouds play a crucial role in the process of star formation by preventing the gravitational auto-collapse

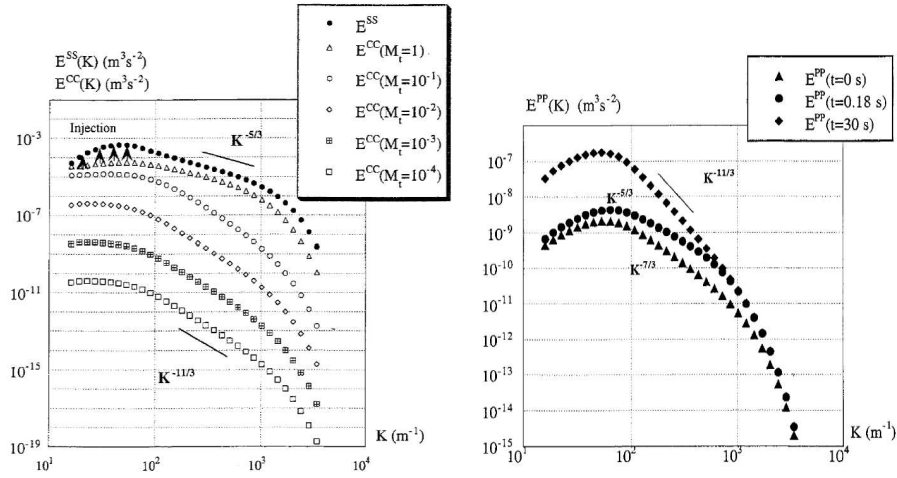


Figure 5.13: Solenoidal and dilatational velocity power spectra for different turbulent Mach numbers at large times (left) and Pressure spectra at different time instants (right) obtained using EDQNM model for weakly compressible turbulence; *Reprinted with permission from Bertoglio et al. (2001); © (2001) AIP publishing LLC.*

of those clouds. A voluminous work has been accomplished in the study of interstellar turbulence and more specifically its compressible aspects. Due to the difficulties in observational studies, several numerical attempts have been carried out in order to study the fundamental aspects of astrophysical turbulence like scaling, different power spectral laws etc. In fact, in most of the cases, interstellar turbulences are modelled by hydrodynamical simulations. The above described numerical works of supersonic turbulence were also designed for understanding interstellar turbulence. The observational studies are comparatively fewer but not negligible. In this part we shall briefly discuss some characteristics of interstellar turbulence in the light of observational data.

Density power spectrum of electrons has been studied (Rickett, 1977, 1990; Armstrong et al., 1995) using diffractive scintillations of small angular diameter radio sources. Interestingly, a Kolmogorov type $k^{-5/3}$ spectrum is observed within length scales $10^8 - 10^{10}$ cm. Moreover, the r.m.s. velocity fluctuations across a length scale l is found to scale approximately as $l^{1/3}$. A possible explanation for this spectrum was given in the framework of compressible (polytropic) MHD turbulence (Lithwick & Goldreich, 2001). Density fluctuations are supposed to originate from the slow magnetosonic and entropy

modes (zero frequency mode in polytropic MHD plasma) which act as passive elements in the cascade of shear Alfvén waves. This cascade generates a $k^{-5/3}$ spectrum which is, in turn, reflected by the density fluctuation spectrum of the same index. However, if the plasma beta is high i.e. the thermal pressure exceeds the magnetic pressure, the slow and entropy modes are damped below the proton diffusion length thereby producing a cut-off length scale for the density fluctuation. Their observational results were justified both by their own theoretical model which was a 'compressible' extension of Goldreich-sridhar model (Goldreich & Sridhar, 1995) and also by the theoretical predictions of Higdon concerning density fluctuation spectrum (Higdon, 1984, 1986) in a collisionless MHD framework.

Compressibility in solar wind turbulence Solar wind (SW) is the most familiar laboratory for space plasma turbulence (A formal introduction of the solar wind is given in chapter 7). Thanks to the feasibility of in-situ measurements, numerous research works have been accomplished on the nature of SW plasma turbulence. Although density fluctuations are present in SW, the fractional density fluctuation is indeed very low in fast solar wind and rarely exceeds 15% whereas for slow solar wind that ratio can be $\sim 25\%$. In both cases the characteristics of SW turbulence is often described satisfactorily in the framework of an incompressible plasma or nearly incompressible turbulence (Montgomery *et al.*, 1987) i.e. the density fluctuations are assumed to merely act as passive scalars. This idea was put into question by Hnat *et al.* (2005). Using ACE spacecraft data (with 64 s. resolution) they compared the extended self-similarity (ESS) curves corresponding to different moments of proton density fluctuations with those of the total magnetic field magnitude fluctuations which are found to fit to the theoretical ESS curves of the passive scalars in incompressible turbulence (Hnat *et al.*, 2005; Bershadskii & Sreenivasan, 2004). Both for fast and slow solar winds, they observed a discrepancy between the two (see figure 5.14) curves which indicates a possible ⁵ **active nature** of the plasma density fluctuations thereby hinting at the compressible nature of SW turbulence.

The most significant observational study (to date) on the compressible aspect of fast solar wind turbulence was realized by Carbone *et al.* (2009) using Ulysses spacecraft data in polar solar wind. Inspired by the numerical works by (Kritsuk *et al.*, 2007*a,b*) of supersonic isothermal turbulence both in hydrodynamics and MHD, they proposed a compressible version (discussed in chapter 6) of the exact relation originally obtained by Politano & Pouquet

⁵Another possibility is that the self similarity curves do not exactly represent the phenomenology which is less realistic.

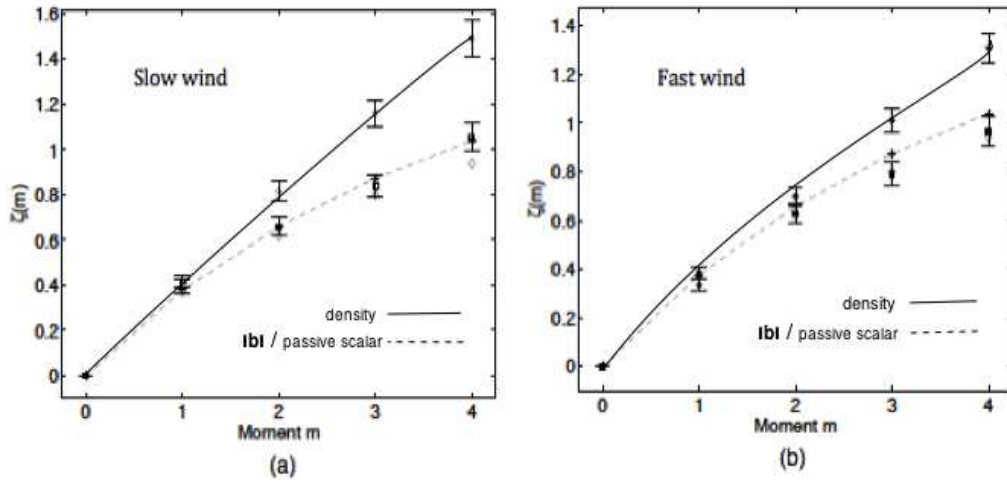


Figure 5.14: Moments of proton density fluctuations and magnetic field magnitude fluctuations as a function of the order of moments in slow (left) and fast (right) solar wind; *Reprinted with permission from Hnat et al. (2005)*; © (2005) American Physical Society. DOI: 10.1103/PhysRevLett.94.204502

(1998a) – hereafter as PP98 – for incompressible MHD (also derived and discussed in details in chapter 6) in order to improve the scaling of velocity structure functions in fast solar wind. For a considerable number of intervals they indeed observed a better scaling (see figure 5.15 in case of compressible moments where the incompressible Elsässer variables (\mathbf{z}^\pm) are replaced by density weighted compressible Elsässer variables ($\mathbf{w}^\pm \equiv \rho^{1/3}\mathbf{z}^\pm$). Despite the improvement in scaling, their relation was not derived analytically. This very point motivated me to establish a compressible counterpart of PP98 exact relation in order to analytically justify their choice of density-weighted variable.

Another important issue is the anomalous heating in fast solar wind. Both Helios and Ulysses data revealed clear signature of local heating by virtue of the temperature profile of solar wind in function of radial distance. Using three dimensional temperature analysis in Helios data, the parallel (with respect to the mean interplanetary magnetic field) temperature of pure fast solar wind was found (Marsch et al., 1982) to decrease as $r^{-0.69}$ and the perpendicular temperature as $r^{-1.17}$ whereas the adiabatic model of non-collisional plasma predicts a temperature fall of r^{-2} in perpendicular direction. Again Ulysses data gives a radial temperature profile of $r^{-1.03}$ for northern hemisphere and that of $r^{-0.81}$ in the southern hemisphere whereas an adiabatic model would give a profile with $r^{-1.33}$ where solar wind is assumed to be composed of mainly

monoatomic gas (rather protons). This discrepancy gave birth to the idea of an intra-wind local source of heating in solar wind. In their article of 2009, Carbone et al. propose compressible turbulence in solar wind to be responsible for this heating. They estimated the energy supply rate by the dissipation rates of pseudo energies (defined in chapter 3) and found that the incompressible pseudo energy dissipation could not provide with sufficient energy whereas the compressible pseudo energy dissipation could (see figure 5.16).

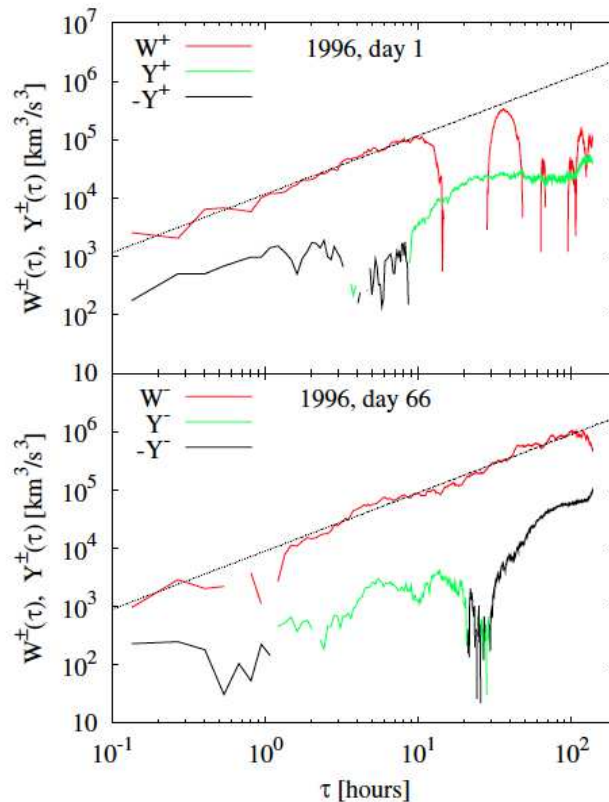


Figure 5.15: Compressible and incompressible scaling (in log-log graph) in time domain of the fast solar wind data obtained from Ulysses spacecraft, Y^\pm W^\pm represent respectively the incompressible and compressible third order moments; Reprinted with permission from Carbone et al. (2009); © (2009) American Physical Society. DOI: 10.1103/PhysRevLett.103.061102

★★ This paper however confronted some criticism (Forman et al., 2010) which principally included their biased choice of data intervals, selection of MHD frequency range (which seemed to span well inferior to the usual MHD frequency range i.e. $10^{-1} - 10^{-4}$ Hz used for the solar wind), their estimation

of turbulent energy dissipation rate by the pseudo-energy rates and some other physical issues. Except the question of validity of chosen MHD interval, all the questions are addressed and explained by the authors in another letter from the authors (Sorriso-Valvo *et al.*, 2010). Some important works on the density and magnetic compressibility have been done using Helios (Bavassano *et al.*, 1982) and Ulysses data (Malara *et al.*, 1996) and specially the effect of compressibility on the Alfvénicity (the correlation between the velocity and magnetic field fluctuations) of the solar wind turbulence. A thorough review on this subject is given in Bruno & Carbone (2005).

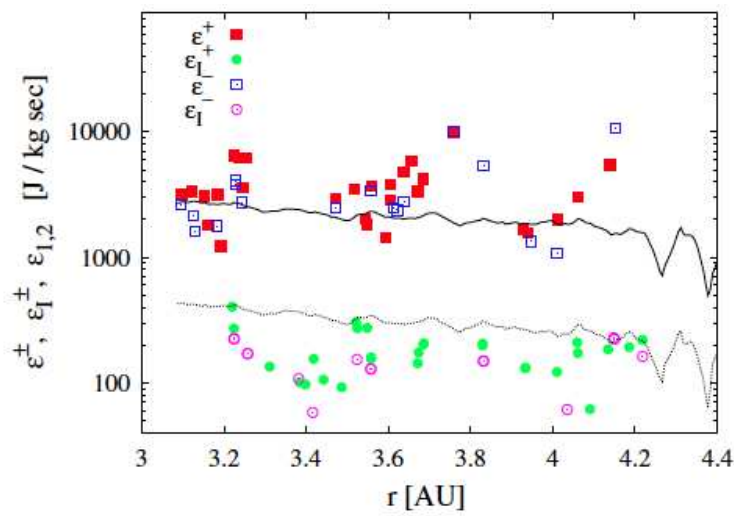


Figure 5.16: Heating energy supply by compressible pseudo-energy ε_I^\pm dissipation (Red and Blue squares) and incompressible pseudo-energy ε_I^\pm dissipation (Green and Violet circles) in comparison with two theoretical estimations of the radial temperature profile for fast solar wind; *Reprinted with permission from Carbone et al. (2009); © (2009) American Physical Society. DOI: 10.1103/PhysRevLett.103.061102*

Exact relations in turbulence

Contents

6.1	Exact relations in incompressible turbulence	109
6.1.1	Incompressible hydrodynamic turbulence	111
6.1.2	Incompressible MHD turbulence	113
6.2	Previous attempts for exact relations in compressible turbulence	116
6.2.1	Heuristic approach by Carbone et al. (2009)	116
6.2.2	FFO approach for a generalized exact equation	117
6.3	New exact relations and phenomenologies in compressible turbulence : My research work	120
6.3.1	Isothermal hydrodynamic turbulence	121
6.3.2	A new phenomenology for compressible turbulence	128
6.3.3	Isothermal MHD turbulence	130
6.3.4	Polytropic hydrodynamic turbulence	137

6.1 Exact relations in incompressible turbulence

EXACT relations in turbulence refer to statistical relations which are derived analytically from the fundamental equations of dynamics (including the closure relations) under different symmetry hypotheses (statistical homogeneity, isotropy, stationarity etc.). Unlike dimensional analysis, the derivation of these 'exact' relations take into account (a) the proper algebraic and differential structure of the parent equations and (b) the exact algebraic value of the variables instead of their order of magnitude. The existing exact-relations in strong¹ turbulence are mainly² the equations relating the divergence of third-

¹In weak turbulence, we have other exact relations which are beyond the scope of this thesis.

²In intermittency, some exact inequalities exist.

order structure function and the mean flux rate of a conserved quantity (total energy, incompressible cross-helicity etc.). These equations are derived for the so called inertial zone (discussed in chapter 4 and 5) in a completely developed turbulence under the assumption of an infinitely large Reynold's number. This type of exact relation was first derived by von Kàrmàn & Howarth (1938) and then they are successfully applied to the inertial zone of incompressible hydrodynamic turbulence by Kolmogorov (Kolmogorov, 1941*b*) where the third-order moment of longitudinal velocity structure function was related to the mean kinetic energy flux rate or the net energy dissipation rate. The Von-Karman Howarth (VKH) form or the divergence form of this exact relation is written as

$$\nabla_{\mathbf{r}} \cdot \langle (\delta v)^2 \delta \mathbf{v} \rangle = -4\varepsilon. \quad (6.1)$$

For isotropic turbulence, this equation can be integrated over a sphere of radius r and can be written as ³

$$\langle (\delta v)^2 \delta v_r \rangle = -\frac{4}{3}\varepsilon r, \quad (6.2)$$

where v_r is the component of \mathbf{v} in the radial direction of the sphere. The expression à la Kolmogorov can be obtained by replacing $\langle (\delta v)^2 \delta v_r \rangle$ by $\langle (\delta v_r)^3 \rangle$ and is expressed as

$$\langle (\delta v_r)^3 \rangle = -\frac{4}{5}\varepsilon r. \quad (6.3)$$

Later these type of relations are derived for convected passive scalars (temperature etc.) by Yaglom (1949). In the year 1998, Politano and Pouquet derived (Politano & Pouquet, 1998*b,a*) an exact relation for incompressible MHD turbulence introducing Elsasser variables. In recent years some exact relations for incompressible Hall MHD and electron MHD turbulence have been derived (Galtier, 2008*b*; Meyrand & Galtier, 2010).

There exist more than one method for deriving these exact relations. The initial ones (von Kàrmàn & Howarth, 1938; Kolmogorov, 1941*b*; Politano & Pouquet, 1998*b*) used the tensorial methods involving isotropy from the very beginning. On the contrary, in this chapter, we shall derive all the exact relations without using tensorial formalism. First, we shall derive the exact relations for incompressible hydrodynamics and MHD turbulence. This part will be followed by the derivation of exact relations of compressible turbulence. In deriving those relations, we assume only statistical homogeneity and the existence of a stationary state corresponding to a conserved quantity. No a priori assumption of statistical isotropy is made. We include an external forcing \mathbf{f} to maintain the turbulent flow. The forcing is chosen to be solenoidal

³For a d-dimensional turbulence, the right hand side is given as $-\frac{4}{d}\varepsilon r$.

and delta-correlated in time (to restore Galilean invariance even after adding forcing term to Navier-stokes equations). We consider two arbitrary points \mathbf{x} and \mathbf{x}' where $\mathbf{x}' = \mathbf{x} + \mathbf{r}$. The primed and non-primed quantities will denote the dynamical variables corresponding to \mathbf{x}' and \mathbf{x} respectively. In addition, for an arbitrary variable ψ , $\delta\psi \equiv \psi' - \psi$ and $\bar{\delta}\psi \equiv (\psi' + \psi)/2$.

6.1.1 Incompressible hydrodynamic turbulence

For a neutral incompressible fluid, the basic equations of dynamics are given by

$$\partial_t \mathbf{v} + (\mathbf{v} \cdot \nabla) \mathbf{v} = -\nabla P + \mathbf{f} + \nu \Delta \mathbf{v}, \quad (6.4)$$

$$\nabla \cdot \mathbf{v} = 0, \quad (6.5)$$

where the symbols have their usual meaning (as in the previous chapters). In the following we shall evaluate the time rate of change of velocity correlator of order two. By the help of the equation (6.4), we can write

$$\begin{aligned} \partial_t \langle \mathbf{v} \cdot \mathbf{v}' \rangle &= \left\langle \mathbf{v} \cdot \frac{\partial \mathbf{v}'}{\partial t} + \frac{\partial \mathbf{v}}{\partial t} \cdot \mathbf{v}' \right\rangle \quad (6.6) \\ &= \langle \mathbf{v} \cdot [-(\mathbf{v}' \cdot \nabla') \mathbf{v}' - \nabla' P' + \nu \Delta' \mathbf{v}' + \mathbf{f}'] + \mathbf{v}' \cdot [-(\mathbf{v} \cdot \nabla) \mathbf{v} - \nabla P + \nu \Delta \mathbf{v} + \mathbf{f}] \rangle. \end{aligned}$$

For an incompressible fluid with statistical homogeneity, we have

$$\langle \mathbf{v} \cdot \nabla' P' \rangle = \nabla_{\mathbf{r}} \cdot \langle P' \mathbf{v} \rangle = -\langle P' (\nabla \cdot \mathbf{v}) \rangle = 0 \quad (6.7)$$

and identically $\langle \mathbf{v}' \cdot \nabla P \rangle = 0$.

Again by using incompressibility, we obtain

$$\mathbf{v} \cdot (\mathbf{v}' \cdot \nabla') \mathbf{v}' = (\mathbf{v}' \cdot \nabla') (\mathbf{v} \cdot \mathbf{v}') = \nabla' \cdot [(\mathbf{v}' \cdot \mathbf{v}) \mathbf{v}'], \quad (6.8)$$

and likewise we show

$$\mathbf{v}' \cdot [(\mathbf{v} \cdot \nabla) \mathbf{v}] = \nabla \cdot [(\mathbf{v} \cdot \mathbf{v}') \mathbf{v}]. \quad (6.9)$$

Now we define E and R_E to be respectively the kinetic energy density and two-point energy correlator⁴ at point \mathbf{x} (same definitions for E' and R'_E at point \mathbf{x}') and can be expressed as

$$E = \frac{\mathbf{v} \cdot \mathbf{v}}{2}, \quad R_E = \frac{\mathbf{v}' \cdot \mathbf{v}}{2}, \quad (6.10)$$

$$E' = \frac{\mathbf{v}' \cdot \mathbf{v}'}{2}, \quad R'_E = \frac{\mathbf{v} \cdot \mathbf{v}'}{2}. \quad (6.11)$$

⁴ For incompressible turbulence two-point energy correlators are the same in \mathbf{x} and \mathbf{x}' .

Using statistical homogeneity, we can then write

$$\begin{aligned}\langle E - R_E \rangle &= \left\langle \frac{(E + E')}{2} \right\rangle - \left\langle \frac{(R_E + R'_E)}{2} \right\rangle \\ &= \left\langle \frac{\mathbf{v} \cdot \mathbf{v} + \mathbf{v}' \cdot \mathbf{v}'}{4} \right\rangle - \left\langle \frac{\mathbf{v} \cdot \mathbf{v}' + \mathbf{v}' \cdot \mathbf{v}}{4} \right\rangle = \left\langle \frac{\delta \mathbf{v} \cdot \delta \mathbf{v}}{4} \right\rangle.\end{aligned}\quad (6.12)$$

Using equations (6.6) to (6.12), we obtain

$$\begin{aligned}\partial_t \langle \mathbf{v} \cdot \mathbf{v}' \rangle &= \partial_t \langle R_E + R'_E \rangle \\ &= \nabla_{\mathbf{r}} \cdot \langle -R_E \delta \mathbf{v} \rangle + D + F \\ &= \nabla_{\mathbf{r}} \cdot \left\langle \left[\frac{(\delta \mathbf{v})^2}{4} - \frac{(E + E')}{2} \right] \delta \mathbf{v} \right\rangle + D + F \\ &= \nabla_{\mathbf{r}} \cdot \left\langle \frac{(\delta \mathbf{v})^2}{4} \delta \mathbf{v} \right\rangle + D + F,\end{aligned}\quad (6.13)$$

where D and F represent resultant dissipative and forcing terms and can explicitly be expressed as

$$D = \nu \langle \mathbf{v} \cdot \Delta' \mathbf{v}' + \mathbf{v}' \cdot \Delta \mathbf{v} \rangle, \quad F = \langle \mathbf{v} \cdot \mathbf{f}' + \mathbf{v}' \cdot \mathbf{f} \rangle.$$

Now if we consider a stationary state where the average energy is conserved by the mutual balance of energy input by forcing term and energy output by viscous term (discussed in chapter 4), the time derivative of the corresponding correlator should also vanish. Moreover, if we are interested well inside the inertial zone, D can be neglected with respect to the other terms. The divergence form of equation (6.1) can simply be obtained if we write $F \equiv \varepsilon$ where ε represents the average kinetic energy injection flux rate. Note that the divergence form is valid for homogeneous three dimensional turbulence of an incompressible neutral fluid. If, in addition, statistical isotropy is assumed, the average flux term can be considered to be a function of $|\mathbf{r}|$ and the equation (6.1) can be simplified to

$$\frac{1}{r^2} \frac{\partial}{\partial r} \left(r^2 \langle (\delta v)^2 \delta v_r \rangle \right) = -4\varepsilon. \quad (6.14)$$

This equation, being integrated over a sphere of radius r, gives the form of well known 4/3 law à la Yaglom. To get the final 4/3 form from the divergence form, we consider the correlation length of the forcing term \mathbf{f} to be very large compared to r so that $\mathbf{f}' \simeq \mathbf{f}$. Under this assumption, we have

$$\varepsilon(r) = \langle \mathbf{v} \cdot \mathbf{f} + \mathbf{v}' \cdot \mathbf{f} \rangle \approx \langle \mathbf{v} \cdot \mathbf{f} + \mathbf{v}' \cdot \mathbf{f}' \rangle = 2 \langle \mathbf{v} \cdot \mathbf{f} \rangle = \varepsilon(0),$$

which render ε to be independent of the variable r thereby leading to the final 4/3 form. The above equation (6.14) is very crucial for understanding fluid turbulence. It shows that for homogeneous and isotropic turbulence the third-order moment of velocity structure function scales linearly with the corresponding length scale r inside the inertial zone. Inversely, inertial zone can, in turn, be defined in the physical space by this relation i.e. [inertial zone is the range of length scales for which the third-order velocity structure function is linear to \$r\$](#) .

Kolmogorov's 4/5 law from Yaglom's 4/3 law: In order to obtain Kolmogorov's 4/5 law given in equation (6.3) from the expression (6.2), we can simply use⁵ the equation (34.15) in [Landau & Lifshitz \(1959\)](#) which gives

$$\langle (\delta v_t)^2 \delta v_r \rangle = \frac{1}{6} \frac{\partial}{\partial r} (r \langle (\delta v_r)^3 \rangle), \quad (6.15)$$

where v_t is the transverse component (perpendicular to the longitudinal direction) of the velocity. Again, one can write

$$\langle (\delta v)^2 \delta v_r \rangle = 2 \langle (\delta v_t)^2 \delta v_r \rangle + \langle (\delta v_r)^3 \rangle.$$

Substituting this expression in relation (6.15) and using equation (6.2), we are left with the following ordinary differential form

$$4ydr + r^4 dy = -4\varepsilon r dr, \quad (6.16)$$

where $y = \langle (\delta v_r)^3 \rangle$. Multiplying both sides by integrating factor x^3 and then integrating, we finally obtain the required Kolmogorov form. In the final solution, we neglected the constant of integration by using the fact that all the structure functions do vanish at $r = 0$.

6.1.2 Incompressible MHD turbulence

In this part, we derive an exact relation for incompressible MHD turbulence of a plasma just by following the same method used in deriving the pure hydrodynamic equation in the previous section. In the current derivation again we use statistical homogeneity and the existence of two stationary states corresponding to total energy (kinetic + magnetic) and cross-helicity conservation whereas in their original derivation, Politano & Pouquet did not use any forcing. Also unlike PP98, (who derived their equation directly in terms of the Elsässer variables) here we shall derive the exact relation in terms of velocity

⁵A complete vectorial proof for -4/5 law is given by [Rasmussen \(1999\)](#) using rotational symmetry.

and magnetic fields (normalized to a velocity) and then we shall re-write that relation in terms of Elsässer variables. The basic equations are given by

$$\partial_t \mathbf{v} + (\mathbf{v} \cdot \nabla) \mathbf{v} = -\nabla P + (\nabla \times \mathbf{v}_A) \times \mathbf{v}_A + \nu \Delta \mathbf{v} + \mathbf{f}, \quad (6.17)$$

$$\partial_t \mathbf{v}_A = \nabla \times (\mathbf{v} \times \mathbf{v}_A) + \eta \Delta \mathbf{v}_A, \quad (6.18)$$

$$\nabla \cdot \mathbf{v} = 0, \quad \nabla \cdot \mathbf{v}_A = 0, \quad (6.19)$$

where $\mathbf{v}_A = \mathbf{b}/\sqrt{\mu_0 \rho}$ with \mathbf{b} being the magnetic field and ρ being the constant density. If the constant density is set to unity (for the sake of simplicity) then we can write $\mathbf{v}_A = \mathbf{b}/\sqrt{\mu_0}$. It is important to specify that in our approach, the system is forced only through momentum equation and not in the Faraday's equation whereas several numerical studies (Alexakis *et al.*, 2006) have been done by forcing the system both in kinetic and magnetic level. The absence of magnetic forcing can be thought to be an assurance of the absence of a magnetic helicity inverse cascade. We can therefore consider only the possibility of direct cascade hereinafter for 3D incompressible MHD turbulence. The total energy density and the cross-helicity density of the plasma are given by

$$E = \frac{1}{2} (v^2 + v_A^2), \quad H = \mathbf{v} \cdot \mathbf{v}_A.$$

The corresponding two-point correlation functions are respectively given by

$$\langle R_E \rangle = \frac{1}{2} \langle \mathbf{v} \cdot \mathbf{v}' + \mathbf{v}_A \cdot \mathbf{v}_A' \rangle, \quad \langle R_H \rangle = \frac{1}{2} \langle \mathbf{v} \cdot \mathbf{v}_A' + \mathbf{v}_A \cdot \mathbf{v}' \rangle.$$

Using the above definitions, one can also show

$$\langle (E + E') - (R_E + R_E') \rangle = \frac{1}{2} \langle (\delta \mathbf{v})^2 + (\delta \mathbf{v}_A)^2 \rangle, \quad (6.20)$$

$$\langle (H + H') - (R_H + R_H') \rangle = \langle \delta \mathbf{v} \cdot \delta \mathbf{v}_A \rangle. \quad (6.21)$$

Now we derive (as in the previous case) the evolution equation of the correlators. By some simple algebra and vector identities, we obtain,

$$\begin{aligned} \partial_t \langle \mathbf{v} \cdot \mathbf{v}' \rangle &= \langle \partial_t \mathbf{v} \cdot \mathbf{v}' + \mathbf{v} \cdot \partial_t \mathbf{v}' \rangle \\ &= \left\langle \left[-(\mathbf{v} \cdot \nabla) \mathbf{v} - \nabla P - \nabla \left(\frac{v_A^2}{2} \right) + (\mathbf{v}_A \cdot \nabla) \mathbf{v}_A \right] \cdot \mathbf{v}' \right. \\ &+ \left. \left[-(\mathbf{v}' \cdot \nabla') \mathbf{v}' - \nabla' P' - \nabla' \left(\frac{v_A'^2}{2} \right) + (\mathbf{v}_A' \cdot \nabla') \mathbf{v}_A' \right] \cdot \mathbf{v} \right\rangle + d_C + f_C \\ &= \langle [-(\mathbf{v} \cdot \nabla) \mathbf{v} + (\mathbf{v}_A \cdot \nabla) \mathbf{v}_A] \cdot \mathbf{v}' - [(\mathbf{v}' \cdot \nabla') \mathbf{v}' - (\mathbf{v}_A' \cdot \nabla') \mathbf{v}_A'] \cdot \mathbf{v} \rangle + d_C + f_C, \end{aligned} \quad (6.22)$$

where d_C and f_C are the resultant dissipative and forcing terms and can be expressed in the same way as that in the pure hydrodynamic case. In arriving

the last line we use the fact that for homogeneous incompressible turbulence the terms $\langle \mathbf{v}' \cdot \nabla P \rangle$, $\langle \mathbf{v} \cdot \nabla' P' \rangle$, $\langle \mathbf{v}' \cdot \nabla (v_A^2/2) \rangle$ and $\langle \mathbf{v} \cdot \nabla' (v_A'^2/2) \rangle$ vanish. Again we have

$$\begin{aligned} \partial_t \langle \mathbf{v}_A \cdot \mathbf{v}_A' \rangle &= \langle \partial_t \mathbf{v}_A \cdot \mathbf{v}_A' + \mathbf{v}_A \cdot \partial_t \mathbf{v}_A' \rangle \\ &= \langle [-(\mathbf{v}_A \cdot \nabla) \mathbf{v} + (\mathbf{v} \cdot \nabla) \mathbf{v}_A] \cdot \mathbf{v}_A' - [(\mathbf{v}_A' \cdot \nabla') \mathbf{v}' - (\mathbf{v}' \cdot \nabla') \mathbf{v}_A'] \cdot \mathbf{v}_A \rangle + d_M, \end{aligned} \quad (6.23)$$

where $d_M = \eta \langle \mathbf{v}_A \cdot \Delta' \mathbf{v}_A' + \mathbf{v}_A' \cdot \Delta \mathbf{v}_A \rangle$ is the magnetic dissipation term. Adding up equations (6.22) and (6.23), we obtain

$$\begin{aligned} \partial_t \langle R_E \rangle &= \partial_t \frac{1}{2} \langle \mathbf{v} \cdot \mathbf{v}' + \mathbf{v}_A \cdot \mathbf{v}_A' \rangle \\ &= \frac{1}{2} \left\langle [-(\mathbf{v} \cdot \nabla) \mathbf{v} + (\mathbf{v}_A \cdot \nabla) \mathbf{v}_A] \cdot \mathbf{v}' - [(\mathbf{v}' \cdot \nabla') \mathbf{v}' - (\mathbf{v}_A' \cdot \nabla') \mathbf{v}_A'] \cdot \mathbf{v} \right. \\ &\quad \left. + [-(\mathbf{v}_A \cdot \nabla) \mathbf{v} + (\mathbf{v} \cdot \nabla) \mathbf{v}_A] \cdot \mathbf{v}_A' - [(\mathbf{v}_A' \cdot \nabla') \mathbf{v}' - (\mathbf{v}' \cdot \nabla') \mathbf{v}_A'] \cdot \mathbf{v}_A \right\rangle + D + F \\ &= \frac{1}{2} \left\langle -(\mathbf{v} \cdot \nabla) [\mathbf{v}' \cdot \mathbf{v} + \mathbf{v}_A' \cdot \mathbf{v}_A] - (\mathbf{v}' \cdot \nabla') [\mathbf{v} \cdot \mathbf{v}' + \mathbf{v}_A \cdot \mathbf{v}_A] \right. \\ &\quad \left. + (\mathbf{v}_A \cdot \nabla) [\mathbf{v}_A' \cdot \mathbf{v} + \mathbf{v}_A \cdot \mathbf{v}'] + (\mathbf{v}_A' \cdot \nabla') [\mathbf{v}_A' \cdot \mathbf{v} + \mathbf{v}_A \cdot \mathbf{v}'] \right\rangle + D + F, \end{aligned} \quad (6.24)$$

where $D = (d_C + d_M)/2$ and $F = f_C/2$. Exploiting the solenoidal character of \mathbf{v} and \mathbf{v}_A and using the identities (6.20) and (6.21), we can write

$$\begin{aligned} \partial_t \langle R_E \rangle &= \frac{1}{2} \left\langle \nabla \cdot [-(\mathbf{v}' \cdot \mathbf{v}) \mathbf{v} + (\mathbf{v}' \cdot \mathbf{v}_A) \mathbf{v}_A + (\mathbf{v}_A' \cdot \mathbf{v}) \mathbf{v}_A - (\mathbf{v}_A' \cdot \mathbf{v}_A) \mathbf{v}] \right. \\ &\quad \left. + \nabla' \cdot [-(\mathbf{v}' \cdot \mathbf{v}) \mathbf{v}' + (\mathbf{v} \cdot \mathbf{v}_A') \mathbf{v}_A' + (\mathbf{v}_A \cdot \mathbf{v}') \mathbf{v}_A' - (\mathbf{v}_A' \cdot \mathbf{v}_A) \mathbf{v}'] \right\rangle + D + F \\ &= \nabla_{\mathbf{r}} \cdot \left\langle \left[-\frac{(\mathbf{v} \cdot \mathbf{v}')}{2} - \frac{(\mathbf{v}_A \cdot \mathbf{v}_A')}{2} \right] \delta \mathbf{v} + \left[\frac{(\mathbf{v} \cdot \mathbf{v}_A')}{2} + \frac{(\mathbf{v}_A \cdot \mathbf{v}')}{2} \right] \delta \mathbf{v}_A \right\rangle + D + F \\ &= \nabla_{\mathbf{r}} \cdot \langle R_E \delta \mathbf{v} + R_H \delta \mathbf{v}_A \rangle + D + F \\ &= \nabla_{\mathbf{r}} \cdot \left\langle \frac{\delta \mathbf{v}}{4} \left[(\delta \mathbf{v})^2 + \left(\frac{\delta \mathbf{v}_A}{2} \right)^2 \right] - 2 \delta \mathbf{v}_A (\delta \mathbf{v} \cdot \delta \mathbf{v}_A) \right\rangle + D + F. \end{aligned} \quad (6.25)$$

Now we consider a stationary state where the left-hand side of the equation (6.25) vanishes. In the inertial zone, we can neglect the dissipation D and moreover assuming the forcing to be the energy source i.e. writing $F = \varepsilon$, we get finally

$$\boxed{\nabla_{\mathbf{r}} \cdot \langle \delta \mathbf{v} [(\delta \mathbf{v})^2 + (\delta \mathbf{v}_A)^2] - 2 \delta \mathbf{v}_A (\delta \mathbf{v} \cdot \delta \mathbf{v}_A) \rangle = -4\varepsilon}, \quad (6.26)$$

which is the primitive form of Politano-Pouquet's exact relation. In isotropic case, integrating the above equation over a sphere of radius r , we obtain

$$\langle \delta v_r [(\delta \mathbf{v})^2 + (\delta \mathbf{v}_A)^2] - 2 \delta v_{Ar} (\delta \mathbf{v} \cdot \delta \mathbf{v}_A) \rangle = -\frac{4}{3} \varepsilon r, \quad (6.27)$$

which is identical to the equation (6) of Politano & Pouquet (1998a) in case of three dimensional turbulence. Performing the same method for cross-helicity correlators, we derive

$$-\langle \delta v_{Ar} [(\delta \mathbf{v})^2 + (\delta \mathbf{v}_A)^2] + 2\delta v_r (\delta \mathbf{v} \cdot \delta \mathbf{v}_A) \rangle = -\frac{4}{3}\varepsilon_c r, \quad (6.28)$$

where ε_c denotes the mean rate of cross-helicity injection flux. Rewriting the equations (6.27) and (6.28) in terms of Elsässer variables $\mathbf{z}^\pm = \mathbf{v} \pm \mathbf{v}_A$, we can finally obtain

$$\boxed{\langle (\delta \mathbf{z}^\pm)^2 \delta z_r^\mp \rangle = -\frac{4}{3}\varepsilon^\pm r,} \quad (6.29)$$

where ε^\pm denotes the mean rate of pseudo-energies ($E^\pm = \frac{1}{2}\mathbf{z}^\pm \cdot \mathbf{z}^\pm$) input flux by virtue of the forcing term. For incompressible case, both of the pseudo energies are inviscid invariants which leads to the possibility of obtaining an exact relation corresponding to each of them. As we shall see, this fact will no longer be true in compressible case thereby eliminating the possibility of two exact relations.

In another paper (Politano & Pouquet, 1998b) preceded by the mentioned one, they also derived the exact relations corresponding to longitudinal structure functions which can be thought to be the MHD version of Kolmogorov's 4/5 law.

6.2 Previous attempts for exact relations in compressible turbulence

Derivation of exact relations in compressible fluid turbulence is not trivial principally due to two reasons: (i) The fluid density is no more a constant thereby affecting the simple symmetric form of the two-point correlators and (ii) The basic assumptions of inertial zone, exclusive large scale forcing with delta correlation in time are not evident in compressible case (as discussed in the previous chapter). In spite of these difficulties, the field of compressible turbulence, which is of significant importance in space plasmas (solar wind, planetary magnetosphere etc.) and astrophysical plasmas (interstellar cloud, dilute interstellar media) demands desperately a sound analytical base in order to verify the universality and also to construct a plausible phenomenology in the mentioned field.

6.2.1 Heuristic approach by Carbone et al. (2009)

The importance of compressibility in solar wind turbulence has been perceived in several papers (Bavassano *et al.*, 1982; Hnat *et al.*, 2005). However, the

aspect of compressible scaling was, for the first time, investigated by [Carbone *et al.* \(2009\)](#). In that paper, they grossly wrote a heuristic relation (analogous to that of the Yaglom's form) for compressible turbulence in order to explain the heating of fast solar wind using the observational data of Ulysses spacecraft. In constructing the relation they used the third-order structure function of density-weighted Elsässer variables ($\mathbf{w}^\pm = \rho^{1/3} \mathbf{z}^\pm$) and they wrote

$$\boxed{\langle (\delta \mathbf{w}^\pm)^2 \delta w_r^\mp \rangle = \frac{4}{3} \langle \rho \rangle \varepsilon^\pm r.} \quad (6.30)$$

Their work was inspired by the numerical simulation of ([Kritsuk *et al.*, 2007a,b](#)) who obtained, for compressible turbulence (with r.m.s. Mach number ~ 6), a reasonable scaling relation and a $-5/3$ spectrum corresponding to the variables \mathbf{w}^\pm . Also in their 2009 paper, they showed some improvements⁶ in the scaling laws of fast solar wind (FSW) turbulence and in the estimation of the heating of FSW when compressible law is used instead of the incompressible version. Nevertheless, their equation (6.30) was not derived analytically from equations of compressible fluid dynamics and cannot therefore be called as an 'exact' relation.

6.2.2 FFO approach for a generalized exact equation

A more rigorous attempt was taken by Falkovich, Fouxon and Oz (FFO) in order to derive a generalized exact relation ([Falkovich *et al.*, 2010](#)) which could include incompressible hydrodynamics and incompressible MHD case as their special limits. Following the same prescription, Fouxon and Oz derived an exact relation for a compressible relativistic fluid too ([Fouxon & Oz, 2010](#)). In the following, we shall derive their exact relation for a non-relativistic fluid using our own notations.

The basic principle behind FFO formulation resides at the construction of a generalized continuity equation associating generalized density Q , generalized current \mathbf{J} and a generalized external source field \mathcal{S} and is given by

$$\partial_t Q + \nabla \cdot \mathbf{J} = \mathcal{S}. \quad (6.31)$$

They use a constitutive relation expressing the current term in terms of the density and a series of its spatial derivatives in order to close the generalized continuity equation. The closure equation is given by

$$J_i = F_i(Q) + \sum_k G_{ik}(Q) \nabla_k Q + \dots, \quad (6.32)$$

⁶Their method of data analysis and conclusions on scaling and heating were put into questions by ([Forman *et al.*, 2010](#)).

where G_{ik} is the Jacobian tensor and the dots represent the higher derivatives. The zeroth-order term $F_i(Q)$ is associated to conservative dynamics whereas the first derivative represents the dissipation. For fluid dynamics, they neglect the higher derivatives and by replacing the closure equation in equation (6.31), they obtain

$$\partial_i Q + \frac{\partial F_i}{\partial r_i} = \mathcal{S} - \frac{\partial}{\partial r_i} \left(\sum_k G_{ik}(Q) \nabla_k Q \right). \quad (6.33)$$

Thereafter, they consider a steady-state condition where $\partial_t \langle Q(0, t) Q(\mathbf{r}, t) \rangle = 0$. Under statistical symmetries, they obtain (according to FF0)

$$\begin{aligned} \partial_t \langle Q(0, t) Q(\mathbf{r}, t) \rangle &= -2 \frac{\partial}{\partial r_i} \langle Q(\mathbf{0}, t) F_i(\mathbf{r}, t) \rangle + \langle Q(\mathbf{0}, t) \mathcal{S}(\mathbf{r}, t) \rangle \\ &\quad - \frac{\delta}{\delta r_i} \left\langle Q(\mathbf{0}, t) \left(\sum_k G_{ik}(\mathbf{r}, t) \nabla_k Q(\mathbf{r}, t) \right) \right\rangle = 0. \end{aligned} \quad (6.34)$$

In the final step of derivation, they assumed a large correlation length for the source term \mathcal{S} (which is identified as the forcing term in standard turbulence) with respect to the length scale r . Under that hypothesis, one can write $\mathcal{S}(\mathbf{r}, t) \approx \mathcal{S}(\mathbf{0}, t)$ and hence $\langle Q(\mathbf{0}, t) \mathcal{S}(\mathbf{r}, t) \rangle \approx \langle Q(\mathbf{0}, t) \mathcal{S}(\mathbf{0}, t) \rangle \equiv \bar{\varepsilon}$, where the constant $\bar{\varepsilon}$ denotes the mean input rate of Q^2 . Furthermore if the concerned length scale is too distant to experience any viscous effect, the resultant relation is given by (equation (2.4), [Falkovich *et al.* \(2010\)](#)):

$$\nabla_i \langle Q(\mathbf{0}, t) F_i(\mathbf{r}, t) \rangle = \bar{\varepsilon}. \quad (6.35)$$

The further assumption of isotropy reduces the above exact relation to

$$\boxed{\langle Q(\mathbf{0}, t) F_i(\mathbf{r}, t) \rangle = \frac{\bar{\varepsilon} r_i}{d}}, \quad (6.36)$$

where d is the spatial dimension.

The equation (6.36) was their generalized exact relation for homogeneous isotropic turbulence. The general form was then reduced to some familiar simplified cases like passive-scalar turbulence, incompressible hydrodynamic turbulence and also the non-trivial case like compressible turbulence with barotropic closure just by some appropriate choice of the generalized density and current. The reduced forms along with corresponding choices of Q and \mathbf{F} (or \mathbf{J}) are given in the following table

Limitations of FFO approach Despite having an analytical base in the derivation, FFO relation(s) suffered from the following subtle mathematical

Nature of flow	Choice of Variables	Exact Relation
Passive scalar turbulence	$Q \equiv \theta$ (passive scalar) & $\mathbf{J} \equiv \theta \mathbf{v} - \kappa \nabla \theta$	$\langle \theta(\mathbf{0}) \theta(\mathbf{r}) \mathbf{v}(\mathbf{r}) \rangle = \frac{\bar{\epsilon} \mathbf{r}}{d}$
Compressible barotropic turbulence	$Q^4 \equiv (\rho \mathbf{v}, \rho), J^4 \equiv Q^4 \mathbf{v}$ & $F \equiv \rho \mathbf{v} \otimes \mathbf{v} + P(\rho) \mathbb{1}$	$\langle \rho(\mathbf{0}) v_j(\mathbf{0}) [\rho(\mathbf{r}) v_j(\mathbf{r}) v_i(\mathbf{r}) + P(\mathbf{r}) \delta_{ij}] \rangle = \frac{\bar{\epsilon} r_i}{d}$
Incompressible hydrodynamic turbulence	$\rho = const., Q \equiv \mathbf{v}$ & $F \equiv \mathbf{v} \otimes \mathbf{v}$	$\langle v_j(\mathbf{0}) v_j(\mathbf{r}) v_i(\mathbf{r}) \rangle = \frac{\bar{\epsilon} r_i}{d}$

and physical shortcomings:

(i) Unlike the exact relations in incompressible turbulence, FFO relations are expressed in terms of the correlation functions instead of structure functions. One should note that for compressible case, the passage between the correlation functions and structure functions is no more trivial and needs additional calculations⁷. Absence of structure functions in the FFO relations prevents one to perform any spectral or phenomenological prediction in terms of the fluctuations and this point constitutes a non-negligible physical limitation of the FFO approach.

(ii) In deriving the divergence form of their equation (equation (2.4)), they unawarely used mirror symmetry or weak isotropy by assuming

$$\begin{aligned} \langle Q(\mathbf{0}, t) F_i(\mathbf{r}, t) \rangle &= \langle Q(\mathbf{r}, t) F_i(\mathbf{0}, t) \rangle \\ \langle Q(\mathbf{0}, t) \mathcal{S}(\mathbf{r}, t) \rangle &= \langle Q(\mathbf{r}, t) \mathcal{S}(\mathbf{0}, t) \rangle. \end{aligned}$$

Note that the above equalities cannot be led by statistical homogeneity without using at least weak isotropy. The point is however left obscure in their paper where just before the above simplification they mentioned "using statistical symmetries" without precising them. They awarely used statistical isotropy to obtain equation (2.5) (JFM, 2010) from (2.4) where they mentioned "Assuming in addition, isotropy one finds ...". This issue clearly makes their derivations more limited than the divergence forms which can be obtained just by statistical homogeneity.

⁷As we shall see later that this passage leads to the introduction of the source terms in the exact relations.

(iii) The third and the most serious issue of FFO approach was their assumption of a stationary state corresponding to the current-density correlation function. From continuity equation and compressible Navier-Stokes equations, we obtain:

$$\begin{aligned}\partial_t \langle \rho \rho' \mathbf{v} \cdot \mathbf{v}' \rangle &= \langle \rho \mathbf{v} \cdot \partial_t (\rho' \mathbf{v}') \rangle + \langle \rho' \mathbf{v}' \cdot \partial_t (\rho \mathbf{v}) \rangle \\ &= -\nabla_{\mathbf{r}} \cdot \langle \rho \rho' (\mathbf{v} \cdot \mathbf{v}') \delta \mathbf{v} + \rho P' \mathbf{v} - \rho' P \mathbf{v}' \rangle + \tilde{d} + \tilde{f},\end{aligned}\quad (6.37)$$

where:

$$\tilde{d} = \tilde{d}(\mathbf{r}) = \langle \rho' \mathbf{v}' \cdot \mathbf{d} + \rho \mathbf{v} \cdot \mathbf{d}' \rangle, \quad \tilde{f} = \tilde{f}(\mathbf{r}) = \langle \rho' \mathbf{v}' \cdot \mathbf{f} + \rho \mathbf{v} \cdot \mathbf{f}' \rangle. \quad (6.38)$$

For homogeneous turbulence we can write:

$$\langle \delta(\rho \mathbf{v}) \cdot \delta(\rho \mathbf{v}) \rangle = 2 \langle \rho^2 \mathbf{v}^2 \rangle - 2 \langle \rho \rho' \mathbf{v} \cdot \mathbf{v}' \rangle, \quad (6.39)$$

which leads to:

$$\partial_t \langle \rho \rho' \mathbf{v} \cdot \mathbf{v}' \rangle = \frac{1}{2} \partial_t \langle \delta(\rho \mathbf{v}) \cdot \delta(\rho \mathbf{v}) \rangle - \partial_t \langle \rho^2 \mathbf{v}^2 \rangle. \quad (6.40)$$

Since the quantity $\rho^2 \mathbf{v}^2$ is *not* the density of an inviscid invariant its time derivative introduces a nonlinear contribution which has a non conservative form, namely:

$$\partial_t \langle \rho^2 \mathbf{v}^2 \rangle = -2 \langle \rho \mathbf{v} \cdot [\nabla \cdot (\rho \mathbf{v} \otimes \mathbf{v})] + \rho \mathbf{v} \cdot \nabla P \rangle + \tilde{d}(0) + \tilde{f}(0). \quad (6.41)$$

In the previous derivations we always considered the stationary state corresponding to average energy which is an inviscid invariant and so does not lead to the appearance of such type of nonlinear contribution. Therefore, it is important to check (e.g. by numerical simulations) if the assumption of stationarity can be applied to the current-density correlation function (whereas it is applicable for the fluctuating part written in terms of structure functions) before deriving exact relations supposing the existence of such a stationary state. In fact, direct numerical simulations (Wagner *et al.*, 2012; Kritsuk *et al.*, 2013) have shown that the FFO relation lack universality and does not give satisfactory scaling. This problem is believed to be generated by their choice of stationary state corresponding to a quantity which is not an inviscid conserved quantity.

6.3 New exact relations and phenomenologies in compressible turbulence : My research work

Due to the abovesaid limitations of the previous attempts, we derived vectorial exact relations for compressible turbulence considering the inviscid conserva-

tion of total energy. We have derived three exact relations for compressible hydrodynamic (Galtier & Banerjee, 2011) and MHD turbulence (Banerjee & Galtier, 2013) with isothermal closure and also for the turbulence in a compressible polytropic neutral fluid (Banerjee & Galtier, 2014). The principal objective of these relations is to understand the different results obtained from the direct numerical simulations (DNS) of compressible turbulence and also to understand the role of compressibility in space plasma turbulence by studying the spacecraft data (for solar wind, planetary magnetosphere etc.). The derivation of these exact relations constitutes the theoretical aspect of my thesis. The derivations will be carried out in a detailed manner in the following.

6.3.1 Isothermal hydrodynamic turbulence

As in incompressible turbulence, here also we start with the basic hypotheses of (a) an infinitely large Reynolds number to ensure a completely developed turbulence and (b) statistical homogeneity. No prior assumption of isotropy is made. In addition, an isothermal closure i.e. $P = C_s^2 \rho$ (where C_s is the constant sound speed of the fluid medium) is used for the current study. The complete set of three-dimensional compressible equations are thus given in the following:

$$\begin{aligned} \partial_t \rho + \nabla \cdot (\rho \mathbf{v}) &= 0, \\ \partial_t (\rho \mathbf{v}) + \nabla \cdot (\rho \mathbf{v} \otimes \mathbf{v}) &= -\nabla P + \mathbf{d} + \mathbf{f}, \\ P &= C_s^2 \rho, \end{aligned}$$

where $\mathbf{d} = \mu \Delta \mathbf{v} + \frac{\mu}{3} \nabla (\nabla \cdot \mathbf{v})$ represents the viscous term and the other symbols have their usual meaning. \mathbf{f} is chosen to be stationary, homogeneous, delta-correlated in time and acting at large scales of the flow.

For a compressible isothermal fluid, the energy density is given as

$$E = \frac{\rho v^2}{2} - \rho \int P d \left(\frac{1}{\rho} \right) = \frac{\rho v^2}{2} - \rho e, \quad (6.42)$$

where $e = C_s^2 \ln(\rho/\rho_0)$ the internal energy per unit mass (ρ_0 is a constant density at equilibrium).

The energy equation then takes the form

$$\partial_t \langle E \rangle = -\mu \langle (\nabla \times \mathbf{v})^2 \rangle - \frac{4}{3} \mu \langle (\nabla \cdot \mathbf{v})^2 \rangle + F, \quad (6.43)$$

where $\langle \rangle$ denotes statistical average and F is the mean rate of energy flux injected at the injection scale(s). We can therefore assume the existence of a

stationary state where the total average energy is unchanged in course of time owing to the mutual balance of the average dissipative and forcing terms.

The relevant two-point energy correlation functions associated to the points \mathbf{x} and \mathbf{x}' can be defined as

$$\langle R \rangle = \left\langle \frac{1}{2} \rho \mathbf{v} \cdot \mathbf{v}' + \rho e' \right\rangle, \quad \langle R' \rangle = \left\langle \frac{1}{2} \rho' \mathbf{v}' \cdot \mathbf{v} + \rho' e \right\rangle. \quad (6.44)$$

Unlike incompressible case, energy correlators corresponding to E and E' are not the same in the compressible case due to the variable character of local density.

Using the above definitions, one can show

$$\langle (E + E') - (R + R') \rangle = \frac{1}{2} \langle \delta(\rho \mathbf{v}) \cdot \delta \mathbf{v} \rangle + \langle \delta \rho \delta e \rangle. \quad (6.45)$$

As we shall see later this relation (6.45) is a key relation for deriving an exact relation for some two-point correlation functions.

Now we shall derive a dynamical equation for $\langle R + R' \rangle$. To do that first we calculate

$$\begin{aligned} \partial_t \langle \rho \mathbf{v} \cdot \mathbf{v}' \rangle &= \langle \rho \mathbf{v} \cdot \partial_t \mathbf{v}' + \mathbf{v}' \cdot \partial_t (\rho \mathbf{v}) \rangle \\ &= \langle \rho \mathbf{v} \cdot (-\mathbf{v}' \cdot \nabla' \mathbf{v}' - \frac{1}{\rho'} \nabla' P') \rangle + \langle \mathbf{v}' \cdot (-\nabla \cdot (\rho \mathbf{v} \mathbf{v}) - \nabla P) \rangle + d_1 + f_1, \end{aligned} \quad (6.46)$$

where

$$d_1 = \left\langle \frac{\rho}{\rho'} \mathbf{v} \cdot \mathbf{d}' + \mathbf{v}' \cdot \mathbf{d} \right\rangle, \quad f_1 = \left\langle \frac{\rho}{\rho'} \mathbf{v} \cdot \mathbf{f}' + \mathbf{v}' \cdot \mathbf{f} \right\rangle,$$

denote respectively the contributions to the correlation of the viscous and forcing terms. In addition using the identities

$$\left\langle \frac{\rho}{\rho'} \mathbf{v} \cdot \nabla' P' \right\rangle = \langle C_s^2 \frac{\rho}{\rho'} \mathbf{v} \cdot \nabla' \rho' \rangle = \langle C_s^2 \rho \mathbf{v} \cdot \nabla' (\ln \rho') \rangle = \langle \nabla' \cdot (\rho e' \mathbf{v}) \rangle,$$

and

$$\langle \mathbf{v}' \cdot \nabla' (\rho \mathbf{v} \cdot \mathbf{v}') \rangle = \langle \nabla' \cdot (\rho (\mathbf{v} \cdot \mathbf{v}') \mathbf{v}') - \rho (\mathbf{v} \cdot \mathbf{v}') (\nabla' \cdot \mathbf{v}') \rangle,$$

we can rewrite (6.46) in the following way

$$\begin{aligned} &\partial_t \langle \rho \mathbf{v} \cdot \mathbf{v}' \rangle \\ &= \langle -\mathbf{v}' \cdot \nabla' (\rho \mathbf{v} \cdot \mathbf{v}') - \nabla' \cdot (\rho e' \mathbf{v}) \rangle - \langle \nabla \cdot (\rho (\mathbf{v} \cdot \mathbf{v}') \mathbf{v} + P \mathbf{v}') \rangle + d_1 + f_1 \\ &= \nabla_{\mathbf{r}} \cdot \langle -\rho (\mathbf{v} \cdot \mathbf{v}') \delta \mathbf{v} + P \mathbf{v}' - \rho e' \mathbf{v} \rangle + \langle \rho (\mathbf{v} \cdot \mathbf{v}') (\nabla' \cdot \mathbf{v}') \rangle + d_1 + f_1. \end{aligned} \quad (6.47)$$

Secondly, we have to complete the computation with

$$\begin{aligned} \partial_t \langle \rho e' \rangle &= \langle \rho \partial_t e' + e' \partial_t \rho \rangle = \langle C_s^2 \frac{\rho}{\rho'} \partial_t \rho' + e' \partial_t \rho \rangle \\ &= \langle -C_s^2 \frac{\rho}{\rho'} \nabla' \cdot (\rho' \mathbf{v}') - e' \nabla \cdot (\rho \mathbf{v}) \rangle \\ &= -\langle \nabla' \cdot (C_s^2 \rho \mathbf{v}') \rangle + \langle \rho' \mathbf{v}' \cdot \nabla' (C_s^2 \frac{\rho}{\rho'}) \rangle - \langle \nabla \cdot (\rho e' \mathbf{v}) \rangle. \end{aligned} \quad (6.48)$$

Again noting that

$$\langle \rho' \mathbf{v}' \cdot \nabla' (C_s^2 \frac{\rho'}{\rho'}) \rangle = -\langle \nabla' \cdot (\rho e' \mathbf{v}') \rangle + \langle e' \nabla' \cdot (\rho \mathbf{v}') \rangle,$$

we obtain after simplification

$$\partial_t \langle \rho e' \rangle = \nabla_{\mathbf{r}} \cdot \langle -\rho e' \delta \mathbf{v} - P \mathbf{v}' \rangle + \langle \rho e' (\nabla' \cdot \mathbf{v}') \rangle. \quad (6.49)$$

The combination of (6.47) and (6.49) leads to

$$\partial_t \langle R \rangle = \nabla_{\mathbf{r}} \cdot \left\langle -R \delta \mathbf{v} - \frac{1}{2} P \mathbf{v}' - \frac{1}{2} \rho e' \mathbf{v}' \right\rangle + \langle (\nabla' \cdot \mathbf{v}') R \rangle + d_1 + f_1. \quad (6.50)$$

By performing the same type of analysis for $\langle R' \rangle$, we get

$$\partial_t \langle R' \rangle = \nabla_{\mathbf{r}} \cdot \left\langle -R' \delta \mathbf{v} + \frac{1}{2} P' \mathbf{v} + \frac{1}{2} \rho' e \mathbf{v}' \right\rangle + \langle (\nabla \cdot \mathbf{v}) R' \rangle + d'_1 + f'_1, \quad (6.51)$$

where d'_1 and f'_1 represent respectively the dissipative and forcing terms. Now adding up equations (6.50) and (6.51), we get

$$\begin{aligned} \partial_t \left\langle \frac{R + R'}{2} \right\rangle &= \frac{1}{2} \nabla_{\mathbf{r}} \cdot \left\langle -(R + R') \delta \mathbf{v} - \frac{1}{2} (P \mathbf{v}' + \rho e' \mathbf{v}' - P' \mathbf{v} - \rho' e \mathbf{v}') \right\rangle \\ &+ \frac{1}{2} \langle (\nabla' \cdot \mathbf{v}') R + (\nabla \cdot \mathbf{v}) R' \rangle + \frac{1}{2} (d_1 + d'_1 + f_1 + f'_1). \end{aligned} \quad (6.52)$$

For the final step of the derivation we shall introduce the usual assumption specific to three-dimensional fully developed turbulence with a direct energy cascade (Frisch, 1995). In particular, we suppose the existence of a statistical steady state in the infinite Reynolds number limit with a balance between forcing and dissipation. We recall that the dissipation is a sink for the total energy and acts mainly at the smallest scales of the system. Then, far in the inertial range we may neglect the contributions of the dissipative terms in equation (6.52) (Aluie, 2011). Writing $f_1 + f'_1 = 2\varepsilon$ and introducing the structure functions we obtain the final form

$$\boxed{-2\varepsilon = \langle (\nabla' \cdot \mathbf{v}') (R - E) \rangle + \langle (\nabla \cdot \mathbf{v}) (R' - E') \rangle + \nabla_{\mathbf{r}} \cdot \left\langle \left[\frac{\delta(\rho \mathbf{v}) \cdot \delta \mathbf{v}}{2} + \delta \rho \delta e - C_s^2 \bar{\delta} \rho \right] \delta \mathbf{v} + \bar{\delta} e \delta(\rho \mathbf{v}) \right\rangle}, \quad (6.53)$$

where ε is the mean total energy injection rate (which is equal to the mean total energy dissipation rate; see relation (6.43)).

Incompressible limit For an incompressible fluid, we have $(\nabla \cdot \mathbf{v}) = (\nabla' \cdot \mathbf{v}') = 0$ which let the source terms vanish. Moreover, we have $\rho = \rho_0$ which leads to $\delta\rho = 0$ and $e = 0$ and indeed we obtain

$$-4\varepsilon = \nabla_{\mathbf{r}} \cdot \langle (\delta\mathbf{v})^2 \delta\mathbf{v} \rangle, \quad (6.54)$$

which can be identified as the primitive form of the Kolmogorov's law.

Phenomenological approach under isotropy Expression (6.53) is the new exact relation for structure functions in fully developed compressible turbulence. It is valid for homogeneous – non necessarily isotropic – three-dimensional compressible isothermal turbulence. When isotropy is additionally assumed this relation can be written symbolically as

$$-2\varepsilon = \mathcal{S}(r) + \frac{1}{r^2} \partial_r (r^2 \mathcal{F}_r), \quad (6.55)$$

where \mathcal{F}_r is the radial component of the isotropic energy flux vector. In comparison with the incompressible case (6.54), expression (6.55) reveals the presence of a new type of term \mathcal{S} which is by nature compressible since it is proportional to the dilatation (i.e. the divergence of the velocity). This term has a major impact on the nature of compressible turbulence since as we will see it acts like a source or a sink for the mean energy transfer rate. Note that \mathcal{S} consists of two terms which account for two-point measurement approach. If we further reduce equation (6.55) by performing an integration over a ball of radius r , after simplification we find

$$-\frac{2}{3}\varepsilon r = \frac{1}{r^2} \int_0^r \mathcal{S}(r) r^2 dr + \mathcal{F}_r(r). \quad (6.56)$$

We start the discussion by looking at the small scale limit of the previous relation which means that the scales are assumed to be small enough to perform a Taylor expansion but not too small to be still in the inertial range. We obtain $\mathcal{S}(r) = \mathcal{S}(0) + r\partial_r\mathcal{S}(0) = r\partial_r\mathcal{S}(0)$ which leads to

$$-\frac{2}{3} \left[\varepsilon + \frac{3}{8} r \partial_r \mathcal{S}(0) \right] r \equiv -\frac{2}{3} \varepsilon_{\text{eff}} r = \mathcal{F}_r(r). \quad (6.57)$$

Note that we do not assume the cancellation of the first derivative of S at $r = 0$ although the function, $R - E$, reaches an extremum at $r = 0$; the reason is that this function is weighted by the dilatation function which may have a non trivial form. We see that at the leading order the main contribution of $\mathcal{S}(r)$ is to modify ε for giving an effective mean total energy injection rate ε_{eff} . Then, the physical interpretation of (6.57) is the following. When the flow is

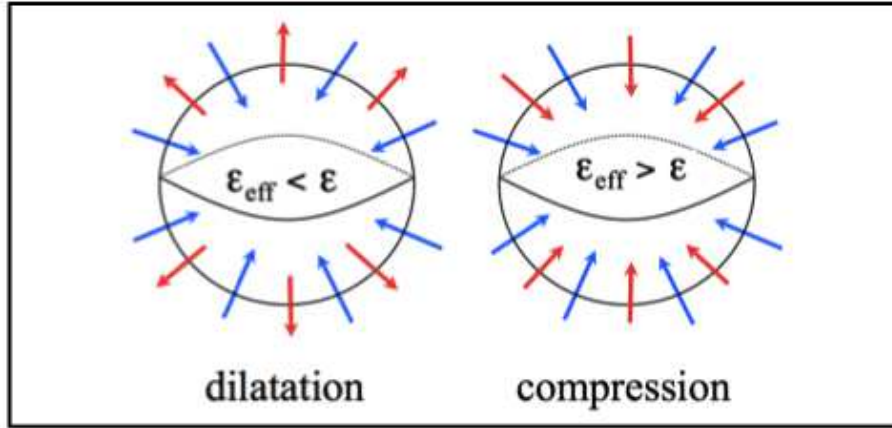


Figure 6.1: Dilatation (left) and compression (right) phases in space correlation for isotropic turbulence. In a direct cascade scenario the flux vectors (blue arrows) are oriented towards the center of the sphere. Dilatation and compression (red arrows) are additional effects which act respectively in the opposite or in the same direction as the flux vectors.

mainly in a phase of dilatation (positive velocity divergence), the additional term is negative and ε_{eff} is smaller than ε . On the contrary, in a phase of compression $\partial_r \mathcal{S}(0)$ is positive and ε_{eff} is larger than ε .

An illustration of dilatation and compression effects in the space correlation is given in figure 6.1. In both cases, the flux vector \mathcal{F} (dashed arrows) is oriented towards the center of the sphere ($r = 0$) since a direct cascade is expected. Dilatation and compression act additionally (solid arrows): in the first case, the effect is similar to a decrease of the local mean total energy transfer rate whereas in the second case it is similar to an increase of the local mean total energy transfer rate.

The discussion may be extended to the entire inertial range (i.e. for larger values of r). In this case the analysis is focused on expression (6.56) for which we have already noted that a term like $R - E$ is mainly negative. It is interesting to note that $\mathcal{S}(r)$ is composed of two types of term which are different by nature. First, there is the dilatation dominated by the smallest scales in the flow – the shocklets – which mainly give a negative contribution with a fast variation (Smith *et al.*, 2000). Secondly, there is the correlation $R - E$ which derives most of its contribution from relatively larger scales - where we mainly feel eddies - with a slower variation. This remark may lead to the assumption that both terms are relatively decorrelated (Aluie, 2011).

Then $\mathcal{S}(r)$ may be simplified as (by using relation (6.45))

$$\mathcal{S}(r) \simeq - \left\langle \bar{\delta}(\nabla \cdot \mathbf{v}) \left[\frac{1}{4} \delta(\rho \mathbf{v}) \cdot \delta \mathbf{v} + \frac{1}{2} \delta \rho \delta e \right] \right\rangle. \quad (6.58)$$

The previous expression is not derived rigorously but it may give us some intuition about its contribution. For example, we may expect a power law dependence close to $r^{2/3}$ for the structure functions. Direct numerical simulations have never shown a scale dependence for the dilatation therefore we may expect that it behaves like a relatively small factor. Then $\mathcal{S}(r)$ will still modify ε as explained in the discussion above, however the power law dependence in r would be now slightly different. In conclusion and according to this simple analysis we see that compression effects (through the dilatation) will mainly impact the scaling law at the largest scales.

Compressible spectrum. We may try to predict a power law spectrum for compressible turbulence. First, we recall that several predictions have been made for the kinetic energy spectrum and also for the spectra associated with the solenoidal or the compressible part of the velocity (Moiseev *et al.*, 1981; Passot *et al.*, 1988). Although these decompositions are convenient for theoretical developments, the associated energies are not inviscid invariants and the predictions are heuristic. For incompressible turbulence the situation is different because a prediction in $k^{-5/3}$ for the kinetic energy spectrum may be proposed by applying a dimensional analysis directly on the exact relation (Frisch, 1995) which in turn gives a stronger foundation to the energy spectrum for which a constant flux is expected. This remark was already noted in particular in recent three-dimensional direct numerical simulations (discussed in the previous chapter) of isothermal turbulence where it is observed that the Kolmogorov scaling is not preserved for the spectra based only on the velocity fluctuations .

We shall now derive a power law spectrum for compressible turbulence by applying a dimensional analysis on equation (6.53). The prediction – although not exact – will have therefore stronger foundation than a pure phenomenological spectral law. Dimensionally, we find $\varepsilon_{\text{eff}} r \sim \rho v^3$. By introducing the density-weighted fluid velocity, $\mathbf{w} \equiv \rho^{1/3} \mathbf{v}$, and following Kolmogorov we obtain

$$E^w(k) \sim \varepsilon_{\text{eff}}^{2/3} k^{-5/3}, \quad (6.59)$$

where $E^w(k)$ is the spectrum associated to the new variable \mathbf{w} . As explained by several authors (Kadomtsev & Petviashvili, 1973; Moiseev *et al.*, 1981) in compressible turbulence we do not expect a constant flux in the inertial range. Here, the same conclusion is reached since we are dealing with an

effective mean energy transfer rate. More precisely if we expect a power law dependence in k for the effective transfer rate one arrives at the conclusion that a steeper power law spectrum may happen at the largest scales. According to relation (6.58) and the simple estimate, $\rho v^2 \sim r^{2/3}$, we could have $E^w(k) \sim k^{-19/9}$. This prediction means that for a small prefactor in (6.58) one needs an extended inertial range to feel the compressible effects on the power spectrum.

Experimental validity Our exact relation has recently been verified by numerical simulations of supersonic turbulence (r.m.s. Mach ~ 6) with 1024^3 resolution ((Kritsuk *et al.*, 2013)) where the authors have pointed out that the exponent of the third-order velocity structure function is close to one if the field used is \mathbf{w} instead of \mathbf{v} . In fact they evaluated both the flux and the source term of equation (6.55) and they found that the flux term is negative whereas the source term is positive but is considerably smaller than the flux term (by magnitude). Finally the sum of the two is found to follow a linear scaling with the fluctuation length scale for nearly two decades of length scales (see figure 6.2). From observational point of view, the solar wind is an interesting

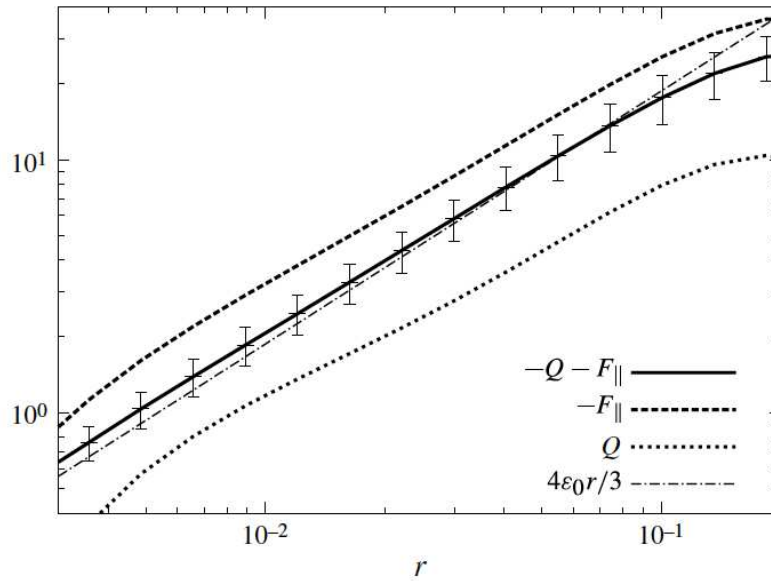


Figure 6.2: Numerical verification of scaling (logarithmic plot) of the flux (F) and the source terms (Q) of equation (6.55) in supersonic turbulence using 1024^3 resolution; *Reprinted with permission from Kritsuk et al. (2013)*; © (2013) Cambridge university press.

example for which a data analysis has revealed such a multiscale behavior at low frequency (burlaga). In addition, this work is believed to found the

primordial base to the findings and conclusions of [Carbone *et al.* \(2009\)](#) using fast solar wind data of Ulysses spacecraft. However, in order to establish a stronger theoretical foundation in the last case one has to deal with plasma thereby inspiring an exact relation in compressible MHD turbulence.

6.3.2 A new phenomenology for compressible turbulence

Construction of a consistent phenomenology is non-trivial and debatable for compressible turbulence as we can no longer think of pure eddies as the compressible velocity field is not solenoidal (divergenceless). Similarly, in case of compressible MHD turbulence, we have to abandon the idea of Alfvén effect because of two compressional modes (magnetosonic waves) co-existing with Alfvén mode which is a pure incompressible mode. The only existing phenomenology for compressible case is using the Burger’s equation which is a one-dimensional equation and predicts a -2 velocity power spectrum for supersonic turbulence using the notion of shock formation ([Frisch, 1995](#)). This phenomenology cannot describe the subsonic regime. As it was discussed in the last chapter, [Kritsuk *et al.* \(2007a\)](#) predict a -5/3 spectrum for subsonic turbulence and a -2 spectrum for supersonic turbulence for three dimensional (3D) compressible isothermal turbulence. A satisfactory phenomenological description for 3D compressible fluid turbulence (and so for MHD) is yet to be developed. Note that unlike incompressible hydrodynamics, in a compressible fluid there is sonic or acoustic wave which is a linear mode. In the following we try to propose ([Banerjee & Galtier, 2012](#)) a possible phenomenological picture (without using directly the shock formation) for understanding the spectra of different regimes (subsonic and supersonic) in compressible turbulence. We start with our derived exact relation which is written as

$$-2\varepsilon = \langle (\nabla' \cdot \mathbf{v}') (R - E) \rangle + \langle (\nabla \cdot \mathbf{v}) (R' - E') \rangle + \nabla_{\mathbf{r}} \cdot \left\langle \left[\frac{\delta(\rho \mathbf{v}) \cdot \delta \mathbf{v}}{2} + \delta \rho \delta e - C_s^2 \bar{\delta} \rho \right] \delta \mathbf{v} + \bar{\delta} e \delta(\rho \mathbf{v}) \right\rangle$$

the first two terms of right hand side present the source terms (exclusive for compressible turbulence) whereas the third one represents the flux term. We note that the source terms are having $(\nabla \cdot \mathbf{v})$ or $(\nabla' \cdot \mathbf{v}')$ as coefficient. Neglecting the dispersive effect of the flow field, we can show (by the basic equations) that the divergence or the dilatation terms propagate with a constant phase velocity C_S (sound speed in the corresponding turbulent medium). Moreover, the total source term can be written approximately as

$$\mathcal{S} \sim \left\langle (\nabla \cdot \mathbf{v}) \left(\frac{1}{2} \rho' \mathbf{v}' \cdot \delta \mathbf{v} \right) \right\rangle \sim \langle (\nabla \cdot \delta \mathbf{v}) (\rho' \mathbf{v}' \cdot \delta \mathbf{v}) \rangle.$$

We can remark that in the flux terms the energy density fluctuations are transported by the fluid velocity fluctuation (represented by the term $\frac{1}{2}[\delta(\rho\mathbf{v}) \cdot \delta\mathbf{v}]$) whereas the source terms represent the transport of the scalar $\rho\mathbf{v} \cdot \delta\mathbf{v}$ by $(\nabla \cdot \mathbf{v})$ where the fluctuating quantity is $\delta\mathbf{v}$. The basic elements describing a possible phenomenology for isothermal compressible hydrodynamic turbulence are the following:

(i) For a given length scale l , there is a competition between the flux and the source terms regarding the transport of their respective fluctuating scalars (as defined above) between two points separated by l .

(ii) Considering turbulence to be a phenomenon without memory, the transport which will cover the distance l later (i.e. with a greater characteristic time) will determine the characteristic non-linear energy transfer time for that length scale l .

(iii) In this case, we can define two characteristic times $\tau_l (= l/v_l)$ and $\tau_C (= l/C_S)$ where $v_l \sim |\delta\mathbf{v}|$.

iv) We assume that the time rate of average total energy is a scale invariant.

Along with these assumptions, we consider three following cases:

(a) **Subsonic turbulence** ($\delta v < C_S$) : In this case, the transport by the flux terms, being slower of the two, governs the effective energy transfer and so the analysis

$$\varepsilon \sim \frac{\rho_l v_l^2}{\tau_l} \sim \frac{\rho_l v_l^3}{l} \Rightarrow E^w(k) \sim \varepsilon^{2/3} k^{-5/3},$$

where $\mathbf{w} \equiv \rho^{1/3}\mathbf{v}$. This prediction is supported by recent numerical simulations of compressible isothermal turbulence (Kritsuk *et al.*, 2007a; Federrath *et al.*, 2010).

(b) **Supersonic turbulence** ($\delta v > C_S$): In this case, the source terms, being slower than the flux terms, governs the interscale energy transfer of the flow and thus the characteristic time is $\tau_{tr} = \tau_C$. Utilizing the exact relation we find

$$\varepsilon \sim \frac{\rho_l v_l^2}{\tau_C} \sim (\rho v) \frac{v_l^2}{l} \Rightarrow E^v(k) \sim \varepsilon k^{-2}.$$

this prediction finds experimental verification in numerical work of Federrath *et al.* (2010).

(c) **Sonic scale** ($\delta v = C_S$): At this scale $v_l = C_S$ and so the characteristic times are also equal. As it is a given scale (k given), we cannot expect a power law for that. But evaluating properly the $E^w(k)$ and $E^v(k)$ and then equalizing them for $l = l_S$ we can estimate the sonic scale (l_S). Schematically, hence we can write the compressible turbulence phenomenology as follows

$$\varepsilon \sim \left\{ \frac{\rho_l v_l^3}{l}, \frac{M_S}{\tau_C} (\rho v) v_l \right\},$$

where $M_S = \frac{v_l}{C_S}$ is the sonic turbulent Mach number and the above two expressions represent the average energy transfer rate respectively in the subsonic and the supersonic regime of compressible hydrodynamic turbulence.

This above phenomenology is based on the scale invariance of ε but it never explains the spectral law as an outcome of a cascade. This type of phenomenology can give an alternative point of view to the familiar one where the power spectrum is supposed to be resulted from a cascade process. The inert role of (ρv) to dimensional analysis can however be a subject of further discussion.

6.3.3 Isothermal MHD turbulence

For constituting an exact relation of compressible MHD turbulence of an isothermal plasma, we rewrite the basic equations (except the continuity equation which is kept unchanged) of ideal MHD in terms of \mathbf{v} and \mathbf{v}_A (Marsch & Mangeney, 1987) as follows:

$$\begin{aligned} \partial_t \rho + \nabla \cdot (\rho \mathbf{v}) &= 0, \\ \partial_t \mathbf{v} + (\mathbf{v} \cdot \nabla) \mathbf{v} &= (\mathbf{v}_A \cdot \nabla) \mathbf{v}_A - \frac{1}{\rho} \nabla \left(P + \frac{1}{2} \rho \mathbf{v}_A^2 \right) - \mathbf{v}_A (\nabla \cdot \mathbf{v}_A) + \mathbf{d}_C + \mathbf{f}_0, \\ \partial_t \mathbf{v}_A + \mathbf{v} \cdot \nabla \mathbf{v}_A &= \mathbf{v}_A \cdot \nabla \mathbf{v} - \frac{\mathbf{v}_A}{2} (\nabla \cdot \mathbf{v}) + \mathbf{d}_M, \\ \mathbf{v}_A \cdot \nabla \rho &= -2\rho (\nabla \cdot \mathbf{v}_A), \end{aligned}$$

where \mathbf{d}_C , \mathbf{d}_M and \mathbf{f}_0 represent respectively the contribution of the kinetic viscosity, magnetic resistivity and the external forcing and the other variables have their usual meaning. The above boxed equations present respectively the continuity equation, the momentum equation, Faraday's induction equation and the zero divergence of magnetic field. Following the same formalism as that of pure hydrodynamic case (Galtier & Banerjee, 2011), we define the relevant two-point correlation functions associated to the total energy and the compressible cross-helicity density as:

$$R_E = \frac{\rho}{2} (\mathbf{v} \cdot \mathbf{v}' + \mathbf{v}_A \cdot \mathbf{v}_A') + \rho e', \quad (6.60)$$

$$R_H = \frac{\rho}{2} (\mathbf{v} \cdot \mathbf{v}_A' + \mathbf{v}_A \cdot \mathbf{v}'), \quad (6.61)$$

and similarly for the primed quantities. Using the above definitions and introducing compressible Elsässer variables $\mathbf{z}^\pm \equiv \mathbf{v} \pm \mathbf{v}_A$, we obtain:

$$(E + E') \pm (H + H') - (R_E \pm R_H + R'_E \pm R'_H) - \delta \rho \delta e = \frac{1}{2} \delta(\rho \mathbf{z}^\pm) \cdot \delta \mathbf{z}^\pm. \quad (6.62)$$

For a statistically homogeneous system, the above relations get reduced to:

$$\langle E \rangle \pm \langle H \rangle - \frac{1}{2} \langle R_E \pm R_H + R'_E \pm R'_H \rangle - \frac{1}{2} \langle \delta \rho \delta e \rangle = \frac{1}{4} \langle \delta(\rho \mathbf{z}^\pm) \cdot \delta \mathbf{z}^\pm \rangle, \quad (6.63)$$

where $\langle \cdot \rangle$ denotes statistical average as usual. Now we shall calculate:

$$\partial_t \langle R_E \pm R_H + R'_E \pm R'_H \rangle, \quad (6.64)$$

which is useful to have a view on the generalized version of the two exact relations of Politano-Pouquet for each of the compressible pseudo-energies ($e^\pm = \rho \mathbf{z}^\pm \cdot \mathbf{z}^\pm$) which are no more conserved in compressible MHD. By using the above boxed equations and basic identities of vector calculus, we obtain after some calculations:

$$\begin{aligned} \partial_t(\rho \mathbf{v} \cdot \mathbf{v}') &= \\ &- \nabla \cdot [\rho(\mathbf{v} \cdot \mathbf{v}')\mathbf{v}] + \nabla \cdot [\rho \mathbf{v}_A(\mathbf{v}' \cdot \mathbf{v}_A)] - (\mathbf{v}' \cdot \mathbf{v}_A) [\nabla \cdot (\rho \mathbf{v}_A)] \\ &- \nabla \cdot (P\mathbf{v}') - \nabla \cdot \left(\frac{1}{2}\rho \mathbf{v}_A^2 \mathbf{v}'\right) - \rho(\mathbf{v}' \cdot \mathbf{v}_A)(\nabla \cdot \mathbf{v}_A) \\ &- \nabla' \cdot [\rho(\mathbf{v} \cdot \mathbf{v}')\mathbf{v}'] + \rho(\mathbf{v} \cdot \mathbf{v}')(\nabla' \cdot \mathbf{v}') + \nabla' \cdot [\rho(\mathbf{v} \cdot \mathbf{v}_A')\mathbf{v}_A'] \\ &- \rho(\mathbf{v} \cdot \mathbf{v}_A')(\nabla' \cdot \mathbf{v}_A') - \frac{\rho}{\rho'} \nabla' \cdot (P'\mathbf{v}) - \frac{\rho}{\rho'} \nabla' \cdot \left(\frac{1}{2}\rho' \mathbf{v}_A'^2 \mathbf{v}\right) \\ &- \rho(\mathbf{v} \cdot \mathbf{v}_A')(\nabla' \cdot \mathbf{v}_A') + d_1 + f_1, \\ \partial_t(\rho \mathbf{v}_A \cdot \mathbf{v}_A') &= \\ &- \nabla \cdot [\rho(\mathbf{v}_A' \cdot \mathbf{v}_A)\mathbf{v}] + \nabla \cdot [\rho \mathbf{v}_A(\mathbf{v} \cdot \mathbf{v}_A')] - (\mathbf{v}_A' \cdot \mathbf{v}) [\nabla \cdot (\rho \mathbf{v}_A)] \\ &- \frac{1}{2}\rho(\mathbf{v}_A \cdot \mathbf{v}_A')(\nabla \cdot \mathbf{v}) - \frac{1}{2}\rho(\mathbf{v}_A \cdot \mathbf{v}_A')(\nabla' \cdot \mathbf{v}') - \nabla \cdot [\rho(\mathbf{v}_A \cdot \mathbf{v}_A')\mathbf{v}'] \\ &+ \rho(\mathbf{v}_A \cdot \mathbf{v}_A')(\nabla' \cdot \mathbf{v}') + \nabla' \cdot [\rho(\mathbf{v}_A \cdot \mathbf{v}')\mathbf{v}_A'] - \rho(\mathbf{v}_A \cdot \mathbf{v}')(\nabla' \cdot \mathbf{v}_A') + d_2, \\ \partial_t(\rho \mathbf{v} \cdot \mathbf{v}_A') &= \\ &- \nabla \cdot [\rho \mathbf{v}(\mathbf{v} \cdot \mathbf{v}_A')] + \nabla \cdot [\rho \mathbf{v}_A(\mathbf{v}_A \cdot \mathbf{v}_A')] - (\mathbf{v}_A' \cdot \mathbf{v}_A) [\nabla \cdot (\rho \mathbf{v}_A)] \\ &- \nabla \cdot (P\mathbf{v}_A') - \nabla \cdot \left(\frac{1}{2}\rho v_A^2 \mathbf{v}_A'\right) - \rho(\mathbf{v}_A' \cdot \mathbf{v}_A)(\nabla \cdot \mathbf{v}_A) \\ &- \nabla \cdot [\rho(\mathbf{v} \cdot \mathbf{v}_A')\mathbf{v}'] + \rho(\mathbf{v} \cdot \mathbf{v}_A')(\nabla' \cdot \mathbf{v}') + \nabla' \cdot [\rho(\mathbf{v} \cdot \mathbf{v}')\mathbf{v}_A'] \\ &- \rho(\mathbf{v} \cdot \mathbf{v}')(\nabla' \cdot \mathbf{v}_A') - \frac{1}{2}\rho(\mathbf{v} \cdot \mathbf{v}_A')(\nabla' \cdot \mathbf{v}') + d_3 + f_2, \\ \partial_t(\rho \mathbf{v}_A \cdot \mathbf{v}') &= \\ &- \nabla \cdot [\rho \mathbf{v}(\mathbf{v}' \cdot \mathbf{v}_A)] + \nabla \cdot [\rho \mathbf{v}_A(\mathbf{v}' \cdot \mathbf{v})] - (\mathbf{v} \cdot \mathbf{v}') [\nabla \cdot (\rho \mathbf{v}_A)] \\ &- \frac{1}{2}\rho(\mathbf{v}' \cdot \mathbf{v}_A)(\nabla \cdot \mathbf{v}) - \nabla' \cdot [\rho(\mathbf{v}_A \cdot \mathbf{v}')\mathbf{v}'] + (\nabla' \cdot \mathbf{v}')(\rho \mathbf{v}_A \cdot \mathbf{v}') \\ &+ \nabla' \cdot [\rho(\mathbf{v}_A \cdot \mathbf{v}_A')\mathbf{v}_A'] - \rho(\mathbf{v}_A \cdot \mathbf{v}_A')(\nabla' \cdot \mathbf{v}_A') - \frac{\rho}{\rho'} \nabla' \cdot [P'\mathbf{v}_A] \\ &- \frac{\rho}{\rho'} \nabla' \cdot \left[\frac{1}{2}\rho' v_A'^2 \mathbf{v}_A\right] - \rho(\mathbf{v}_A \cdot \mathbf{v}_A')(\nabla' \cdot \mathbf{v}_A') + d_4 + f_3, \\ \partial_t(\rho e') &= -\nabla' \cdot (\rho e' \mathbf{v}') - \nabla \cdot (\rho e' \mathbf{v}) - \nabla' \cdot (P'\mathbf{v}') + \rho e' (\nabla' \cdot \mathbf{v}'), \end{aligned}$$

where d_1, d_2, d_3 and d_4 represent the dissipative terms which are expressible in terms of \mathbf{d}_M and f_1, f_2 and f_3 represent the forcing contributions which can

be expressed in terms of \mathbf{f}_0 . Hence we have all the necessary elements for the dynamic equation of R_E and R_H . Similarly we can write (by symmetry) the expressions of R'_E and R'_H just by carefully interchanging the primed and the unprimed quantities. Now if we apply statistical averaging operator on each term, after judicious re-arrangement of all the terms we finally obtain:

$$\begin{aligned}
& \partial_t \langle R_E \pm R_H + R'_E \pm R'_H \rangle \\
&= \nabla_r \cdot \left\langle \left[\frac{1}{2} \delta(\rho \mathbf{z}^\pm) \delta \mathbf{z}^\pm + \delta \rho \delta e \right] \delta \mathbf{z}^\mp + \bar{\delta} \left(e + \frac{v_A^2}{2} \right) \delta(\rho \mathbf{z}^\pm) \right\rangle \\
&- \frac{1}{4} \left\langle \frac{v_A'^2}{c_s^2} \nabla' \cdot (\rho \mathbf{z}^\pm e') + \frac{v_A^2}{c_s^2} \nabla \cdot (\rho' \mathbf{z}'^\pm e) \right\rangle + D_\pm + F_\pm \\
&+ \left\langle (\nabla \cdot \mathbf{v}) \left[R'_E \pm R'_H - E' \mp H' \mp \frac{\bar{\delta} \rho}{2} (\mathbf{v}_A \cdot \mathbf{z}'^\pm) - \frac{P'}{2} + \frac{P'_M}{2} \right] \right\rangle \\
&+ \left\langle (\nabla' \cdot \mathbf{v}') \left[R_E \pm R_H - E \mp H \mp \frac{\bar{\delta} \rho}{2} (\mathbf{v}_A' \cdot \mathbf{z}^\pm) - \frac{P}{2} + \frac{P_M}{2} \right] \right\rangle \\
&+ \left\langle (\nabla \cdot \mathbf{v}_A) \left[R_H \pm R_E - R'_H \mp R'_E \pm E' + H' - \bar{\delta} \rho (\mathbf{v}_A \cdot \mathbf{z}'^\pm) \pm \frac{5P'}{2} \pm \frac{P'_M}{2} \right] \right\rangle \\
&+ \left\langle (\nabla' \cdot \mathbf{v}_A') \left[R'_H \pm R'_E - R_H \mp R_E \pm E + H - \bar{\delta} \rho (\mathbf{v}_A' \cdot \mathbf{z}^\pm) \pm \frac{5P}{2} \pm \frac{P_M}{2} \right] \right\rangle,
\end{aligned}$$

where $P_M = (1/2)\rho v_A^2$ is the magnetic pressure. D_\pm and F_\pm represent respectively the averaged resultant dissipative and forcing terms and can explicitly be written as

$$\begin{aligned}
D_\pm &= \frac{1}{2} [(d_1 + d_2 + d'_1 + d'_2) \pm (d_3 + d_4 + d'_3 + d'_4)], \\
F_\pm &= \frac{1}{2} [(f_1 + f'_1) \pm (f_2 + f_3 + f'_2 + f'_3)].
\end{aligned}$$

The above boxed expression consists of two equations which represent the generalized form (to compressible MHD) of the coupled equations (4) and (6) of (Politano & Pouquet, 1998a). As it was already shown (Marsch & Mangeney, 1987), for compressible flows the compressible cross-helicity (whose density is written as $H_C = \rho \mathbf{v} \cdot \mathbf{v}_A$) is no longer conserved and we cannot let the term $\partial_t \langle R_E \pm R_H + R'_E \pm R'_H \rangle$ vanish to the extent of a stationary state where the average forcing term and the average resultant dissipative (kinetic + magnetic) terms cancel each other to ensure the conservation of total energy and total cross-helicity. Hence for the compressible case, these two equations individually do not lead to any exact relation. However, if we add both we find:

$$\begin{aligned}
 & \partial_t \langle R_E + R'_E \rangle \\
 &= \frac{1}{2} \nabla_r \cdot \left\langle \left[\frac{1}{2} \delta(\rho \mathbf{z}^-) \cdot \delta \mathbf{z}^- + \delta \rho \delta e \right] \delta \mathbf{z}^+ + \left[\frac{1}{2} \delta(\rho \mathbf{z}^+) \cdot \delta \mathbf{z}^+ + \delta \rho \delta e \right] \delta \mathbf{z}^- + \bar{\delta} \left(e + \frac{v_A^2}{2} \right) \delta(\rho \mathbf{z}^- + \rho \mathbf{z}^+) \right\rangle \\
 & - \frac{1}{8} \left\langle \frac{v_A'^2}{c_s^2} \nabla' \cdot (\rho \mathbf{z}^+ e') + \frac{v_A^2}{c_s^2} \nabla \cdot (\rho' \mathbf{z}'^+ e) + \frac{v_A'^2}{c_s^2} \nabla' \cdot (\rho \mathbf{z}^- e') + \frac{v_A^2}{c_s^2} \nabla \cdot (\rho' \mathbf{z}'^- e) \right\rangle \\
 & + \left\langle (\nabla \cdot \mathbf{v}) \left[R'_E - E' - \frac{\bar{\delta} \rho}{2} (\mathbf{v}_{\mathbf{A}'} \cdot \mathbf{v}_{\mathbf{A}}) - \frac{P'}{2} + \frac{P'_M}{2} \right] + (\nabla' \cdot \mathbf{v}') \left[R_E - E - \frac{\bar{\delta} \rho}{2} (\mathbf{v}_{\mathbf{A}} \cdot \mathbf{v}_{\mathbf{A}'}') - \frac{P}{2} + \frac{P_M}{2} \right] \right\rangle \\
 & + \left\langle (\nabla \cdot \mathbf{v}_{\mathbf{A}}) \left[R_H - R'_H + H' - \bar{\delta} \rho (\mathbf{v}' \cdot \mathbf{v}_{\mathbf{A}}) \right] + (\nabla' \cdot \mathbf{v}_{\mathbf{A}'}) \left[R'_H - R_H + H - \bar{\delta} \rho (\mathbf{v} \cdot \mathbf{v}_{\mathbf{A}'}) \right] \right\rangle + D + F,
 \end{aligned}$$

where $D = (D_+ + D_-)/2$ and $F = (F_+ + F_-)/2$. Now to establish the final relation, we assume that in the limit of infinite (kinetic and magnetic) Reynold's numbers, the system attains a stationary state associated with average total energy. Under this assumption, the left hand term of the above equation vanishes. Now if we concentrate far in the inertial zone where the dissipative terms are negligible with respect to the other terms, we are left with:

$$\begin{aligned}
 -2\varepsilon &= \frac{1}{2} \nabla_r \cdot \left\langle \left[\frac{1}{2} \delta(\rho \mathbf{z}^-) \cdot \delta \mathbf{z}^- + \delta \rho \delta e \right] \delta \mathbf{z}^+ + \left[\frac{1}{2} \delta(\rho \mathbf{z}^+) \cdot \delta \mathbf{z}^+ + \delta \rho \delta e \right] \delta \mathbf{z}^- + \bar{\delta} \left(e + \frac{v_A^2}{2} \right) \delta(\rho \mathbf{z}^- + \rho \mathbf{z}^+) \right\rangle \\
 & - \frac{1}{4} \left\langle \frac{1}{\beta'} \nabla' \cdot (\rho \mathbf{z}^+ e') + \frac{1}{\beta} \nabla \cdot (\rho' \mathbf{z}'^+ e) + \frac{1}{\beta'} \nabla' \cdot (\rho \mathbf{z}^- e') + \frac{1}{\beta} \nabla \cdot (\rho' \mathbf{z}'^- e) \right\rangle \quad (6.65) \\
 & + \left\langle (\nabla \cdot \mathbf{v}) \left[R'_E - E' - \frac{\bar{\delta} \rho}{2} (\mathbf{v}_{\mathbf{A}'} \cdot \mathbf{v}_{\mathbf{A}}) - \frac{P'}{2} + \frac{P'_M}{2} \right] + (\nabla' \cdot \mathbf{v}') \left[R_E - E - \frac{\bar{\delta} \rho}{2} (\mathbf{v}_{\mathbf{A}} \cdot \mathbf{v}_{\mathbf{A}'}) - \frac{P}{2} + \frac{P_M}{2} \right] \right\rangle \\
 & + \left\langle (\nabla \cdot \mathbf{v}_{\mathbf{A}}) \left[R_H - R'_H + H' - \bar{\delta} \rho (\mathbf{v}' \cdot \mathbf{v}_{\mathbf{A}}) \right] + (\nabla' \cdot \mathbf{v}_{\mathbf{A}'}) \left[R'_H - R_H + H - \bar{\delta} \rho (\mathbf{v} \cdot \mathbf{v}_{\mathbf{A}'}) \right] \right\rangle,
 \end{aligned}$$

where ε denotes the mean total energy injection rate (which is equal to the mean total energy dissipation rate). In the above equation the flux terms are deliberately written in terms of the compressible Elsässer variables \mathbf{z}^\pm whereas the source terms are expressed in terms of the velocity and the compressible Alfvén velocity. This writing is expected to be useful for (i) an attempt to generalise the Alfvén effect (introduced by Kraichnan) to describe the phenomenology of compressible MHD turbulence and (ii) understanding separately the contribution of the velocity field and the Alfvén term in the source term. It is interesting to note that in the second part of our flux, the isothermal β parameter (*i.e.* $2C_S^2/v_A^2$) appears which can help us understand (or obtain) the different limits depending upon its value. The above equation, being considerably bulky, is laborious to handle. For quick references, we give below a schematic view of that equation:

$$-2\varepsilon \approx \left\langle \Phi_1 + \frac{1}{\beta} \Phi_2 + (\nabla \cdot \mathbf{v}) S_1 + (\nabla \cdot \mathbf{v}_{\mathbf{A}}) S_2 \right\rangle, \quad (6.66)$$

where each term in the R.H.S of the equation (6.66) corresponds to different lines of equation (6.65).

Relevant limits

(a) Incompressible MHD: In this limit, all the source terms vanish. Moreover, the compressible energy term becomes zero (evident from its definition as for incompressible case $\rho = \rho_0$) and we get finally (normalising the density to unity):

$$-2\varepsilon = \frac{1}{4} \nabla_r \cdot \langle (\delta \mathbf{z}^-)^2 \delta \mathbf{z}^+ + (\delta \mathbf{z}^+)^2 \delta \mathbf{z}^- \rangle. \quad (6.67)$$

Note that the term $\nabla_r \cdot \langle \bar{\delta}(v_A^2/2) \delta(\mathbf{z}^- + \mathbf{z}^+) \rangle$ can be shown to be zero in incompressible case by expanding it and letting the ∇_r enter inside the average operator in a judicious manner. A rewriting of the \mathbf{z}^\pm in terms of \mathbf{v} and \mathbf{v}_A (assuming the constant density to be normalised to unity) help us recognise the equations obtained in incompressible MHD case.

(b) Compressible hydrodynamic case: To verify the hydrodynamic limit, we put $\mathbf{v}_A = 0$ and so $\mathbf{z}^+ = \mathbf{z}^- = \mathbf{v}$; we are left with:

$$\begin{aligned} -2\varepsilon = & \nabla_r \cdot \left\langle \left[\frac{1}{2} \delta(\rho \mathbf{v}) \cdot \delta \mathbf{v} + \delta \rho \delta e \right] \delta \mathbf{v} + \bar{\delta} e \delta(\rho \mathbf{v}) \right\rangle \\ & + \left\langle (\nabla \cdot \mathbf{v}) \left[R'_E - E' - \frac{P'}{2} \right] + (\nabla' \cdot \mathbf{v}') \left[R_E - E - \frac{P}{2} \right] \right\rangle, \end{aligned} \quad (6.68)$$

which is nothing but equation (6.53) obtained in compressible hydrodynamic case. Although here the pressure terms are written as the source terms whereas previously those were considered to contribute in flux terms.

(c) High and low β plasmas: Without problem we admit that in the limit where the beta parameter of the plasma tends to infinity (very large value), i.e. the plasma becomes almost incompressible (although not entirely), the flux term Φ_2/β becomes negligible with respect to Φ_1 of equation (6.66). On the contrary for a very small beta value, where the plasma can be assumed to be cold and magnetised (kinetic pressure negligible with respect to magnetic pressure), the term Φ_2/β dominates over Φ_1 term and at that situation the effective flux term becomes (after rearrangement):

$$-\frac{1}{2} \left\langle \frac{1}{\beta'} \nabla' \cdot (\rho \mathbf{v} e') + \frac{1}{\beta} \nabla \cdot (\rho' \mathbf{v}' e) \right\rangle, \quad (6.69)$$

where each term of the above expression corresponds to the different lines of equation (6.65).

Presence of an external magnetic field

Relation (6.65) comprises the total magnetic field at each point of the flow field. This total field \mathbf{b} of each point can be supposed (a realistic case) to have a fluctuating part (vary in space and time) $\tilde{\mathbf{b}}$ superimposed on a constant external magnetic field \mathbf{B}_0 . In the following, we shall investigate the flux and the source terms under the said situation. The part of the total flux term which contains \mathbf{B}_0 can be expressed as:

$$\begin{aligned} \langle \Phi_{\mathbf{B}_0} \rangle = & \frac{\nabla_r}{2\mu_0} \cdot \left\langle \delta \left(\frac{1}{\sqrt{\rho}} \right) \delta(\sqrt{\rho}) [\mathbf{B}_0 \times (\delta\mathbf{v} \times \mathbf{B}_0)] + \delta(\sqrt{\rho}) [\mathbf{B}_0 \times (\delta\mathbf{v} \times \delta\tilde{\mathbf{v}}_{\mathbf{A}})] \right. \\ & + \delta \left(\frac{1}{\sqrt{\rho}} \right) [\delta(\rho\tilde{\mathbf{v}}_{\mathbf{A}}) \times (\delta\mathbf{v} \times \mathbf{B}_0) + \delta(\rho\mathbf{v}) \times (\delta\tilde{\mathbf{v}}_{\mathbf{A}} \times \mathbf{B}_0)] \\ & - \delta^2 \left(\frac{1}{\sqrt{\rho}} \right) [\delta(\rho\mathbf{v}) \cdot \mathbf{B}_0] \mathbf{B}_0 + B_0^2 \bar{\delta} \left(\frac{1}{\rho} \right) \delta(\rho\mathbf{v}) + 2 \left[\mathbf{B}_0 \cdot \bar{\delta} \left(\frac{\tilde{\mathbf{v}}_{\mathbf{A}}}{\sqrt{\rho}} \right) \right] \delta(\rho\mathbf{v}) \left. \right\rangle \\ & - \frac{1}{2\mu_0} \left\langle \frac{B_0^2}{2\rho'^2} \rho\mathbf{v} \cdot \nabla' \rho' + \frac{\mathbf{B}_0 \cdot \tilde{\mathbf{b}}}{\rho'^2} \rho\mathbf{v} \cdot \nabla' \rho' + \frac{B_0^2}{2\rho'^2} \rho'\mathbf{v}' \cdot \nabla \rho + \frac{\mathbf{B}_0 \cdot \tilde{\mathbf{b}}'}{\rho'^2} \rho'\mathbf{v}' \cdot \nabla \rho \right\rangle, \end{aligned} \quad (6.70)$$

where $\tilde{\mathbf{v}}_{\mathbf{A}} = \tilde{\mathbf{b}}/\sqrt{\rho}$. Now if we assume the external field \mathbf{B}_0 to be very strong so that $B_0 \gg |\tilde{\mathbf{b}}|$ and also $B_0 \gg |\delta\mathbf{v}|$, we shall just consider the terms weighted by B_0^2 . After some straightforward calculations, we obtain the resultant flux term (the magnetic terms without B_0 and with single power of B_0 are neglected) which is written simply as:

$$\langle \Phi_{\mathbf{B}_0} \rangle \simeq \frac{\nabla_r}{2} \cdot \left\langle \delta \left(\frac{1}{\sqrt{\rho}} \right) \delta(\sqrt{\rho}) [\mathbf{B}_0 \times (\delta\mathbf{v} \times \mathbf{B}_0)] - \delta^2 \left(\frac{1}{\sqrt{\rho}} \right) [\delta(\rho\mathbf{v}) \cdot \mathbf{B}_0] \mathbf{B}_0 \right\rangle. \quad (6.71)$$

Of course the above expression gives the modifying part of the flux in the presence of a strong constant magnetic field applied externally. The pure kinetic terms of the flux are always there. One can easily understand that the modification is purely due to compressibility. It is also interesting to notice that in expression (6.71) the fluctuations are exclusively kinetic in nature (because of the absence of e.g. Hall type term in the basic equations). One can easily understand that the $\delta\mathbf{v}$ of first term and the $\delta(\rho\mathbf{v})$ of the second term of the above expression can be replaced by $\delta\mathbf{v}_{\perp}$ and $\delta(\rho\mathbf{v}_{\parallel})$ respectively where $\delta\mathbf{v}_{\perp} \perp \mathbf{B}_0$ and $\delta\mathbf{v}_{\parallel} \parallel \mathbf{B}_0$. The pure kinetic terms can however be omitted by assuming the external magnetic contribution to be dominant with respect to the velocity and the density fluctuations.

The source terms are also modified due to the effect of a strong external magnetic field. The terms of type $\langle (\nabla \cdot \mathbf{v}) S_1 \rangle$ get reduced to (keeping just the terms with B_0^2)

$$\langle \Psi_{\mathbf{v}} \rangle \simeq \frac{B_0^2}{2} \left\langle \delta(\nabla \cdot \mathbf{v}) \delta \left(\frac{1}{\sqrt{\rho}} \right) \bar{\delta}(\sqrt{\rho}) - \bar{\delta}(\nabla \cdot \mathbf{v}) \right\rangle, \quad (6.72)$$

and the source terms like $\langle (\nabla \cdot \mathbf{v}_A) S_2 \rangle$ are rewritten as:

$$\begin{aligned} \langle \Psi_{\mathbf{v}_A} \rangle &\simeq \mathbf{B}_0 \cdot \left\langle \nabla \left(\frac{1}{\sqrt{\rho}} \right) \left[(\mathbf{B}_0 \cdot \mathbf{v}') \left\{ \rho' \delta \left(\frac{1}{\sqrt{\rho}} \right) \right\} - (\mathbf{B}_0 \cdot \mathbf{v}) \frac{\delta \rho}{2\sqrt{\rho'}} \right] \right. \\ &\quad \left. - \nabla' \left(\frac{1}{\sqrt{\rho'}} \right) \left[(\mathbf{B}_0 \cdot \mathbf{v}) \left\{ \rho \delta \left(\frac{1}{\sqrt{\rho}} \right) \right\} - (\mathbf{B}_0 \cdot \mathbf{v}') \frac{\delta \rho}{2\sqrt{\rho}} \right] \right\rangle. \end{aligned} \quad (6.73)$$

Simplifying one step further, if we assume that the velocity field vector at each point of the flow field is perpendicular to the external magnetic field i.e. $v_{\parallel} = v'_{\parallel} = 0$, then $\mathbf{v} \equiv \mathbf{v}_{\perp}$. In that case, $\langle \Psi_{\mathbf{v}_A} \rangle$ vanishes and so is the second term of $\langle \Phi_{Bz} \rangle$ and then the corresponding reduced exact relation can be written as:

$$\begin{aligned} -2\varepsilon &\simeq \frac{B_0^2}{2} \nabla_{r_{\perp}} \cdot \left\langle \delta \left(\frac{1}{\sqrt{\rho}} \right) \delta(\sqrt{\rho}) \delta \mathbf{v}_{\perp} \right\rangle \\ &\quad - \frac{B_0^2}{4} \left\langle (\nabla_{\perp} \cdot \mathbf{v}_{\perp}) \left(1 + \sqrt{\frac{\rho}{\rho'}} \right) + (\nabla'_{\perp} \cdot \mathbf{v}'_{\perp}) \left(1 + \sqrt{\frac{\rho'}{\rho}} \right) \right\rangle. \end{aligned} \quad (6.74)$$

Construction of different spectra

In this section we try to make predictions on compressible spectra using the derived theoretical relations. The simplified relation (6.74) is considerably indicative for phenomenological intuition. The existence of strong external magnetic field \mathbf{B}_0 renders the energy transfer in parallel (w.r.t. \mathbf{B}_0) direction negligible in comparison to the transverse transfer. From the flux term of (6.74), dimensionally we can have (for instance keeping the source terms aside)

$$\varepsilon \sim (\rho_l v_{Al}^2) v_{l\perp} k_{\perp}, \quad (6.75)$$

where the above expression represents the perpendicular transfer of magnetic energy due to \mathbf{B}_0 with a characteristic time $\tau_l \sim (l_{\perp}/v_{l\perp})$. Now if we define two new variables

$$W_l = \rho_l^{1/3} v_{l\perp}, \quad B_l = \rho_l^{1/3} v_{Al} = \rho_l^{-1/6} B_0, \quad (6.76)$$

we obtain,

$$\varepsilon \sim U_l B_l^2 k_{\perp} \sim (E^U(k_{\perp}) k_{\perp})^{1/2} E^B(k_{\perp}) k_{\perp}^2, \quad (6.77)$$

whence we get finally

$$E^B \cdot E^{U^{1/2}} \sim \varepsilon k_{\perp}^{-5/2}. \quad (6.78)$$

Taking into consideration of the source terms will just modify ε to ε_{eff} (likewise the compressible hydrodynamic case). A compressional effect ($\nabla \cdot \mathbf{v}$ is

negative) will increase the effective energy flux rate whereas a dilatational effect ($\nabla \cdot \mathbf{v}$ is positive) will reduce ε_{eff} as it is evident from the source terms of (6.74). With an additional hypothesis of axisymmetry (symmetry in the plane perpendicular to \mathbf{B}_0), we can describe the effect of the source terms by the help of the figure (6.3).

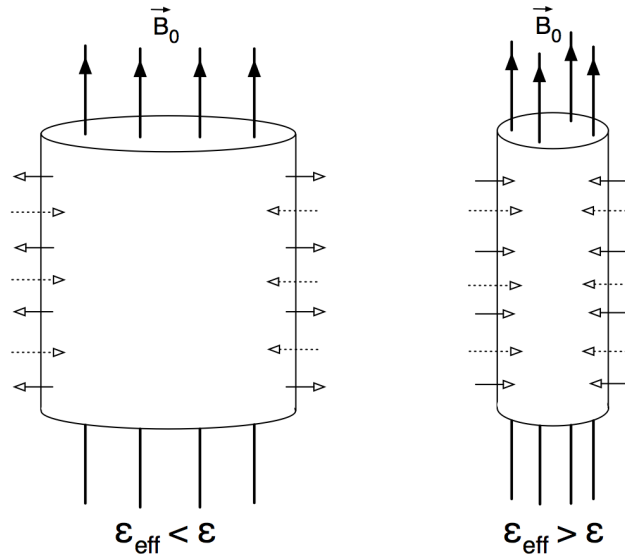


Figure 6.3: Phenomenological view of compressible MHD turbulence in the presence of a strong directive magnetic field; An axisymmetric total energy cascade is predicted in the perpendicular direction of the strong directive magnetic field following the same phenomenology of the hydrodynamic case; Source: Banerjee & Galtier (2013).

6.3.4 Polytopic hydrodynamic turbulence

The use of isothermal closure in the previous derivations was due to the sake of simplicity. Astrophysical plasmas are often modelled (Tu & Marsch, 1997; Hu *et al.*, 1997) as polytopic fluid ($P = k\rho^\gamma$) with variable polytopic index γ . In the current study, we shall derive an exact relation for a polytopic fluid whose polytopic index is fixed with respect to space and time. This derivation is more complicated than isothermal case due to two reasons : (i) The sound speed is no longer a constant and (ii) Fluid pressure is no longer linear to fluid density. As we shall see the fluctuating sound speed plays a key role in determining the nature of polytopic turbulence.

The basic equations governing the dynamics of a compressible polytopic

fluid are:

$$\partial_t \rho + \nabla \cdot (\rho \mathbf{v}) = 0, \quad (6.79)$$

$$\partial_t (\rho \mathbf{v}) + \nabla \cdot (\rho \mathbf{v} \otimes \mathbf{v}) = -\nabla P + \mathbf{d} + \mathbf{f}, \quad (6.80)$$

$$P = K \rho^\gamma, \quad (6.81)$$

where the symbols have their usual meaning. The terms \mathbf{d} and \mathbf{f} represent, respectively, the contributions of the dissipation and the external forcing. As in the previous cases, forcing is assumed to be stationary, homogeneous, delta-correlated in time and acting at large scales only. The sound speed is defined as:

$$C_s^2 = \frac{\partial P}{\partial \rho} = \gamma P / \rho. \quad (6.82)$$

Our objective is to set up an exact relation associated with the correlators of the total energy density which is defined as:

$$E = \frac{1}{2} \rho \mathbf{v} \cdot \mathbf{v} + \rho e, \quad (6.83)$$

where e accounts for the compressible energy which is expressed as:

$$e = - \int P d \left(\frac{1}{\rho} \right) = \frac{P}{\rho(\gamma - 1)} = \frac{C_s^2}{\gamma(\gamma - 1)}. \quad (6.84)$$

We shall define the two-point correlation functions for the total energy density. The correlators are given by the trace of the matrices $\rho \mathbf{v} \otimes \mathbf{v}'$ and $\rho' \mathbf{v}' \otimes \mathbf{v}$. Unlike the isothermal case, here the sound speed is also a flow variable which leads us to write the energy density correlators in the following way:

$$\langle R_E \rangle = \left\langle \rho \left(\frac{\mathbf{v} \cdot \mathbf{v}'}{2} + \frac{C_s C_s'}{\gamma(\gamma - 1)} \right) \right\rangle, \quad (6.85)$$

$$\langle R'_E \rangle = \left\langle \rho' \left(\frac{\mathbf{v}' \cdot \mathbf{v}}{2} + \frac{C_s' C_s}{\gamma(\gamma - 1)} \right) \right\rangle. \quad (6.86)$$

Using the above expressions we obtain:

$$\langle (E + E') - (R_E + R'_E) \rangle = \left\langle \frac{\delta(\rho \mathbf{v}) \cdot \delta \mathbf{v}}{2} + \frac{\delta(\rho C_s) \delta C_s}{\gamma(\gamma - 1)} \right\rangle. \quad (6.87)$$

Under statistical homogeneity, the above equation gets reduced to :

$$\left\langle \frac{(R_E + R'_E)}{2} \right\rangle = \langle E \rangle - \left\langle \frac{\delta(\rho \mathbf{v}) \cdot \delta \mathbf{v}}{4} + \frac{\delta(\rho C_s) \delta C_s}{2\gamma(\gamma - 1)} \right\rangle. \quad (6.88)$$

Now we have to find the partial time derivative of the left-hand side member of equation (6.88). By a straightforward calculation, we find:

$$\partial_t \langle \rho \mathbf{v} \cdot \mathbf{v}' \rangle = \nabla_{\mathbf{r}} \cdot \langle -\rho(\mathbf{v} \cdot \mathbf{v}') \delta \mathbf{v} + P \mathbf{v}' - \rho h' \mathbf{v} + \rho(\mathbf{v} \cdot \mathbf{v}')(\nabla' \cdot \mathbf{v}') \rangle + d_1 + f_1, \quad (6.89)$$

$$\partial_t \langle \rho' \mathbf{v}' \cdot \mathbf{v} \rangle = \nabla_{\mathbf{r}} \cdot \langle -\rho'(\mathbf{v}' \cdot \mathbf{v}) \delta \mathbf{v} - P' \mathbf{v} + \rho' h \mathbf{v}' + \rho'(\mathbf{v}' \cdot \mathbf{v})(\nabla \cdot \mathbf{v}) \rangle + d'_1 + f'_1, \quad (6.90)$$

where h is the enthalpy ($h = \gamma e$); d_1 , f_1 and d'_1 and f'_1 correspond respectively to the dissipative and the forcing terms in equations (6.89) and (6.90). Explicit expressions for them can be given as follows:

$$d_1 = \left\langle \mathbf{d} \cdot \mathbf{v}' + \frac{\rho}{\rho'} \mathbf{d}' \cdot \mathbf{v} \right\rangle, \quad f_1 = \left\langle \mathbf{f} \cdot \mathbf{v}' + \frac{\rho}{\rho'} \mathbf{f}' \cdot \mathbf{v} \right\rangle, \quad (6.91)$$

$$d'_1 = \left\langle \mathbf{d}' \cdot \mathbf{v} + \frac{\rho'}{\rho} \mathbf{d} \cdot \mathbf{v}' \right\rangle, \quad f'_1 = \left\langle \mathbf{f}' \cdot \mathbf{v} + \frac{\rho'}{\rho} \mathbf{f} \cdot \mathbf{v}' \right\rangle. \quad (6.92)$$

We also find:

$$\partial_t \left\langle \frac{\rho C_s C'_s}{\gamma(\gamma-1)} \right\rangle = - \left\langle \left(1 + \frac{\gamma-1}{2} \right) \frac{C'_s C_s}{\gamma(\gamma-1)} \nabla \cdot (\rho \mathbf{v}) + \frac{\rho}{2\rho'\gamma} C'_s C_s \nabla' \cdot (\rho' \mathbf{v}') \right\rangle, \quad (6.93)$$

$$\partial_t \left\langle \frac{\rho' C'_s C_s}{\gamma(\gamma-1)} \right\rangle = - \left\langle \left(1 + \frac{\gamma-1}{2} \right) \frac{C_s C'_s}{\gamma(\gamma-1)} \nabla' \cdot (\rho' \mathbf{v}') + \frac{\rho'}{2\rho\gamma} C_s C'_s \nabla \cdot (\rho \mathbf{v}) \right\rangle. \quad (6.94)$$

Adding up Eqs. (6.89) to (6.94) and also adding and subtracting the term, $\langle (\nabla \cdot \mathbf{v})(\rho' C'_s C_s) + (\nabla' \cdot \mathbf{v}')(\rho C_s C'_s) \rangle / \gamma(\gamma-1)$, we get by using the definition of the correlators:

$$\begin{aligned} \partial_t \langle R_E + R'_E \rangle = & \quad (6.95) \\ \nabla_{\mathbf{r}} \cdot \left\langle - (R_E + R'_E) \delta \mathbf{v} - \frac{P' \mathbf{v}}{2} + \frac{P \mathbf{v}'}{2} + \frac{\rho' h \mathbf{v}'}{2} - \frac{\rho h' \mathbf{v}}{2} \right\rangle & + \langle (\nabla \cdot \mathbf{v}) R'_E + (\nabla' \cdot \mathbf{v}') R_E \rangle \\ + \frac{1}{\gamma(\gamma-1)} \langle (\rho C'_s \mathbf{v} + \rho' C_s \mathbf{v}) \cdot (\nabla C_s) + (\rho' C_s \mathbf{v}' + \rho C_s \mathbf{v}') \cdot (\nabla' C'_s) \rangle & \\ - \frac{1}{2\gamma} \left\langle C_s C'_s \left(1 + \frac{\rho'}{\rho} \right) \nabla \cdot (\rho \mathbf{v}) + C_s C'_s \left(1 + \frac{\rho}{\rho'} \right) \nabla' \cdot (\rho' \mathbf{v}') \right\rangle & + \mathcal{D} + \mathcal{F}, \end{aligned}$$

where $\mathcal{D} = (d_1 + d'_1)/2$ and $\mathcal{F} = (f_1 + f'_1)/2$ represent, respectively, the resultant dissipative and forcing terms. By introducing in the above expression relation (6.87) without the statistical average, we obtain eventually:

$$\begin{aligned}
\partial_t \langle R_E + R'_E \rangle = & \tag{6.96} \\
& \nabla_{\mathbf{r}} \cdot \left\langle \frac{1}{2} (\delta(\rho \mathbf{v}) \cdot \delta \mathbf{v}) \delta \mathbf{v} + \frac{1}{\gamma(\gamma-1)} \delta(\rho C_s) \delta C_s \delta \mathbf{v} \right\rangle + \mathcal{D} + \mathcal{F} \\
& + \left\langle (\nabla \cdot \mathbf{v}) \left(R'_E - E' + \frac{P'}{2} \right) + (\nabla' \cdot \mathbf{v}') \left(R_E - E + \frac{P}{2} \right) \right\rangle \\
& + \frac{1}{\gamma(\gamma-1)} \langle (\rho C'_s \mathbf{v} + \rho' C'_s \mathbf{v}') \cdot (\nabla C_s) + (\rho' C_s \mathbf{v}' + \rho C_s \mathbf{v}) \cdot (\nabla' C'_s) \rangle \\
& + \left\langle \left[\frac{C_s'^2}{2(\gamma-1)} - \frac{C_s C'_s}{2\gamma} \left(1 + \frac{\rho'}{\rho} \right) \right] \nabla \cdot (\rho \mathbf{v}) + \left[\frac{C_s^2}{2(\gamma-1)} - \frac{C_s C'_s}{2\gamma} \left(1 + \frac{\rho}{\rho'} \right) \right] \nabla' \cdot (\rho' \mathbf{v}') \right\rangle.
\end{aligned}$$

Now we introduce the usual assumptions specific to three-dimensional fully developed turbulence with a direct energy cascade. We consider a steady state for which the partial time derivative of the average energy correlators vanishes. We consider a small enough viscosity such that the dissipative term will not affect the inertial range. For incompressible turbulence the dissipation is a sink localized mainly at the smallest scales of the system but in the present situation this property is not guaranteed. For example with the one dimensional Burgers equation – a simple archetype equation for very high Mach number flows – the contribution of the dissipation term is not concentrated at small scales but is rather constant throughout the whole inertial range. Its value tends to zero only as the viscosity goes to zero. Note that this is true for regular shocks but might even become wrong for shocks of Alfvénic type where dissipation may affect large scales as it is shown in one dimensional simulations (Laveder *et al.*, 2013). The mean energy injection rate is determined by the resultant forcing which is in fact, under our assumptions, $\mathcal{F} = 2\varepsilon$ (Galtier & Banerjee, 2011). Note that the question of a forcing acting at large scales only has been discussed recently in (Kritsuk *et al.*, 2013) in a numerical context for which it is not an obvious implementation. Then, far in the inertial zone (infinite Reynolds number limit is assumed) where the dissipative terms are negligible (Aluie, 2013), the exact relation writes:

$$\boxed{
\begin{aligned}
-2\varepsilon = & \nabla_{\mathbf{r}} \cdot \left\langle \frac{1}{2} (\delta(\rho \mathbf{v}) \cdot \delta \mathbf{v}) \delta \mathbf{v} + \frac{1}{\gamma(\gamma-1)} \delta(\rho C_s) \delta C_s \delta \mathbf{v} + \bar{\delta} h \delta(\rho \mathbf{v}) \right\rangle \\
& + \left\langle D \left(R'_E - E' + \frac{P'}{2} - \frac{1}{\gamma} \bar{\delta} \rho C_s C'_s \right) + D' \left(R_E - E + \frac{P}{2} - \frac{1}{\gamma} \bar{\delta} \rho C_s C'_s \right) \right\rangle,
\end{aligned}
} \tag{6.97}$$

where D and D' denote respectively $(\nabla \cdot \mathbf{v})$ and $(\nabla' \cdot \mathbf{v}')$. Note that in the derivation we have used the relation, $(\mathbf{v} \cdot \nabla) C_s = ((\gamma - 1)C_s/2\rho)\mathbf{v} \cdot \nabla\rho$.

Expression (6.97) is the required exact relation for three dimensional polytropic hydrodynamic turbulence. (Banerjee & Galtier, 2014). It is composed of the divergence of a flux \mathbf{F} (first line in the right hand side) and of a purely compressible term \mathcal{S} (second line) which leads us to use for the discussion the simplified writing:

$$-2\varepsilon = \nabla_{\mathbf{r}} \cdot \mathbf{F} + \mathcal{S}(\mathbf{r}). \quad (6.98)$$

As for isothermal turbulence, \mathcal{S} may be seen as a source or a sink for the mean energy transfer rate. But unlike the isothermal case, here the determination of the sign of the source term is not immediate in general and depends on the competition between $R'_E - E'$ (which is mainly negative) and $\bar{\delta}\rho C_s C'_s / \gamma - P'/2$ (whose sign is more difficult to define although it is positive at small scales since it tends to $P/2$ when $r \rightarrow 0$). Thus, $\mathcal{S}(r)$ contributes to modify ε for giving an effective mean total energy injection rate ε_{eff} (with $\varepsilon_{\text{eff}} \equiv \varepsilon + \mathcal{S}/2$) possibly larger than ε in the compression case and smaller than ε in the dilatation case with possibly an inverse cascade if $\varepsilon_{\text{eff}} < 0$. An illustration of dilatation and compression effects in the space correlation is given in figure (6.1).

Incompressible limit

An incompressible behaviour can be expected for a polytropic fluid in the limit $\gamma \rightarrow +\infty$ (Biskamp, 2008). First of all, let us check the incompressible limit of a polytropic fluid, i.e. $\gamma \rightarrow +\infty$. For that limit, we obtain $D = 0$ and a uniform density at every point of the flow field. We also get for the second term of the flux, $\delta(\rho C_s)\delta C_s \sim C_s^2 \sim \gamma$ (as all of them tend to infinite value), which does not lead to a singularity thanks to the presence of $\gamma(\gamma - 1)$ in the denominator. The third term also goes away in the incompressible limit under the following justification:

$$\nabla_{\mathbf{r}} \cdot \langle \bar{\delta}h\delta(\rho\mathbf{v}) \rangle = \nabla_{\mathbf{r}} \cdot \langle \gamma\bar{\delta}\varepsilon\delta(\rho\mathbf{v}) \rangle = \nabla_{\mathbf{r}} \cdot \left\langle \frac{\gamma}{2(\gamma - 1)} \left(\frac{P}{\rho} + \frac{P'}{\rho'} \right) \delta(\rho\mathbf{v}) \right\rangle. \quad (6.99)$$

In the limit where $\gamma \rightarrow +\infty$, we have $\rho = \rho' = \text{constant}$ and we get (using $D = D' = 0$):

$$\begin{aligned} \nabla_{\mathbf{r}} \cdot \langle \bar{\delta}h\delta(\rho\mathbf{v}) \rangle &= \frac{1}{2} \nabla_{\mathbf{r}} \cdot \langle P'\mathbf{v}' + P\mathbf{v}' - P'\mathbf{v} - P\mathbf{v} \rangle \\ &= \frac{1}{2} \langle P(\nabla' \cdot \mathbf{v}') + P'(\nabla \cdot \mathbf{v}) \rangle = 0. \end{aligned} \quad (6.100)$$

The term \mathcal{S} vanishes automatically due to the solenoidal velocity field and the uniform density. Then, the Kolmogorov's exact relation is reproduced

properly (Antonia *et al.*, 1997). At this point of discussion, we like to stress on the fact that the exact relation (6.97) for compressible turbulence include third-order structure function as in the incompressible case and not a fourth order structure function because

$$[\delta(\rho\mathbf{v}) \cdot \delta\mathbf{v}] \delta\mathbf{v} \neq \delta\rho (\delta\mathbf{v} \cdot \delta\mathbf{v}) \delta\mathbf{v}.$$

Dimensional analysis and spectra

To start with the spectral prediction, we keep the source term \mathcal{S} aside and investigate what happens dimensionally for the spectral prediction just with the flux term (isotropy is assumed). Additionally, we will not consider any intermittency correction which can modify slightly our conclusion about the scaling laws. At this point of discussion, it is necessary to justify the scale invariance of the mean total energy density injection rate ε in the compressible case. According to (Falkovich *et al.*, 2010) even in compressible turbulence a scale invariant mean energy flux rate can be assumed if the forcing correlation length scale is much larger than the inertial range length scales. A discussion around this question has been developed in Wagner *et al.* (2012) and Kritsuk *et al.* (2013) where it is claimed that a very short time correlation for the large scale acceleration or a very small length correlation for the density functions is necessary for the scale invariance of ε . Under this assumption, the exact relation can be written mainly as:

$$-2\varepsilon \simeq \frac{(\rho v)_\ell v_\ell^2}{\ell} \left(\frac{1}{2} + \frac{1}{\gamma(\gamma-1)M_{\rho\ell}M_\ell} + \frac{1}{(\gamma-1)\mathcal{M}_\ell^2} + \frac{1}{4(\gamma-1)M_\ell^2} \right), \quad (6.101)$$

where:

$$M_{\rho\ell} \equiv \frac{\delta(\rho v)}{\delta(\rho C_s)} \sim \frac{(\rho v)_\ell}{(\rho C_s)_\ell}, \quad M_\ell \equiv \frac{\delta v}{\delta C_s} \sim \frac{v_\ell}{C_{s\ell}}, \quad \mathcal{M}_\ell \equiv \frac{\delta v}{\delta C_s} \sim \frac{v_\ell}{C_s}, \quad (6.102)$$

are respectively the **current Mach number**, the **gradient Mach number** (which is not defined for isothermal turbulence where the sound speed is constant) and the **turbulent Mach number**. The third one is familiar in turbulence studies whereas the first and the second one have been defined for the sake of our current study. It is not obvious to built up any spectral assumption from the above expression (6.101). Insofar as we assume further simplifications like $(\rho v)_\ell v_\ell^2 \sim \rho_\ell v_\ell^3$ and $(\rho v)_\ell / (\rho C_s)_\ell \sim v_\ell / C_{s\ell}$, we can approximately write:

$$-4\varepsilon \simeq \frac{\rho_\ell v_\ell^3}{\ell} \left(1 + \frac{(\gamma+4)}{2\gamma(\gamma-1)M_\ell^2} + \frac{2}{(\gamma-1)\mathcal{M}_\ell^2} \right). \quad (6.103)$$

6.3. New exact relations and phenomenologies in compressible turbulence : My research work 143

Additionally, if we assume that $M_\ell \sim \ell^\alpha$ and $\mathcal{M}_\ell \sim \ell^\beta$, expression (6.103) can be re-written as:

$$-4\varepsilon \sim \frac{\rho \ell v_\ell^3}{\ell} (1 + \Gamma_1 \ell^{-2\alpha} + \Gamma_2 \ell^{-2\beta}), \quad (6.104)$$

with the coefficients $\Gamma_1 = (\gamma + 4)/[2\gamma(\gamma - 1)]$ and $\Gamma_2 = 2/(\gamma - 1)$. One can easily verify that $\Gamma_1 \sim \Gamma_2$ and so none of the second and the third terms can be neglected with respect to one another just from their coefficient consideration. From this step after some straightforward calculations, one can predict that the power spectrum of density-weighted velocity $w \equiv \rho^{1/3}v$ scales as:

$$E_k^w \sim \varepsilon^{2/3} k^{-5/3} (1 + \Gamma_1 k^{2\alpha} + \Gamma_2 k^{2\beta})^{-2/3}. \quad (6.105)$$

For supersonic turbulence for which $\delta v \gg \bar{\delta}C_s$ and $\delta v \gg \delta C_s$, the second and the third terms become negligible compared with the first one and we have:

$$E_k^w \sim \varepsilon_{\text{eff}}^{2/3} k^{-5/3}, \quad (6.106)$$

whereas for $\delta v \gg \bar{\delta}C_s$ but $\delta v \ll \delta C_s$ (which is less probable but still possible), we have:

$$E_k^w \sim (\varepsilon_{\text{eff}}/\Gamma_1)^{2/3} k^{-\frac{(5+4\alpha)}{3}}, \quad (6.107)$$

where ε_{eff} reflects the non-negligible effect of the source terms in the supersonic turbulence regime (see next subsection).

For subsonic turbulence we may have two possible situations. First, we have the case $\delta v \ll \bar{\delta}C_s$ but $\delta v \gg \delta C_s$ for which the spectral relation takes the form:

$$E_k^w \sim (\varepsilon/\Gamma_2)^{2/3} k^{-\frac{(5+4\beta)}{3}}. \quad (6.108)$$

One may immediately notice that if the scale dependence of the gradient or the turbulent Mach number is weak, i.e. α or β takes a small value, the power spectrum for w tends to the Kolmogorov value. Finally, when $\delta v \ll \bar{\delta}C_s$ and $\delta v \ll \delta C_s$, we are left with:

$$E_k^w \sim \varepsilon^{2/3} k^{-5/3} (\Gamma_1 k^{2\alpha} + \Gamma_2 k^{2\beta})^{-2/3}, \quad (6.109)$$

which is no more a pure power law but a non-trivial combination of two power laws. A power law can nonetheless be recovered if $\alpha \simeq \beta$. Note that the above analysis cannot be used in the isothermal limit as Γ_1 and Γ_2 are undefined for $\gamma = 1$. The basic reason for this problem is our total energy expression whose compressive part is undefined in the isothermal case and cannot be obtained as a limit of a polytropic case (for which $\gamma \rightarrow 1$).

Source term contributions

The contribution of \mathcal{S} is expected to be non negligible at supersonic ($\mathcal{M}_\ell \gg 1$) scales. An intuitive argument for this can be found in [Biskamp \(2008\)](#) where the dilatation term D is shown to be approximately proportional to the Mach number squared. Following the same formalism as carried out by [Kritsuk et al. \(2013\)](#) for isothermal turbulence, we may rewrite the polytropic source term as:

$$\mathcal{S} = \left\langle \frac{1}{2} [\delta(\rho \mathbf{v} D) - 2\bar{\delta} D \delta(\rho \mathbf{v})] \cdot \delta \mathbf{v} + \left[\frac{\delta(\rho C_s D)}{\gamma(\gamma - 1)} + \frac{(\gamma - 3)}{\gamma(\gamma - 1)} \bar{\delta} D \delta(\rho C_s) \right] \delta C_s - PD \right\rangle. \quad (6.110)$$

In the subsonic case, irrespective of the sub-regimes, $C_s (\sim \bar{\delta} C_s)$ is larger than δv and δC_s and hence the source term comes to be simply $\langle -PD \rangle$. This expression, bereft of any fluctuation, can hardly be expected to participate in turbulence and spectral construction, which in turn justifies why for subsonic turbulence the basic contribution is from flux terms.

On the other hand, for supersonic regime (with moderate γ) where $\delta v \gg C_s$ and $\delta v \gg \delta C_s$, the source term is reduced to:

$$\mathcal{S} = \left\langle \frac{1}{2} [\delta(\rho \mathbf{v} D) - 2\bar{\delta} D \delta(\rho \mathbf{v})] \cdot \delta \mathbf{v} \right\rangle. \quad (6.111)$$

This expression is similar to Eq. (2.10) in [Kritsuk et al. \(2013\)](#) where a relatively small contribution has been found numerically for isothermal supersonic turbulence. We can therefore conclude that in the supersonic turbulence regime ($\mathcal{M}_\ell > 1$) the source is weakly affected by the polytropic terms at moderate values of γ . This point can be quantified numerically for polytropic turbulence by comparing the relative importance of each term in \mathcal{S} .

Different values of polytropic index γ

For the discussion, we shall consider the isothermal case ([Galtier & Banerjee, 2011](#)) as a reference against which the polytropic law will be compared. We see that the polytropic closure leads to the appearance of new terms in the flux and the source. From expression (6.103), one can immediately see that the contribution of the second and third terms in the flux may enhance that of the first one for $\gamma > 1$ but opposes when $\gamma < 1$. More precisely, for $\gamma < 1$ we may expect even the possibility of an inverse cascade of total energy if the first term becomes subdominant which practically corresponds to Eq. (6.109). From a theoretical point of view this situation may arise at low gradient and turbulent Mach number for which the sound speed and its fluctuations are relatively large with respect to the velocity fluctuations of the fluid. This property could be investigated numerically by looking at the relative importance of

each term inside the flux. Besides $\gamma = 1$ (which is discussed above) the flux contains another singularity for $\gamma = 0$ due to the presence of the second term in Eq. (6.103).

For the source terms the effect of γ is subtle. The second term of expression (6.110) – the one multiplied by δC_s – depends on the γ values. For $\gamma > 3$, both members of the second term have positive coefficients. For $1 < \gamma < 3$, the coefficient of the first member ($1/[\gamma(\gamma - 1)]$) is positive whereas it is negative for the second one ($(\gamma - 3)/[\gamma(\gamma - 1)]$). If $0 < \gamma < 1$, the opposite case to the previous one will occur. For astrophysical interest, it is however possible to get negative values of gamma too (Horedt, 2004). For that situation, the first and second terms may contribute with a different sign. In order to verify numerically these effects, it is needed to consider a flow with very low gradient Mach number (M_ℓ) for which the first term (multiplied by δv) of the source contributes weakly with respect to the second term of the source (multiplied by δC_s). At the same time, it is also essential to weaken the effect of the third term i.e. $\langle -PD \rangle$ which is probably not obvious to satisfy. In reality, the case $\gamma < 0$ corresponds, in general, to the thermal instability in the outer envelopes of giant molecular clouds (Renard & Chieze, 1993) and therefore requires a more complicated model.

Solar wind data analysis

Contents

7.1	Introduction	147
7.2	The solar wind	148
7.2.1	The heliosphere	148
7.2.2	Prediction for the solar wind	149
7.2.3	The fast and the slow solar wind	149
7.2.4	Exploration of the solar wind	151
7.2.5	MHD fluctuations in the solar wind	152
7.2.6	Nature of the solar wind turbulence	152
7.3	Data source	154
7.3.1	The THEMIS mission	154
7.3.2	A brief description of instruments	154
7.4	Judicial selection of data	157
7.4.1	Selection of intervals	157
7.4.2	Relevant spatial and temporal scales	162
7.5	Analysis of the selected data	164

7.1 Introduction

THIS chapter is dedicated to the study of observational data from the THEMIS spacecraft with a view to understanding the role of compressibility in the solar wind turbulence. More elaborately, in the course of this chapter, we shall try to understand the applicability of the exact relation for compressible MHD turbulence (Banerjee & Galtier, 2013) to the solar wind which is a collisionless space plasma and can be modeled as an MHD fluid at large scales. A great advantage of the solar wind is the availability of in-situ measurements from several spacecraft. In the following, we shall briefly

describe the solar wind and its characteristics¹. This part will be followed by the description of the THEMIS mission, the process of analyzing in-situ data for our study. Finally we shall discuss some preliminary results which are obtained in the course of my thesis.

7.2 The solar wind

The very high temperature ($\sim 10^6 K$) of stellar corona renders the coronal plasma gravitationally unstable. This plasma expands into the outer space when the stellar magnetic field is not sufficient to confine it by the magnetic loops. This energetic flow is called the **stellar wind**. For the sun, the corresponding wind is called the **solar wind**.

7.2.1 The heliosphere

The plasma of the solar wind contains mostly protons and electrons of energy ranging between $10^4 - 10^5$ eV. This energetic outflow extends almost freely upto a distance of approximately 70 AU (and so beyond the planetary system ~ 50 AU) until it gets slowed down by the **termination shock**. The region permeated by the solar wind defines the **heliosphere** (see figure (7.1)). The shape of the heliosphere is however not spherical but

- (i) it has a magnetic spiral structure due to the solar rotation and
- (ii) it is equatorially (helmet streamer configuration) due to the solar dipolar magnetic field.

The solar wind, which consists of mainly ionized hydrogen(96%) and a small proportion (4%) of ionized helium, attains very soon super sonic and super-Alfvénic speeds. Both of the sound speed and the Alfvén speed of the solar wind (near 1 AU) vary between 50 – 100 km/s. whereas the flow velocity is in general about 300 – 800 km/s. After having travelled approximately 70 AU distance with an approximate velocity of several hundreds of kilometers per second, finally the solar wind starts to interact with the stellar wind of the interstellar medium and gets slower to a sub-sonic flow. This region of interaction is called the **terminal shock**. This is a fast MHD shock which propagates towards the Sun and is found to exist between 75 – 90 AU. The interaction retards the solar wind resulting in important compressible fluctuations and heating of the terminal shock region. The next zone of sub-sonic solar wind flow is called the **heliosheath**. The termination of heliosheath is

¹Although I have already discussed various aspects and works of the solar wind turbulence in previous chapters under a broader context, in this chapter I wish to give a formal introduction to the solar wind.

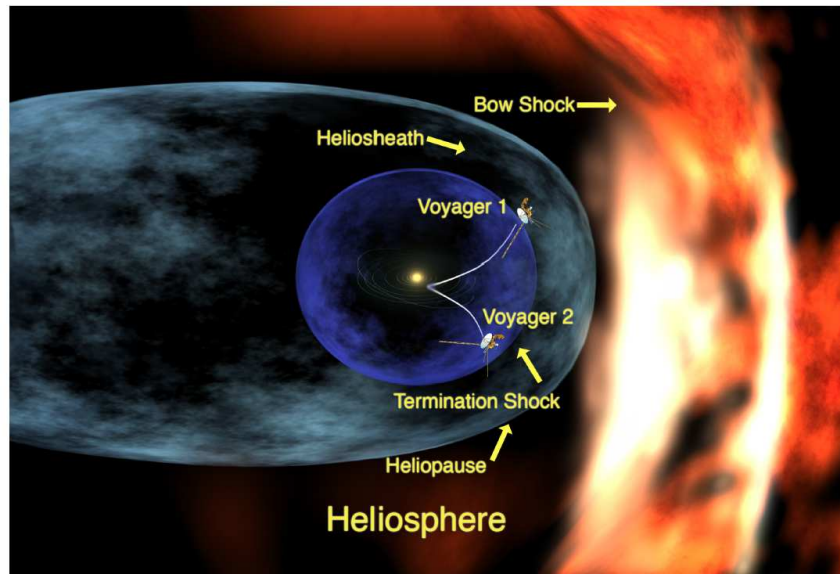


Figure 7.1: A schematic figure of the heliosphere; Credit: NASA.

defined when the particles of the solar wind cannot push the interstellar wind any longer and thus gets effectively stopped thereby forming a stagnant but locally unstable (due to important kinetic and magnetic fluctuations) region, called the **heliopause**, at about a distance of 100 AU from the Sun.

7.2.2 Prediction for the solar wind

The existence of the solar wind was theoretically predicted by **Eugene Parker** (Parker, 1958) and was detected directly by Soviet satellite Luna 1 in the very next year (January, 1959). In his model, he assumed the existence of a stationary radial outflow (from the Sun) driven by the pressure and the gravity. He neglected the effect of the solar magnetic field as a primitive step. By the help of ideal gas approximation and polytropic closure, he succeeded in predicting a supersonic flow which is flowing outwards. However, an improved version of this work was given later by **Weber & Davis (1967)** taking the solar magnetic field into account.

7.2.3 The fast and the slow solar wind

The structure of the magnetic field prevents the solar wind to be radially symmetric even at a considerable distance from the complex coronal loops. The wind generated from the central part of the coronal holes flows at a speed of approximately 550 – 750 km/s. and is called the **fast solar wind**.

On the other hand, the speed of the wind emanated from the neighborhood of the solar equatorial region is about 250-400 km/s. and is called the **slow solar wind**. Analyzing the data from various missions, we can find out the following characteristics of the solar wind:

a) Because of very high density of the slow solar wind, the resultant mass flow by the slow wind is greater than that by the fast one.

b) The fast wind is fairly uniform whereas the slow one undergoes considerable fluctuations. The boundaries between the two is however sufficiently sharp (see figure (7.2)).

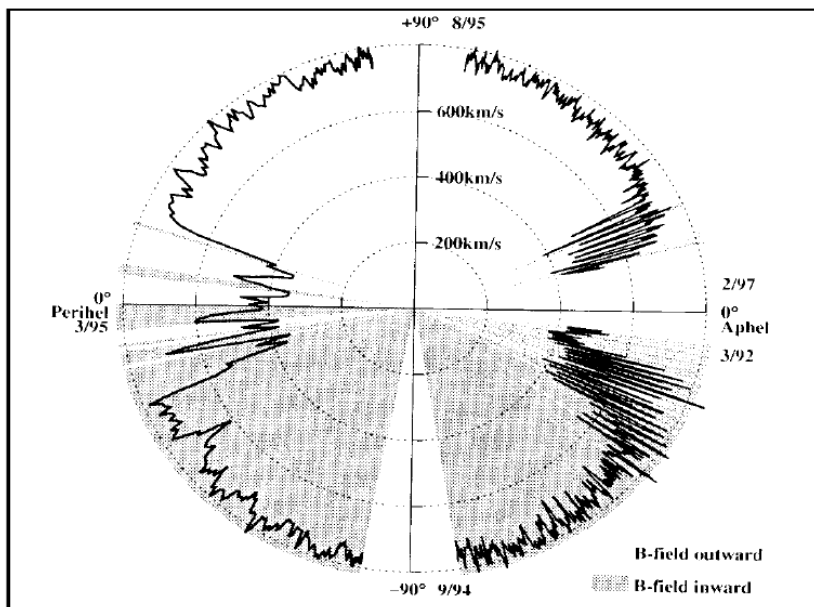


Figure 7.2: Solar wind speed and the magnetic field polarity observations from the Ulysses spacecraft covering almost all the latitudes from the equatorial to the polar region; *Reprinted with permission from Biskamp (2008); © (2003) Cambridge university press.*

c) The proton temperature drops more rapidly with distance in the slow wind than in fast wind. For the slow wind the law $T \propto r^{-1.33}$ represents nearly adiabatic expansion where for the fast one the law $T \propto r^{-0.8}$ accounts for a semi- isothermal expansion thereby indicating a sufficient amount of local input of heat energy in the fast wind. This anomalous heating can possibly be attributed to the compressible turbulence in the fast solar wind (Carbone *et al.*, 2009) and is discussed in the chapter 5.

d) iv) Due to the solar rotation, the fast wind catches up the slow solar wind forming a compression region of high density and magnetic field which is called

the **corotating interaction region** (CIR) and this region gets steepened in a sharp shock front at larger heliospheric distance.

The reason behind the acceleration of the fast wind is still not very clear. Considering the free expansion of the coronal plasma along the magnetic field lines in the coronal holes and using the Parker's hydrodynamic model we get a velocity ~ 500 km/s at a coronal temperature $\sim 10^6$ K whereas in reality, we obtain fast solar wind stream of ~ 700 km/s. velocity from the coronal holes of temperature $\sim 10^5$ K. Some are of the opinion that the enormous acceleration can be attributed to the dissipation of intense high frequency Alfvén waves originating from the convection zone which leads to a high-energy ion population. Observations from strongly broadened spectral lines indicate an effective temperature upto 10^8 K which is sufficient to explain the acceleration process. The scientists are, however, still in search of firm theoretical explanation.

Obscurity exists also in explaining the origin of the slow wind. From the figure we notice that the slow wind emanates from the equatorial belt which is magnetically complex and due to the scarcity of open field lines, this region gives birth to the wind of lower velocities. Yet a better understanding can be obtained by the study of the fluctuations of the MHD turbulence riding on the mean solar wind flow.

7.2.4 Exploration of the solar wind

The first study of the solar wind plasma was carried out by Neugebauer & Snyder (1962) exploiting the data of the Mariner 2 spacecraft, which was actually planned as a probe for the study of Venus. Since then more than 10 spacecraft have been launched to study the solar wind, either as the principal objective (like Helios A and B, Wind, ACE, Ulysses etc.), or as a secondary goal (SOHO, Cluster, THEMIS etc).

The inner heliosphere from 0.3 AU to 1 AU has been explored by the two spacecraft of Helios mission (1975-1976). This mission, although was launched in the 1970s, has provided with very rich data which constitute the basis of the study of solar wind turbulence. The spacecraft WIND and ACE studied the equatorial wind at about 1 AU distance. The outer heliosphere beyond 1 AU has been investigated by Pioneers 10 and 11 and Voyagers 1 and 2. All these said spacecraft have had their orbits very near to the ecliptic region whereas Ulysses possessing a highly inclined orbit becomes able to collect the data of polar wind (ranging from 1 AU to 5 AU) which is very little affected by the solar activities unlike the equatorial wind.

7.2.5 MHD fluctuations in the solar wind

The observations of Mariner 2 already confirmed the fact that solar wind plasma is not at all steady and is associated with fluctuations of substantial amount of different quantities such as velocity, magnetic field, density, temperature etc. As outside the corona, this plasma is practically collisionless and thus a fluid description for the solar wind can therefore be questioned. Nevertheless, an MHD formalism is appropriate for the fluctuations whose wavelengths are much larger than the ion inertial scale ($\sim 100km$) and the ion Larmor radius ($\sim 100km$). In course of our study we shall concentrate on these type of fluctuations (will be discussed in details later in this chapter). However, the collisionless character of the coronal plasma demands a kinetic approach for describing the wave dissipation in the solar wind where the dissipative effects are necessarily attributed to the plasma collective effects like cyclotron resonance effect (for a detailed discussion see Balogh & Treumann (2013) and Belmont *et al.* (2014)).

The presence of fluctuations is not surprising as the wind originates in corona which is the site of intense magnetic activity occurring practically at all available scales. This wind undergoes turbulence dynamics in the solar convection zone and gets modulated by the waves in the convective region through nonlinear interaction. Besides the instabilities in the solar wind driven by the sheared flows, shocks, particle beams and anisotropies bring about a continuous resuscitation of turbulence thereby leading to a sustaining turbulent flow in the solar wind.

7.2.6 Nature of the solar wind turbulence

The nature of the solar wind turbulence depends on the velocity-magnetic field correlation. For a very high velocity-magnetic field correlation (where one of the two Alfvén waves are dominant) the fluctuations are thought to be of pure Alfvénic nature whereas for a weak correlation, fully developed Kolmogorov turbulence (with well defined scaling and cascade) can be expected. The Alfvénic school emphasizes the coronal origin of the fluctuations whereas the other one pays importance to the local instabilities (Roberts & Goldstein, 1991; Marsch, 1991; Biskamp, 2008).

For distances which are not too large, say $r < 0.5$ AU, large-amplitude fluctuations of magnetic field and velocity (transverse to the mean field) show strong correlation which can be expressed by $\delta\mathbf{v} \simeq \pm\delta\mathbf{b}$. From the construction of Elsässer variables (discussed in chapter 4), we can easily admit the fact that strong correlation corresponds to the dominance of one of the two Alfvén waves. In practice the dominating part is found to be the outward

wave propagation. In a collisionless plasma as the compressive wave modes i.e. the fast and slow magnetosonic modes get dissipated very fast (Belcher & Davis, 1971) and the only surviving mode is the incompressible Alfvén mode, the large scale turbulence of the solar wind can be treated to be nearly incompressible. This point is also supported by the fact that the mean density fluctuation of the fast solar wind is always about 10 – 15%.

In the region very close to the Sun i.e. $r \leq 0.3$ AU, the outward propagating wave-spectrum in the fast wind is found to follow an approximate k^{-1} power law (Marsch & Tu, 1990a). In order to explain this phenomenon, Velli *et al.* (1989) showed that the linear coupling of the outgoing waves to the large scale inhomogeneity of the solar wind generates a very weak ingoing wave whose non-linear interaction with the first gives finally an approximate k^{-1} spectrum. It is also found that the separation between the spectra of the outward and the inward wave gets reduced with distance and at distance $r = 1$ AU, the two spectra merge to the Kolmogorov's $k^{-5/3}$ power law. The explanation for this phenomenon can be given by the theory of decaying turbulence (Biskamp, 2008).

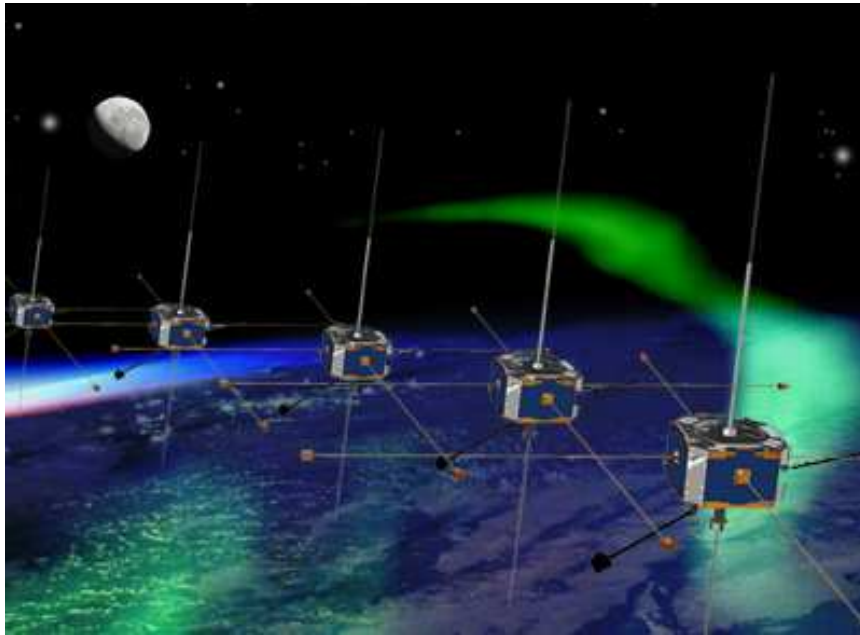


Figure 7.3: An artist view of the five spacecraft of the THEMIS mission; Credit: NASA.

However, for the solar wind at about 1AU, some recent works of Hnat *et al.* (2005); Carbone *et al.* (2009) etc. have shown the importance of compressibility in the solar wind turbulence (discussed in chapter 5) for the scaling and

heating issues of the fast solar wind. In this chapter we are going to address this unsolved question by the help of in-situ data analysis of the fast solar wind.

Finally, I should mention that the high frequency fluctuations of the solar wind (above 0.1 Hz) also constitute an enormous field of research. Sophisticated models like Hall MHD, Electron MHD, Landau-fluid, gyrokinetic and pure kinetic models are used in order to understand the nature of this high-frequency "dissipation range" turbulence in the solar wind. This part is beyond the scope of my thesis and has been investigated in recent research papers (for detailed discussions, see [Passot & Sulem \(2007\)](#); [Sulem & Passot \(2008\)](#); [Galtier \(2008a\)](#); [Howes *et al.* \(2008\)](#); [Schekochihin *et al.* \(2009\)](#); [Sahraoui *et al.* \(2009, 2010\)](#); [Alexandrova *et al.* \(2009\)](#)).

7.3 Data source

7.3.1 The THEMIS mission

In scope of my thesis, I studied the nature of solar wind turbulence by exploiting the in-situ data of THEMIS B (renamed later as ARTEMIS 1), which belongs to the mission THEMIS or **Time History of Events and Macroscale Interactions during Substorms**. The mission consists of five NASA satellites : Themis A, B, C, D and E. As the mission title suggests, THEMIS was launched in 2007 to study substorms in magnetosphere and the resulting plasma processes near the poles. Later (end 2009) three of the five satellites (A, D, E) were made to stay in the terrestrial magnetosphere and the two others are brought to orbits near the moon in order to study the interaction of the moon and the solar wind. The new mission has been named to **Acceleration, Reconnection, Turbulence and Electrodynamics of the Moon's Interaction with the Sun** (ARTEMIS) and THEMIS B and C have become ARTEMIS 1 and 2 respectively. Solar wind data can thus be obtained from those two satellites by choosing the suitable time intervals over which they were travelling in the free streaming solar wind i.e. the wind free from the terrestrial bow shock.

7.3.2 A brief description of instruments

THEMIS B consists of several field and plasma instruments designed to achieve the science goals of the mission. In the current context we shall be interested in two of them: (i) Fluxgate Magnetometer (FGM), which provides the magnetic data and (ii) Electrostatic analyzer (ESA), which provides the

plasma data (ion and electron distribution functions yielding the corresponding fluid density, velocity, temperature etc.). The description and the working principle of these two instruments are given in the following:

(i) **Fluxgate Magnetometer (FGM)**: FGM measures the background magnetic field and its fluctuations with a maximum sampling frequency of 64 Hz. Onboard THEMIS FGM is particularly designed for studying the abrupt changes in the magnetic configuration of the terrestrial magnetosphere at the onset of a sub-storm. This instrument possesses an extremely high offset stability of 0.2 nT/hr and is sufficiently sensitive to detect the magnetic field variation of the order of 0.01 nT. In the upper limit, this instrument can measure approximately upto 25000 nT. FGM is thus an efficient magnetometer with a range of operation spanning over $10^{-2} - 10^4$ nT. Higher time resolution magnetic data with time resolution upto 0.015 s can be obtained (in burst mode) thanks to this magnetometer. For the current purpose, we are interested in MHD scales which correspond to a maximum frequency of the order of 0.1Hz (the reason will be explained in subsection 7.3.2) and thus we use the spin resolution magnetic data with time resolution of 3 seconds.

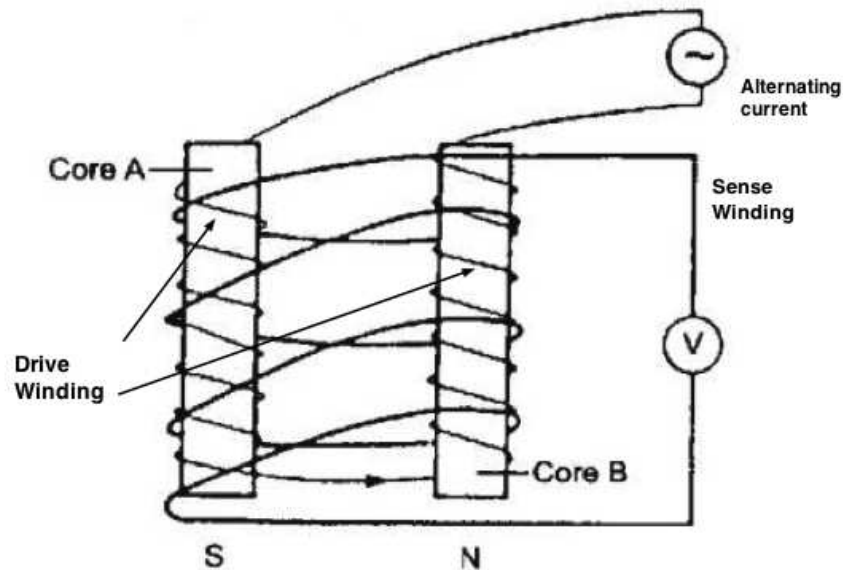


Figure 7.4: Working principle of the fluxgate magnetometer (FGM).

Fluxgate magnetometer sensor consists of two small ring cores made of highly permeable alloy around which copper wires are wound in mutually opposite sense (see figure 7.4). Alternating currents are then driven through these windings (called drive winding) which leads, in those two cores, to the

generation of alternating magnetic fields which are mutually opposing. In the absence of external magnetic field no global magnetic field is perceived in the secondary winding (called sense winding) and so no electric current flows through it. The presence of an external field affects that symmetry and reinforces the field in one ring while weakening in the other one. A net non-zero flux is then perceived in the secondary winding which generates a current by which the corresponding external magnetic field intensity is measured. For measuring three components of that external magnetic field, a 'triad' of such arrangement is used. FGM can measure a continuous magnetic field as well as an alternating field.

(ii) **Electrostatic Analyzer (ESA)**: THEMIS has two electrostatic analyzers for obtaining the plasma data by measuring the velocity distribution functions of electrons and ions. The working principle of the onboard THEMIS ESAs is described in the following:

- A pair of "top hat" electrostatic analyzers with common 180° by 6° fields-of-view detect particles over 4π steradians each 3s spin period (see figure 7.5). Each analyzer consists of two concentric hemispheric plates in the form of a shell. The plates (and "hat") are maintained at different voltages. This causes the electrons and ions, the charged particles, to move in a circle inside the shell. Only the charged particles with just the right energy will follow the curve of the instrument's hemispheric shell and arrive at the particle detector at the exit (principle of cyclotron). At this point, the detector registers the number of particles that hit it. By varying the voltages, we can find out how many particles are within each specified energy. Typically ions having energy ranging from 3 - 25 keV and electrons with energy upto 30 keV are detected by this analyzer.
- After being detected the particles are binned into six distributions whose energy, angle, and time resolution depend upon instrument mode. We thus obtain three dimensional velocity distribution functions of ions and electrons every 3 seconds (spin resolution of the spacecraft).
- Density, velocity (analogous to the fluid velocity), temperature (calculated from pressure) are then calculated as the different order moments of the particle distribution function following the definitions given in the chapter 3.

For studying the solar wind plasma, this instrument proves to be crucial for providing high time resolution plasma data. The 3s time resolution (the spin resolution) thereby allowing us to probe into almost all the inertial range of MHD (explained quantitatively in subsection 7.3.2.2). The advantage of

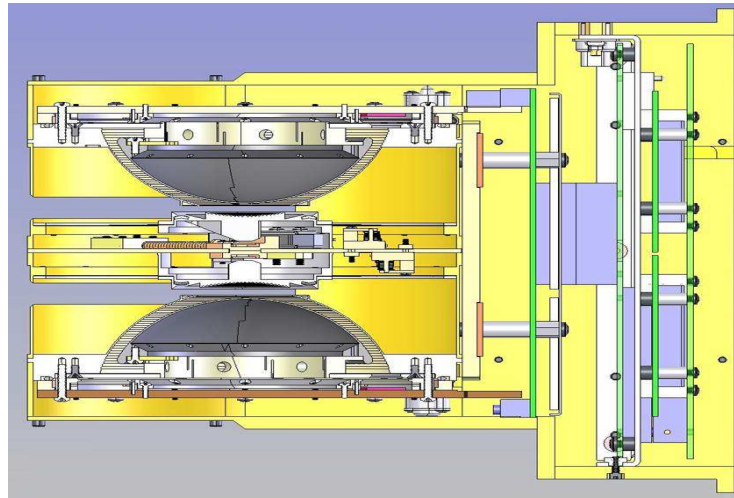


Figure 7.5: A schematic view of ESA; Credit: Berkeley.

THEMIS mission is that even with 3s resolution, several continuous (without gaps) datasets are available (typically of 7-8 hours).

(iii) **Other instruments:** In addition to the above two instruments, Themis has

- (a) an electric field instrument (EFI) for measuring electric fields in three dimensions,
- (b) a search coil magnetometer (SCM) for measuring magnetic fluctuations ranging from 0.1 Hz to 4 kHz,
- (c) a solid state telescope (SST) to measure the distribution function of superthermal (~ 25 keV - ~ 6 MeV) particles,
- (d) an instrument data processing unit (IDPU) to control the electronics of the above mentioned instruments and
- (e) some ground based instruments including an imager and some gate magnetometers. A representative diagram of the spacecraft with its onboard instruments is shown in the figure (7.6).

7.4 Judicial selection of data

7.4.1 Selection of intervals

For the sake of obtaining solar wind data, we choose² certain periods from years 2008 and 2009. This primary selection is made thanks to the Berkeley

²There exist several long intervals of solar wind in ARTEMIS but as an initial step, we have limited our study to the years 2008 and 2009.

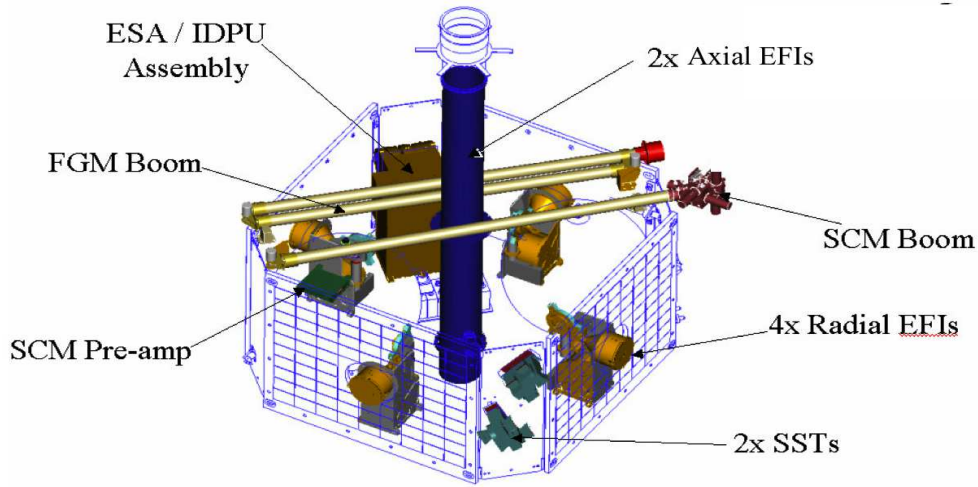


Figure 7.6: THEMIS spacecraft with its onboard instruments; Credit: NASA and oral presentation of Le Contel et al.

website of THEMIS mission (<http://themis.ssl.berkeley.edu/>) by which we make sure that during those periods THEMIS B passes through free streaming solar wind (not connected to the Earth bow shock). As can be seen from figure (7.7), among nine situations only two situations (highlighted by red border) can provide us with solar wind data i.e. the periods (i) from 15/06/2008 to 15/10/2008 and (ii) from 15/06/2009 to 30/09/2009. For those two intervals the apogees of the orbits are located approximately at a distance of $30 R_E$ (with $R_E = \text{Earth radius} \approx 6400 \text{ km.}$) from the Earth and well inside the free streaming solar wind.

This next step of selection has been realized by the help of a NASA sponsored software **SSC Orbit Viewer**. By using this software, for a given interval, we can get (i) precise trajectory of the spacecraft along with the positions of magnetopause and bow-shock, (ii) the distance of the spacecraft from the Earth, magnetopause and bow-shock during that interval. The trajectories along with the distances are provided in the figure (7.8) for the intervals for which the spacecraft is far away from the bow-shock region.

However, enough care should be taken in choosing the data which are not affected significantly by the particles reflected from the terrestrial bow-shock. It is therefore necessary to examine the energy (or the temperature) of the ionic fluid corresponding to the chosen interval and to verify whether there is any considerable fluctuation in the temperature profile. The verification of such a 24 hour interval on 14/07/2008 – 15/07/2008 is given in the figure (7.9) where the ion temperature is found to vary weakly about 100 eV along with some eventual peaks.

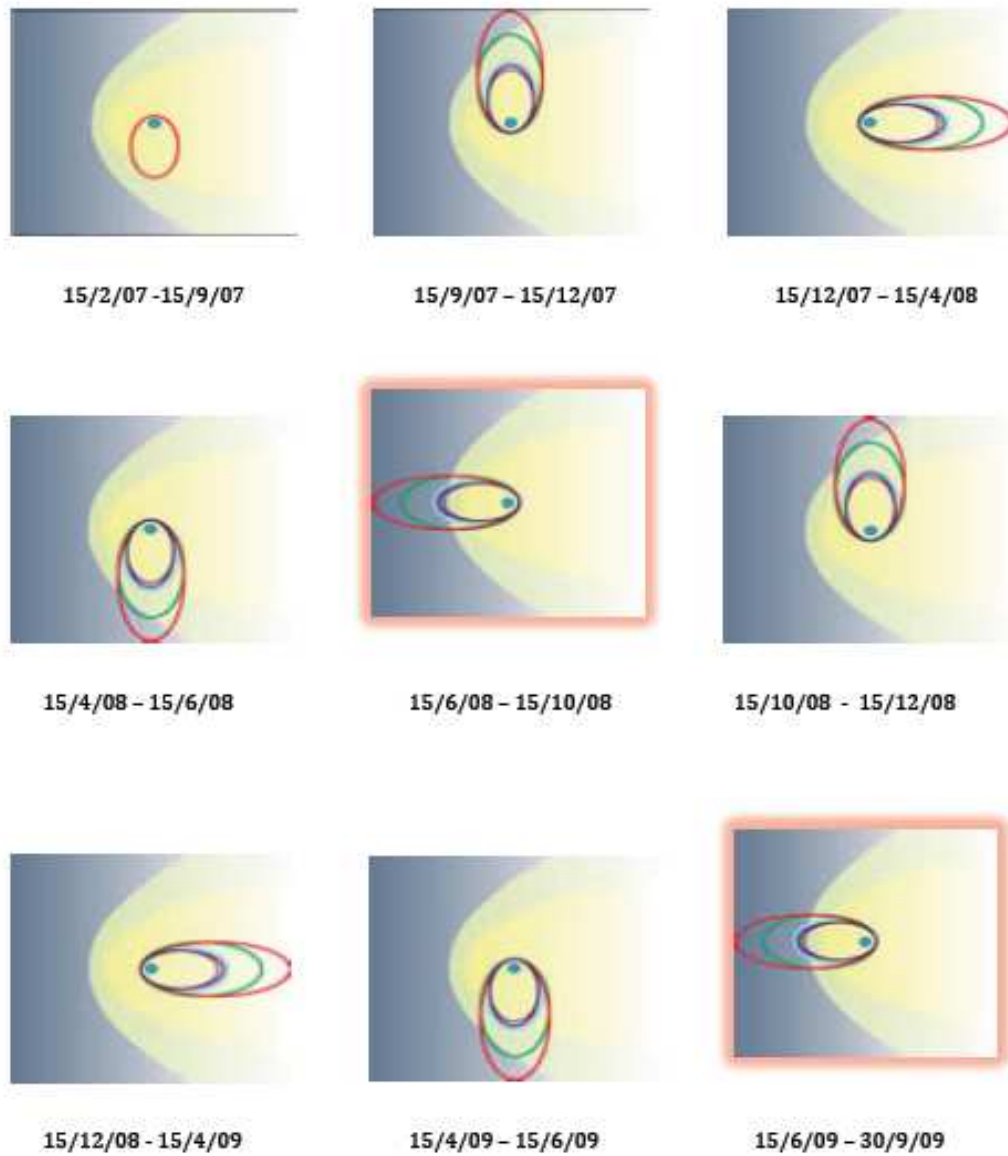


Figure 7.7: THEMIS spacecraft orbits during different periods; the red trajectory corresponds to THEMIS B and the grey region represents the solar wind; Credit : <http://themis.ssl.berkeley.edu/> .

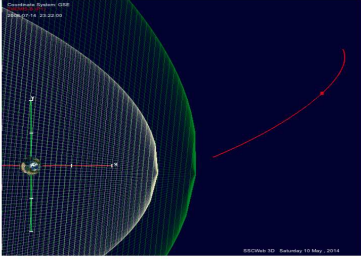
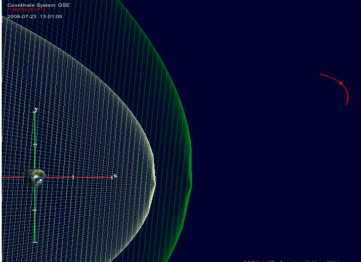
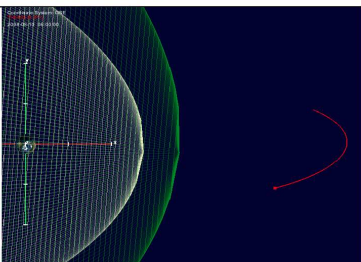
Interval	Spacecraft trajectory	D_{1x} (in R_E)	D_{2x} (in R_E)	D_{3x} (in R_E)
14/7/08 06h – 15/7/08 18h		20-30	8 - 20	5 - 16
23/7/08 01h – 21h		27-28	18-19	14-15
10/8/08 06h – 12/08/08 00h		23-30	14-20	10-14

Figure 7.8: Spacecraft trajectories (red line) obtained by SSC Orbit Viewer along with the positions of the magnetopause (off-white net like region) and bow-shock (green net like region). D_{1x} , D_{2x} , D_{3x} represent respectively the distance of the spacecraft from the Earth, the magnetopause and the bow-shock along the x-direction.

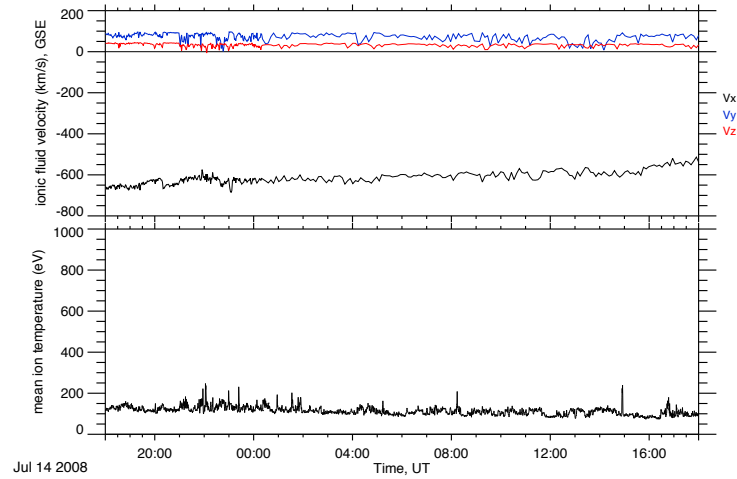


Figure 7.9: Examination of the ionic fluid temperature for a 24-hour interval on 14/07/2008-15/07/2008.

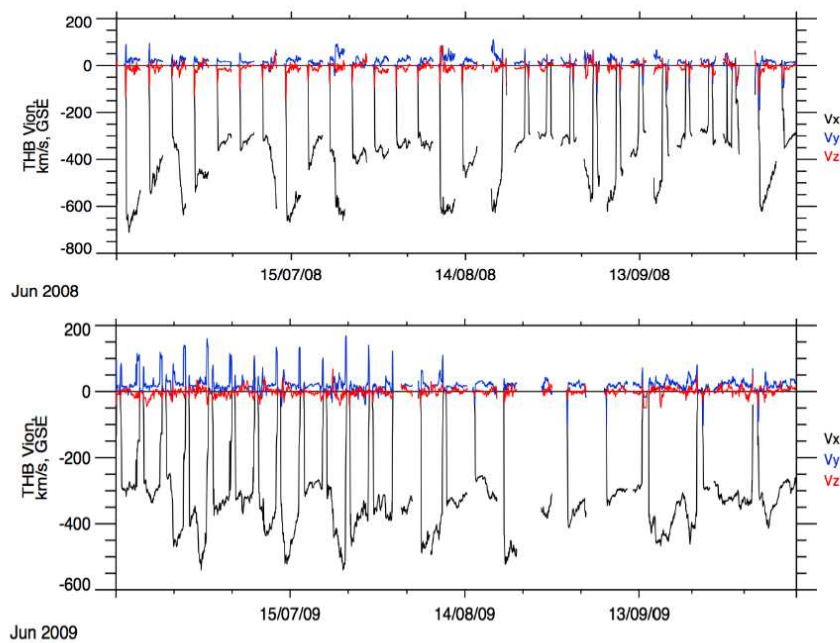


Figure 7.10: Selection of Fast solar wind data for the periods of 15/06/2008 - 10/10/2008 and 15/06/2009 - 10/10/2009, the three components of velocity (in km/s) are given in three different colors (as explained in the image).

In order to understand the compressible turbulence in the fast solar wind, we start by searching periods of this specific type of solar wind. We use local data source of AMDA (Automated Multi Dataset Analysis) to obtain the velocity of the solar wind for the two above-said intervals (see figure (7.10)). We use GSE (Geocentric Solar Ecliptic) coordinate system where the positive x-direction corresponds to the longitudinal direction from the Earth to the Sun and the z direction corresponds to the ecliptic north pole.

We can see that both in the year 2008 and 2009, we have several intervals with $|v_x| \geq 500$ km/s representing the streams of the fast solar wind. Once such an interval is chosen, we checked furthermore whether the corresponding datasets are continuous (without data gaps) or not. By thorough inspection, we have sorted out a number of intervals of 2008 for which we obtain clean (without gaps) data set both for the plasma (obtained by ESA) and the magnetic field (obtained by FGM) from AMDA local data base. We have also tried as much as possible to avoid abrupt and sharp discontinuities in data. The selected intervals are listed in the table (7.1).

Time interval	Duration of clean dataset
14/7/08 06 hrs. - 15/7/08 18 hrs.	36 hours
16/7/08 00 hrs. - 16/7/08 12 hrs.	12 hours
23/7/08 01 hrs. - 23/7/08 21 hrs.	20 hours
9/8/08 18 hrs. - 11/8/08 00 hrs.	30 hours
11/8/08 06 hrs. - 11/8/08 12 hrs	6 hours
11/8/08 15 hrs. - 12/8/08 00 hrs	9 hours

Table 7.1: Selected intervals of the fast solar wind with continuous data set

7.4.2 Relevant spatial and temporal scales

7.4.2.1 The Taylor's hypothesis

As mentioned above, the principal objective of the current study is to verify the validity of the exact scaling relation for compressible MHD turbulence in the solar wind turbulence. The original scaling relation relates third-order structure functions to the fluctuation length scales (in isotropic turbulence). In the case of spacecraft data analysis, what we obtain instead, is a time series of different dynamical variables (velocity, density, temperature, electric field, magnetic field etc.). Moreover the time series do not correspond to a single point in space but correspond to the space points crossed by the spacecraft along its trajectory. Now if we measure the frequency (ω') of the fluctuations at a specific point in space (i.e. the apparent frequency), it will be given

by the original frequency ω_p (perceived in the rest frame of the plasma flow) modulated by the relative motion between the spacecraft and the solar-wind bulk plasma. The Doppler relation is thus given by

$$\omega' = \omega_p + \mathbf{k} \cdot \mathbf{V}_R, \quad (7.1)$$

where V_R is the relative velocity between the solar wind and the spacecraft and \mathbf{k} is the propagation wave vector. Considering the intrinsic fluctuations to be principally caused by the Alfvén waves, we can write $\omega_p = \mathbf{k} \cdot \mathbf{V}_A$ and hence

$$\omega' = \mathbf{k} \cdot (\mathbf{V}_A + \mathbf{V}_R). \quad (7.2)$$

Now using the super Alfvénicity of the solar wind flow i.e. $|\mathbf{V}_R| \gg |\mathbf{V}_A|$, one can simplify the above relation to be

$$\omega' \approx \mathbf{k} \cdot \mathbf{V}_R.$$

Furthermore, considering the relative motion to be essentially in the direction³ of the fluctuation propagation, we can finally write (Matthaeus & Goldstein, 1982)

$$\omega' \approx kV_R. \quad (7.3)$$

This relation enables us to relate linearly the time series data to the corresponding fluctuation length scales and hence for an arbitrary variable, we have the following equivalence

$$\delta\psi \equiv \psi(r+l) - \psi(r) \equiv \psi(t+\tau) - \psi(t). \quad (7.4)$$

7.4.2.2 Suitable choice of the frequency range

In order to correctly determine the frequency range of our interest, we should recall the fact that the MHD mono-fluid description can be appropriate to describe the dynamics of a plasma if the corresponding length scales are larger than the ion inertial scale (λ_i) at which the ions start to decouple themselves from the electronic population (which still behaves like a fluid) and the magnetic field comes to be frozen in the electronic fluid instead of the bulk plasma. For the solar wind plasma at 1 AU, the ionic density (n_i) is approximately 5 particles cm^{-3} . The corresponding λ_i is then approximately

$$\lambda_i = \frac{\text{speed of light } (c)}{\text{ion plasma frequency } (\omega_{pi})} = \sqrt{\frac{m_i}{n_i e^2 \mu_0}} \approx 10^5 m \equiv 100 km. \quad (7.5)$$

³This assumption may, however, be invalid as the angle between the fluctuation propagation and the direction of solar wind flow was found to be $\sim 45^\circ$ (Sahraoui *et al.*, 2010).

Now considering the average fast solar wind velocity to be approximately 500 km/s, the corresponding frequency scale is of the order of 0.1 Hz. This determines the upper bound of the MHD frequency range. The lower bound, on the other hand is independent of the plasma parameters and should be determined by the forcing or energy injection scale. It is still a matter of debate to determine the effective injection scale for the solar wind turbulence. For practical purposes, this value is estimated by the lower bound of the $-5/3$ frequency spectrum of magnetic energy⁴ power density. In several studies, this range is found to span roughly within $10^{-4} - 10^{-1}$ Hz. For our current study, we have varied the time lag (τ) from 3 s to 3000 s resolution which allows us to sweep over the frequency range of $[10^{-4}, 10^{-1}]$ Hz.

7.5 Analysis of the selected data

The basic objective is to compare, for a selected interval, the incompressible and compressible energy fluxes (we keep the source terms aside) in order to point out the effect of the density fluctuations in the flux. We have chosen nearly 25 intervals of 3 hours with 3 s. resolution. The calculation is done by a simple code using FORTRAN 77/90. The final plots are drawn in direct scale (and not in logarithmic scale) and so the original sign (positive or negative) of the third order structure functions are kept intact. For the sake of simplicity, the GSE x-direction is chosen to be the direction of measurement. More precisely, we test the scaling of the expression $S_3 = \langle [\delta(\rho\mathbf{z}^+) \cdot \delta\mathbf{z}^+] \delta z_x^- + [\delta(\rho\mathbf{z}^-) \cdot \delta\mathbf{z}^-] \delta z_x^+ \rangle$ as a function of time lag τ . In calculating⁵ incompressible flux, the plasma density in the selected interval is just replaced by the mean density of that interval where for the compressible calculation, we leave the density⁶ as an ordinary variable. Along with the aforesaid plot, a measure of compressibility is given for each interval. Coefficient of variation (the ratio of standard deviation to the mean value) of the ion density fluctuations is chosen to be the measure of compressibility in the following studies. In the figure (7.11), we have three panels. The first one represents the data corresponding to three components of velocity, density and three components of magnetic field fluctuations corresponding to the interval of 8h and 11h on 11/08/2008. The second panel presents the fluctuations

⁴Considering a constant ratio of kinetic and magnetic energy in incompressible MHD, one can show that the power density spectrum of magnetic energy is sufficient to represent the spectral index for the total energy. In compressible case, this is not valid due to the presence of compressible energy.

⁵All the calculations are done in S.I. unit system.

⁶One should not however forget that the density is present also in the expression of Elsässer variables which should also be taken care with.

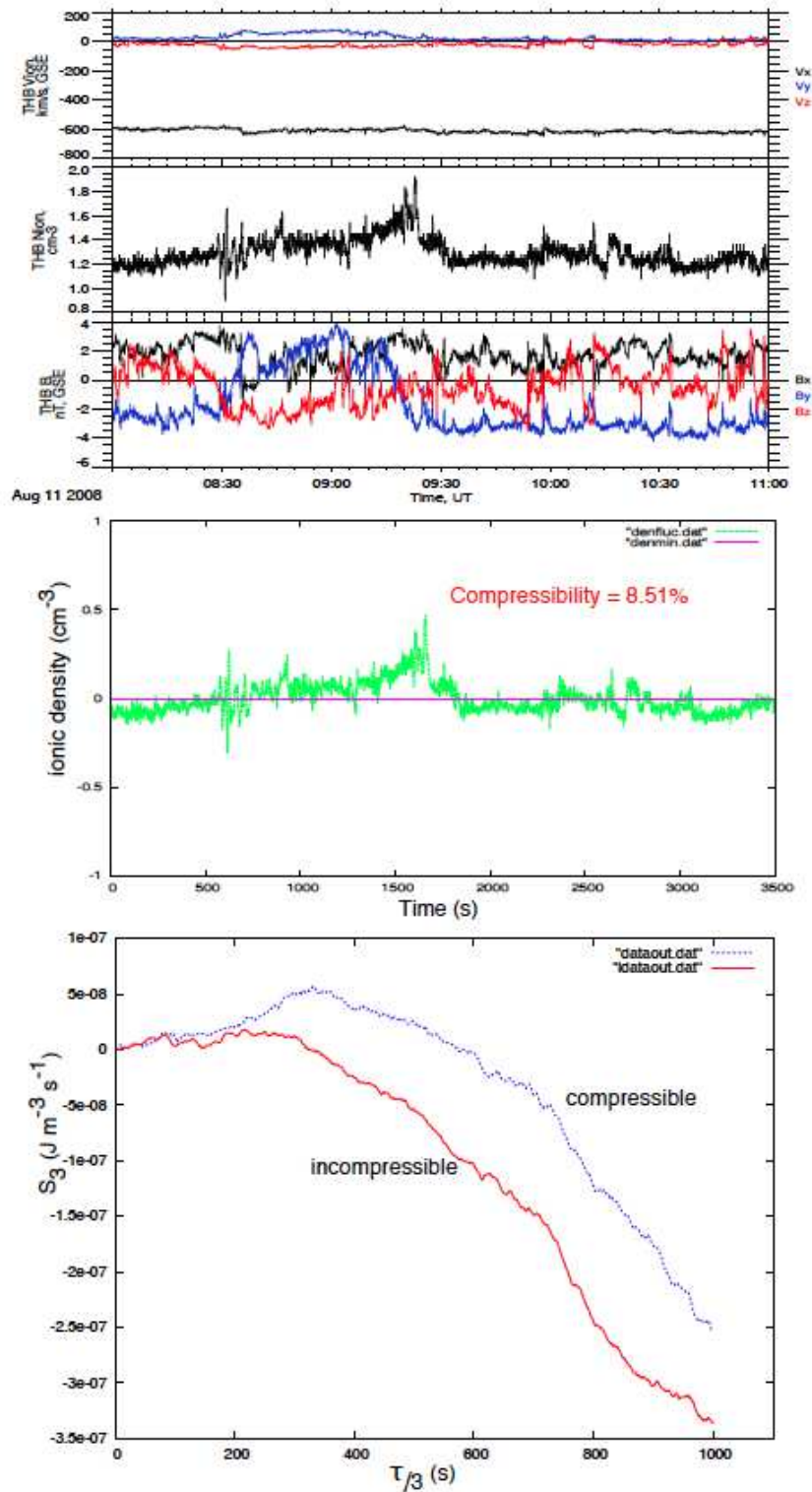


Figure 7.11: The fluctuation data scheme of 8h-11h of 11/08/2008 obtained from AMDA - the ion velocity components, ion density and magnetic field components are given in the respective three panels (top figure); calculated density fluctuations (in green) about the mean value (in violet) (middle panel) and the scaling of incompressible (in red) and partial compressible flux (in blue) as a function of time lag τ (bottom panel).

of the ion density about the mean value for that interval and the third one represents the scaling of the incompressible and compressible moments.

For this interval the compressibility is very weak ($\sim 8\%$) and we can observe that the incompressible and compressible scalings are not very different. Moreover for this interval, both the flux terms are principally negative. However, this is not the same picture that we get for other intervals. In fact, we obtain a random mixture of positive and negative moments both in the incompressible and compressible case. Here, we present four such intervals (see figures (7.12) and (7.13)) where different combinations of the flux signs are obtained.

These intervals are taken from the same day (14 July, 2008). The compressibility (here defined as the coefficient of variation of the density fluctuations) does not exceed 20% in any of the intervals. A plausible explanation for this random behaviour can be given using the high Alfvénicity of the fast solar wind where non-linear cascade is very weak due to a strong velocity magnetic field correlation (Carbone *et al.*, 2009). Despite the above discussed random behaviour, it is however found that, in most of the cases, the gap between the two is more pronounced when the compressibility is higher and vice-versa (see figure (7.14)).

Comparison of different flux terms for solar wind at 1 A.U. The compressible flux term used above was just a part of the total flux term obtained for compressible MHD turbulence. We recall the newly obtained exact relation for compressible MHD turbulence in an isothermal plasma in the following:

$$\begin{aligned}
-2\varepsilon = & \frac{1}{2} \nabla_r \cdot \left\langle \left[\frac{1}{2} \delta(\rho \mathbf{z}^-) \cdot \delta \mathbf{z}^- + \delta \rho \delta e \right] \delta \mathbf{z}^+ + \left[\frac{1}{2} \delta(\rho \mathbf{z}^+) \cdot \delta \mathbf{z}^+ + \delta \rho \delta e \right] \delta \mathbf{z}^- + \bar{\delta} \left(e + \frac{v_A^2}{2} \right) \delta(\rho \mathbf{z}^- + \rho \mathbf{z}^+) \right\rangle \\
& - \frac{1}{4} \left\langle \frac{1}{\beta'} \nabla' \cdot (\rho \mathbf{z}^+ e') + \frac{1}{\beta} \nabla \cdot (\rho' \mathbf{z}'^+ e) + \frac{1}{\beta'} \nabla' \cdot (\rho \mathbf{z}^- e') + \frac{1}{\beta} \nabla \cdot (\rho' \mathbf{z}'^- e) \right\rangle \\
& + \left\langle (\nabla \cdot \mathbf{v}) \left[R'_E - E' - \frac{\bar{\delta} \rho}{2} (\mathbf{v}_{\mathbf{A}'} \cdot \mathbf{v}_{\mathbf{A}}) - \frac{P'}{2} + \frac{P'_M}{2} \right] + (\nabla' \cdot \mathbf{v}') \left[R_E - E - \frac{\bar{\delta} \rho}{2} (\mathbf{v}_{\mathbf{A}} \cdot \mathbf{v}_{\mathbf{A}'}) - \frac{P}{2} + \frac{P_M}{2} \right] \right\rangle \\
& + \left\langle (\nabla \cdot \mathbf{v}_{\mathbf{A}}) \left[R_H - R'_H + H' - \bar{\delta} \rho (\mathbf{v}' \cdot \mathbf{v}_{\mathbf{A}}) \right] + (\nabla' \cdot \mathbf{v}_{\mathbf{A}'}) \left[R'_H - R_H + H - \bar{\delta} \rho (\mathbf{v} \cdot \mathbf{v}_{\mathbf{A}'}) \right] \right\rangle,
\end{aligned}$$

The first two lines of the above relation represent the flux terms whereas the following two lines consist of the source terms. Unlike the incompressible case, here we have more than one candidate in the flux term. It is therefore reasonable to investigate the relative importance of those terms in order to confirm whether any term becomes identically negligible with respect to the others. The exact relation can schematically be written as

$$-2\varepsilon = \frac{1}{2} \nabla_r \cdot \langle \mathcal{F}_1 + \mathcal{F}_2 + \mathcal{F}_3 + \mathcal{F}_4 \rangle + \langle \Phi \rangle + \text{source terms}, \quad (7.6)$$

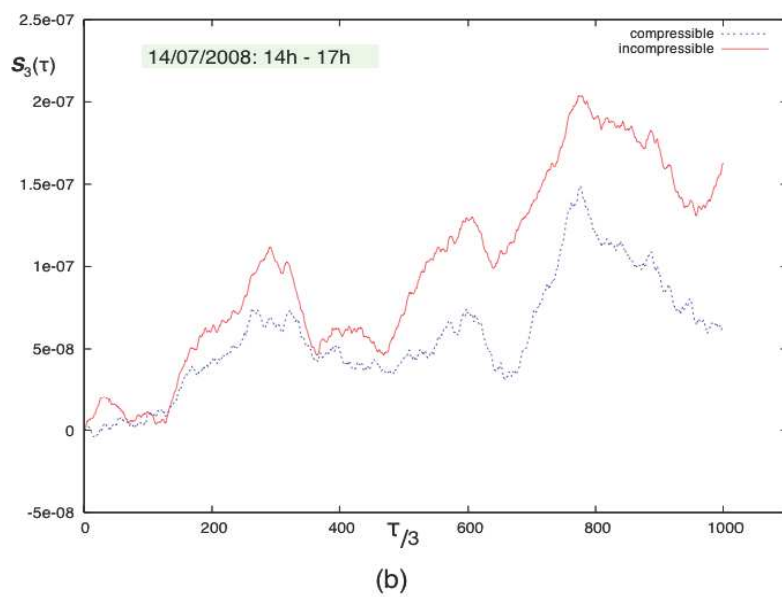
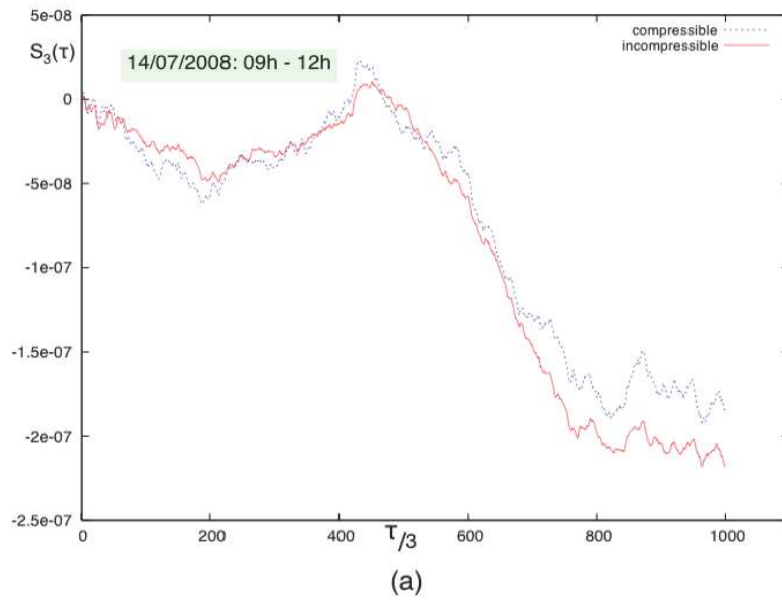


Figure 7.12: (a) Interval with negative incompressible and compressible flux, (b) Interval with positive incompressible and compressible flux.

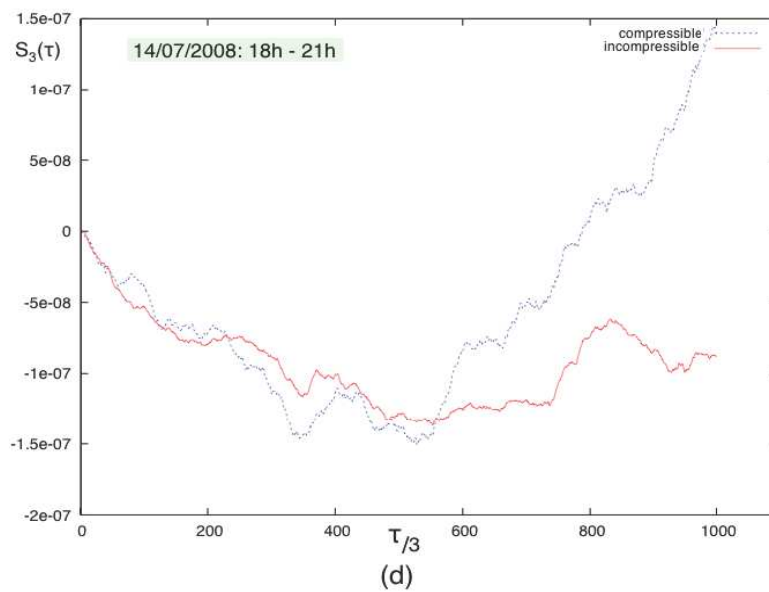
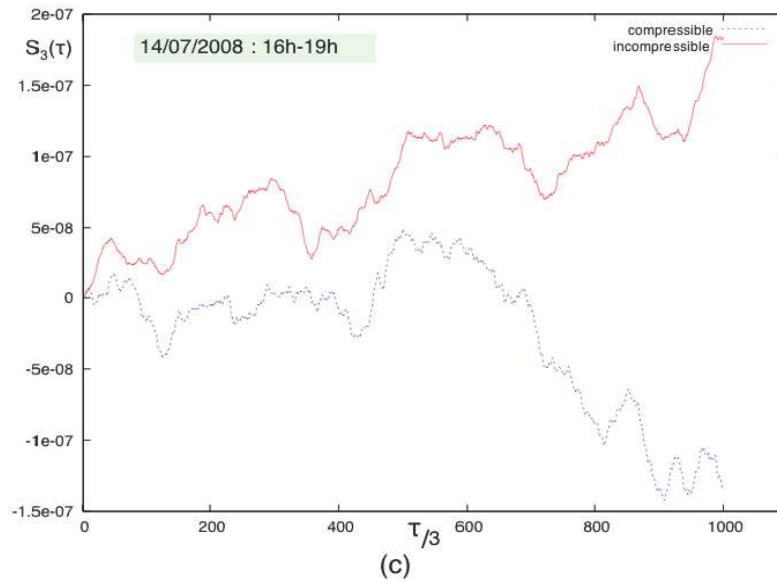


Figure 7.13: (c) Interval with positive incompressible flux and negative compressible flux, (d) Interval with negative incompressible flux and positive compressible flux.

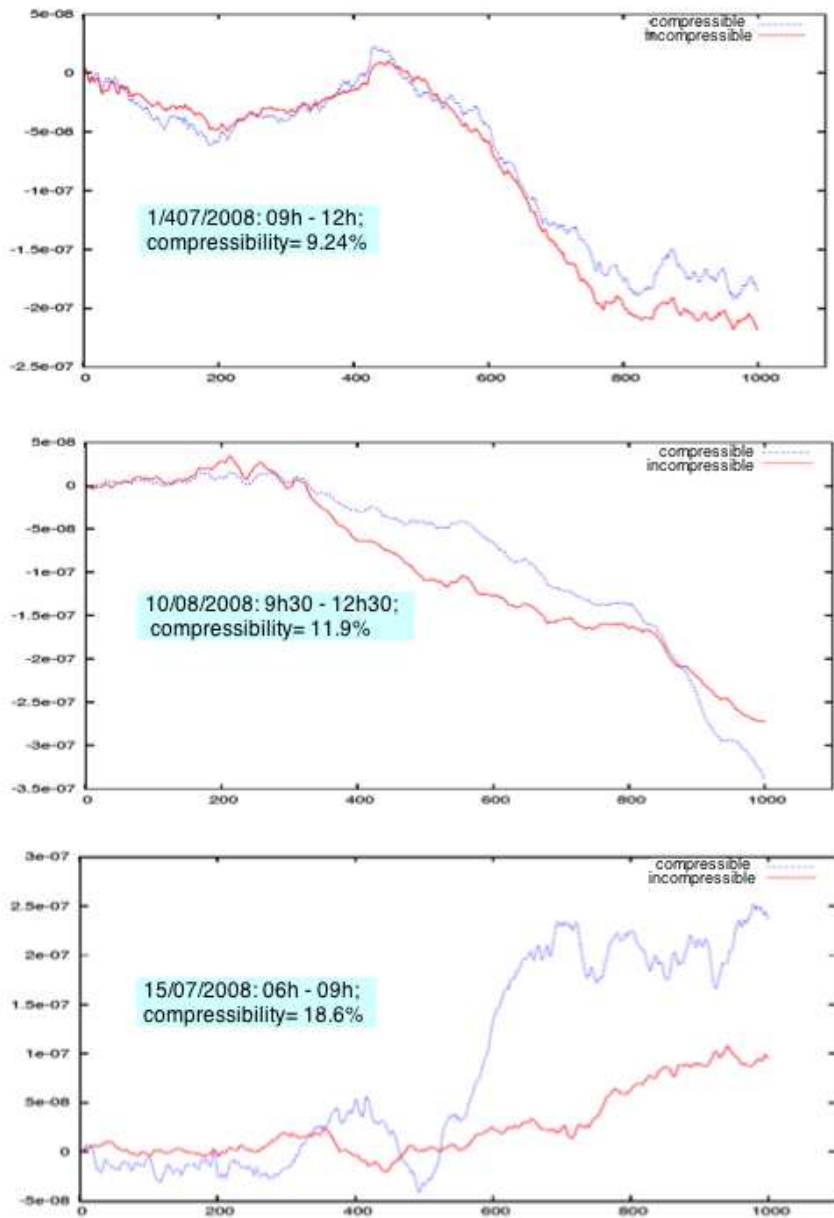


Figure 7.14: The effect of compressibility on the discrepancy between the incompressible and compressible flux.

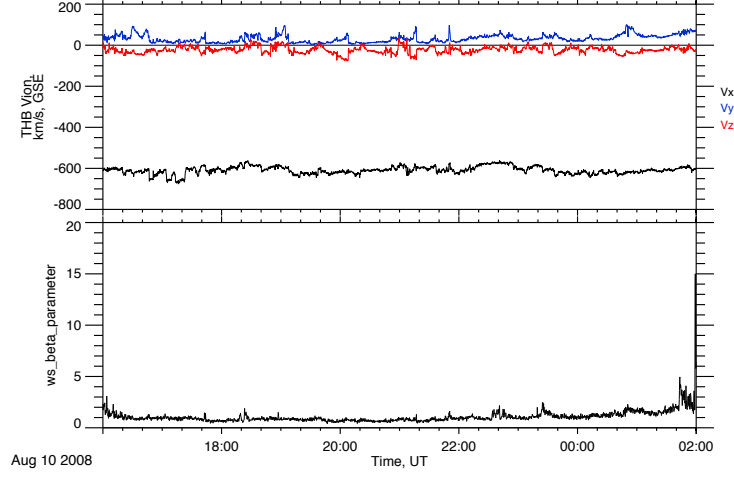


Figure 7.15: Almost constant plasma beta parameter of order unity during a 10 hour interval of 10/08/2008 -11/10/2008 (second panel)

where

$$\begin{aligned}
 \langle \mathcal{F}_1 \rangle &= \left\langle \left[\frac{1}{2} \delta(\rho \mathbf{z}^-) \cdot \delta \mathbf{z}^- \right] \delta \mathbf{z}^+ \right\rangle, \\
 \langle \mathcal{F}_2 \rangle &= \left\langle \left[\frac{1}{2} \delta(\rho \mathbf{z}^+) \cdot \delta \mathbf{z}^+ \right] \delta \mathbf{z}^- \right\rangle, \\
 \langle \mathcal{F}_3 \rangle &= \langle 2\delta\rho\delta e\delta\mathbf{v} \rangle, \\
 \langle \mathcal{F}_4 \rangle &= \left\langle 2\bar{\delta} \left(e + \frac{v_A^2}{2} \right) \delta(\rho\mathbf{v}) \right\rangle, \\
 \langle \Phi \rangle &= -\frac{1}{2} \left\langle \frac{1}{\beta'} \nabla' \cdot (\rho\mathbf{v}e') + \frac{1}{\beta} \nabla \cdot (\rho'\mathbf{v}'e) \right\rangle.
 \end{aligned}$$

The term Φ cannot be written in pure divergence form. However, for the solar wind at 1 AU., we have found certain intervals (see fig. 7.15) for which the plasma beta is almost constant and is of the order unity (see figure (7.15)). For those intervals, we can have $\beta \approx \beta' \sim 1$ and hence we can write

$$\langle \Phi \rangle \approx -\frac{1}{2} \nabla_{\mathbf{r}} \cdot \langle \rho\mathbf{v}e' - \rho'\mathbf{v}'e \rangle = \nabla_{\mathbf{r}} \cdot \langle \bar{\delta}e\delta(\rho\mathbf{v}) \rangle \quad (7.7)$$

We try to establish an approximate ordering by using the typical order of magnitudes of the dataset of current interest. For several intervals of the fast

solar wind, we get,

$$\begin{aligned} |\mathbf{v}| &\sim 550 \text{ km/s.}, |\delta\mathbf{v}| \sim 5 \text{ km/s.} \\ |\mathbf{v}_A| &\sim 100 \text{ km/s.}, |\delta\mathbf{v}_A| \sim 2 \text{ km/s.} \\ \rho &\sim 2 \times 10^{-21} \text{ kg.m}^{-3}, \delta\rho \sim 0.05 \times 10^{-21} \text{ kg.m}^{-3}, \delta(\rho v) \sim 5 \times 10^{-17} \text{ kg.m}^{-2}.\text{s}^{-1}. \end{aligned}$$

The average sound speed is about 60 km/s. Using all these order of magnitudes⁷, we finally obtain

$$|\mathcal{F}_1| \approx |\mathcal{F}_2| \approx 10^3 |\mathcal{F}_3| \approx 10^{-3} |\mathcal{F}_4|. \quad (7.8)$$

But this ordering is not very useful in the current study because the contribution of each term comes from their statistical average. In fact, in some intervals, the fluctuations are switching enormously within positive and negative values. We have indeed found some intervals where $|\mathcal{F}_1| \approx |\mathcal{F}_3|$ or $|\mathcal{F}_1| \approx |\mathcal{F}_4|$ after being averaged over the selected interval (see table (7.2)). It is thus concluded that none of these contributions can be eliminated in a gross way just by their numerical order of magnitudes.

Time interval	$\langle\mathcal{F}_1\rangle$	$\langle\mathcal{F}_3\rangle$	$\langle\mathcal{F}_4\rangle$
14/07/08 09 hrs. - 12 hrs.	1.95×10^{-8}	-2.6×10^{-12}	-1.3×10^{-10}
11/08/08 08 hrs. - 11 hrs.	4.7×10^{-11}	1.86×10^{-12}	3.8×10^{-10}
21/08/09 01 hrs. - 04 hrs.	-6.2×10^{-11}	-2.65×10^{-11}	5.28×10^{-10}

Table 7.2: Average values of the flux terms (for 3 s. lag) for a number of three-hour intervals

It is therefore logical to investigate the scaling property with the complete flux term (of course for the intervals with almost uniform beta for simplicity). With the complete flux term, we have studied more than 6 intervals of 6 hours (it was harder to get continuous intervals of 6 hours than those of 3 hours) and we vary the time lag (τ) from 3 s. to 9000 s so as to cover as much as possible the MHD range. When the scaling is plotted in logarithmic scale, we found a remarkably improved scaling (see figures 7.16 and 7.17) with respect to the incompressible scaling (Politano & Pouquet, 1998b) and the empirical compressible scaling (Carbone *et al.*, 2009). Unlike the previous two scalings, the new scaling gives

(a) a regular scaling with no sign change (i.e. in logarithmic scale the scaling does not contain any hole or discontinuity).

⁷One should however remember that in the final scaling relation, the vectorial fluctuation part associates essentially the longitudinal fluctuations which is almost identical to the x component in our study.

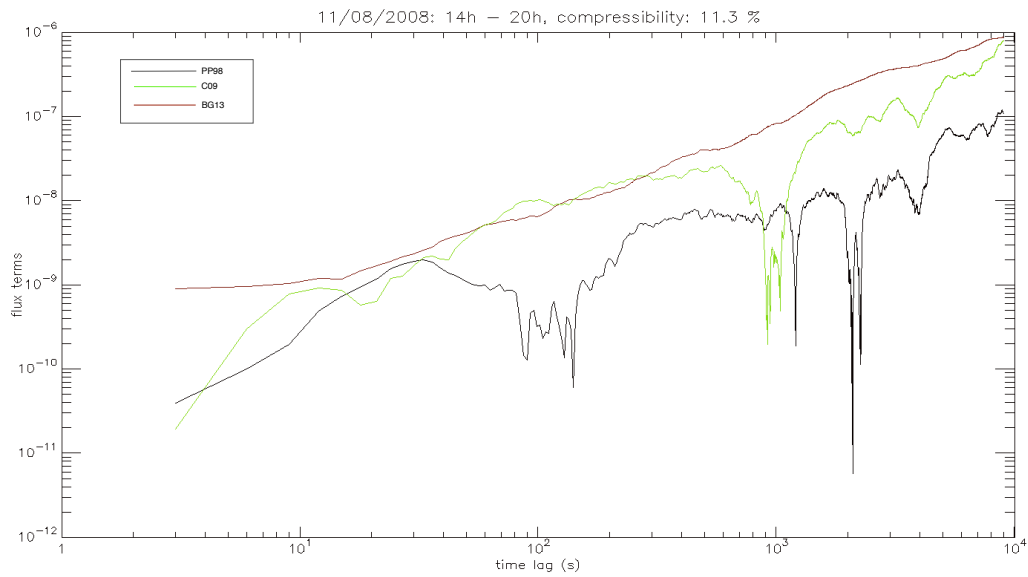


Figure 7.16: Comparison of incompressible (in black), heuristic compressible (in green) and analytical compressible (in red) scalings in a 6-hour interval of 2008

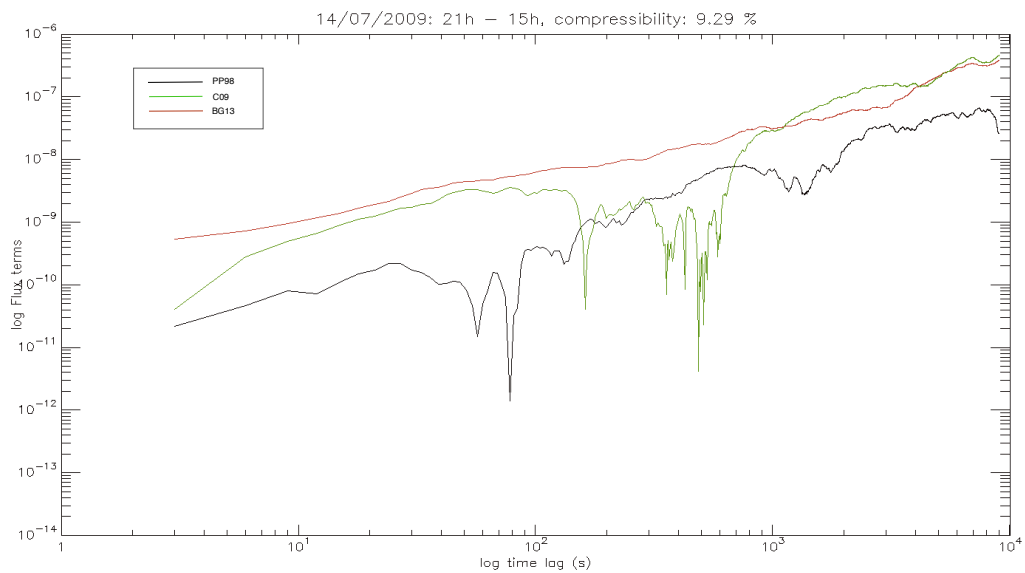


Figure 7.17: Comparison of incompressible (in black), heuristic compressible (in green) and analytical compressible (in red) scalings in a 6-hour interval of 2009

(b) a consistent power-law behaviour (in fact almost linear behaviour) for at least three decades of fluctuation time (or length) scales.

Interestingly, the order of magnitude of the compressible third-order structure function is found to be almost the same (10-15 times greater than the incompressible value) as that obtained by [Carbone *et al.* \(2009\)](#). This fact justifies that the new scaling is adequate for explaining the anomalous heating of the fast solar wind on the basis of compressible fluctuations in the corresponding turbulence. The contribution is found to come from the fluctuations of the currents (terms like $\delta(\rho\mathbf{v})$) and not from mere density fluctuations $\delta\rho$.

During the scope of my thesis, only a preliminary study is performed on the fast solar wind turbulence using in-situ THEMIS spacecraft data. The next step is, of course, to perform an elaborated study with the complete compressible scaling law including the source terms. In order to estimate the source terms, one has to evaluate the local divergence terms of the source term. Multi-spacecraft data from the two ARTEMIS spacecraft could be used to estimate the spatial gradients along the direction of separation between them. Moreover, the role of compressibility in the slow solar wind turbulence is not studied in the course of my thesis. A comparative study on the compressible effects in fast and slow solar wind turbulence could enlighten the physics behind the solar wind turbulence. It is also planned to test the simplified scaling law which we obtained ([Banerjee & Galtier, 2013](#)) in the presence of a very strong (w.r.t. the fluctuations) magnetic field for certain intervals of the solar wind data having a strong mean magnetic field.

Resuming and looking ahead...

Contents

8.1	Answered and unanswered issues of compressible turbulence	175
8.2	Some future projects	177

8.1 Answered and unanswered issues of compressible turbulence

MY research work was primarily dedicated to the development of analytical theories in compressible turbulence. Unlike the incompressible turbulence, we have meagre theoretical development for the turbulence in compressible fluids. Several analytical exact relations were derived for incompressible turbulence in neutral fluids and in plasmas (Kolmogorov, 1941*b*; Yaglom, 1949; Politano & Pouquet, 1998*b,a*; Galtier, 2008*b*; Meyrand & Galtier, 2010) etc. It is seventy years (1941-2011) after Kolmogorov's work that we derived the first Kolmogorov-like exact relation for compressible turbulence (Galtier & Banerjee, 2011). This work finds its significance in explaining the universality in compressible turbulence in terms of the cube-root density weighted velocity ($\rho^{1/3}\mathbf{v}$) supporting previous high resolution numerical results of Kritsuk *et al.* (2007*a*) and Federrath *et al.* (2010) for isothermal supersonic turbulence. In addition to the flux terms, compressible exact relation consists of source terms which are proportional to the dilatation and is believed to modify the global energy transfer rate. Under the assumption of a direct energy cascade, a possible phenomenology based on the global dilatation and compression is also proposed from the said relation. According to this phenomenology, a global compressional effect would enhance a direct energy cascade whereas a global dilatational effect would weaken it. In our entire derivation, a direct cascade is assumed for the total energy which is the sum of kinetic and internal compressive energies and is a global inviscid invariant of the system. This point can be put in question in the current framework. Recent numerical works

(Aluie *et al.*, 2012) assures a direct cascade for the kinetic energy (which is not an invariant of compressible turbulence) in subsonic and transonic turbulence. The basic reason of this kinetic energy cascade is due to the large scale exclusivity of the pressure dilatation term which falls as k^{-1} and practically decouples the internal energy to the kinetic energy inside the inertial zone thereby leading to a direct energy cascade for the later. However, for supersonic turbulence, this fact is not verified and gives birth to an open issue. Furthermore the existence of a so-called inertial zone is also debatable in compressible turbulence. Several works (Federrath *et al.*, 2010; Wagner *et al.*, 2012; Kritsuk *et al.*, 2013) find considerable forcing sensitivity of the scaling and spectral properties in compressible strong turbulence. Moreover, till date, no rigorous proof exists to justify a direct energy cascade of total energy in strong compressible turbulence. However, an inverse energy cascade has already been reported in two-dimensional weakly compressible turbulence (Dahlburg *et al.*, 1990) using solenoidal forcing.

Polytropic model is more realistic in case of the solar wind (Marsch & Tu, 1990b) and in astrophysical plasmas. An extension of our first work (Galtier & Banerjee, 2011) has been accomplished in case of a polytropic fluid (Banerjee & Galtier, 2014) in order to understand the role of sound speed fluctuations in compressible turbulence. In this work, we have defined three Mach Numbers. Depending on the scaling properties of those Mach numbers, we have predicted some spectral power laws which are subject to future numerical and observational verifications.

Another main result of my thesis is the derivation of an exact relation of compressible MHD turbulence of an isothermal plasma (Banerjee & Galtier, 2013). This work justified analytically the scaling relations and Kolmogorov type spectral laws for density weighted Elsässer variables. Unlike the incompressible case (Politano & Pouquet, 1998a), here we do not have two separate scaling laws for two pseudo-energies but one relation corresponding to the conservation of total energy. Therefore the theoretically derived proper scaling variable is $\rho^{1/3}(\mathbf{z}^{+2}\mathbf{z}^- + \mathbf{z}^{-2}\mathbf{z}^+)^{1/3}$ instead of $\rho^{1/3}\mathbf{z}^\pm$. No phenomenology was proposed for general compressible MHD turbulence and is still an open question. Nevertheless, the situation becomes much simpler when we consider a very strong mean magnetic field. A possible phenomenology is proposed following Galtier & Banerjee (2011) to explain an energy cascade in the perpendicular direction of that mean magnetic field. However, no conclusion is made on the possibility of a cascade in the parallel direction and is surely a matter of further investigation. Under this strongly anisotropic condition, a power law of $-5/2$ has been predicted for coupled (kinetic and magnetic) energy power spectra. No prediction for the individual parts of energy (kinetic, magnetic or compressive) and even for the total energy was possible to made

from our exact relation.

The last part of my thesis was dedicated in the analysis of in-situ fast solar wind data of THEMIS spacecraft. For several intervals I have performed comparative study between the incompressible and compressible fluxes (as a preliminary step, source terms are kept aside). For a fixed interval, the discrepancy between the two scalings are found to reflect (to some extent) the density fluctuations or the degree of compressibility of the said interval. Finally a crude estimation of the order of magnitude for different candidates of flux terms has been carried out in the case of the solar wind at 1 AU in order to understand the relative importance of each term. However, in practice, the local fluctuations change significantly their sign and therefore, no term can be considered to be neglected identically in the statistical studies.

8.2 Some future projects

THE field of theoretical compressible turbulence is developed very little due to its greater complexity and less symmetry than its incompressible counterpart. A large scope of possible theoretical projects can therefore be prospected. An exact relation in case of compressible polytropic plasma (which is not done during my thesis due to lack of time) can be thought to be an immediate offspring of my thesis work. Several regimes depending on the sonic and Alfvénic Mach number need to be investigated. A thorough development of this relation could indeed be useful in understanding the role of turbulence in the star formation mechanism which is still obscure to the astrophysicists. The inclusion of gravitational field can obviously sophisticate the model. The question whether the gravitational field works as a forcing candidate being effective only at the large scales or can modify the flow at all scales is subject to future numerical studies including gravitational field. Interestingly, inclusion of gravitational field as an all-scale entity is shown to hardly affect the incompressible scaling relations (see Appendix A). Will it play the identical role in compressible turbulence or not still remains an open question.

The nature of astrophysical turbulence is essentially convective i.e. governed by thermal instability which leads to a variable energy flux. A more realistic theoretical model can thus be thought of by closing the system in terms of third or higher order moments. A possibility of two-point closures in compressible turbulence (where the compressibility is not necessarily weak) can be relevant in this context (Bertoglio *et al.*, 2001).

A fundamental assumption of our derivation is based on the statistical homogeneity. In practice, a supersonic turbulent flow leads to the formation of

shocks and discontinuities which effectively render the flow statistically inhomogeneous or rather globally inhomogeneous. The type of turbulence developed at the back and the forth of a shock thus need to be studied separately. A detailed thorough theoretical work is thus needed in case of inhomogeneous turbulence in order to understand the supersonic turbulence from a phenomenological point of view.

Intermittency in compressible turbulence is another subject of immense complexity and obscurity. Intuitive approaches (Schmidt *et al.*, 2008) for modelling compressible intermittency in the same framework of incompressible turbulence has also produced, to some extent, good agreements with the numerical results. However, a proper model with suitable phenomenology for compressible turbulence is yet to be developed. In fact, such models can possibly be developed starting from our newly derived exact relations and hence opens another possibility of theoretical investigation.

Concerning the projects of spacecraft data analysis, the first objective is to complete the current study (as discussed in the chapter 7). Parallely, it would be interesting to test the simplified scaling law which we obtained (Banerjee & Galtier, 2013) in the presence of a very strong (w.r.t. the fluctuations) magnetic field for the magnetospheric plasmas near magnetosheath which is governed by a very strong mean magnetic field. For a number of intervals, positive correlation between the fluctuations of the local density and the local magnetic field components have been observed in fast solar wind data. A study (which is not discussed in the scope of this thesis) relating local magnetic field fluctuations and local ionic density fluctuation is also in progress and can be indicative in understanding the proper nature and reason of density and magnetic field coupling and its effect in solar wind turbulence.

References

- ALEXAKIS, A., MININNI, P. D. & POUQUET, A. 2006 On the inverse cascade of magnetic helicity. *The Astrophysical Journal* **640** (1), 335. (Cited on page 114.)
- ALEXANDROVA, O., SAUR, J., LACOMBE, C., MANGENEY, A., MITCHELL, J., SCHWARTZ, S. J. & ROBERT, P. 2009 Universality of solar-wind turbulent spectrum from mhd to electron scales. *Phys. Rev. Lett.* **103**, 165003. (Cited on page 154.)
- ALFVÉN, H. 1942 Existence of electromagnetic–hydrodynamic waves. *Nature* **150**, 405–406. (Cited on page 32.)
- ALLEN, T. K., BAKER, WILLIAM R., PYLE, ROBERT V. & WILCOX, JOHN M. 1959 Experimental generation of plasma alfvén waves. *Phys. Rev. Lett.* **2**, 383–384. (Cited on pages vii, 32 and 34.)
- ALUIE, H. 2011 Compressible turbulence: The cascade and its locality. *Physical Review Letter* **106**, 174502. (Cited on pages 123 and 125.)
- ALUIE, H. 2013 Scale decomposition in compressible turbulence. *Physica D* **247**, 54–65. (Cited on page 140.)
- ALUIE, H., LI, S. & LI, H. 2012 Conservative cascade of kinetic energy in compressible turbulence. *The Astrophysical Journal Letters* **751** (2), L29. (Cited on page 176.)
- ANTONIA, R. A., OULD-ROUIS, M., ANSELMET, F. & ZHU, Y. 1997 Analogy between predictions of Kolmogorov and Yaglom. *Journal of Fluid Mechanics* **332**, 395–409. (Cited on pages 61 and 142.)
- ARMSTRONG, J. W., RICKETT, B. J. & SPANGLER, S. R. 1995 Electron density power spectrum in the local interstellar medium. *The Astrophysical Journal* **443**, 209–221. (Cited on pages 2 and 103.)
- BALOGH, A. & TREUMANN, R.A. 2013 *Physics of Collisionless Shocks: Space Plasma Shock Waves*. Springer. (Cited on page 152.)
- BANERJEE, S. & GALTIER, S. 2012 Compressible turbulence: A different physics? *Proceedings SF2A, Scientific Highlights, Boissier et al. Eds.* pp. 277–279. (Cited on page 128.)

- BANERJEE, S. & GALTIER, S. 2013 Exact relation with two-point correlation functions and phenomenological approach for compressible magnetohydrodynamic turbulence. *Physical Review E* **87**, 013019. (Cited on pages xi, 6, 40, 121, 137, 147, 173, 176 and 178.)
- BANERJEE, S. & GALTIER, S. 2014 A kolmogorov-like exact relation for compressible polytropic turbulence. *Journal of Fluid Mechanics* **742**, 230–242. (Cited on pages 6, 121, 141 and 176.)
- BATCHELOR, G. K. & PROUDMAN, I. 1956 The large-scale structure of homogeneous turbulence. *Philosophical Transactions of the Royal Society of London. Series A, Mathematical and Physical Sciences* **248** (949), 369–405. (Cited on page 69.)
- BATCHELOR, G. K. & TOWNSEND, A. A. 1949 The nature of turbulent motion at large wave-numbers. *Proceedings of the Royal Society of London. Series A. Mathematical and Physical Sciences* **199** (1057), 238–255. (Cited on page 75.)
- BATEMAN, H. 1915 Some recent researches on the motion of fluids. *Monthly Weather Review* **43**, 163–170. (Cited on page 17.)
- BAVASSANO, B., DOBROWOLNY, M., FANFONI, G., MARIANI, F. & NESS, N. F. 1982 Statistical properties of mhd fluctuations associated with high-speed streams from helios-2 observations. *Solar Physics* **78**, 373–384. (Cited on pages 107 and 116.)
- BELCHER, J. W. & DAVIS, LEVERETT 1971 Large-amplitude alfvén waves in the interplanetary medium, 2. *Journal of Geophysical Research* **76** (16), 3534–3563. (Cited on page 153.)
- BELMONT, G., GRAPPIN, R., MOTTEZ, F., PANTELLININ, F. & PELLETIER, G. 2014 *Collisionless plasmas in astrophysics*. Wiley-vch, Weinheim. (Cited on pages 3 and 152.)
- BENZI, R., CILIBERTO, S., TRIPICCIONE, R., BAUDET, C., MASSAIOLI, F. & SUCCI, S. 1993 Extended self-similarity in turbulent flows. *Physical Review E* **48**, R29–R32. (Cited on page 80.)
- BERSHADSKII, A. & SREENIVASAN, K. R. 2004 Intermittency and the passive nature of the magnitude of the magnetic field. *Physical Review Letters* **93**, 064501. (Cited on page 104.)

- BERTOGLIO, J. P., BATAILLE, F. & MARION, J. D. 2001 Two-point closures for weakly compressible turbulence. *Physics of Fluids (1994-present)* **13** (1), 290–310. (Cited on pages x, 102, 103 and 177.)
- BISKAMP, D. 2008 *Magnetohydrodynamic Turbulence*. Cambridge University Press, Cambridge. (Cited on pages xi, 52, 54, 57, 59, 66, 72, 80, 90, 102, 141, 144, 150, 152 and 153.)
- BITTENCOURT, J.A. 2003 *Fundamentals of Plasma Physics*, 3rd edn. INPE. (Cited on pages 24, 26 and 30.)
- BOROVSKY, J. E. & GARY, S. P. 2008 The viscosity of the collisionless solar wind and the reynolds number of its mhd turbulence. *AGU Fall Meeting Abstracts* p. A2. (Cited on page 68.)
- BOYD, T.J.M. & SANDERSON, J.J. 2003 *The Physics of Plasmas*. Cambridge University Press. (Cited on page 30.)
- BRACHET, M. E., MENEGUZZI, M. & SULEM, P. L. 1986 Small-scale dynamics of high-reynolds-number two-dimensional turbulence. *Physical Review Letters* **57**, 683–686. (Cited on page 92.)
- BRUNO, R. & CARBONE, V. 2005 The solar wind as a turbulence laboratory. *Living Reviews in Solar Physics* **2** (4). (Cited on pages 2 and 107.)
- BURGERS, J.M. 1948 A mathematical model illustrating the theory of turbulence **1**, 171 – 199. (Cited on pages 4, 17 and 84.)
- CARBONE, V., MARINO, R., SORRISO-VALVO, L., NOULLEZ, A. & BRUNO, R. 2009 Scaling laws of turbulence and heating of fast solar wind: The role of density fluctuations. *Physical Review Letters* **103**, 061102. (Cited on pages x, 5, 85, 104, 106, 107, 117, 128, 150, 153, 166, 171 and 173.)
- CHANDRASEKHAR, S. 1951 The fluctuations of density in isotropic turbulence. *Proceedings of the Royal Society of London. Series A. Mathematical and Physical Sciences* **210** (1100), 18–25. (Cited on page 86.)
- CHANDRASEKHAR, S. 1954 *The theory of turbulence; Editor: Edward A. Spiegel*. Springer. (Cited on pages 44 and 83.)
- COLELLA, P. & WOODWARD, P. R. 1984 The piecewise parabolic method (ppm) for gas-dynamical simulations. *Journal of Computational Physics* **54** (1), 174 – 201. (Cited on page 91.)
- CONSTANTIN, P & FEFFERMAN, C 1994 Scaling exponents in fluid turbulence: some analytic results. *Nonlinearity* **7** (1), 41. (Cited on page 53.)

- CORRSIN, S. 1959 Outline of some topics in homogeneous turbulent flow. *Journal of Geophysical Research* **64** (12), 2134–2150. (Cited on page 68.)
- DAHLBURG, J. P., DAHLBURG, R. B., GARDNER, J. H. & PICONE, J. M. 1990 Inverse cascades in two-dimensional compressible turbulence. i. incompressible forcing at low mach number. *Physics of Fluids A: Fluid Dynamics (1989-1993)* **2** (8), 1481–1486. (Cited on page 176.)
- DAHLBURG, R. B. & PICONE, J. M. 1989 Evolution of the orszag-tang vortex system in a compressible medium. i. initial average subsonic flow. *Physics of Fluids B: Plasma Physics (1989-1993)* **1** (11), 2153–2171. (Cited on page 90.)
- DAI, W. & WOODWARD, P. R. 1994 Two-dimensional simulations for the impulsive penetration of a solar wind filament into the magnetosphere. *Journal of Geophysical Research: Space Physics* **99** (A5), 8577–8584. (Cited on page 91.)
- DITLEVSEN, P.D. 2010 *Turbulence and Shell Models*. Cambridge University Press. (Cited on pages 57 and 58.)
- ELMEGREEN, B. G. & SCALO, J. 2004 Interstellar turbulence i: Observations and processes. *Annual Review of Astronomy & Astrophysics* **42**, 211–273. (Cited on page 68.)
- ELSÄSSER, W. M. 1950 The hydromagnetic equations. *Physical Review* **79**, 183–183. (Cited on pages 4, 39 and 63.)
- FALKOVICH, G., FOUXON, I. & OZ, Y. 2010 New relations for correlation functions in Navier-Stokes turbulence. *Journal of Fluid Mechanics* **644**, 465. (Cited on pages 117, 118 and 142.)
- FEDERRATH, C., KLESSEN, R. S. & SCHMIDT, W. 2008 The density probability distribution in compressible isothermal turbulence: Solenoidal versus compressive forcing. *The Astrophysical Journal Letters* **688** (2), L79. (Cited on page 99.)
- FEDERRATH, C., ROMAN-DUVAL, J., KLESSEN, R. S., SCHMIDT, W. & LOW, M. MAC 2010 Comparing the statistics of interstellar turbulence in simulations and observations: Solenoidal versus compressive turbulence forcing. *Astronomy & Astrophysics* **512**, A81. (Cited on pages x, 5, 11, 71, 85, 99, 100, 101, 129, 175 and 176.)

- FINE, R. A. & MILLERO, F. J. 1973 Compressibility of water as a function of temperature and pressure. *The Journal of Chemical Physics* **59** (10), 5529–5536. (Cited on page 8.)
- FJORTOFT, R. 1953 On the changes in the spectral distribution of kinetic energy for twodimensional, nondivergent flow. *Tellus* **5** (3), 225–230. (Cited on page 72.)
- FLECK, R. C., JR. 1991 Vorticity generation behind interstellar shock fronts. *Astrophysics and Space Science* **182** (1), 81–84. (Cited on page 20.)
- FORMAN, M. A., SMITH, C. W. & VASQUEZ, B. J. 2010 Comment on "scaling laws of turbulence and heating of fast solar wind: The role of density fluctuations". *Physical Review Letters* **104**, 189001. (Cited on pages 106 and 117.)
- FOUXON, I. & OZ, Y. 2010 Exact scaling relations in relativistic hydrodynamic turbulence. *Physics Letters B* **694** (3), 261 – 264. (Cited on page 117.)
- FRISCH, U. 1995 *Turbulence: the legacy of A. N. Kolmogorov*. Cambridge University Press, Cambridge. (Cited on pages viii, 45, 48, 52, 68, 69, 71, 73, 77, 78, 81, 83, 123, 126 and 128.)
- FRISCH, U. & BEC, J. 2001 *Turbulence, Les Houches - Ecole d'Été de Physique Théorique*, vol. 74. Springer Berlin Heidelberg. (Cited on page 47.)
- FRISCH, U., SULEM, P. L. & NELKIN, M. 1978 A simple dynamical model of intermittent fully developed turbulence. *Journal of Fluid Mechanics* **87**, 719–736. (Cited on page 77.)
- GALTIER, S. 2008a Exact scaling laws for 3d electron mhd turbulence. *Journal of Geophysical Research: Space Physics* **113**. (Cited on page 154.)
- GALTIER, S. 2008b von karman-howarth equations for hall magnetohydrodynamic flows. *Physical Review E* **77**, R015302. (Cited on pages 110 and 175.)
- GALTIER, S. 2013 *Magnéto-hydrodynamique: Des plasmas de laboratoire à l'astrophysique*. Vuibert. (Cited on pages 30, 33 and 54.)
- GALTIER, S. & BANERJEE, S. 2011 Exact relation for correlation functions in compressible isothermal turbulence. *Physical Review Letters* **107**, 134501. (Cited on pages 5, 121, 130, 140, 144, 175 and 176.)
- GARNIER, J., LISAK, M. & PICOZZI, A. 2012 Toward a wave turbulence formulation of statistical nonlinear optics. *Journal of the Optical Society of America B Optical Physics* **29**, 2229. (Cited on page 1.)

- GIBSON, C. H. & SCHWARZ, W. H. 1963 The universal equilibrium spectra of turbulent velocity and scalar fields. *Journal of Fluid Mechanics* **16**, 365–384. (Cited on pages [viii](#) and [62](#).)
- GOLDREICH, P. & SRIDHAR, S. 1995 Toward a theory of interstellar turbulence. 2: Strong alfvénic turbulence. *The Astrophysical Journal* **438**, 763–775. (Cited on page [104](#).)
- GRAPPIN, R., LEORAT, J. & POUQUET, A. 1983 Dependence of mhd turbulence spectra on the velocity field-magnetic field correlation. *Astronomy & Astrophysics* **126**, 51–58. (Cited on page [65](#).)
- HARTEN, A., ENGQUIST, B., OSHER, S. & CHAKRAVARTHY, S. R. 1987 Uniformly high order accurate essentially non-oscillatory schemes, III. *Journal of Computational Physics* **71**, 231–303. (Cited on page [91](#).)
- HAWLEY, J. F. & STONE, J. M. 1995 MOCCT: A numerical technique for astrophysical MHD. *Computer Physics Communications* **89**, 127–148, numerical Methods in Astrophysical Hydrodynamics. (Cited on page [90](#).)
- HELMHOLTZ, H. 1867 On integrals of the hydrodynamical equations, which express vortex-motion. *Philosophical Magazine and J. Science* **33** (226), 485–512. (Cited on page [10](#).)
- HENNEBELLE, P. & AUDIT, E. 2007 On the structure of the turbulent interstellar atomic hydrogen. I. physical characteristics. influence and nature of turbulence in a thermally bistable flow. *Astronomy & Astrophysics* **465**, 431–443. (Cited on page [85](#).)
- HIGDON, J. C. 1984 Density fluctuations in the interstellar medium: Evidence for anisotropic magnetogasdynamic turbulence. i - model and astrophysical sites. *The Astrophysical Journal* **285**, 109–123. (Cited on page [104](#).)
- HIGDON, J. C. 1986 Density fluctuations in the interstellar medium: Evidence for anisotropic magnetogasdynamic turbulence. II - Stationary structures. *The Astrophysical Journal* **309**, 342–361. (Cited on page [104](#).)
- HNAT, B., CHAPMAN, S. C. & ROWLANDS, G. 2005 Compressibility in solar wind plasma turbulence. *Physical Review Letters* **94**, 204502. (Cited on pages [x](#), [104](#), [105](#), [116](#) and [153](#).)
- HOPF, E. 1952 Statistical hydromechanics and functional calculus. *Journal of Rational Mechanics Anal* **1**, 87–123. (Cited on page [87](#).)

- HORED T, G. P. 2004 *Polytropes: Applications in astrophysics and related fields*. Kluwer Academic Publishers. (Cited on page 145.)
- HOWES, G. G., COWLEY, S. C., DORLAND, W., HAMMETT, G. W., QUATAERT, E. & SCHEKOCHIHIN, A. A. 2008 A model of turbulence in magnetized plasmas: Implications for the dissipation range in the solar wind. *Journal of Geophysical Research: Space Physics* **113** (A5). (Cited on page 154.)
- HU, Y. Q., ESSER, R. & HABBAL, S. R. 1997 A fast solar wind model with anisotropic proton temperature. *Journal of Geophysical Research* **102**, 14661–14676. (Cited on page 137.)
- IROSHNIKOV, P. S. 1964 Turbulence of a conducting fluid in a strong magnetic field. *Soviet Astronomy* **7**, 566. (Cited on page 63.)
- KADOMTSEV, B. B. & PETVIASHVILI, V. I. 1973 On acoustic turbulence. *Doklady Akademii Nauk* **218**, 794–796. (Cited on pages 87 and 126.)
- VON KÀRMÀN, T. & HOWARTH, L. 1938 On the statistical theory of isotropic turbulence. *Proceedings of the Royal Society of London A* **164**, 192–215. (Cited on page 110.)
- KIDA, S. & ORSZAG, S. A. 1990 Energy and spectral dynamics in forced compressible turbulence. *Journal of Scientific Computing* **5** (2), 85–125. (Cited on page 11.)
- KIDA, S. & ORSZAG, S. A. 1992 Energy and spectral dynamics in decaying compressible turbulence. *Journal of Scientific Computing* **7** (1), 1–34. (Cited on pages 11 and 90.)
- KLEIN, R. I. & MCKEE, C. F. 1994 , vol. 630, p. 251. Cambridge: Univ. Press. (Cited on page 20.)
- KOLMOGOROV, A. N. 1941a Degeneration of isotropic turbulence in an incompressible viscous liquid. *Doklady Akademii Nauk SSSR* **31**, 538–540. (Cited on page 52.)
- KOLMOGOROV, A. N. 1941b Dissipation of energy in the locally isotropic turbulence. *Doklady Akademii Nauk SSSR* **32**, 16–18. (Cited on pages 54, 110 and 175.)
- KOLMOGOROV, A. N. 1962 A refinement of previous hypotheses concerning the local structure of turbulence in a viscous incompressible fluid at high reynolds number. *Journal of Fluid Mechanics* **13**, 82–85. (Cited on page 79.)

- KRAICHNAN, R. H. 1953 The scattering of sound in a turbulent medium. *Journal Acoustical Society of America* **25**, 1096–1104. (Cited on page 92.)
- KRAICHNAN, R. H. 1965 Inertial range spectrum in hydromagnetic turbulence. *Physics of Fluids* **8**, 1385–1387. (Cited on page 63.)
- KRAICHNAN, R. H. 1967*a* Inertial ranges in two-dimensional turbulence. *Physics of Fluids (1958-1988)* **10** (7), 1417–1423. (Cited on pages 59 and 73.)
- KRAICHNAN, R. H. 1967*b* Intermittency in the very small scales of turbulence. *Physics of Fluids (1958-1988)* **10** (9), 2080–2082. (Cited on page 75.)
- KRAICHNAN, R. H. & MONTGOMERY, D. 1980 Two-dimensional turbulence. *Reports on Progress in Physics* **43** (5), 547. (Cited on page 73.)
- KRITSUK, A.G., WAGNER, R. & NORMAN, M.L. 2013 Energy cascade and scaling in supersonic isothermal turbulence. *Journal of Fluid Mechanics Rapid* **729**, R1. (Cited on pages x, 120, 127, 140, 142, 144 and 176.)
- KRITSUK, A. G., NORMAN, M. L., PADOAN, P. & WAGNER, R. 2007*a* The statistics of supersonic isothermal turbulence. *The Astrophysical Journal* **665**, 416–431. (Cited on pages ix, xiii, 5, 11, 71, 85, 94, 95, 96, 97, 104, 117, 128, 129 and 175.)
- KRITSUK, A. G., PADOAN, P., WAGNER, R. & NORMAN, M. L. 2007*b* Scaling laws and intermittency in highly compressible turbulence. *AIP Conference Proceedings* **932** (1), 393–399. (Cited on pages ix, 5, 85, 97, 98, 104 and 117.)
- KRITSUK, A. G., USTYUGOV, S. D., NORMAN, M. L. & PADOAN, P. 2009 Simulations of Supersonic Turbulence in Molecular Clouds: Evidence for a New Universality. In *Numerical Modeling of Space Plasma Flows: ASTRONUM-2008* (ed. N. V. Pogorelov, E. Audit, P. Colella & G. P. Zank), *Astronomical Society of the Pacific Conference Series*, vol. 406, p. 15. (Cited on pages ix, 95 and 98.)
- KRITSUK, A. G., USTYUGOV, S. D., NORMAN, M. L. & PADOAN, P. 2010 Self-organization in Turbulent Molecular Clouds: Compressional Versus Solenoidal Modes. In *Numerical Modeling of Space Plasma Flows, Astronomum-2009* (ed. N. V. Pogorelov, E. Audit & G. P. Zank), *Astronomical Society of the Pacific Conference Series*, vol. 429, p. 15. (Cited on pages 5 and 99.)

- LANDAU, L.D. & LIFSHITZ, E.M. 1959 *Fluid Mechanics (Volume 6 of A Course of Theoretical Physics)*. Pergamon Press. (Cited on page 113.)
- LAVEDER, D., PASSOT, T. & SULEM, P.L. 2013 Intermittent dissipation and lack of universality in one-dimensional alfvénic turbulence. *Physics Letters A* **377**, 1535–1541. (Cited on page 140.)
- LÉORAT, J. & POUQUET, A. 1986 In *DRET Onera colloquium, Poitiers, Ecole normale supérieure de mécanique et aérotechnique*. (Cited on page 92.)
- LESIEUR, M. 2008 *Turbulence in Fluids*. Springer. (Cited on page 54.)
- LIGHTHILL, M. J. 1955 The effect of compressibility on turbulence. In *Gas Dynamics of Cosmic Clouds, IAU Symposium*, vol. 2, p. 121. (Cited on page 95.)
- LINDBORG, E., HALLBÄCK, M. & BURDEN, A.D. 1993 EDQNM and DNS – comparative calculations. *Applied Scientific Research* **51** (1-2), 353–358. (Cited on page 102.)
- LITHWICK, Y. & GOLDREICH, P. 2001 Compressible magnetohydrodynamic turbulence in interstellar plasmas. *The Astrophysical Journal* **562** (1), 279. (Cited on page 103.)
- LIU, X., OSHER, S. & CHAN, T. 1994 Weighted essentially non-oscillatory schemes. *Journal of Computational Physics* **115**, 200–212. (Cited on page 91.)
- MAC LOW, M. M., KLESSEN, R. S., BURKERT, A. & SMITH, M. D. 1998 Kinetic energy decay rates of supersonic and super-alfvénic turbulence in star-forming clouds. *Physical Review Letters* **80**, 2754–2757. (Cited on page 71.)
- MALARA, F., PRIMAVERA, L. & VELTRI, P. 1996 Compressive fluctuations generated by time evolution of alfvénic perturbations in the solar wind current sheet. *Journal of Geophysical Research: Space Physics* **101** (A10), 21597–21617. (Cited on page 107.)
- MARSCH, E. 1991 *MHD Turbulence in the Solar Wind*, pp. 159–241. (Cited on page 152.)
- MARSCH, E. & MANGENEY, A. 1987 Ideal mhd equations in terms of compressive Elsässer variables. *Journal of Geophysical Research: Space Physics* **92** (A7), 7363–7367. (Cited on pages 4, 39, 40, 130 and 132.)

- MARSCH, E., MÜHLHAÜSER, K.-H., ROSENBAUER, H., SCHWENN, R. & NEUBAUER, F. M. 1982 Solar wind helium ions: Observations of the helios solar probes between 0.3 and 1 au. *Journal of Geophysical Research: Space Physics* **87** (A1), 35–51. (Cited on page 105.)
- MARSCH, E. & TU, C.-Y. 1990a On the radial evolution of mhd turbulence in the inner heliosphere. *Journal of Geophysical Research: Space Physics* **95** (A6), 8211–8229. (Cited on page 153.)
- MARSCH, E. & TU, C.-Y. 1990b Spectral and spatial evolution of compressible turbulence in the inner solar wind. *Journal of Geophysical Research: Space Physics* **95** (A8), 11945–11956. (Cited on page 176.)
- MATTHAEUS, W. H. & GOLDSTEIN, M. L. 1982 Measurement of the rugged invariants of magnetohydrodynamic turbulence in the solar wind. *Journal of Geophysical Research: Space Physics* **87** (A8), 6011–6028. (Cited on page 163.)
- MEYER-VERNET, N. 2007 *Basics of the Solar Wind*. Cambridge University Press. (Cited on pages viii and 84.)
- MEYRAND, R. & GALTIER, S. 2010 A universal law for solar-wind turbulence at electron scales. *The Astrophysical Journal* **721**, 1421–1424. (Cited on pages 3, 110 and 175.)
- MOFFATT, H. K. 1969 The degree of knottedness of tangled vortex lines. *Journal of Fluid Mechanics* **null**, 117–129. (Cited on page 38.)
- MOISEEV, S.S., PETVIASHVILY, V.I., TOOR, A.V. & YANOVSKY, V.V. 1981 The influence of compressibility on the selfsimilar spectrum of subsonic turbulence. *Physica D: Nonlinear Phenomena* **2** (1), 218 – 223. (Cited on pages 87, 92 and 126.)
- MONIN, A.S., YAGLOM, A.M. & LUMLEY, J.L. 1975 *Statistical fluid mechanics: mechanics of turbulence*. *Statistical Fluid Mechanics: Mechanics of Turbulence* v. 2. MIT Press. (Cited on pages 52, 54 and 81.)
- MONTGOMERY, D., BROWN, M. R. & MATTHAEUS, W. H. 1987 Density fluctuation spectra in magnetohydrodynamic turbulence. *Journal of Geophysical Research: Space Physics* **92** (A1), 282–284. (Cited on page 104.)
- NAZARENKO, S. 2011 *Wave Turbulence*. Springer. (Cited on pages 55, 62, 72 and 73.)

- NEUGEBAUER, M. & SNYDER, C. W. 1962 Solar plasma experiment. *Science* **138** (3545), 1095–1097. (Cited on page 151.)
- NIE, Q. & TANVEER, S. 1999 A note on third-order structure functions in turbulence. *Proceedings of the Royal Society of London. Series A: Mathematical, Physical and Engineering Sciences* **455** (1985), 1615–1635. (Cited on page 54.)
- NORDLUND, A. & BRANDENBURG, AXEL 1992 Dynamo action in stratified convection with overshoot. *The Astrophysical Journal* (392), 647–652. (Cited on page 90.)
- NORDLUND, A. & PADOAN, P. 2003 Star formation and the initial mass function **614**, 271–298. (Cited on page 99.)
- OBOUKHOV, A. M. 1962 Some specific features of atmospheric turbulence. *Journal of Fluid Mechanics* **13**, 77–81. (Cited on page 79.)
- ORSZAG, S. A. 1970 Analytical theories of turbulence. *Journal of Fluid Mechanics* **41**, 363–386. (Cited on page 102.)
- PADOAN, P., JIMENEZ, R., NORDLUND, A. & BOLDYREV, S. 2004 Structure function scaling in compressible super-alfvénic mhd turbulence. *Physical Review Letters* **92**, 191102. (Cited on page 97.)
- PARKER, E. N. 1958 Dynamics of the interplanetary gas and magnetic fields. *The Astrophysical Journal* **128**, 664. (Cited on page 149.)
- PASSOT, T. & POUQUET, A. 1987 Numerical simulation of compressible homogeneous flows in the turbulent regime. *Journal of Fluid Mechanics* **181**, 441–466. (Cited on pages 20, 90 and 92.)
- PASSOT, T., POUQUET, A. & WOODWARD, P. 1988 On the plausibility of kolmogorov-type spectra in molecular clouds. *Astronomy & Astrophysics* **197**, 228–234. (Cited on pages ix, 85, 91, 92, 101 and 126.)
- PASSOT, T. & SULEM, P. L. 2007 Collisionless magnetohydrodynamics with gyrokinetic effects. *Physics of Plasmas (1994-present)* **14** (8). (Cited on page 154.)
- PASSOT, T. & VAZQUEZ-SEMADINI, E. 1998 Density probability distribution in one-dimensional polytropic gas dynamics. *Physical Review E* **58**, 4501–4510. (Cited on pages viii, 88 and 91.)
- PEDLOSKY, J. 1987 *Geophysical Fluid Dynamics, 2nd edition*. Springer-Verlag. (Cited on page 16.)

- POLITANO, H. & POUQUET, A. 1998*a* Natural length scales for structure functions in magnetized flows. *Geophysical Research Letters* **25**, 273–276. (Cited on pages 104, 110, 116, 132, 175 and 176.)
- POLITANO, H. & POUQUET, A. 1998*b* A von karman-howarth equation for mhd fluids and its consequences on third-order longitudinal structure and correlation functions. *Physical Review E* **57**, R21–R24. (Cited on pages 110, 116, 171 and 175.)
- PORTER, D. H., POUQUET, A. & WOODWARD, P. R. 1992 Three-dimensional supersonic homogeneous turbulence : A numerical study. *Physical Review Letters* **68**, 3156–3159. (Cited on pages ix and 93.)
- PORTER, D. H., POUQUET, A. & WOODWARD, P. R. 1994 Kolmogorov-like spectra in decaying three-dimensional supersonic flows. *Physics of Fluids* **6**, 2133–2142. (Cited on pages ix, 93 and 94.)
- PROMENT, D., NAZARENKO, S. & ONORATO, M. 2009 Quantum turbulence cascades in the gross-pitaevskii model. *Physical Review A* **80**, 051603. (Cited on page 1.)
- RASMUSSEN, H. O. 1999 A new proof of kolmogorov's 4/5-law. *Physics of Fluids (1994-present)* **11** (11), 3495–3498. (Cited on page 113.)
- RAX, J.M. 2005 *Physique des plasmas*. Dunod. (Cited on page 23.)
- RENARD, M. & CHIEZE, J. P. 1993 The fragmentation of molecular clouds: critical(jeans) mass in the vicinity of thermal instability and influence of visible extinction variations. *Astronomy & Astrophysics* **267**, 549–558. (Cited on page 145.)
- REYNOLDS, O. 1883 An experimental investigation of the circumstances which determine whether the motion of water shall be direct or sinuous, and of the law of resistance in parallel channels. *Philosophical Transactions of the Royal Society of London* **174**, 935–982. (Cited on page 47.)
- RICHARDSON, L.F. 1922 *Weather Prediction by Numerical Process*. Cambridge University Press. (Cited on pages 2, 60 and 71.)
- RICHTMYER, R.D. & MORTON, K.W. 1967 *Difference methods for initial-value problems*. Interscience Publishers. (Cited on page 90.)
- RICKETT, B. J. 1977 Interstellar scattering and scintillation of radio waves. *Annual Review of Astronomy & Astrophysics* **15**, 479–504. (Cited on page 103.)

- RICKETT, B. J. 1990 Radio propagation through the turbulent interstellar plasma. *Annual Review of Astronomy & Astrophysics* **28**, 561–605. (Cited on page 103.)
- ROBERTS, D. A. & GOLDSTEIN, M. 1991 Turbulence and waves in the solar wind. *Reviews of Geophysics* **29**, 932–943. (Cited on page 152.)
- ROSE, H.A. & SULEM, P.L. 1978 Fully developed turbulence and statistical mechanics. *Le journal de physique, France* **39** (5), 441–484. (Cited on page 58.)
- ROTT, N 1990 Note on the history of the reynolds number. *Annual Review of Fluid Mechanics* **22** (1), 1–12. (Cited on page 47.)
- SAHRAOUI, F., GOLDSTEIN, M. L., BELMONT, G., CANU, P. & REZEAU, L. 2010 Three dimensional anisotropic k spectra of turbulence at subproton scales in the solar wind. *Phys. Rev. Lett.* **105**, 131101. (Cited on pages 154 and 163.)
- SAHRAOUI, F., GOLDSTEIN, M. L., ROBERT, P. & KHOTYAINTESEV, YU. V. 2009 Evidence of a cascade and dissipation of solar-wind turbulence at the electron gyroscale. *Phys. Rev. Lett.* **102**, 231102. (Cited on page 154.)
- SALEM, C., MANGENEY, A., BALE, S. D. & VELTRI, P. 2009 Solar wind magnetohydrodynamics turbulence: Anomalous scaling and role of intermittency. *The Astrophysical Journal* **702** (1), 537. (Cited on pages viii and 75.)
- SALEM, C. S., HOWES, G. G., SUNDKVIST, D., BALE, S. D., CHASTON, C. C., CHEN, C. H. K. & MOZER, F. S. 2012 Identification of kinetic alfvén wave turbulence in the solar wind. *The Astrophysical Journal Letters* **745** (1), L9. (Cited on page 3.)
- SALMON, R. 1998 *Lectures on Geophysical Fluid Dynamics*. Oxford University Press. (Cited on page 49.)
- SCHEKOCHIHIN, A. A., COWLEY, S. C., DORLAND, W., HAMMETT, G. W., HOWES, G. G., QUATAERT, E. & TATSUNO, T. 2009 Astrophysical gyrokinetics: Kinetic and fluid turbulent cascades in magnetized weakly collisional plasmas. *The Astrophysical Journal Supplement Series* **182** (1), 310. (Cited on page 154.)
- SCHMIDT, W. 2009 Large Eddy Simulations of Supersonic Turbulence. *ArXiv e-prints* . (Cited on pages 85 and 99.)

- SCHMIDT, W. 2013 *Numerical Modelling of Astrophysical Turbulence*. Springer International Publishing. (Cited on page 90.)
- SCHMIDT, W., FEDERRATH, C., HUPP, M., KERN, S. & NIEMEYER, J. C. 2009 Numerical simulations of compressively driven interstellar turbulence. I. Isothermal gas. *Astronomy & Astrophysics* **494**, 127–145. (Cited on pages 85 and 99.)
- SCHMIDT, W., FEDERRATH, C. & KLESSEN, R. 2008 Is the scaling of supersonic turbulence universal? *Physical Review Letters* **101**, 194505. (Cited on pages 97, 99 and 178.)
- SHE, Z. S. & LEVEQUE, E. 1994 Universal scaling laws in fully developed turbulence. *Physical Review Letters* **72**, 336–339. (Cited on pages 79 and 97.)
- SMITH, M. D., MAC LOW, M.-M. & ZUEV, J. M. 2000 The shock waves in decaying supersonic turbulence. *Astronomy & Astrophysics* **356**, 287–300. (Cited on page 125.)
- SOMMERFELD, A. 1908 Ein beitrag zur hydrodynamisehen erkliirung der turbulenten flfissigkeitsbewegung. *4th International Congress of Mathematics, Rome* **3**, 116–124. (Cited on page 47.)
- SORRISO-VALVO, L., CARBONE, V., MARINO, R., NOULLEZ, A., BRUNO, R. & VELTRI, P. 2010 Sorriso-valvo et al. reply:. *Physical Review Letters* **104**, 189002. (Cited on page 107.)
- STOKES, G. G. 1851 On the effect of the internal friction of fluids on the motion of pendulums. *Transactions of the Cambridge Philosophical Society* **9**, 8. (Cited on page 47.)
- STONE, J. M., MIHALAS, D. & NORMAN, M. L. 1992 Zeus-2d: A radiation magnetohydrodynamics code for astrophysical flows in two space dimensions. iii - the radiation hydrodynamic algorithms and tests. *The Astrophysical Journal Supplementary Series* **80**, 819–845. (Cited on page 90.)
- STONE, J. M. & NORMAN, M. L. 1992a Zeus-2d: A radiation magnetohydrodynamics code for astrophysical flows in two space dimensions. i - the hydrodynamic algorithms and tests. *The Astrophysical Journal Supplementary Series* **80**, 753–790. (Cited on page 90.)
- STONE, J. M. & NORMAN, M. L. 1992b Zeus-2d: A radiation magnetohydrodynamics code for astrophysical flows in two space dimensions. ii. the magnetohydrodynamic algorithms and tests. *The Astrophysical Journal Supplementary Series* **80**, 791. (Cited on page 90.)

- STRANG, G. 1968 On the construction and comparison of different splitting schemes. *SIAM Journal of Numerical Analysis* **5**, 506–517. (Cited on page 91.)
- SULEM, P.L. & PASSOT, T. 2008 Flr-landau fluids for collisionless plasmas. *Communications in Nonlinear Science and Numerical Simulation* **13** (1), 189–196, vlasovia 2006: The Second International Workshop on the Theory and Applications of the Vlasov Equation. (Cited on page 154.)
- THOMSON, W. (LORD KELVIN) 1869 On vortex motion. *Transactions of the Royal Society of Edinburgh*. **25**, 217–260. (Cited on page 14.)
- TOKUNAGA, H. 1976 The statistical theory of one-dimensional turbulence in a compressible field. *Journal of the Physical Society of Japan* **41** (1), 328–337. (Cited on pages viii, 88 and 89.)
- TU, C.-Y. & MARSCH, E. 1997 Two-Fluid Model for Heating of the Solar Corona and Acceleration of the Solar Wind by High-Frequency Alfvén Waves. *Solar Physics* **171**, 363–391. (Cited on pages 3 and 137.)
- VÁZQUEZ-SEMADENI, E., PASSOT, T. & POUQUET, A. 1996 Influence of cooling-induced compressibility on the structure of turbulent flows and gravitational collapse. *The Astrophysical Journal* **473**, 881–893. (Cited on pages 18, 19, 20 and 85.)
- VELLI, MARCO, GRAPPIN, ROLAND & MANGENEY, ANDRÉ 1989 Turbulent cascade of incompressible unidirectional alfvén waves in the interplanetary medium. *Phys. Rev. Lett.* **63**, 1807–1810. (Cited on page 153.)
- WAGNER, R., FALKOVICH, G., KRITSUK, A. G. & NORMAN, M. L. 2012 Flux correlations in supersonic isothermal turbulence. *Journal of Fluid Mechanics* **713**, 482–490. (Cited on pages 120, 142 and 176.)
- WEBER, E. J. & DAVIS, JR., L. 1967 The Angular Momentum of the Solar Wind. *The Astrophysical Journal* **148**, 217–227. (Cited on page 149.)
- WENSINK, H. H., DUNKEL, J., HEIDENREICH, S., DRESCHER, K., GOLDSTEIN, R. E., LÖWEN, H. & YEOMANS, J. M. 2012 Meso-scale turbulence in living fluids. *Proceedings of the National Academy of Sciences* . (Cited on page 1.)
- WOLFRAM, S. 2002 *A New Kind of Science*. Wolfram Media. (Cited on page 47.)

-
- WOLTJER, L. 1958 A theorem on force-free magnetic fields. *Proceedings of the National Academy of Sciences* **44** (6), 489–491. (Cited on pages 36 and 37.)
- WU, J.Z., MA, H. & ZHOU, D. 2007 *Vorticity and Vortex Dynamics*. Springer. (Cited on page 14.)
- YAGLOM, A. M. 1949 Local structure of the temperature field in a turbulent flow. *Doklady Akademii Nauk SSSR* **69**, 743. (Cited on pages 110 and 175.)
- ZAKHAROV, V. E. 1965 Weak turbulence in media with decay spectrum. *Prikladnaya Mekhanika i Tekhnicheskaya Fizika* **4**, 35–39. (Cited on page 87.)
- ZAKHAROV, V. E. & SAGDEEV, R. Z. 1970 Spectrum of acoustic turbulence. *Soviet Physics Doklady* **15**, 439. (Cited on pages 15 and 86.)

Résumé

Ma thèse a pour but de comprendre le rôle de la compressibilité dans la turbulence aux basses fréquences dans les plasmas spatiaux (le vent solaire, les plasmas magnétosphériques etc.) et astrophysiques (nuage moléculaire interstellaire, le cœur d'une étoile etc.). Trois nouvelles relations exactes ont été déduites dans le cadre de la turbulence compressible dans un fluide isotherme et polytrophe et dans un plasma MHD isotherme afin de comprendre différentes propriétés universelles de la turbulence compressible. De plausibles phénoménologies ont été proposées aussi en vue d'une compréhension de différentes lois de spectre obtenues grâce aux simulations numériques de la turbulence compressible. Une distinction qualitative entre la turbulence sous-sonique et supersonique est ainsi décrite.

Une analyse utilisant des données d'observation des sondes spatiales THEMIS est également réalisée dans le but d'expliquer l'effet de la compressibilité dans la turbulence du vent solaire rapide.

Keywords: [Turbulence](#), [turbulence compressible](#), [plasmas spatiaux](#), [plasmas astrophysiques](#), [vent solaire](#), [analyse des données](#)

Abstract

My thesis work is principally dedicated to the understanding of the role of compressibility in low frequency turbulence of space plasmas (the solar wind, the magnetosphere etc.) and astrophysical plasmas (interstellar molecular cloud, the core of a star etc.). Three new exact relations have been derived analytically in the framework of isothermal and polytropic hydrodynamic turbulence and for isothermal MHD turbulence. By using these relations, various universal scaling properties of compressible turbulence have been investigated. In addition, plausible phenomenologies have been proposed in order to theoretically reproduce different power-laws for the total energy power spectra which had been obtained in previous numerical simulations of compressible turbulence. A semi-qualitative distinction between sub-sonic and supersonic regimes of turbulence is hence concluded.

In the second part, an analysis using THEMIS spacecraft data is also performed in a view to explaining the effect of the compressibility in the turbulence of the fast solar wind.

Keywords: [Turbulence](#), [compressible turbulence](#), [space plasmas](#), [astrophysical plasmas](#), [theory](#), [exact relation](#), [solar wind](#), [data analysis](#)
